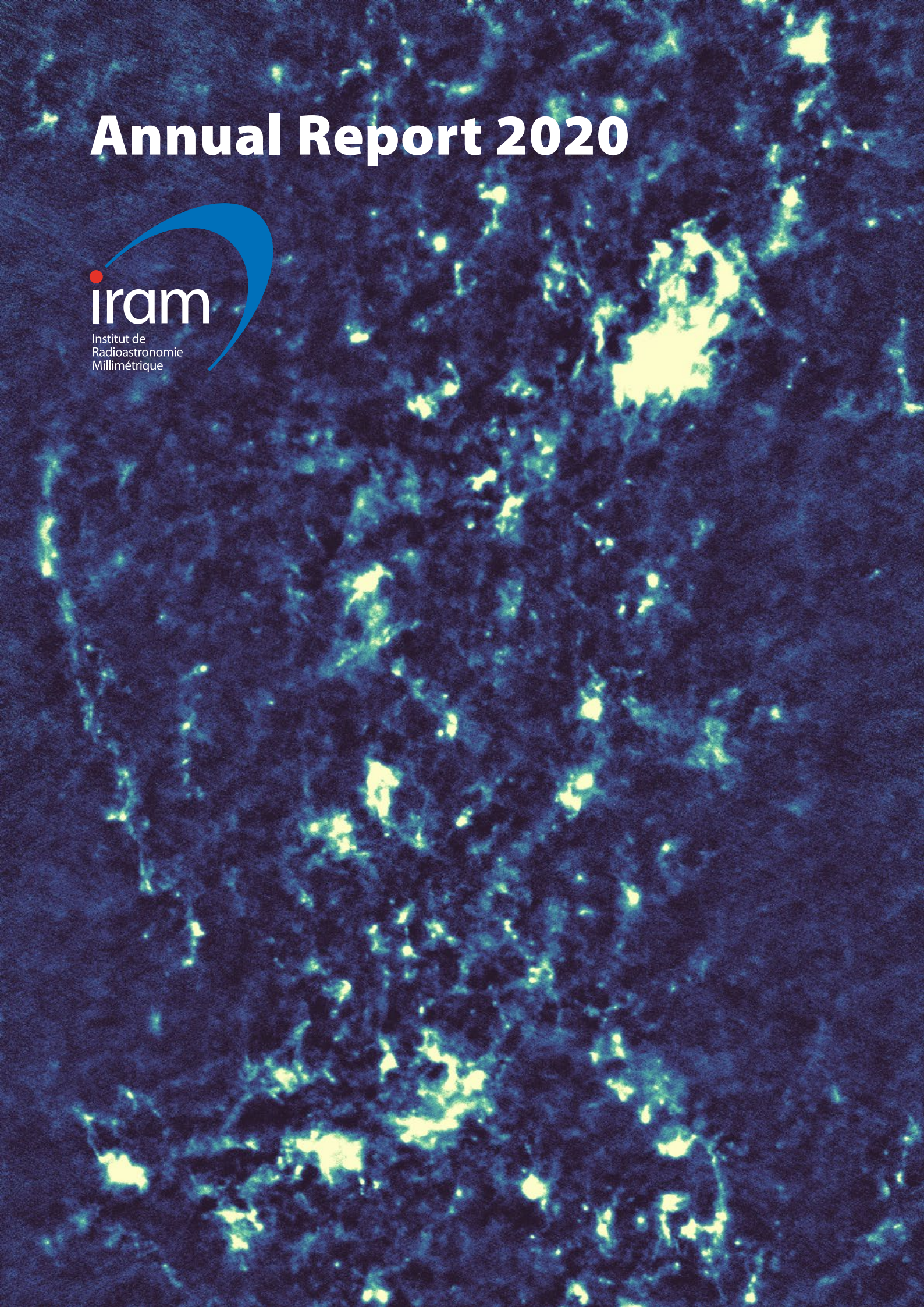


# Annual Report 2020



# IRAM Annual Report 2020

**Published by IRAM © 2021**

Director of publication Karl-Friedrich Schuster

Edited by Frédéric Gueth, Sonja Moreau

**With contributions from:**

Sébastien Blanchet, Antonio Córdoba, Eduard Driessen, Bertrand Gautier, Olivier Gentaz, Romain Messmer, Santiago Navarro, Roberto Neri, Juan Peñalver, Jérôme Pety, Francesco Pierfederici, Christophe Risacher, Miguel Sánchez Portal, Karl-Friedrich Schuster



# Contents

Introduction.....	4
Highlights of research with the IRAM telescopes.....	6
30-meter telescope.....	20
NOEMA.....	28
Grenoble headquarters.....	38
Backend Group.....	38
Frontend Group.....	41
Superconducting Devices Group.....	45
Mechanical Group.....	47
Computer Group.....	49
Science Software.....	50
IRAM ARC Node.....	52
Personnel & Finance.....	54
Annexes.....	58
Telescope schedules.....	58
Publications.....	72
Committees.....	90



# Introduction

The reader of this annual report may easily imagine that the year 2020 was for IRAM totally dominated by the struggle to adapt to the constraints of the Covid-19 pandemic. And indeed, this took a very important part of our energy on all levels: personal, institutional and also societal. Safety for the staff and their families was and is the main concern and this had to be combined with a continuous questioning and re-definition of rules and ways of doing.

It is all the more absolutely remarkable what was achieved over the year. Let me first thank here the entire IRAM staff who knew to stick together, to adapt and to move forward while keeping the spirits high despite the very numerous difficulties in professional and everyday personal life. We have been witnesses of the old truth that people show their great qualities in important crises. Only in the aftermath of the current situation it will become clear how much depended on keeping the everyday business going. On the one side, we wanted to avoid too disruptive situations for the staff and on the other side, it was important to continue best possible service to the scientific user community under the given circumstances.

In fact, as soon as the rapidly degrading situation requested a first general lockdown in March 2020 in France and Spain, a huge effort was made between the safety coordinators as well as the group leaders and the station managers to insure safety at the IRAM observatories and the headquarter including creation of information channels, reorganization of work flows and installation of a vast number of safety measures.

At the observatories, this immense work and the exceptional motivation of the staff allowed to overcome the very difficult situation in the first weeks of the pandemic including a lot of problems generated by the fact that the related ski stations for both observatories went into full stop with no service provided to IRAM. Despite these difficulties to access the observatories, the IRAM 30-meter telescope only had to go into survival mode for four weeks before switching successfully to a totally new operation mode with exclusive remote user support from operators and astronomers on duty. NOEMA even could seamlessly continue science operation and only antenna assembly work was interrupted for eight weeks. With all these challenges, it was nevertheless possible to finish assembly and

commission of the 11<sup>th</sup> NOEMA antenna in September 2020. At the same time, the French partner CNRS could confirm his commitment to fully finance Antenna 12 with completion of this final NOEMA antenna foreseen for fall 2021.

Likewise, an incredible number of projects made very important progress in the laboratories. Among many other projects and developments, one might mention the first dual-band receiver that was installed at NOEMA showing very promising performance. It is further notable, that the 2<sup>nd</sup> water vapour radiometer generation went from prototype status into production and that the NOEMA VLBI phasing has seen first very successful tests.

Three outstanding events added onto this in the second half of the year 2020 which I will mention here in temporal order. Beginning of October, our executive council member for more than 30 years, Reinhard Genzel was awarded the Nobel prize for Physics. Throughout the decades, Reinhard Genzel has been a key person to support the progress and evolution of IRAM and we all were extremely happy and proud about this reward. Then in beginning of November came the news that the Spanish science ministry awarded very important structural funds to support the refurbishment and ambitious upgrade of our iconic workhorse, the IRAM 30-meter telescope. And finally, end of November 2020, the IRAM partners signed the extension of the collaboration agreement until 2034. Needless to say, that this is received by the IRAM staff as a confirmation of the high esteem and trust from the partner organisations into the persons at work and in IRAM as a whole.

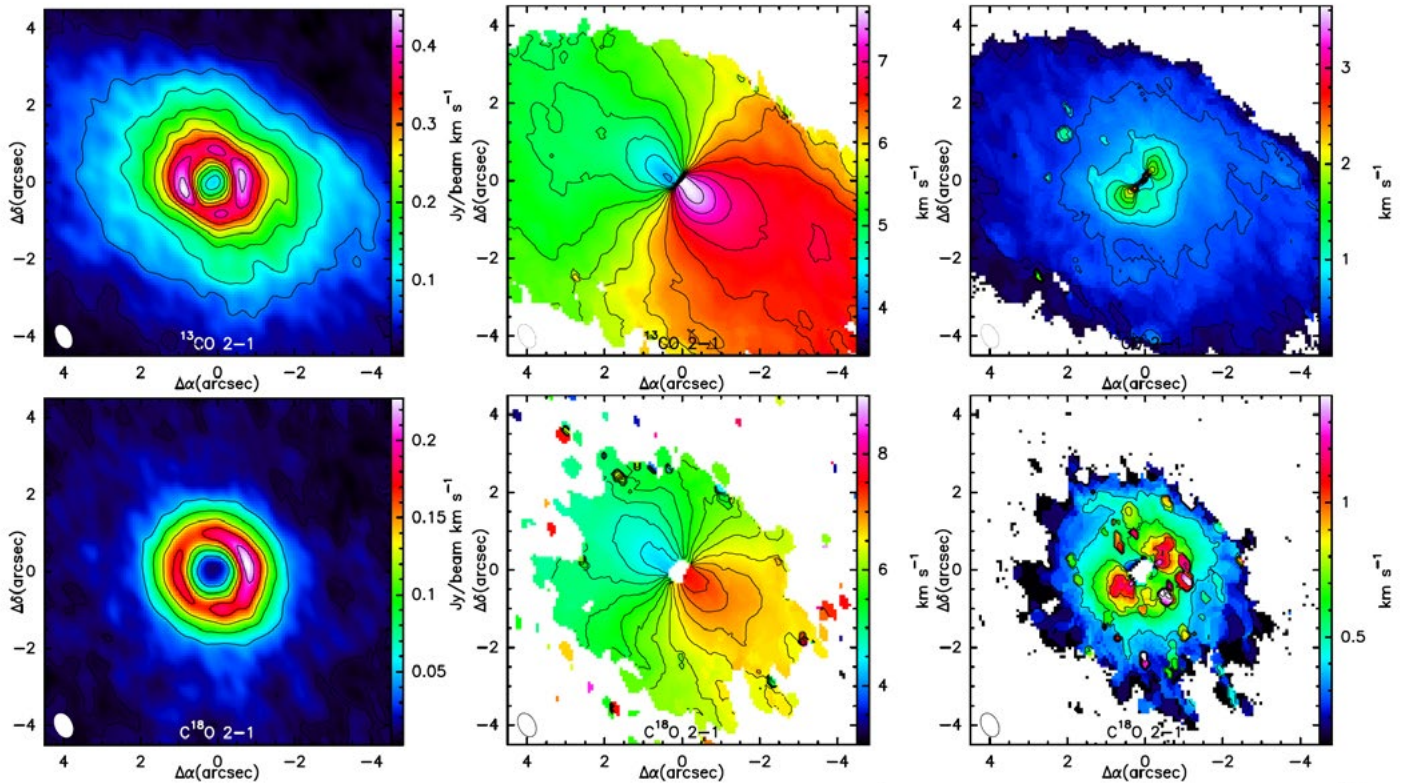
This leaves us with a bittersweet look onto 2020 where so much suffering and problems on all levels are side by side with a large number of achievements and positive events in our institute. My hope is that the health urgency can soon be overcome and we can find ways to duly celebrate together at least part of these achievements.

With best regards

Karl-Friedrich Schuster  
Director



# Highlights of research with the IRAM telescopes



Credit: Pablo Rivière-Marichalar et al.

## A protostellar binary system fed by a 10500 AU gas streamer

One of the key challenges in the field of star formation is the formation of binary stars. Among the possible routes for the formation of close-companion stars is the fragmentation of a gravitationally unstable disk around a protostar early in the star formation process. As the disk grows in mass, it eventually becomes gravitationally unstable and fragments, forming one or more new protostars orbiting each other. This scenario is supported by models where the small-scale disk asymmetries observed around young protostars and possibly resulting from an eccentric fragmentation of the large-scale disk environment, are at the origin of the formation of a close binary.

In an attempt to explore the environment of a Class 0 binary system, a team of scientists led by Jaime Pineda (MPE/Garching) used NOEMA to observe, at disk-forming scales, the dynamical properties of the gas in the proto-stellar system Per-emb-2 (IRAS 03292+3039). The high-resolution observations revealed the presence of a large reservoir of fresh material in almost free-fall that narrows down to an elongated gas stream of 10500 AU under the gravitational pull of the innermost part of the core. The stream carries large amounts of gas ( $0.1 M_{\odot}$ ) with chemicals such as  $\text{HC}_3\text{N}$ ,  $\text{C}_2\text{S}$ ,  $^{13}\text{CS}$ , which are channeled at a rate of  $7 \cdot 10^{-7} M_{\odot}/\text{yr}$  onto the disk surrounding the binary star system. According to the authors, both the locations and the speed of the gas are well matched by a theoretical model of a stream of material free-falling from large to small scales, and are

thereby confirming that the streamer's dynamics are controlled by the densest central region of the system. From the streamer density, the depletion timescale is estimated to  $\sim 20000$  yr, which is comparable to the free-fall time scale but much shorter than the canonical  $\sim 100000$  yr duration of the Class 0 phase.

The results of this study provide impressive evidence that the large-scale environment around forming stars has an important influence on small-scale disk formation and evolution. Moreover, they show that the non-axisymmetric enrichment of fresh material injected into the disk is a possible trigger for the formation of binary and possibly multiple star systems. Finally, they provide new support for studies claiming that streamer-like features seen on disk scales are the result of strong envelope accretion.

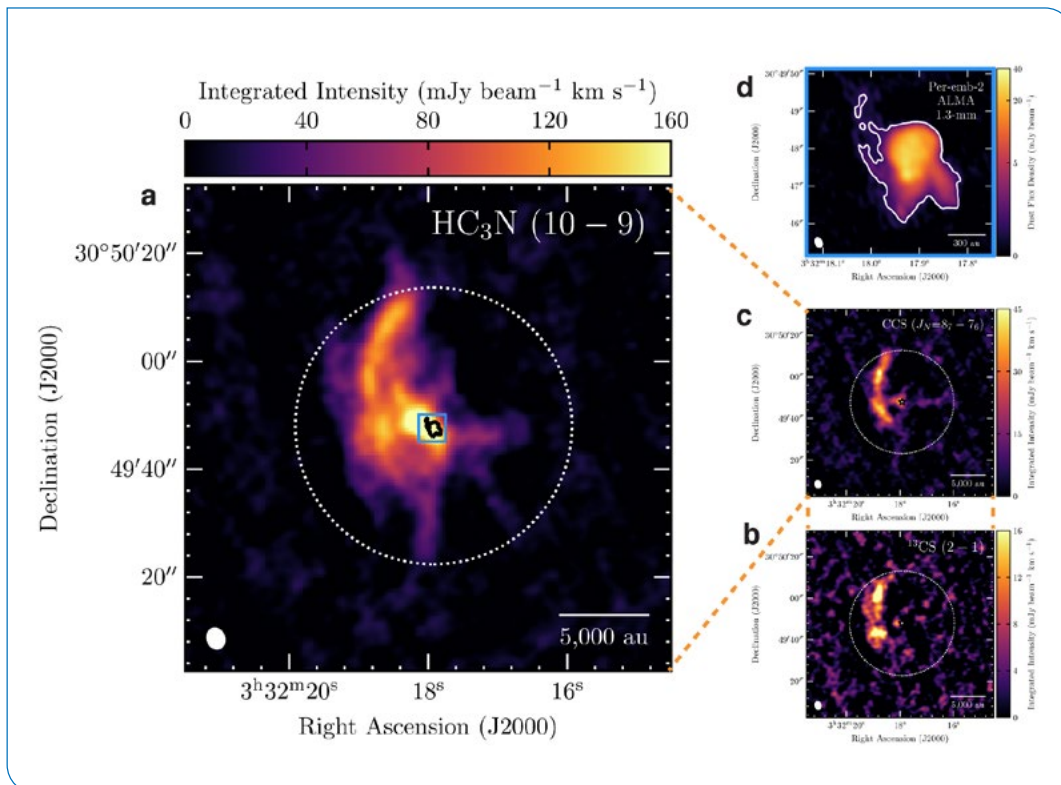


Image of the 'streamer' feeding chemically fresh material from a distance of about 10500 AU to the proto-star at the centre of the image. The three images use different molecules as tracers, indicated in the top right corner, and all show the streamer in action. The colour coding is according to the integrated intensity of the signal. The 1.3mm continuum panel at the top right is from ALMA.

Work by Pineda et al. 2020, Nature, 4, 1158

## Cold gas accretion mode of star formation in AzTEC2?

Several lines of evidence suggest that the global production of stars in galaxies is mainly regulated by the steady accretion of gas from the intergalactic medium. This process of galaxy evolution is believed to be responsible for the widespread star formation in galactic disks over giga-year timescales. It is known as the "cold gas accretion mode" of star formation, which differs from the rather short-lived but more intensive production of stars often triggered by major/minor galaxy mergers. Whereas both regimes of star formation have been widely explored out to intermediate redshifts ( $z \sim 2$ ), the relative role of the cold gas accretion and merger mode in driving the intense production of stars in galaxies at higher redshifts ( $z \sim 3$ ) remains an open issue.

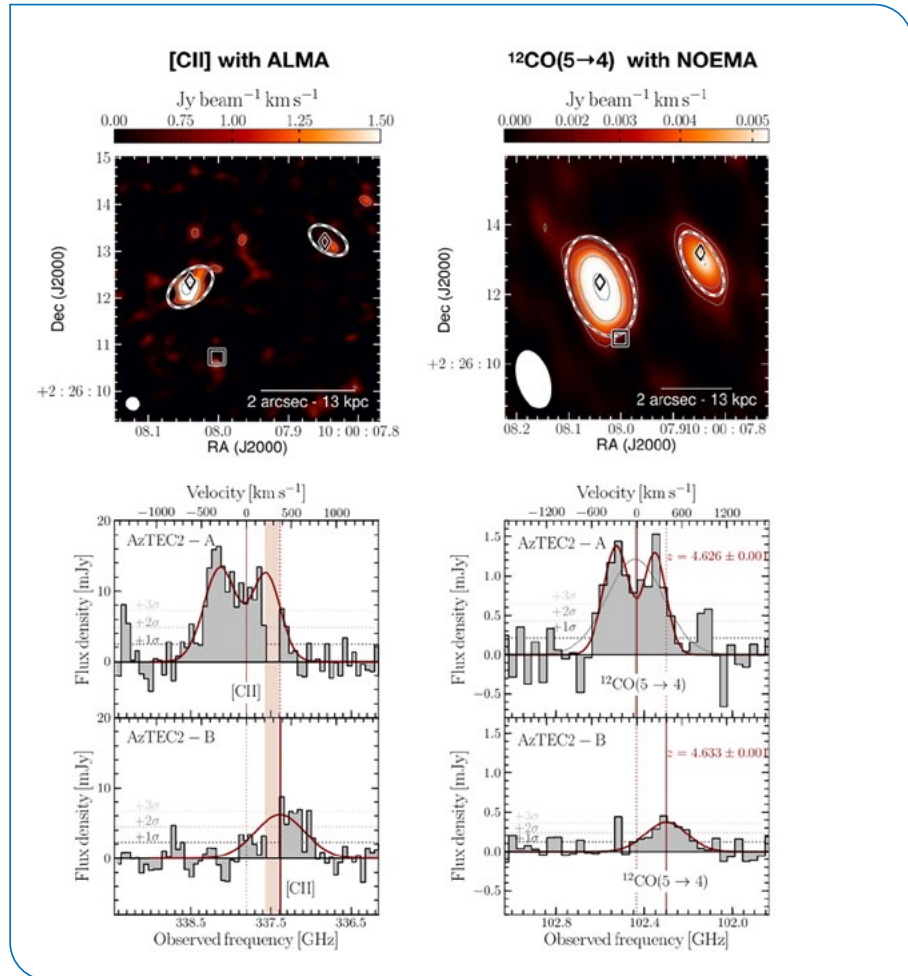
To investigate the role of cold gas accretion in star formation at higher redshift, a team of astronomers led by Jiménez-Andrade (NRAO/Charlottesville) studied AzTEC2, the second brightest SMG in the COSMOS field, which consists of a massive, star-forming disk and a smaller companion galaxy. By combining observations from NOEMA and ALMA, the authors assessed the redshift and confirmed that AzTEC2 is binary galaxy system at a redshift of 4.63, and thereby ruled out previous associations with a galaxy at  $z \sim 1$ .

By using the  $^{12}\text{CO} (5-4)$  line emission and adopting typical SMG-like gas excitation conditions, and a gas mass-to-luminosity conversion factor  $\alpha_{\text{CO}} = 2.5$ , Jiménez-Andrade and collaborators estimated the molecular gas mass to  $3.2 \cdot 10^{11} M_{\odot}$  for AzTEC2-A, and to  $0.8 \cdot 10^{11} M_{\odot}$  for AzTEC2-B. With infrared-derived star formation



Upper panels: velocity-integrated intensity maps of [CII]158 $\mu$ m and  $^{12}\text{CO}$  (5–4) detected towards AzTEC2-A and AzTEC2-B with ALMA and NOEMA, respectively. Lower panels: [CII]158 $\mu$ m and  $^{12}\text{CO}$  (5–4) spectra of AzTEC2-A and AzTEC2-B. The red solid line represents the model. The velocities displayed in the spectra are relative to the central frequency of the  $^{12}\text{CO}$  (5–4) line emission in AzTEC2-A.

Work by Jiménez-Andrade et al. 2020, *ApJ*, 890, 171

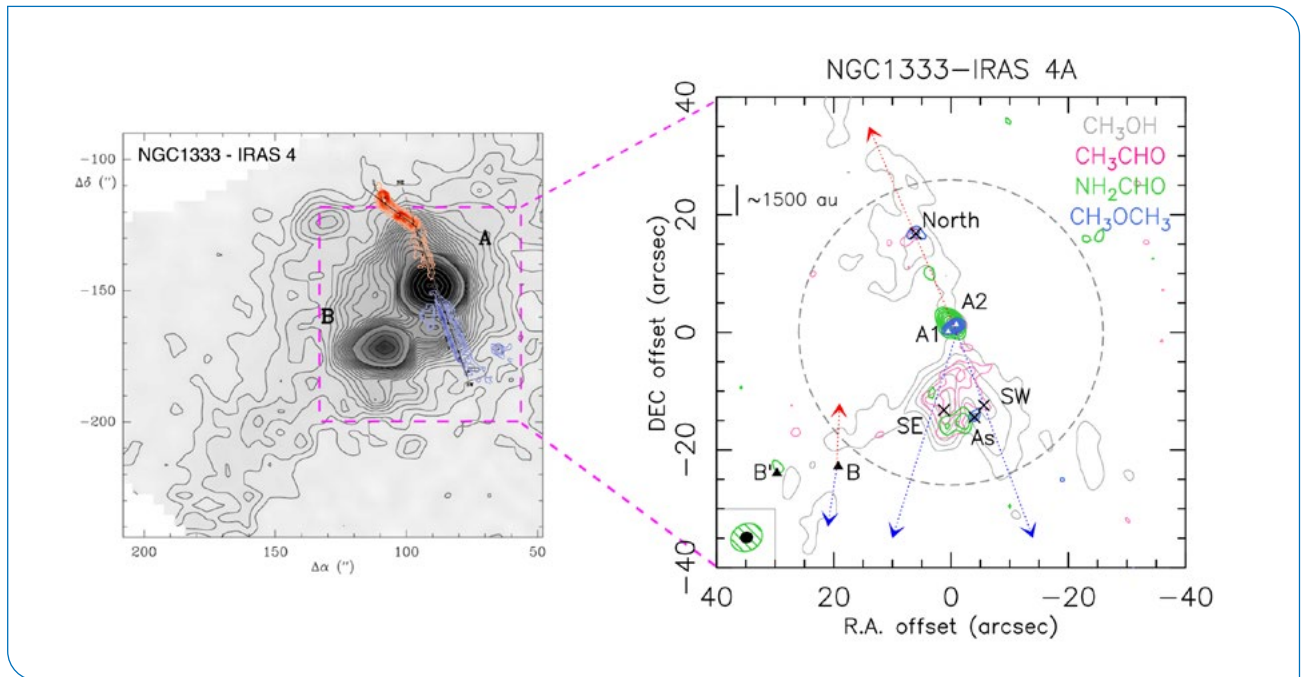


rates of 1920  $M_{\odot}/\text{yr}$  and 710  $M_{\odot}/\text{yr}$  for AzTEC2-A and AzTEC2-B respectively, their current gas reservoirs are expected to be depleted within 30–200 Myr. Their results indicate that AzTEC2-A hosts a massive, rotation-dominated disk with a de-projected rotation velocity of 660 km s $^{-1}$  where star formation occurs at intense levels. According to the authors, this indicates that even disk galaxies that harbour vast gas reservoirs could sustain intense star formation activity that resembles that of merger-driven SMGs.

This study supports the emerging consensus whereby the population of single-dish selected SMGs is rather heterogeneous, including both interacting systems and galaxies that form stars through a smoother mode of star formation sustained by cold gas accretion. Further systematic studies are already planned to verify this scenario.

## Complex organic molecules in IRAS 4A

The presence of complex organic molecules (iCOMs) around solar-type protostars has raised the question of their role in the chemical origins of biotic molecules and thus in the emergence of life on Earth. While their possible importance for the occurrence of life is undisputed today, iCOMs pose a challenge to astrochemistry, as their synthesis is far from obvious. Nowadays, two main paradigms are proposed, according to which iCOMs are synthesized either on the surfaces of dust grains or in the gas phase via sputtering. Although both pathways require the formation of simple hydrogenated molecules on dust grains during the pre-stellar phase, both pathways can lead to the synthesis of iCOMs. However, which of the two is the more efficient and under what conditions iCOMs form remain open questions.



Overlay (left) of the 1.25 mm continuum emission (grey contours, IRAM 30-meter telescope) and the SiO emission tracing the outflows (colored, VLA). Zoomed-in image (right) of the IRAS 4A system observed with NOEMA. The dashed blue and red arrows indicate the directions of the blue- and red-shifted outflows from 4A1, 4A2 and 4B. The velocity integrated maps of the iCOMs listed in the top right corner are colored accordingly.

Work by De Simone et al. 2020, A&A, 640, A75

One method that turns out to be efficient in disentangling the two formation routes is to compare observations toward low-mass outflow shocks with model predictions. Indeed, shocks that sweep through the outflows drive the chemical evolution of the outflows over time, allowing observed molecular abundances to be compared with model predictions and thereby constraining the formation pathways of iCOMs.

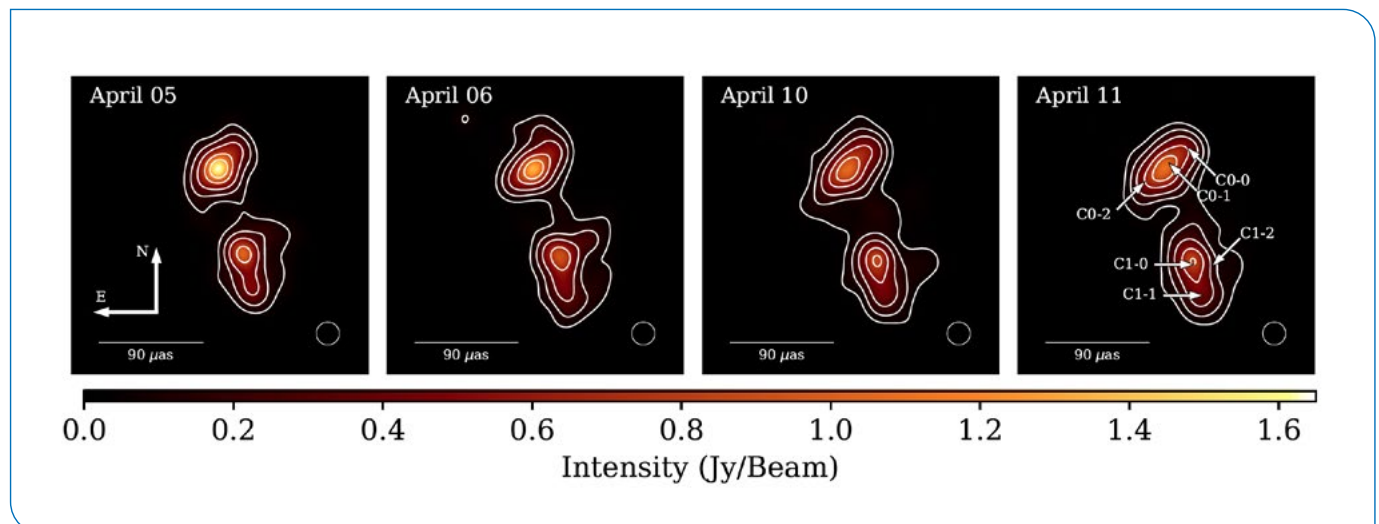
To shed new light on the iCOM chemistry in the outflows of NGC1333-IRAS 4A, a research group led by Marta De Simone (IPAG/Grenoble) reported the detection of four iCOMs with NOEMA: methanol ( $\text{CH}_3\text{OH}$ ), acetaldehyde ( $\text{CH}_3\text{CHO}$ ), formamide ( $\text{NH}_2\text{CHO}$ ), and dimethyl ether ( $\text{CH}_3\text{OCH}_3$ ). The researchers were able to observe significant differences in the iCOM abundances between the southeastern outflow driven by IRAS 4A1, and the north-southwestern outflow driven by the hot corino in IRAS 4A2. By using an astrochemical gas-phase model (GRAINOBLE), the authors show that the different distribution of some iCOMs can be explained by gas-phase reaction, and in particular for acetaldehyde. Indeed, although laboratory experiments show that acetaldehyde can be formed on the surfaces of dust grains, the comparison of their models with the observed gas distribution provides strong evidence that the gas-phase formation route cannot be neglected for acetaldehyde, and that it depends very little on the details of the modeling.

The authors conclude that gas-phase reactions do indeed appear to be the dominant process in the IRAS 4A outflows, and that the chemical differentiation between the two outflows is presumably related to their different kinematical age. Further observations of outflows at different ages are planned to corroborate these results.

## Event Horizon Telescope observations of the blazar 3C279

Relativistic jets in active galactic nuclei (AGN) are believed to originate from the vicinity of a supermassive black hole (SMBH) at the center of the galaxy. Understanding the detailed physical processes that lead to the formation, acceleration, collimation, and the subsequent propagation of a jet is one of the major quests in modern astrophysics. Extensive high-resolution AGN studies have been conducted on these topics over the past decades, but it is only through observations such as those allowed by the Event Horizon Telescope (EHT) Collaboration that a significant breakthrough seems possible.

To resolve the fine-scale structures of jets in the vicinity of SMBHs, a critical precondition to better understand both the accretion phase and the way jets evolve, Jae-Young Kim (MPIfR/Bonn) and collaborators made use of the EHT, and so of the IRAM 30-meter telescope, to observe the 230 GHz continuum emission in the innermost jet regions of 3C279, one of the brightest known blazars. The EHT observations, which were obtained at  $20 \mu\text{s}$  resolution, show that the core region (C0 region) in 3C279 consists of three bright substructures (C0-0, C0-1, C0-2) oriented perpendicular to an elongated structure, and separated by 30–40  $\mu\text{s}$ , which corresponds to a projected spatial scale of  $\sim 3000 R_s$  for  $M_{\text{BH}} = 8 \cdot 10^8 M_\odot$ . The EHT observations were supplemented by quasi-simultaneous VLBA (43 GHz) and GMVA (85 GHz) maps of the large-scale core and jet features. According to the authors the three substructures are associated with either a curved jet or a linear, nodular structure such as a site of large-scale magnetic reconnection or of plasma instabilities. The fact that the three core substructures show proper motions of  $\sim 1.4 \mu\text{s}/\text{day}$  and high flux variability suggests that they have something to do with how the jets meet the accretion disc surrounding the black hole. According to the authors, the rather low intrinsic brightness temperature ( $T \leq 10^{10}$  K) of the core and its morphological complexity also suggest that the core region of 3C279 becomes optically thin at short (mm) wavelengths, or that the innermost jet is dominated by magnetic energy if the synchrotron turn-over frequency were close to 230 GHz.



EHT images of 3C279 on April 5 to 11 generated by averaging the images obtained using three different imaging pipelines. The circular  $20 \mu\text{s}$  restoring beam is shown in the bottom right corner of each panel. The IRAM 30-meter telescope is part of the GMVA and EHT networks.

Work by Kim et al. 2020, A&A, 640, A69

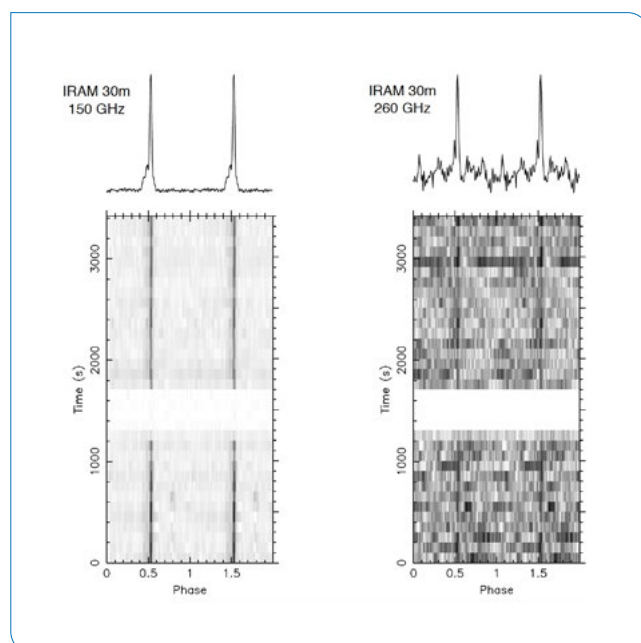
## NIKA2 detects strong pulses in the magnetar XTE J1810-197

Pulsars are fast spinning, highly magnetized neutron stars capable of generating beamed radiation that appears as periodic pulses. While the physical mechanism of pulsar radio emission remains poorly understood, observational evidence suggests that it must be due to some coherent radiation mechanism. Unfortunately, neither the exact mechanism nor its origin is clear. Measuring pulsar emission across the electromagnetic spectrum is thus important for constraining theoretical models, and in this regard the poorly explored window between the radio and optical is of particular relevance.

To investigate whether pulsars can be detected in the mm-wavelength range with kinetic inductance detectors (KID), IRAM researcher Pablo Torne and collaborators, have managed to detect broadband pulsations from the X-ray pulsar XTE J1810-197 using the NIKA2 camera installed at the IRAM 30-meter telescope. XTE J1810-197 was inactive for about three years, but it recently showed pulsar emission again, which shows that the source is highly variable.

According to the researchers, this is the first time a pulsar was detected in the millimeter band using receivers based on KID technology, and the first time that synchrotron pulses were detected from XTE J1810-197 in the millimeter range.

Using the complex readout system, in which signals are sampled at a rate of 23.48 Hz, short radiation pulses were observed at 150 and 260 GHz, the two frequency bands of operation of NIKA2. The extremely high brightness of the single pulses, which was estimated to be  $T_b > 10^{17}$  at 150 GHz, is a strong indication that the emission region is radiating coherently. The authors of the study believe that although the pulses at 260 GHz could not be detected individually despite the high sensitivity of NIKA2, the emission mechanism is likely the same because of the high similarity between the continuum-equivalent flux density and the averaged pulse profile. According to them this result is another step forward in the quest to uncover the pulsar radio emission mechanism.



**Average pulse profiles (*top*) and signal intensities (*bottom*) of the magnetar XTE J1810-197 observed with NIKA2 at 150 GHz (left) and 260 GHz (right). The pulsar orbital period is  $\sim 5.54$  s. Integration time bins are 43 ms on the horizontal axis, 1.7 min on the vertical axis. The white gap corresponds to the time when the telescope was not observing the source.**

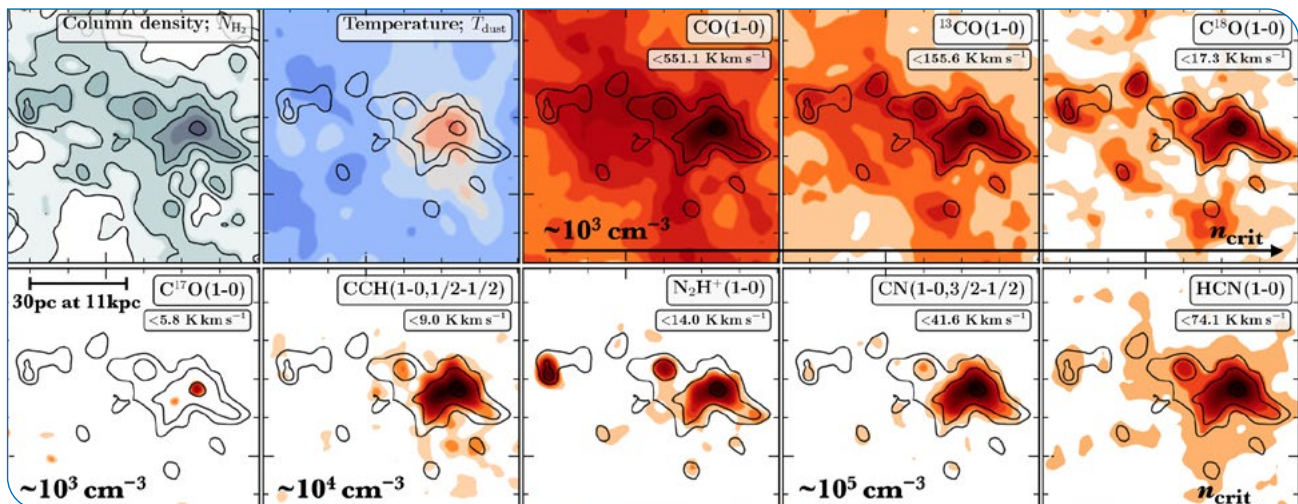
*Work by Torne et al. 2020, A&A, 640, L2*

## A LEGO offspring – a chemical survey of the massive star forming region W49

The process of star formation from dense molecular clouds is still one of the major unsolved problems in astronomy. Many fundamental open questions are still hotly debated, such as understanding the relative balance of turbulence, magnetic field, and gravitational energy, how these properties can be observationally determined, how these properties may vary with the environment, and if they are important for the fraction of dense gas that is eventually converted into stars. Developing a better understanding of the emission properties of dense gas tracers across a broad range of environments is of critical importance to address these questions.

For this purpose, Ashley Barnes (AlfA/Bonn) and collaborators investigated the molecular environment of a  $0.01 \text{ kpc}^2$  region centred on the star-forming region W49, which was observed with the IRAM 30-meter telescope in the frame of the “Line Emission as a Tool for Galaxy Observations” (LEGO) Large Program.

The researchers found that the spatial extent or brightness of the molecular line transitions are not well correlated with their critical densities, highlighting the fact that abundance and optical depth must be considered when estimating line emission characteristics. By exploring how the total emission and line emission vary as a function of the molecular hydrogen column density and dust temperature, they found that there is not a single region of this parameter space responsible for the brightest and most efficiently emitting gas for all species. It turns out for example, that the HCN (1-0) transition shows high emission efficiency at high column densities ( $10^{22} \text{ cm}^2$ ) and moderate temperatures (35 K), whilst for instance  $\text{N}_2\text{H}^+$  emits most efficiently towards lower temperatures ( $10^{22} \text{ cm}^2$  and  $<20 \text{ K}$ ). The authors determine  $X_{\text{CO}(1-0)} \sim 0.3 \text{ } 10^{20} \text{ cm}^{-2} (\text{K km s}^{-1})^{-1}$  and  $\alpha_{\text{HCN}(1-0)} \sim 30 \text{ } M_{\odot} (\text{K km s}^{-1} \text{ pc}^2)^{-1}$ , which both differ significantly from the commonly adopted values. All in all, these results provide new evidence that when interpreting molecular emission, the typical assumptions that CO probes the bulk gas properties in galaxies, while molecular species such as HCN and  $\text{HCO}^+$  potentially characterize the densest gas environment, should be viewed with caution.



IRAM 30-meter telescope maps towards W49 of the integrated intensity of selected molecular gas tracers. The upper left two panels show the column density and dust temperature determined from data obtained with the Herschel Space Observatory. Overlaid on the upper left panels are contours of  $\text{NH}_2$ . All maps are smoothed to  $60''$  and ordered by increasing critical density of the molecular transition.

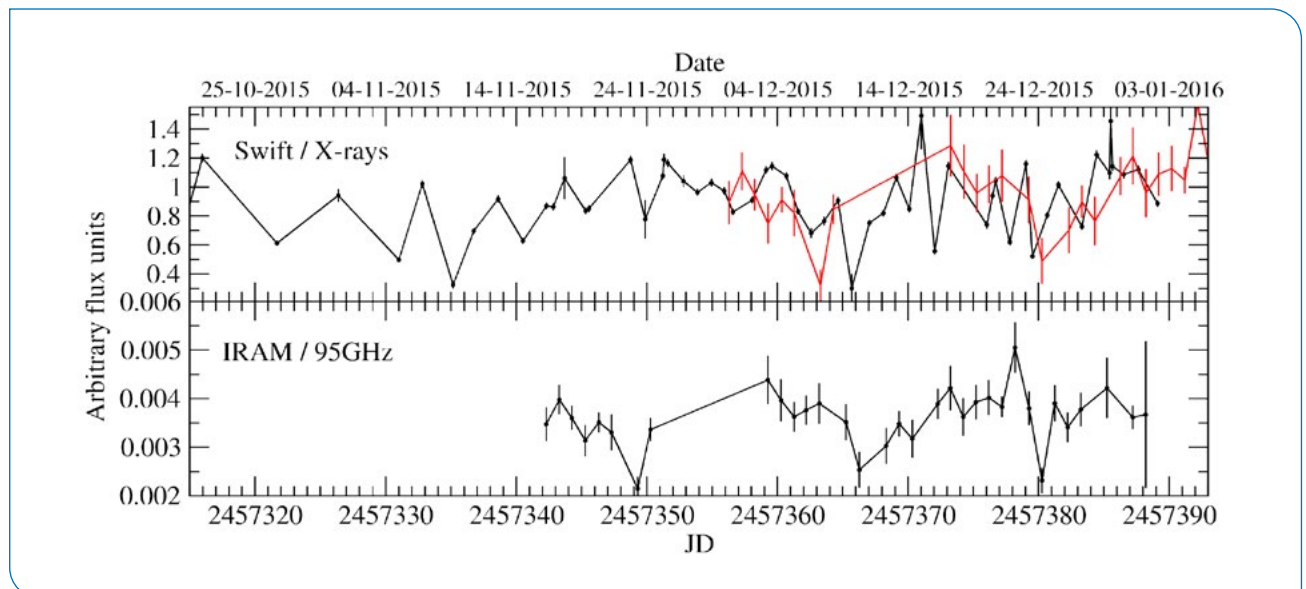
Work by Barnes et al. 2020, MNRAS, 497, 1972

## Coronal activity in the accretion disk of NGC 7469?

Radio-quiet active galactic nuclei (AGN) differ from radio-loud nuclei in that they exhibit emission that is several orders of magnitude fainter. While the high brightness temperature of these sources suggests the presence of hot, non-thermal electrons, the actual physical origin and location of the radio emission source in radio-quiet AGN remains controversial. Current understanding is that the radio emission from radio-quiet AGN may be due to weak jets, nuclear star formation, or even coronal activity on the surface of the accretion disk.

In an effort to improve the understanding of the origin of radio-quiet AGN emission, Ehud Behar (Technion Physics Department/Haifa) and collaborators report on the flux monitoring over several weeks of the Seyfert galaxy NGC 7469 around 95 and 143 GHz with the IRAM 30-meter telescope, and in the optical, UV and X-ray with the Swift, XMM-Newton and WISE observatories. According to the authors it is the first time that light curves were measured simultaneously at millimetre-wave and in X-rays towards this source. While the flux density in both millimetre bands showed changes of about 50% over the 36-day observing period, consistent with the variability observed in previous observing campaigns, the X-ray light curve showed much larger flux variations of up to a factor of 5 over the same period. The high degree of variability in both millimetre bands and in the X-ray suggests that both sources of radiation originate from the same physical component of the AGN, and very likely from the corona of the accretion disk. Indeed, a tentative correlation between the millimetre and X-ray light curves suggests the presence of a ~14-day lag of the X-ray emission. If real, the lag could imply that magnetically heated electrons produce the millimetre waves, and ultimately lose most of their energy by emitting X-rays. Simultaneous monitoring in eight UV/optical bands shows much less variability than in the millimetre bands and X-ray, implying this source of radiation is originating from a different AGN component, likely the accretion disc itself.

More precise millimetre-band measurements of a sample of X-ray-variable AGN are now needed, preferably also on time-scales of less than a day where X-rays vary dramatically, in order to properly test the physical connection between the two bands. Such campaigns require higher sensitivity than that available with the IRAM 30-meter telescope and would possibly make use of facilities such as NOEMA and ALMA.



Light curves of NGC 7469 in X-rays (*top*) and at 95 GHz (*bottom*). A tentative 14-day lag is overlaid in the top panel (*red curve*) that shows the 95 GHz light curve shifted forward by 14 days.

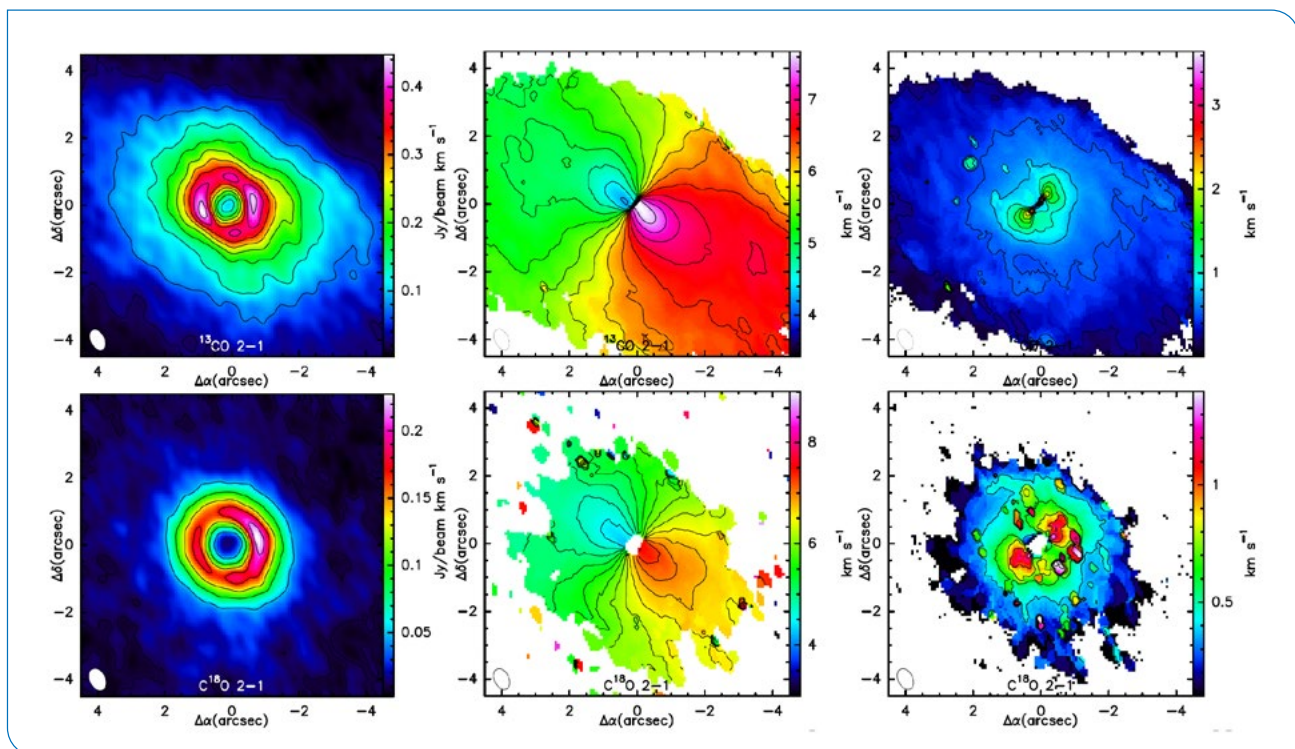
Work by Behar et al. 2020, MNRAS, 491, 3523

## AB Aur, a Rosetta stone for studies of planet formation

Planets are known to form in circumstellar systems of gas and dust called protoplanetary disks, but the exact mechanism leading to planet formation remains unclear. While the gas in these systems is a key factor in the dynamical evolution of the protoplanetary disk, and in particular the dispersion of the gas appears to set the timescale for the formation of giant planets, key parameters such as the gas-to-dust ratio remain largely unknown. Therefore, a thorough characterization of the physical conditions and chemical composition of the gas is of utmost importance for understanding the disk evolution.

In an effort to characterize the gaseous disk around the Herbig Ae star AB Aur, a team of researchers led by Pablo Rivière-Marichalar (OAN/Madrid) performed a thorough spectroscopic study to determine the physical and chemical conditions in the disk using NOEMA. A total of 23 transitions from different species were observed, including  $^{12}\text{CO}$ ,  $^{13}\text{CO}$ ,  $\text{C}^{18}\text{O}$ ,  $^{13}\text{C}^{17}\text{O}$ ,  $\text{p-H}_2\text{CO}$ ,  $\text{SO}$ ,  $\text{SiO}$ ,  $\text{DCO}^+$ ,  $\text{HC}_3\text{N}$ ,  $\text{OCS}$ ,  $\text{CCS}$ ,  $^{13}\text{CN}$ ,  $^{13}\text{CS}$  and  $\text{CO}^+$ . The authors used the integrated intensity maps and stacked spectra to derive reliable estimates of disk temperature and calculated the gas-to-dust ratio throughout the disk by combining the  $^{13}\text{CO}$  and  $\text{C}^{18}\text{O}$  data. Column density maps for the different species were also derived and used to calculate abundance maps. Finally, the observational results were compared with a series of astrochemical models to gain insight into the properties of the disk. The molecules observed show different spatial distributions, and the peaks of the distributions were found to not correlate with the molecules' binding energy. Using  $\text{H}_2\text{CO}$  and  $\text{SO}$  lines, a mean disk temperature of 39 K was derived. The gas-to-dust ratio ranges from 10 to 40 across the disk, and abundance of  $\text{SO}$  ( $2 \cdot 10^{-4}$ ) with respect to  $^{13}\text{CO}$  is found to be almost one order of magnitude larger than the value derived for  $\text{H}_2\text{CO}$  ( $1.6 \cdot 10^{-5}$ ).

The authors of the study thus show that AB Aur hosts a peculiar transition disk characterized by a high gas and dust temperature, a low gas-to-dust ratio, and large sulfur depletion. By determining for the first time the gas temperature and the gas-to-dust ratio across the disk, the researchers provide new information to further constraining hydrodynamical simulations.



NOEMA integrated intensity maps (left), intensity-weighted velocity maps (center) and velocity dispersion maps (right). Species shown are  $^{13}\text{CO}$  (2-1) (top),  $\text{C}^{18}\text{O}$  (2-1) (bottom). The white ellipses in the bottom left corner of each map shows the synthesized beam at each wavelength.

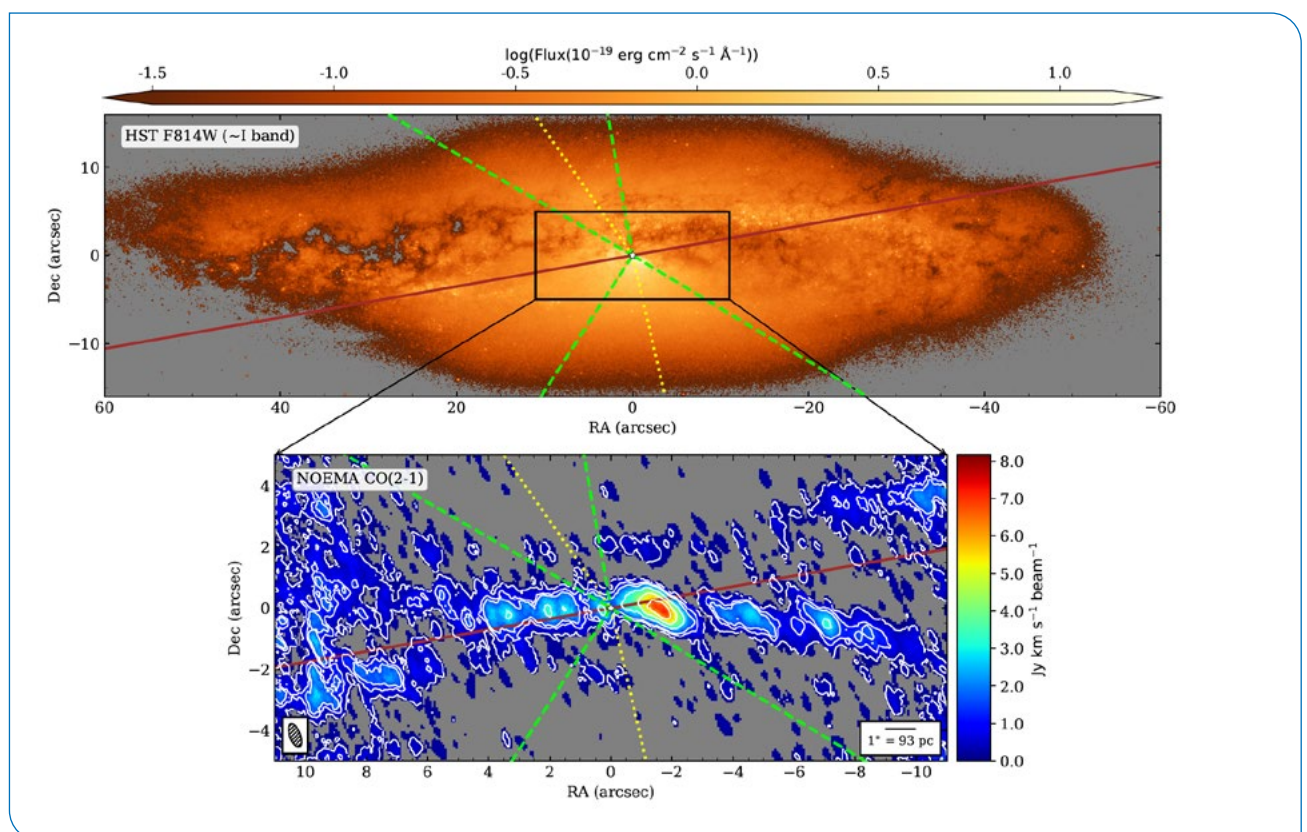
Work by Rivière-Marichalar et al. 2020, A&A, 642, 32

## A search for outflows in the nuclear regions of Seyfert galaxies

Star-AGN coexistence makes galaxies excellent laboratories for the study of stellar and AGN outflows and their feedback. Outflows provide negative feedback when redistributing gas on a large scale in the interstellar and intergalactic environment, but can also provide positive feedback when associated with vigorous star formation. AGN-driven outflows are believed to play an important role in regulating the growth of galaxies, mostly via negative feedback. However, their effects on their hosts are far from clear, especially for low and moderate luminosity Seyfert galaxies.

To investigate this issue, Antonio Domínguez-Fernández (OAN/Madrid and IPARCOS-UCM/Madrid) and collaborators have obtained cold molecular gas observations, traced by the  $^{12}\text{CO}$  (2-1) transition, using the NOEMA interferometer of five nearby Seyfert galaxies. The spatial resolution ( $\sim 30\text{-}100$  pc) and field of view ( $\sim 5000$  pc) of NOEMA allowed the researchers to investigate the CO (2-1) morphology and kinematics from the outer edges of the galaxy disks down to the nuclear regions.

CO (2-1) emission was detected in all five galaxies with disk- or circumnuclear ring like morphologies. Cold molecular gas masses were derived on nuclear (100 pc) and circumnuclear (650 pc) scales in the range from  $10^6$  to  $10^7 M_{\odot}$  and from  $10^7$  to  $10^8 M_{\odot}$ , respectively. It appears that although non-circular motions are also present, most of the gas rotates in the plane of the galaxies. In NGC 4253, NGC 4388 and NGC 7465, the streaming motions are related to the presence of a large-scale bar. In Mrk 1066 and NGC 4388, the non-circular motions in the nuclear regions are explained as outflowing material due to the interaction of the AGN wind with molecular gas in the galaxy disk.



HST/WFC3 I-band image of NGC 4388 (top), NOEMA  $^{12}\text{CO}$  (2-1) integrated intensity map (bottom). The star marks the assumed location of the AGN, which corresponds to the 21-cm continuum peak from VLBI observations. Masked pixels are shown in grey. The green dashed lines represent the edges of the ionization cone and the dashed yellow line the cone axis. The brown solid lines are the position angle of the major axis of the main bars.

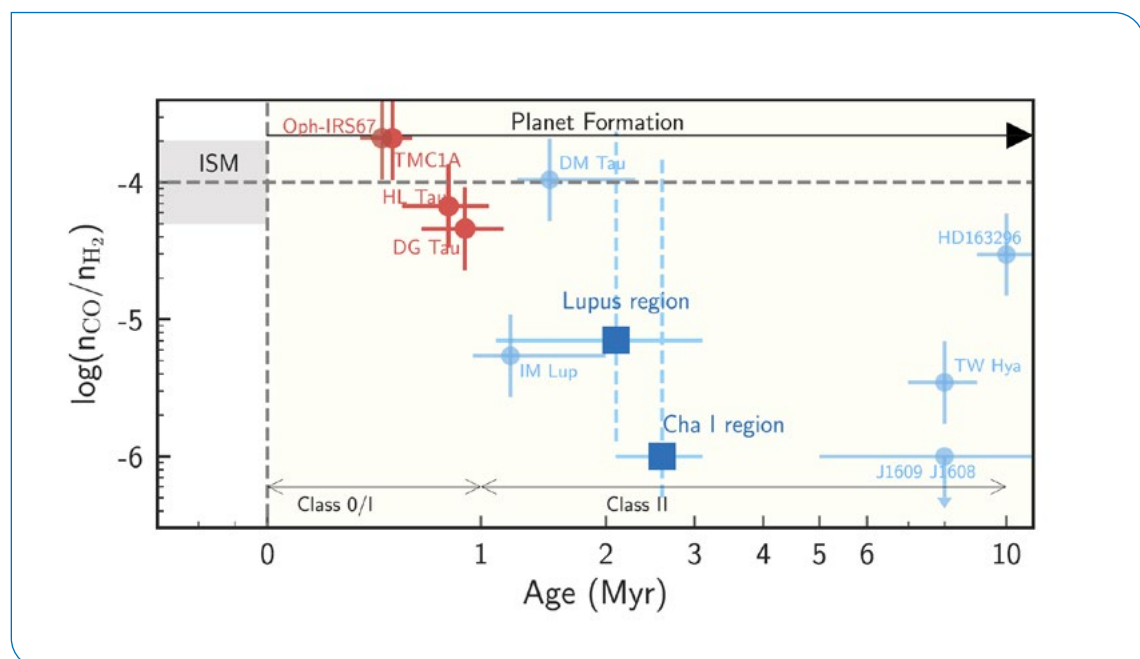
Work by Domínguez-Fernández et al. 2020, A&A, 643, 127



Although the spatial resolution may have an impact on the results achieved, the study clearly shows that it is only in cases of favourable geometry that it will be possible to detect molecular outflows. The authors conclude that the presence of galactic bars, present and past AGN-wind disk interactions, interactions with companion galaxies, and information about the kinematics of the ionized gas are necessary for an unambiguous and accurate interpretation of the kinematics of the cold molecular gas.

### Evolution of volatile CO from the protostellar to the protoplanetary stage

Recent observations show that the CO gas abundance, relative to  $H_2$ , in many 1–10 Myr (Class II) old protoplanetary disks may be heavily depleted by a factor of 10–100 compared to the canonical interstellar medium (ISM) value of  $10^{-4}$ . When and how this depletion happens can significantly affect the compositions of planetesimals and the atmospheres of giant planets. It is therefore important to constrain whether the depletion already occurs at the earliest protostellar disk stage.



CO gas abundance measurements in protostellar and protoplanetary disks. The protostellar disks (<1 Myr) and protoplanetary disks (1–10 Myr) are in red and blue, respectively. The filled circles are for individual disks and the squares for averaged values of star formation regions. The TMC1A, HL Tau, and DG Tau data are from this work.

Work by Zhang et al. 2020, ApJ, 891, L17

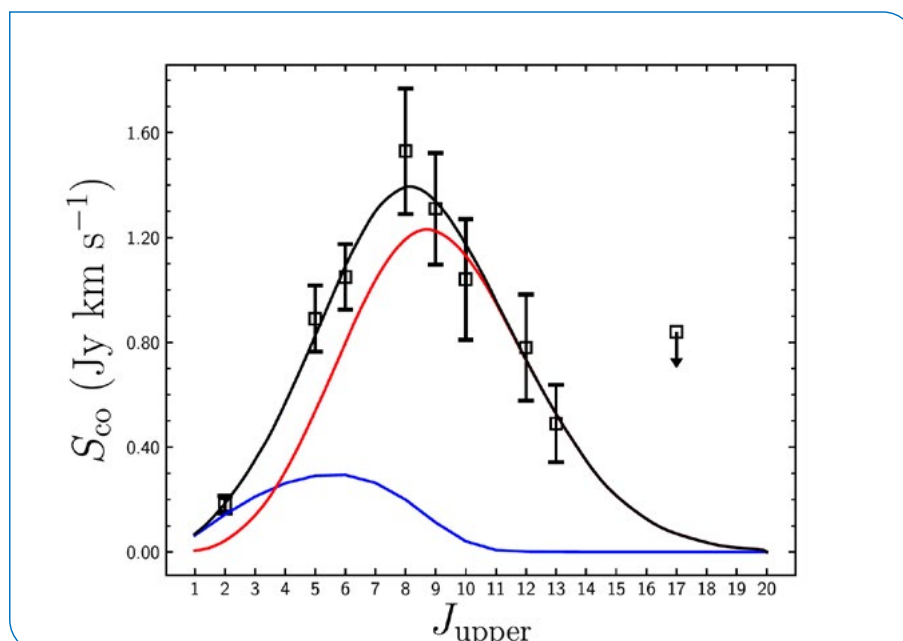
Zhang Ke (University of Michigan/Ann Arbor) and collaborators used NOEMA to obtain spatially resolved observations of  $C^{18}O$ ,  $C^{17}O$  and  $^{13}C^{18}O$   $J=2-1$  lines in three protostellar disks. They show that the  $C^{18}O$  line emits from both the disk and the inner envelope, while the  $C^{17}O$  and  $^{13}C^{18}O$  lines are consistent with a disk origin. The line ratios indicate that both  $C^{18}O$  and  $C^{17}O$  lines are optically thick in the disk region, and only the  $^{13}C^{18}O$  line is optically thin. The line profiles of the  $^{13}C^{18}O$  emissions are best reproduced by Keplerian gaseous disks at similar sizes as their mm-continuum emission suggests small radial separations between the gas and mm-sized grains in these disks, in contrast to the large separation commonly seen in protoplanetary disks. Assuming a gas-to-dust ratio of 100, they find that the CO gas abundances in these protostellar disks are consistent with the ISM abundance within a factor of 2, nearly one order of magnitude higher than the average value of 1–10 Myr

old disks. If these CO abundances are representative of protostellar disks  $< 1$  Myr, then there are two important implications: first, the CO gas depletion seen in Class II disks are results of processes that occurred inside disks rather than the infalling envelopes; second, the process is extremely efficient, as it depletes volatile CO gas by a factor of 10 within 1 Myr. The timescale of the CO depletion process therefore is comparable with the general timescale of planetesimal and planet formation. Whatever mechanisms drive the CO depletion, it can significantly affect the final compositions of planets. These results suggest that there is a fast,  $\sim 1$  Myr, evolution of the abundance of CO gas from the protostellar disk stage to the protoplanetary disk stage.

## Probing the SLED of a quasar-starburst system at $z=6$

Quasars at  $z \sim 6$  are first representatives of the coeval evolution of supermassive black holes (SMBHs) and their host galaxies. A large fraction of these early systems shows host galaxies with dynamical masses of  $10^{10}$ – $10^{11} M_{\odot}$ . The huge amounts of dust and gas they contain are warmed up by massive star formation activity ( $10^2$ – $10^3 M_{\odot}/\text{yr}$ ) and traced by their bright  $^{12}\text{CO}$  emission. Observations of this molecule appear to be crucial to understand the physical and chemical conditions, the kinematics of the multiphase interstellar medium, and to study SMBHs and their host galaxies in the earliest stages of coevolution.

To investigate the molecular environment of a quasar-starburst galaxy at high redshift, a team of researchers led by Jianan Li (Peking University, Beijing) combined NOEMA observations of  $^{12}\text{CO}$  (5–4), (6–5), (12–11), and (13–12) and ALMA observations of  $^{12}\text{CO}$  (8–7), (9–8),  $\text{H}_2\text{O}$  ( $2_{0,2}-1_{1,1}$ ), and  $\text{OH}^+$  ( $1_1-0_1$ ) of the  $z = 6.003$  quasar SDSS J231038.88+185519.7. They constructed the CO spectral line energy distribution (SLED), which they analyzed with the radiative transfer code MOLPOP-CEP. The best-fitting result suggests that two gas components, a warm ( $T_{\text{kin}} = 306$  K) and a cold one ( $T_{\text{kin}} = 50$  K), are necessary to explain the CO spectral distribution. The molecular gas density of the warm (cold) component is estimated to  $\log(n(\text{H}_2)/\text{cm}^{-3}) = 5.25$  (4.20), and the corresponding column density to  $\log(N(\text{CO})/\text{cm}^{-2}) = 15.5$  (18.0). Compared to samples of local ULIRGs, starburst galaxies, and high-redshift submillimeter galaxies, J231038.88+185519.7 exhibits higher CO excitation at  $J \geq 8$ , like other high-redshift quasars. The authors conclude that the high CO excitation, together with the enhanced  $L_{\text{H}_2\text{O}}/L_{\text{IR}}$ ,  $L_{\text{H}_2\text{O}}/L_{\text{CO}}$  and  $L_{\text{OH}^+}/L_{\text{H}_2\text{O}}$  ratios, suggest that besides the UV radiation from young massive stars, other mechanisms such as shocks, cosmic-rays, and X-rays might also be responsible for the heating and ionization of the molecular gas. In the nuclear region any of these mechanisms might be present due to the powerful quasar and the starburst activity.



$^{12}\text{CO}$  SLED of J2310+1855 fitted with a two-component model. The black squares are the CO fluxes measured with NOEMA and ALMA. The CO (5–4), (6–5), (8–7), (9–8), (12–11) and (13–12) data are from this work. The blue and red lines are the best-fitted cold and warm gas components.

Work by Li et al. 2020, *ApJ*, 889, 162

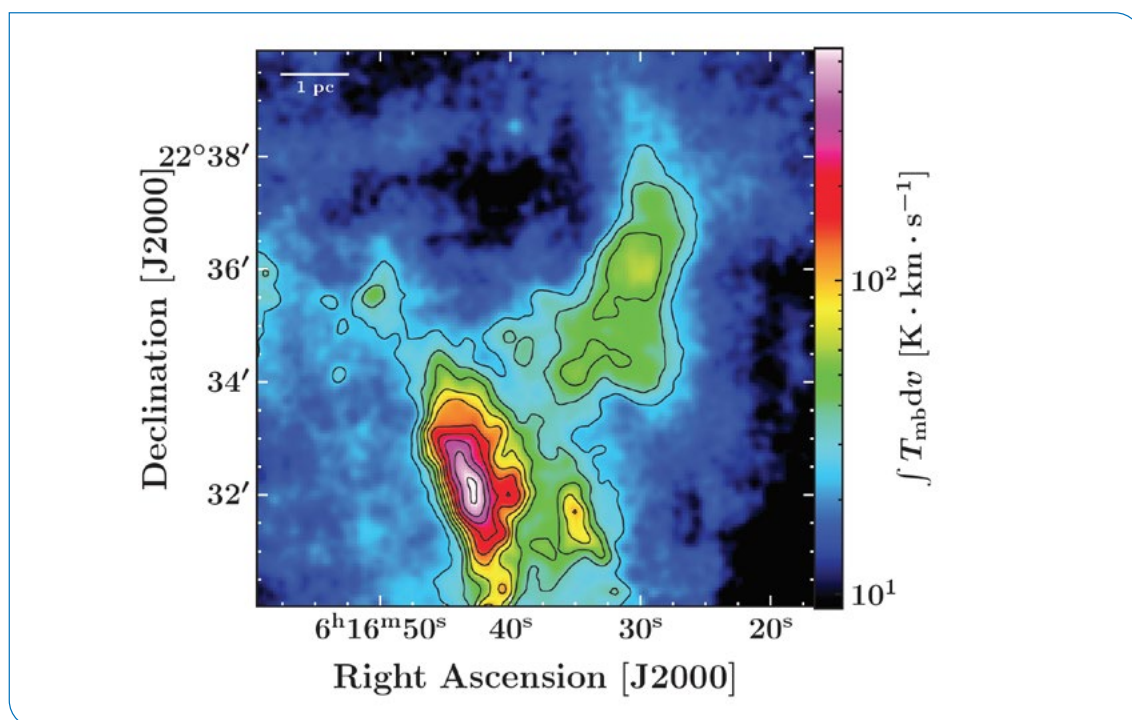
## Interstellar anatomy the G region in the IC443 supernova remnant

Supernova remnants (SNRs) represent a major feedback source from stars in the interstellar medium of galaxies. During the late stages of supernova explosions, shock waves produced by the initial blast modify the chemistry of gas and dust, inject kinetic energy into the surroundings that gradually decays in turbulence and thereby alters star formation characteristics. Cosmic rays (CRs) accelerated in the earlier stages of the explosion and trapped in the shock fronts, interact with the dense medium and can generate strong  $\gamma$ -ray emission.

To characterize the mechanisms of energy injection by an evolved SNR, its effects on local star formation, and identify all possible sources of ongoing acceleration of CRs by the SNR, a group of researchers led by Pierre Dell'Ova (ENS/Paris and Observatoire de Paris) started to investigate the stellar and interstellar contents of IC443, an evolved shell-type SNR at a distance of 1.9 kpc with an estimated age of 30 kyr. The researchers aimed at measuring the mass of the gas and characterize the nature of infrared point sources within the extended G region, which corresponds to the peak of  $\gamma$ -ray emission. The region was mapped with the IRAM 30-meter telescope in  $^{12}\text{CO}$  and  $^{13}\text{CO}$ , and complemented them with  $\text{C}^{18}\text{O}$  observations at the APEX telescope.

The observations reveal four molecular structures: a shocked molecular clump associated with emission lines, a quiescent, dark cloudlet, a narrow ring-like structure, and a shocked knot. Masses of the four structures were estimated to  $\sim 230$ ,  $\sim 90$ ,  $\sim 210$ , and  $\sim 4 M_{\odot}$ , respectively, and a total mass of  $\sim 1100 M_{\odot}$  was estimated throughout the rest of the field of observations. candidates. The results indicate that the shocked clump holds only a fraction of the total molecular mass in the extended G region, which shows that the mass associated with the ring-like structure and the cloudlet cannot be neglected when quantifying the interaction of CRs with the dense local medium.

The team finds 144 protostars in the G region, and concludes that they might provide a fresh source of CRs, which must also be taken into account in the interpretation of the strong  $\gamma$ -ray observations in the region.



Velocity-integrated map of the  $^{12}\text{CO}$  (2–1) observations carried out with the IRAM 30-meter telescope over the extended G region. The colour scale is logarithmic to enhance the dynamic range and emphasize the fainter molecular cloudlet.

Work by Dell'Ova et al. 2020, *A&A*, 644, 64



Credit: Manuel Castillo Fraile



Credit: André Rambaud

# 30-meter telescope



Credit: Stefano Berta & Bilal Ladjelate

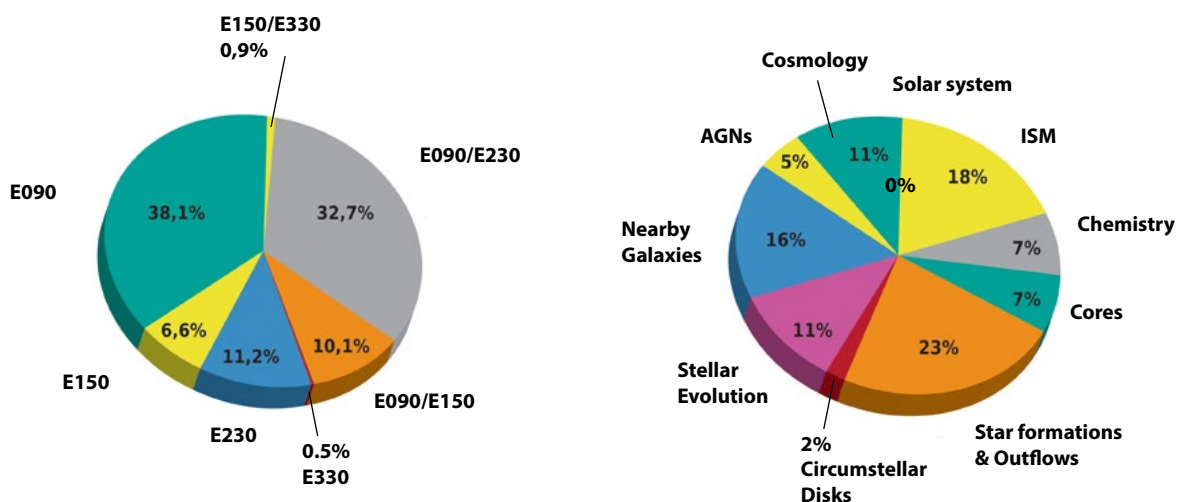
The Covid-19 pandemic has obviously strongly impacted the activity of the 30-meter observatory and Granada offices. The lockdown period and the strict safety measures imposed changes in the work patterns. The Granada premises were kept closed until early May and the staff worked exclusively in home office mode. Since mid-May, the offices started to be intermittently populated with strict protective measures. These measures are still in place early 2021. The attendance was limited to 50% of the nominal staffing. At the telescope site, the work patterns also changed, trying to set the occupancy of the observatory to a strict minimum for safe and efficient operation. The most noticeable change is that on-site visiting observers have no longer been allowed since March 2020 and are replaced by a fully remote visitor mode.

2020 was also marked by some very good news: after a very busy period of preparation, IRAM was eventually able to initiate the long-sought upgrade of the 30-meter telescope, namely the full renewal of the servo control system for the telescope mount, sub-reflector and wobbler by state-of-the-art hardware and software components, and the improvement of the surface of the primary reflector for better efficiency at any elevation and in day and night times. A thorough proposal for EU co-financing through the European Regional Development Funds (ERDF) programme was submitted in the last days of March, 2020 and has been awarded funding in July, for a total amount of 4.8 million Euro. The upgrade project will be hopefully completed by early 2023, ensuring that the 30-meter will be kept on the leading edge of research in the coming years.

## Astronomical projects

Despite the Covid-19, pandemic, science observations at the 30-meter telescope continued almost without interruptions. Only during a short period of a couple of weeks in March/April, the telescope had to be stopped due to the lockdown in Spain. In May, telescope operation fully resumed with no visiting astronomers anymore and most observations done remotely. During the year, a total of 191 projects were observed. This number includes 9 large programs with EMIR or NIKA2, 7 Director's time projects, and 13 VLBI projects. About 21% of these projects were scheduled in pool weeks. The percentage of remote observations increased to 69% averaged over the full year. Galactic topics were addressed by two-thirds of the scheduled projects, while a third of the projects were devoted to nearby galaxies and more distant objects. EMIR was used during almost 81% of the observing hours, while HERA was used for less than 1% of the time, and NIKA2 usage increased to 19%.

During the scheduling year, astronomers could only visit the 30-meter telescope during the first months. In total, only 72 astronomers visited the telescope to support projects, 42 of which came to support the observing pools. Two groups of master students and their tutors visited the telescope to observe short projects as part of their training courses just in time before the lockdown started.



Usage of EMIR bands in 2020.

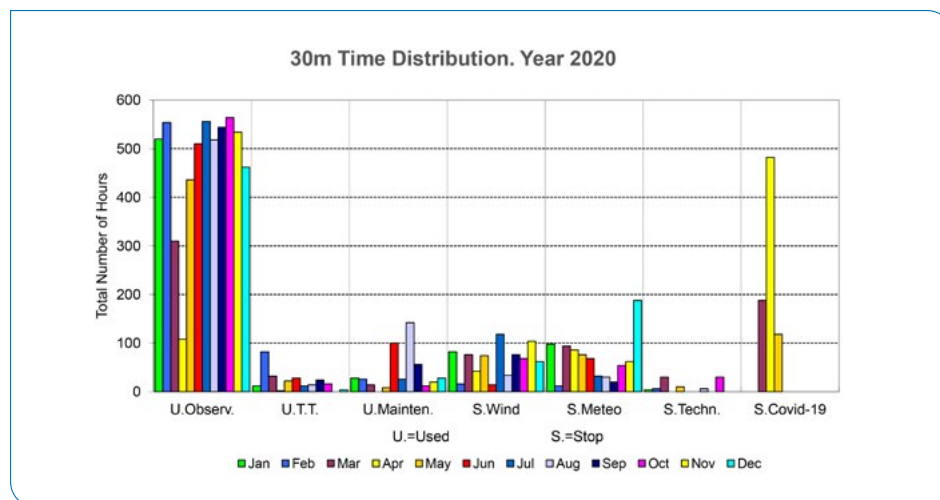
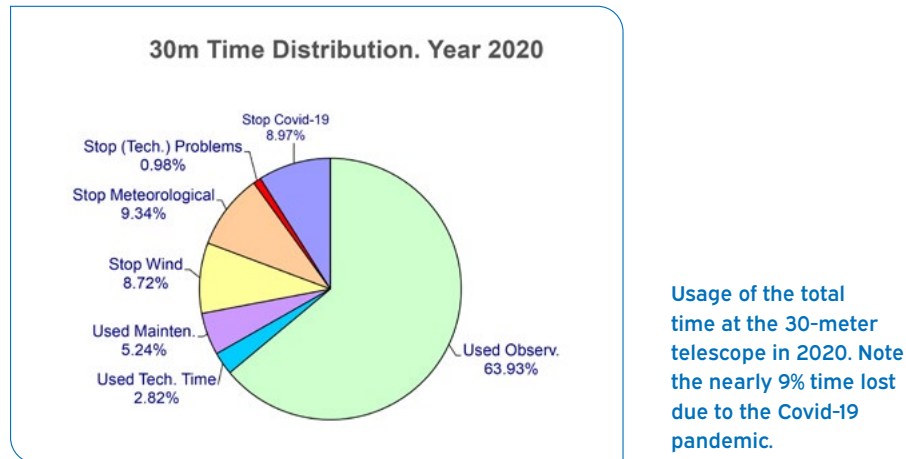
Time distribution of scientific categories observed in 2020.

## Observatory operation

With the start of the first Covid-19 pandemic, on-site personnel at the observatory was been reduced to an absolute minimum, with just one transport per week. The company operating the Sierra Nevada ski resort completely (and suddenly) stopped operations, and the cable-car was no longer operational thereafter. Telescope operations were stopped for 3 weeks and were reduced to 12h night shifts due to the lack of personnel for another 4 weeks. However, since May 12 normal 24h shifts were resumed. All AOD shifts were done remotely until approximately mid-September. The visits of external observers to the observatory were stopped and replaced by the remote visitor mode. When remote visitor observations are not possible (e.g. inexperienced observers), they are carried out in service mode.

In spite of the difficult situation described above, the observing efficiency has been outstanding: around 64% of the total available time was allocated to scientific observations with either EMIR, HERA or NIKA2. The fraction of time lost due to the Covid-19 crisis was nearly 9%, and was partially compensated by the reduction of the time loss due to poor weather conditions (around 18%, versus 23% in 2019). The time fraction spent in maintenance and technical time was around 8% (this includes the telescope stop period due to the replacement of the tower cladding). Finally, the time lost due to technical problems remains extremely low, less than 1%.

In spite of the many restrictions in the activities of contractors imposed by the pandemic, several important refurbishment activities were started or resumed.



Monthly time distribution of observing time, technical projects (T.T.), maintenance, time lost due to weather conditions (wind, snow etc.) and technical problems. Notice the time lost due to Covid-19 in March, April and May.

The most important and visible action was the replacement of the antenna pedestal cladding: the original plates were made of fibre cement with a substantial fraction of asbestos, a material proven to be very toxic. The refurbishment was carried out in two stages: first, the fibre-cement plates were removed taking all safety measures for workers; the wooden frame supporting the old plates and the insulating material were also removed. In a second stage, the new metallic supporting frame and sandwich panels made of steel sheets with rock wool isolation were installed. The new cladding is behaving very well: on the one hand, the day-time

thermal behavior is similar to the original, and on the other, the new cladding shows a good resilience to the impact of ice pieces falling from the upper telescope structure that usually caused breakage of the fragile fibre-cement plates every Winter.

A second important upgrade in the telescope area was the replacement of the air conditioning unit in the room hosting the spectrometers and computers. The old Liebert machine has been replaced by two new Stulz units of enhanced cooling capacity, each one with 22.2 kW frigorific power.



Removal of original fibre-cement plate.



Installation of the new asbestos-free cladding.



The 30-meter telescope with its new facelift.



## Instruments

### Radioelectric protection

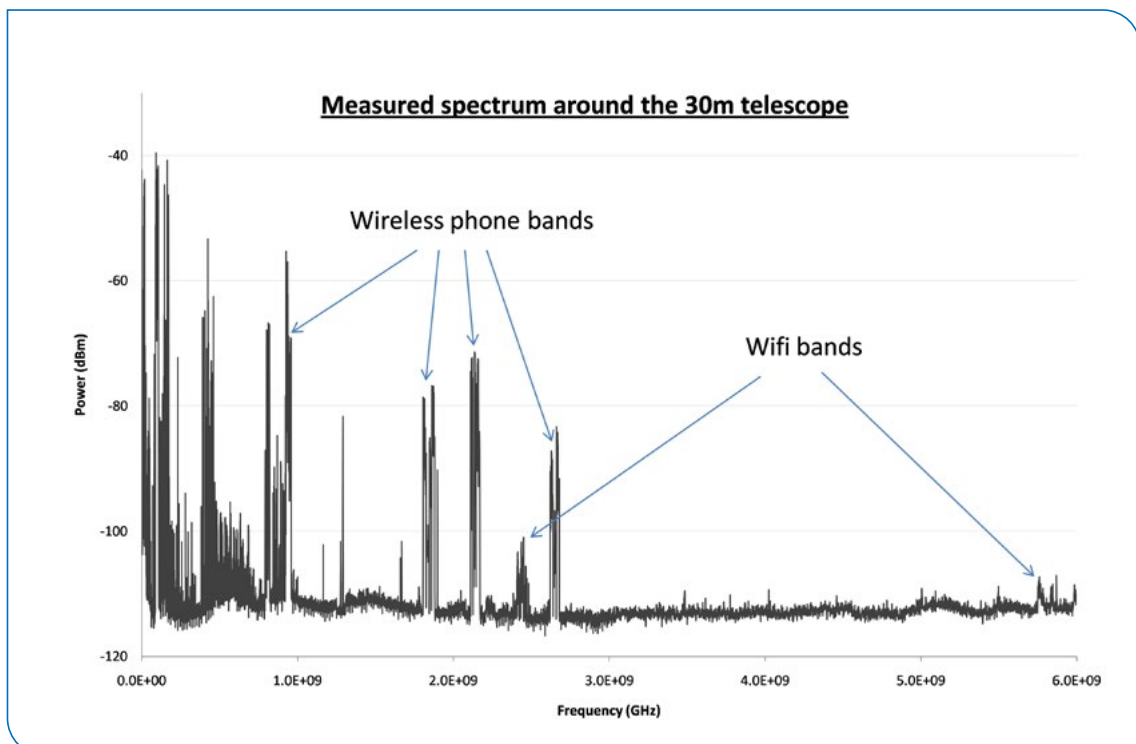
As the car collision radars, mobile phone technology and other wireless applications evolve, the spectrum around the 30-meter telescope is likely to get contaminated by radio-electric interferences. A recent event was the installation of a communication pylon in close proximity of the telescope. The tower, planned to be used as a private communication system for the ski resort, includes several low frequency (<1 GHz) sector antennas and a parabolic dish working over 10GHz. After explaining the risks of EM interference from such transmitters on the observatory operation, these antennas were finally moved to a much further distance from the telescope.



In order to ascertain the situation concerning possible sources of EM interference around the observatory, a survey on the 0 – 20 GHz band was performed. Two very broad band omnidirectional disc-cone antennas, a low-frequency commercial one and a homemade smaller design for the higher bands, were used for the signal acquisition. Despite the high sensitivity of the instrumentation, no signal was detected above 6 GHz.

The data were acquired during the month of June 2020, a very quiet period due to the inactivity of the ski station and the current pandemic situation. The spectrum can thus be considered as very close to the best scenario and used to compare with future RFI surveys.

Setup used for the measurements of radio-frequency interferences in the IF bandwidth of the receivers.



Measured spectrum in the 0-6 GHz frequency range.

## Backend

A significant VESPA maintenance effort was undertaken to ensure its availability for the next few years, fixing mostly the sampler boards whose stock had dwindled down to a critical level. A new version of the firmware and software for the broadband continuum detectors was prepared, which will enable faster sampling for pulsar observations and improved analysis of the power fluctuations of the heterodyne receivers. After validation of the prototype, a set of 6 barycentric references was built. The integration in the system still depends on further work on the interface and control software.

## VLBI

In January 2020, a general EHT dress rehearsal was carried out at 1.3 mm, successfully obtaining fringes in several baselines involving the 30-meter telescope. However, the restrictions derived from the pandemic forced the cancellation of both the EHT (1 mm) and GMVA (3 mm) Spring sessions. Eventually, in October 2020 the global GMVA (3 mm) session took place; fringes were successfully obtained on the baselines joining the 30-meter and the other European telescopes. In December 2020, the first test at 3 mm between the phased-NOEMA (pNOEMA) array, comprising 8 antennas, the IRAM 30-meter and the OAN 40-meter Yebes telescopes took place. Fringes were successfully obtained on all baselines. To ease future VLBI sessions, in particular the increased need for flexibility in their scheduling, an automatic, remote switching between VLBI and normal operations has been fully implemented.

An important recognition was received in February 2020: several IRAM scientists and engineers involved in the production of the first image of the shadow of the supermassive black hole of M87 were awarded by the Andalusian Regional Government (Junta de Andalucía) with the "Bandera de Andalucía 2020" for the province of Granada in the category of Research, Science and Health.

## Computers & software

Regular operations changed dramatically in 2020 because of the Covid-19 pandemic. The IRAM staff switched to home-office, while the 30% fraction of remote observations rapidly increased to, and continues to be, 100%. To adapt to this new situation, the computer group strengthened the remote access infrastructure and logistics for both internal and external users. The OpenVPN server worked and is working exceptionally well. The VoIP system for telephones also allows calls to be answered on a regular computer with the use of commonly available, open-source software. In addition, several video-conference tools were set-up

A number of important improvements were implemented: first, the archive storage system was upgraded (both the master and the copy) increasing its capacity to close to 900 TB of usable space. We are currently at 55% capacity. Second, two critical machines (mrt-lx1 and mrt-lx3) were eventually virtualized allowing for



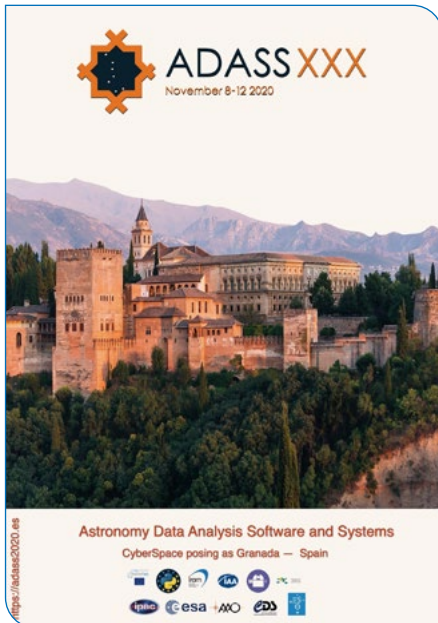
New layout of the telescope operators' (left) and astronomers' (right) working areas.

greater resilience in case of failures and easy rollback of changes. The two virtual machines are currently working flawlessly. The operator and observer workstations were upgraded to faster computers with four 27" screens each in a 2x2 layout .

The Granada data center work was eventually finished. The new data center has almost twice usable space, better electrical installation and cooling, and three racks for servers, communications and storage respectively. The floor was also sealed from the parking space underneath. The second copy of the archive system was relocated to the refurbished Granada data center.

In the area of the operational software, PaKo has been adapted to the GFortran compiler, in order not to depend anymore on the extensive Intel Fortran Compiler. It is hoped this will allow IRAM users to install PaKo more easily at their home institute, in order to test scripts before starting their observing campaigns. The IMBFits for NIKA2 has been further developed to include support for polarization and also for the calibration source. Soon after the observations, the IMBFits are written to the archives in Granada and then mirrored in Grenoble.

A highlight of the year was the organization, as an on-line event, of the ADASS XXX conference. This multi-wavelengths conference focusses on "Astronomy Data Analysis Software and Systems" and gathers every year hundreds of experts in the field. It was a very successful event with almost 600 participants from all over the world and five full days of tutorials talks and BoFs ("birds of a feather", i.e. discussion groups). All contributions were recorded and are available online.



## Facilities

An important highlight regarding the improvement of life conditions at the observatory was the installation of a new digital TV system, available in each and every bedroom. Spanish, but also French, English, and German channels are now available to all residents and visitors, making their stay more enjoyable.

Work was also performed to improve the security at entrances of the telescope and main building: electromagnetic locks and video-intercoms at the entrances have been installed. This responds to the evolving situation: since the inauguration of the 30-meter telescope, the access to its premises is much easier through the road or ski station, hence increasing the risk of intrusion.



The IRAM 30-meter cooks' team attended a course of vegetarian cooking.



# NOEMA



Credit: Patrick Grillet

The highlight this year was the addition of the 11<sup>th</sup> antenna to the NOEMA array. First fringes were observed with Antenna 11 on August 19, and after a successful science commissioning phase, NOEMA started regular science observations with all eleven antennas. In parallel, the observatory continued to be engaged in the next milestones: the transformation of NOEMA into a very-long-baseline interferometry (VLBI) station, and the assembly of Antenna 12. While work on these projects progressed relatively well, their schedule could not be fully met in 2020 due to the Covid-19 pandemic.

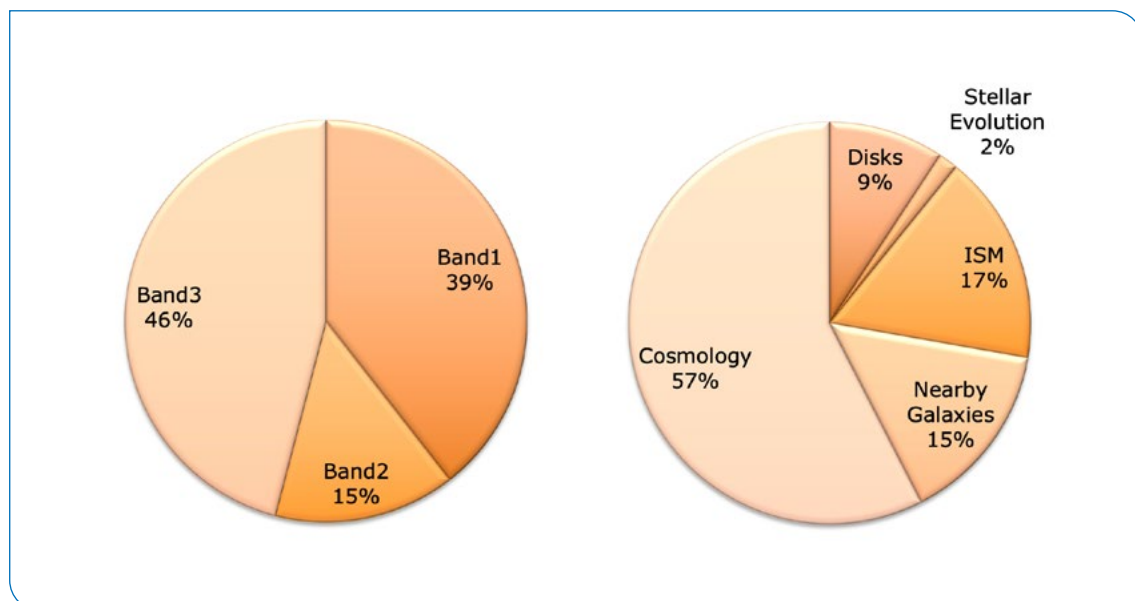
As in previous years, the NOEMA observatory continued its efficient operation, characterized by a high availability of antennas and instruments and a low technical downtime. The antennas, receivers and the correlator all performed well throughout the year. The combination of high system reliability and structured organization of work at the observatory helped to keep the scientific productivity at the highest level. To take advantage of the best weather periods and the most extended configuration (A) of NOEMA, technical activities were kept to the strict minimum during the winter period. All scientific observations were performed in service observation mode only.

To fully exploit the winter conditions at the beginning of the year, the interferometer reached its most extended configuration (A) at the end of January, operating with all ten available antennas. The antennas

were moved into the intermediate configuration (C) at the end of February and into the most compact configuration (D) in early April. Despite the complicated lockdown situation in spring, the observatory continued to observe, and thanks to exceptionally good weather conditions, even obtained a significantly higher scientific yield (by 14%) in the March-May period than in the two previous years over the same period. Despite difficult Covid-19 related working conditions, the NOEMA observatory was able to deliver Antenna 11, retrofit three first-generation antennas, perform the annual maintenance on the NOEMA antennas, pursue commissioning activities, and maintain full scientific productivity with the 10-antenna NOEMA array through the end of the summer semester. By the end of November, NOEMA was ready to start regular astronomical observations and to enter the winter semester 2020/2021 with all eleven antennas.

The program committee met twice during the year, around four weeks after the deadlines for the submission of proposals. It reviewed 219 regular proposals and recommended 142 of them (15% more than 2019). Over the year, NOEMA also received and accepted 7 Director's Discretionary Time (DDT) proposals. Including the backlog of projects from 2019, science goals from 115 proposals were scheduled in 2020 at the NOEMA observatory, including science from 2 Large Programs, 5 Max-Planck-IRAM Observatory Programs (MIOP), and 10 DDT proposals. This corresponds to 291 individual sub-projects (same number as in 2019) that received time on the interferometer.

As in previous years, NOEMA continued to provide unique and exciting scientific results and to demonstrate its effectiveness at exploring the interstellar medium in our Galaxy and in the high-redshift universe. As in previous years, the observing time requested to carry out galactic research was less than the time requested for extragalactic science. This testifies to the enduring and widespread interest of the extragalactic community, which has been persistently growing over the past years. The largest amount of observing time was invested in the compact and intermediate configurations of the interferometer between spring and autumn. The percentage of observing time invested in 2020 on science programs for the user community was on average 49% of the total time, or equivalently, 178 days. An additional 17% were invested on technical operations and developments: software work, commissioning, technical verifications and installation of new equipment (11%), array reconfigurations (4%), and receiver tunings for user projects (2%). The remaining 34% were lost due to weather constraints.



Requested observing time by receiver band and science category.

## Ongoing work and activities



Science observations with Antenna 11.

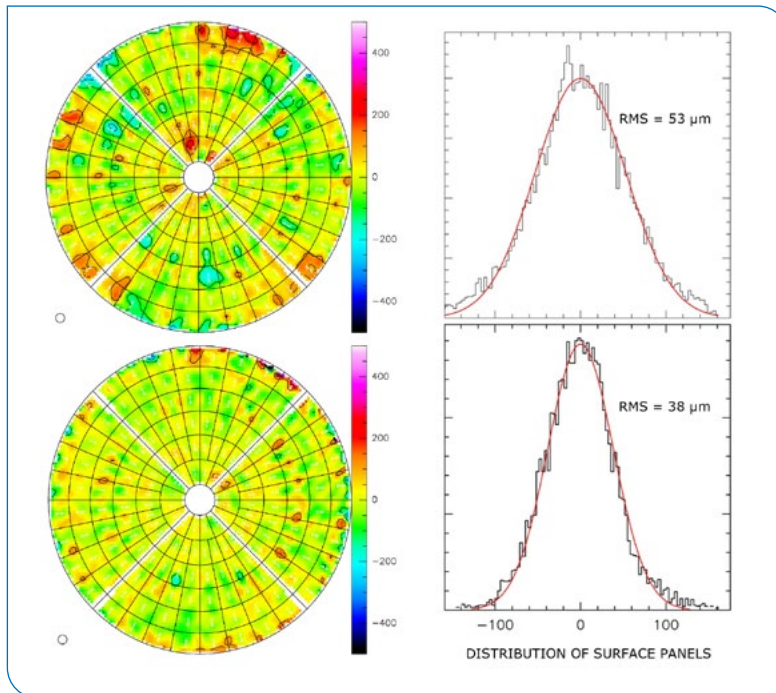
### **Antenna 11 commissioning**

The integration of Antenna 11 into the NOEMA array was the most significant event and among the most exciting activities of the commissioning and science operations (NCSO) team in 2020. The start of the NCSO phase of Antenna 11 began on August 17, 2020, with the delivery of the antenna to the commissioning team. The goal of the NCSO was to take the antenna from the stage reached at the end of construction to an instrument that meets scientific requirements. This stage, which is aimed at checking that all parameters are within the specifications, provides first quantitative information on the antenna performance in terms of sensitivity, image quality and accuracy. To achieve this objective, the NCSO team worked in close collaboration with the computing, engineering and construction teams, and used specific test procedures already applied to the previous antennas. The commissioning activities included antenna safety checks, pointing, focus and tracking accuracy verifications, improvements of the surface accuracy using phase-coherent holography, and the assessment of a number of key performance indicators such as the antenna interferometric efficiency. First results from the NCSO of Antenna 11 helped to improve operational reliability and to identify areas where further work had to be done. For instance, due to an error in the manufacturing process, the panels of rings 1 to 4 were found not to fully meet the specifications and will have to be replaced in 2021. Ultimately, after the successful commissioning campaign, which demonstrated NOEMA's once again increased performance, Antenna 11 joined the array and began routine scientific operations.

### **Antenna upgrade project**

The antenna upgrade project is aimed at bringing first generation antennas (1-6) to the same technological and operational standard as the new NOEMA antennas (7-12). In the frame of this project, another important milestone was achieved in the fall of 2020 with the completion of the electro-technical refurbishment phase on Antennas 2, 3 and 6. To ensure that technical modifications were in line with science requirements, the NCSO team ran a series of test procedures. At the end of November, the antennas were declared technically ready for science operations and made available for routine science observations. Work on the retrofitting of the remaining first-generation antennas will continue in 2021.

As in previous years, the surface quality of all antennas was verified by means of holographic measurements and readjusted during the maintenance period, and iteratively improved when deemed necessary. All in all, the primary surfaces of all six antennas show excellent stability and a median accuracy of  $36\mu\text{m}$  RMS.



Surface panel distributions of Antenna 11 relative to the ideal paraboloidal surface (*left*) and associated surface RMS (*right*). On the top, holographic results of the antenna surface after delivery to astronomical commissioning; on the bottom, improved antenna surface after three iterations of panel adjustments.

### Commissioning of the 14-channel radiometer

After the initial testing period in 2019, the new generation 14-channel radiometer underwent an optimization phase in the Grenoble frontend laboratory and was then installed again on Antenna 8. In particular, internal temperature stability and homogeneity were significantly improved and the load table mechanism was revised. The radiometer was integrated into the real-time observing and data recording system, and has been correcting the atmospheric phase turbulence on the baselines of Antenna 8 since December 2020. Although the radiometer is currently operating in an emulation mode that uses only 4 of its 14 channels, its performance is already comparable to the best first-generation radiometers. Work was underway at the end of the year to use the data from all 14 channels for even more sensitive atmospheric phase corrections. Current plans are to equip two more antennas with a 14-channel radiometer by the end of 2021, and to have all antennas equipped with a radiometer in 2022.

### Large IF bandwidth observing mode

As part of the development of new observing modes for NOEMA, the feasibility of covering frequency ranges larger than the IF bandwidth by cyclically switching between two LO frequencies separated by 7.744 GHz was investigated. Such mode would offer the possibility of performing spectral scans over contiguous bandwidths of 32 GHz, under practically identical observing conditions. First very promising tests conducted in late 2020 with a subset of antennas have shown that switching LO tunings between two selected frequencies shows repeatable and stable performance within specifications. Should further investigations in 2021 validate the feasibility and efficiency of the observing mode, first science demonstration observations could then be conducted during the year.

### User support

The NOEMA Science Operations Group (SOG) has been largely successful in meeting the goals and overcoming the organizational and technical development challenges in the NOEMA project despite the constraints of the pandemic.

The central mission of the SOG is to ensure that the NOEMA Observatory provides users with the means to conduct state-of-the-art research. The SOG astronomers work towards optimizing the scientific performance,

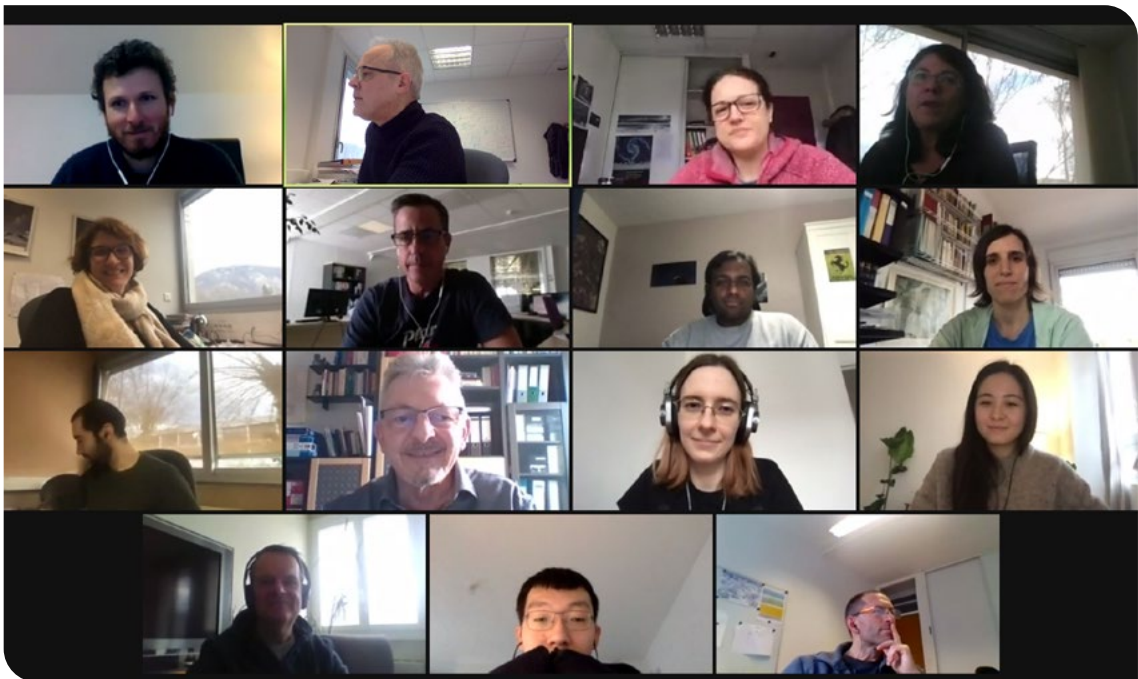


efficiency and return of the interferometer, either on site or remotely from the Grenoble headquarters. They provide technical support and expertise on NOEMA to researchers and visiting astronomers who have questions about the instruments, observing procedures, data reduction and calibration, pipeline data processing, and archiving of NOEMA data. Providing the best science data is at the core of the SOG mission.

Internally, the SOG interacts with the scientific software group on developments that may impact the long-term future of the interferometer, performs the technical review of scientific proposals, works with the technical groups to ensure that operational requirements are met, keeps user documentation up to date, and performs operational testing and commissioning tasks. Among the most important activities in 2020 were the commissioning of Antenna 11, performance assessments of the retrofitted first-generation antennas, of the 14-channel prototype water vapor radiometer installed on Antenna 8, and of the dual-band receiver installed on Antenna 9, and support for two VLBI test campaigns.

In normal times, IRAM headquarters hosts a regular stream of visiting astronomers from around the world who stay at the institute for periods ranging from a few days to a few months.

Starting March 2020, advice and assistance to calibrate and analyze 56 NOEMA projects remotely from their home institutes were provided to 63 astronomers from Europe and overseas for a total of 326 days. Prior to the lockdown period, face-to-face assistance was also given to 8 investigators visiting IRAM Grenoble. In total, the SOG invested 357 days (27% more compared to 2019) to reduce and analyze data from the interferometer. 63 science projects received support and advice. Compared to previous years and as a result of the global Covid-19 measures, the overall level of remote user support increased drastically. IRAM astronomers have been leading or collaborating on 50 projects in which they were directly involved. Given the increasing demands for support and supervision of external investigators, the computer system and network infrastructure at IRAM headquarters were reorganized to provide full computing power to individual users when necessary.



Members of the NOEMA Science Operations Group (SOG) at a Zoom meeting.

## Data Archive

The data headers of observations carried out with the NOEMA and the former Plateau de Bure Interferometer are archived at the Centre de Données astronomiques de Strasbourg (CDS), and are available for viewing via the CDS search tools. In 2020, the archive contained coordinates, on-source integration time, frequencies, observing modes, array configurations, project identification codes, etc. for observations carried out in the period from December 1991 to September 2019. The archive is updated at the CDS every 6 months (May and October) and with a delay of 12 months from the end of a scheduling semester in which a project was observed in order to keep some of the information confidential until that time.

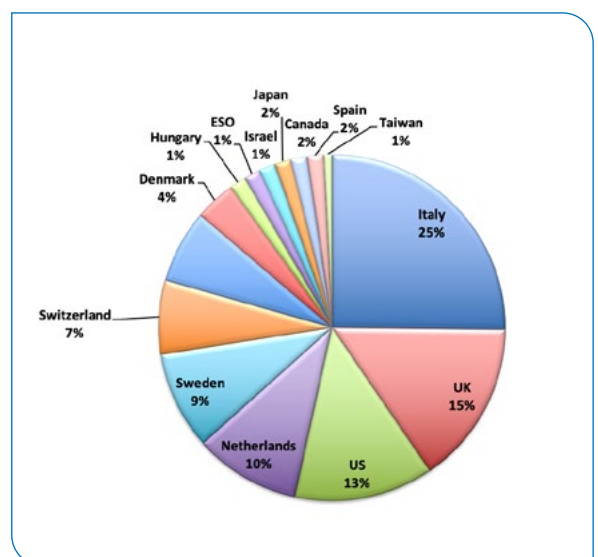
Access to the science data is initially limited to the principal investigators of the observing programs and their delegates. While the proprietary period of Large Programs is set to end 18 months after the end of the last scheduling semester in which the program was observed, the proprietary period of science data from standard NOEMA observing programs is set to terminate 36 months after the end of the last scheduling semester.

The IRAM Data Archive is the collection point for research carried out at the IRAM observatories in the framework of a Large Program and of regular science projects. The goal is to provide open access to calibrated images, data cubes, and visibility data from NOEMA, the former Plateau de Bure interferometer, and the 30-meter telescope. During the last year we have received more and more requests for data from the archives, and as we expect this number to grow in the coming years, developments are planned to facilitate access to the archives via the web in the future.

The science-ready products of Large Programs are made available to the astronomical community at the end of the regular data proprietary period. The archive is the result of a joint effort between IRAM, the principal investigators of the Large Programs and their collaborators.

## Radionet transnational access

The interest of the European community in using the NOEMA facility has remained high during the 2017 to 2020 period covered by the Horizon 2020 initiative. NOEMA received more than 800 observing proposals from more than 1500 unique users originating from 45 countries. In the same period, NOEMA counted over 300 RadioNet eligible proposals submitted by researchers affiliated to scientific institutions from 10 European countries (IT, IE, UK, SE, CH, NL, DK, HU, DE, ES), one intergovernmental organization (ESO) and 4 non-European countries (TW, US, JP, CA) and organizations. Observing time was granted to 68 RadioNet eligible proposals. The observing capabilities offered to RadioNet eligible groups benefitted more than 130 researchers with a well-balanced distribution between senior scientists (66%) and younger PhD students and post-doctoral researchers (34%), and with an increasingly balanced distribution between female (44%) and male scientists (56%). Seven eligible teams benefited from financial support of their travel costs to visit IRAM headquarters in Grenoble and reduce their data with the help of IRAM experts. Despite the fact that RadioNet has come to an end in 2020, this successful Europe-wide initiative will continue in the coming years under the Opticon-RadioNet Pilot (ORP) program, still within the Horizon 2020 research framework program.



RadioNet PI User Distribution, 2017-2020.

## VLBI

NOEMA participated in the Event Horizon Telescope (EHT) dress rehearsal on January 23 and 24, 2020, operating in single dish mode. However due to the Covid-19 pandemic and its impact on the EHT operations around the world, the EHT session scheduled for March-April 2020 was cancelled. As a result, NOEMA also did not participate in the Global Millimeter VLBI Array (GMVA) spring campaign. First 3 mm VLBI observations, which validated the full phased capabilities of the interferometer, were successfully performed in December together with the IRAM 30-meter telescope and the Yebes 40-meter telescope. While the fringe analysis by MPIfR Bonn indicated that work remained to be done to cope with long observing sessions, the December test demonstrated the excellent sensitivity of the phased NOEMA array for upcoming VLBI observing campaigns.

Compared to the previous phased array mode that was dismantled in 2017 with the arrival of PolyFiX, progress is considerable: where the old system worked for a maximum of 6 phased antennas with a maximum data rate of 1 GB/sec corresponding to a maximum bandwidth of 256 MHz on the sky, the present system is ready for 64 GB/s data rates and 12 phased antennas, with the possibility to go to 128 GB/s if the recording capabilities are upgraded. The new active beamformer allows to optimize the antenna phasing in real-time, improving efficiency over all observed bands.

While further tests with the interferometer are still planned in 2021, NOEMA is expected to participate in the spring 2021 science observing campaigns. NOEMA will join the IRAM 30-meter telescope as key elements of the EHT and GMVA networks and strengthen the role of European observatories in these global networks.



**VLBI Mark 6 recorders  
installed at NOEMA.**

## Observatory operations

Following the outbreak of Covid-19 in France and the lockdown imposed mid-March, the activity of the NOEMA observatory has been deeply impacted, but has not stopped.

At first, a strict protocol was put in place where only the 3 teams operating the instrument (7 persons) were allowed on site. These 3 teams took turns to ensure the site and instrument security, and operate the observatory in a nominal way until the end of April. Science observations were not stopped. During that period, other NOEMA staff members have worked in home-office or on tasks to be carried out off-site.

Taking advantage of this period, a sanitary protocol was designed to allow as many activities as possible to be carried out on the site. These rules were implemented at the beginning of May, allowing to resume the construction of the antennas and the maintenance operations, in addition to the science observation activities.

It was however decided to strictly limit or postpone any other activity which was not essential to the good operation of the site.

## Maintenance, construction and retrofit of antennas

For the eighth consecutive year, maintenance was carried out simultaneously with the construction of new NOEMA antennas. However, and contrary to previous years, in order to accelerate the delivery of the last antennas, the assembly of Antenna 12 started while Antenna 11 was still under construction in the hall, which had the direct consequence of occupying the whole maintenance & construction hall. Hence, the maintenance

of the antennas in operation was not possible in the hall until Antenna 11 was moved outside on August 10 for its commissioning.

Due to these organizational constraints, only the first-generation antennas (Antennas 1 to 6) were maintained in the hall, from mid-August until early December. Antennas 7 to 10 have been inspected outside, and the most urgent corrective maintenance operations have been performed on-site.

In parallel to the usual maintenance operations, the upgrade of the azimuth and elevation drive systems, which started the previous year on Antenna 1, was successfully continued on Antennas 2, 3 and 6. Each of these operations required 4 weeks of work, carried out in parallel with the usual maintenance operations in order to minimize the impact on the schedule.

The construction of Antenna 12, the last antenna in the frame of the NOEMA project, was on schedule at the end of 2020. It is planned that it will be available for scientific observations in the winter semester 2021/2022.



Construction  
of Antennas 11 and 12.

## Site Maintenance

Among the tasks achieved despite the constraints imposed by the Covid pandemic are important maintenance works on the cable-car. One of the 43-tons carrying rope was successfully replaced, and the old cable was cut into a dozen sections before being removed. During this shutdown phase, the carriage and the suspension of the passenger cabin were sent for maintenance, thus bringing forward by a few months the regular date of their inspection.

All these operations were carried out according to a rigorous schedule and the cable-car could be put back into service after only a few weeks stop.



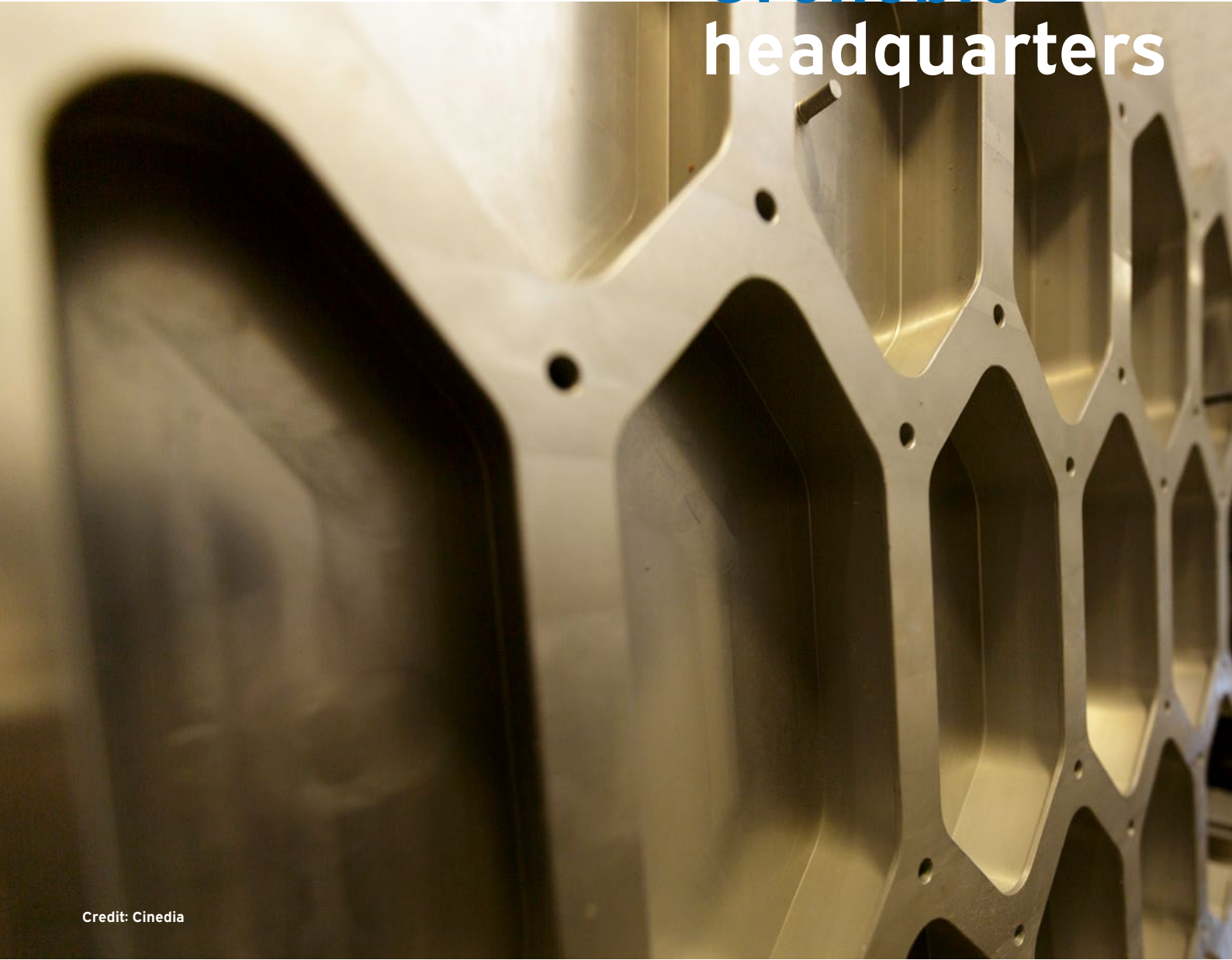
Transport of the new track rope by exceptional convoy.



Section of the old cable composed of numerous strands.



# Grenoble headquarters



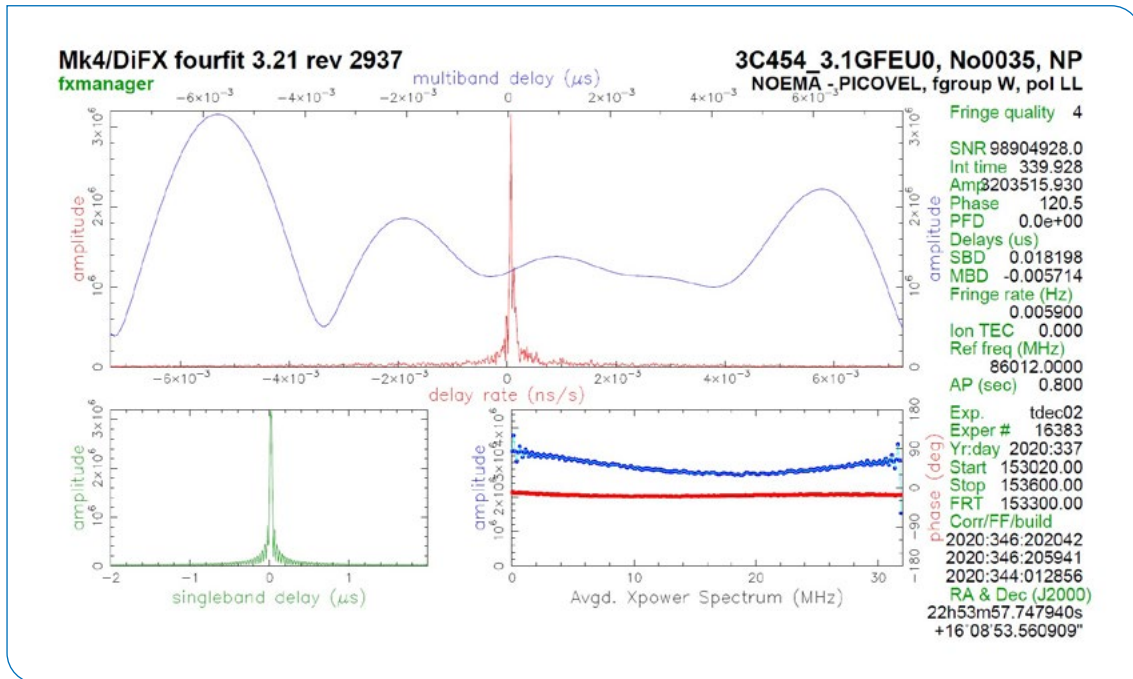
Credit: Cinedia

## BACKEND GROUP

### NOEMA phasing project

Work on the VLBI observing mode has been pursued during 2020. Early January, a new master synthesizer with an improved phase noise has been installed in view of the 2020 EHT dress rehearsal and spring observing session (finally canceled due to the pandemic situation).

Then, by fall 2020, the development of the VDIF formatter board has been resumed to correct for some minor flaws in the hardware. Also, the firmware in charge of encapsulating the beamformer data into VLBI standard digital frames (for transmission to the Mark6 recorders) has undergone extensive testing in collaboration with the MPIfR VLBI technology division.



First NOEMA Fringes in Phased-Array  
mode on 02 Dec. 2020.

Despite some remaining but non-blocking issues in the firmware, it was decided to run a test in phased-array mode by early December (4GHz 1SB Dual Polarization). With participation of the IRAM 30-meter telescope, fringes at 3 mm at a 32 Gbps recording rate were successfully obtained for the very first time with NOEMA/PolyFIX with 8 active antennas in the phased array. This validated several parts of the VLBI setup, including the real-time control of the beamformer associated with the phase solver software.

Following this milestone, the fabrication of a new batch of VDIF formatter boards has been launched to complete the frequency coverage as required by the EHT frequency plan. Thus, support of the full EHT configuration (4GHz 2SB Dual polarization @64 Gbps) is expected to take place in 2021.

## Antenna reference transmission over fiber

Following the lessons learned from the 2019 test campaign, additional hardware and software tools have been developed in order to acquire data with a more convenient and reliable test setup. New on-site measurements of the LOREFoF (LO Reference over Fiber) subsystem were then able to take place during spring 2020.

Loopback tests in a very distant station with the current coaxial cables or with fibers have shown a similar phase drift on short time scales but significant differences over long time scales. This is in coherence with the higher temperature sensitivity of fibers that was characterized last year. Sensitivity of the LOREFoF demonstrator module to EMI has also been highlighted during the tests, especially regarding spurious magnetic fields likely radiated by power-supplies.

With these findings in mind, a first prototype has been developed with the goal of an installation in the limited space available within the receiver cabin to perform in-antenna tests in a configuration as close as possible to the final configuration.





The Test of Reference over Fiber subsystem.

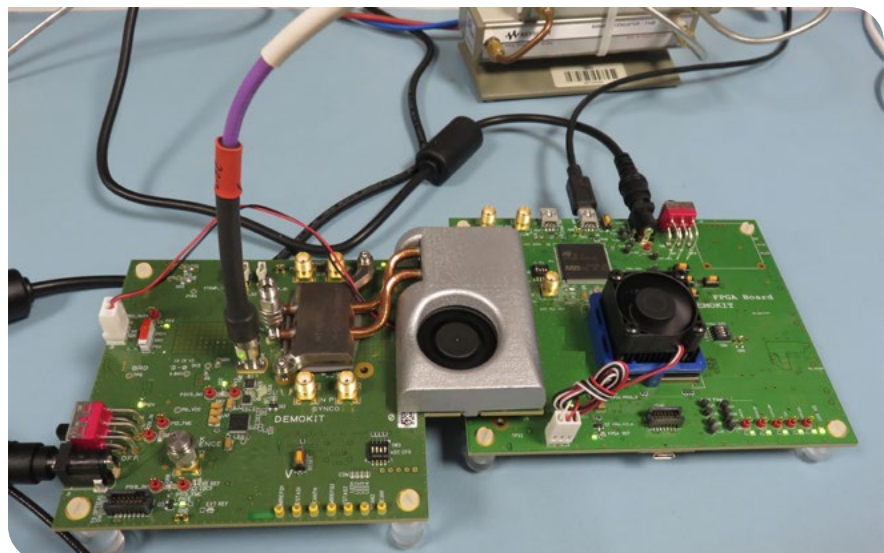
## Digital correlators

Additional digitizer cards have been installed in PolyFiX to support the 11<sup>th</sup> antenna delivered in September 2020. In parallel, work on the second correlator PolyFiX-2 has continued, to prepare for the arrival of the dual-band receivers system. Procurement of some critical components has continued. For instance, a new batch of optical links has been ordered to get rid of the fluctuating manufacturing delays usually encountered on this kind of specific products. At the same time, the correlator boards for PolyFiX-2 have been fabricated. Test of the cards has been started and will extend throughout next year.

## Evaluation of very wide bandwidth A/D converters

The next multi-beam receivers currently under development will generate a so far never offered bandwidth. Processing the numerous IF bandwidth implies direct digitization in the receiver cabin. In collaboration with a leading company in A/D converters, some measurements have been performed on a preliminary prototype ADC chip which should be able to digitize at least a 4 to 12GHz instantaneous bandwidth.

Very promising performances have been measured, validating the ADC selected architecture. A design iteration is foreseen to match the high level of integration required from the chip level up to the boards and system levels.



Measurements on an Ultra-Wideband ADC Demo Kit.

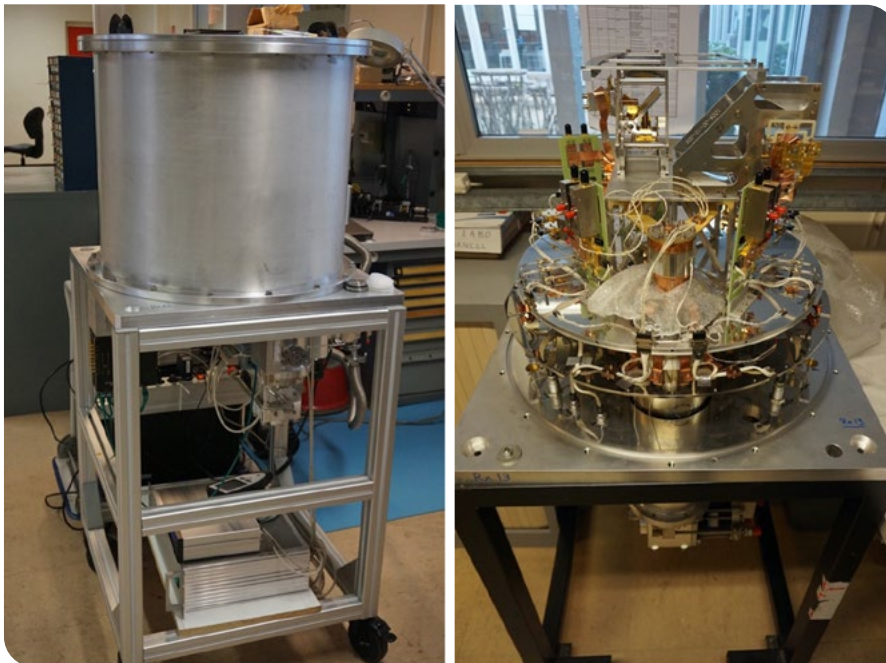
## FRONTEND GROUP

### NOEMA operation and maintenance

The NOEMA receivers and cryocooler systems could not be properly serviced during the maintenance of 2020, due to the Covid-19 impact and restrictions on operations. It is planned to recover this delay during the upcoming maintenance of 2021. Similarly, almost all of the planned upgrades could not be performed and should take place normally in 2021.

### NOEMA receivers

In 2020, the last receiver for the NOEMA 12<sup>th</sup> antenna was assembled, together with an additional spare receiver (Rx13) for the Grenoble facilities, allowing an operational receiver to be always available in the IRAM laboratory facilities for testing upgrades .



**The two final NOEMA receivers. Left: Receiver for the antenna 12. Right: spare receiver almost completely integrated.**

### New local oscillators for the NOEMA receivers

Two prototypes for local oscillators for band 1 and bands 2/3 using YIG oscillators were validated. The Band 1 YIG local oscillator is essentially a copy of the existing one used currently in Antennas 7 to 11. A version integrating a power amplifier was tested, allowing to get much more power, as needed for future multibeam receivers. In 2021, the production of all Band 1 YIG oscillators will be completed and we can aim at having only YIG-based oscillators at the observatory by the beginning of 2022.

The Bands 2/3 YIG oscillator was first tested with the Antenna 10 in 2018, but a parasitic signal made part of the LO unusable. It was therefore upgraded and modified in such way as to remove this harmonic (originating from the YIG oscillator fundamental frequency intermodulations at various multipliers). That modification was verified on Antenna 7 in 2020 and after successful validation, the production series for the

12 YIG-based local oscillators can start, to equip all antennas by end of 2022. The goal is therefore that by that time, there will only be YIG-based LOs at NOEMA, which will considerably improve reliability and tuning times, and will allow implementing new observing modes, with fast LO switching capabilities.

### Dual-band NOEMA receivers

The first receiver with dual-band capabilities was installed in November 2019 on Antenna 9. In 2020, several commissioning tests were performed, allowing to compare the performance of that receiver compared to optimized single pixel observations. While the results were generally good, a point of concern was the decreased efficiency seen in Band 3 with the new optics of that receiver. In particular the addition of a lens to adjust the focus of Band 3 is likely to be responsible for this 10% degradation. New lens designs were produced in 2020 to correct for this problem.

Two new dual-band systems are under assembly. To this effect, two receiver support frames (so-called “chassis-A”) were manufactured in 2020, allowing to accommodate dual-band receivers. An upgrade was also done to replace the translation stage used in the prototype by a similar model but 2.5 times faster. In 2021, if used in combination with the two receivers available in the laboratory, two new full dual-band systems could be installed.

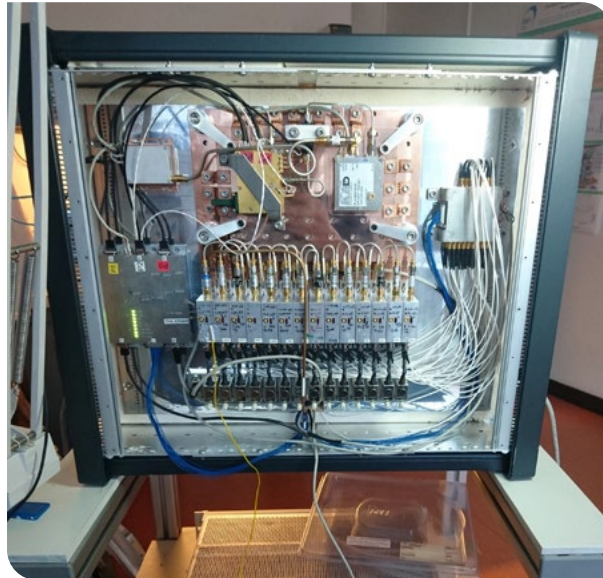
In parallel, since this dual-band mode of observing will deliver twice the IF bandwidth, the Frontend group started in 2020 the design and production of the components needed to double the number of warm IF channels and laser-based transport of the IF signal via optical fibers.



**Two new frames called “chassis-A” were manufactured specifically for the dual-band mode of operation. They are partially integrated with the translation stages, optics and moving mechanism used for the calibration.**

## NOEMA new generation water vapor radiometers

The first prototype of the second-generation water vapor radiometers (WVR-2G) was considerably improved in 2020. A substantial effort was carried out in order to make it more stable by decoupling it from the varying temperature conditions of the receiver cabin. It performed at least as good as the best existing radiometers but with many more channels (14 compared to 3). It also provides added robustness against electro-magnetic perturbations coming from satellites or other microwave links. The series production for 7 new generation radiometers has started in fall 2020. The first two radiometers will be available end of 2021, and all of them will be produced by summer 2022.

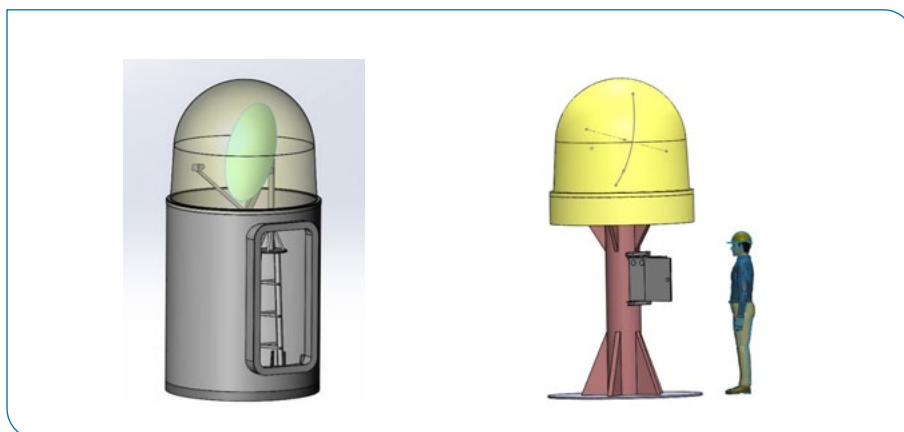


**Radiometer prototype in the laboratory after the final upgrades in January 2020, before re-installation on Antenna 8 in February 2020.**

## Phase monitoring project

This project which started in 2018 in collaboration with the SMA group from the Center for Astrophysics (Harvard, USA), aims at providing a real-time, permanent monitoring system of the observing conditions at the NOEMA site.

In 2020, the final testing of a two-antenna prototype system took place with two parabolic antennas enclosed in protective 1.5 m radomes, separated by 378 m. From September to November, both parabolas were pointed towards the satellite Thor 6 at  $0.8^\circ$  West. The goal was mainly to test new Low Noise Blocks (LNB) that are collecting the satellite incoming signal on the antennas. The system provides real-time atmospheric phase variation to the operators through a web-based page.



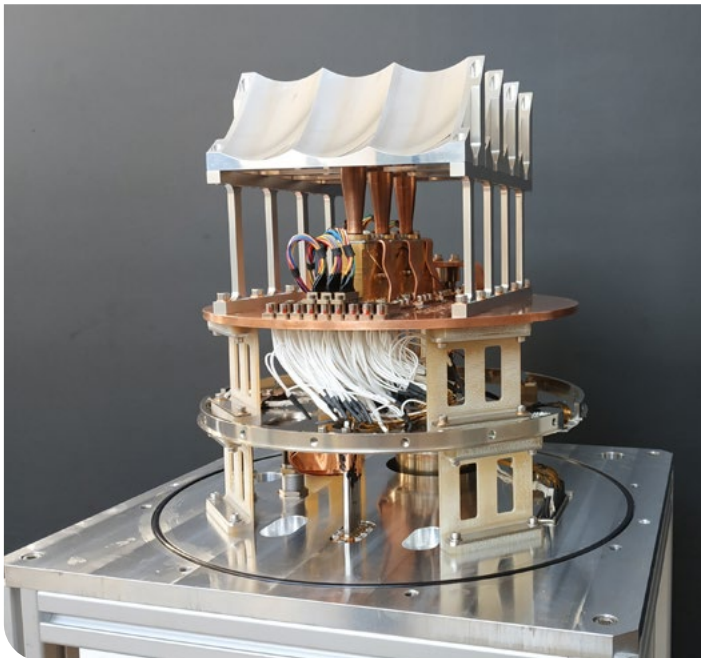
**Possible solutions for the infrastructure of the phase monitoring project. The parabola has to be enclosed in a protective radome, and installed at sufficient height to prevent snow accumulation.**

As the results were very promising, it was agreed that a permanent 3-station system will be installed on the Plateau de Bure in the years to come. After a first infrastructure draft, two simpler versions are under study. Data acquisition system, electronics racks, and software will also have to be improved for better maintainability.

### AETHRA Radionet - Multibeams

2020 was the last year for the European project Radionet-AETHRA, in which IRAM has been specifically working on the development of small size array receivers using 1) direct amplifiers (LNAs) in the 70-116 GHz frequency range, and 2) 1x7 pixels at 230 GHz, with mixers, amplifiers, and LO distribution integrated in the same mechanical blocks.

In 2020, the cryostats for both projects were fabricated by two external companies. The impact of the Covid-19 pandemic was high and created substantial delays. Still, the cryostats were delivered and assembled in the IRAM laboratories.



**AETHRA 3 mm array receiver. View of the inner contents of the cryostat. Two cold stages are used at 60K and 12K. The cold optics can also be seen. One full line of 3 pixels will populate the receiver.**



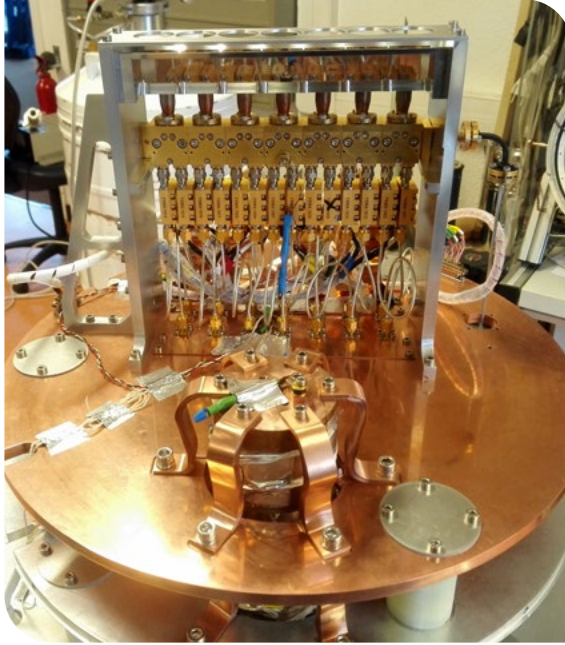
**Test setup, with the cryostat at the middle left. A new spectrum analyzer with noise figure measurement capabilities was purchased in 2020 allowing to noticeably speed up testing.**

#### **100GHz 3x3 HEMT receiver**

This project is done in close collaboration with the MPIfR in Bonn, the Fraunhofer Institute in Karlsruhe and INAF in Italy. The array includes a 1x3 pixels line for the 75-110 GHz band using active OMT blocks (with HEMT amplifiers integrated in the OMT block). The design is done for 3x3 pixels, but currently, only 3 active OMT blocks are available, sufficient for proper demonstration and testing.

#### **230GHz 1x7 SIS mixer receiver**

The 1x7 pixels for the 200-270 GHz band is using 2SB SIS mixers developed during the previous Radionet project AETHER. The cryostat is based on the NOEMA cryostat, scaled down slightly, and uses the same cold head, a 3-stage Sumitomo Industries RDK-3ST allowing to cool down the detectors to about 4K. The cryostat was delivered in November 2020 and integration followed soon afterwards.



AETHRA 1x7 pixels for 230 GHz using 2SB SIS mixers. The cryostat is a scaled version of the NOEMA cryostats and will use the same Sumitomo 3 stage cold heads, allowing to reach temperatures below 4 K.

### CMD test cryostat

A new test receiver was designed at IRAM. It will be used in the Grenoble headquarters to measure cold mirror deformations (CMD) at temperatures down to 4K. It is particularly interesting to measure the NIKA-2 dichroic thermal deformations during the cooling process. To do so, the system will use a laser array and measure the reflected signal positions during the cooling phase to estimate deformations. This setup will eventually be available to measure any optical or electrical components at cold conditions.

## SUPERCONDUCTING DEVICES GROUP

As in the last few years, the superconducting devices group has been able to focus most of its work to development of new technologies for upcoming instruments. At the same time, the group has continued to work on upgrading the machine park, to be ready for future demanding projects such as the multibeam receivers for the 30-meter telescope. Despite a total stop of the clean room during the 8 weeks of lockdown in spring, noticeable advancements on all fields were possible.

### Machine park upgrades

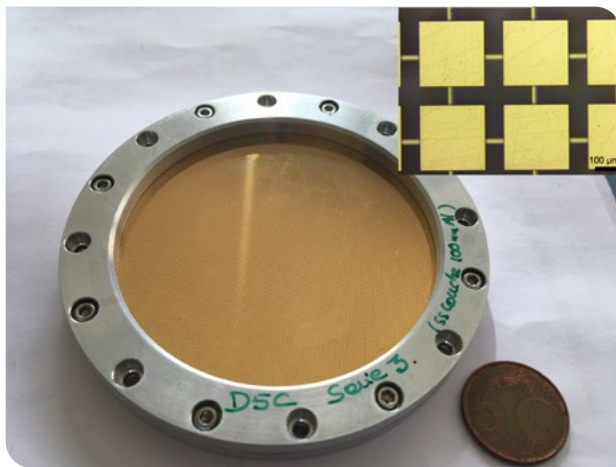
After a significant investment in 2019 in a new e-beam lithography system, attention has been focused on defining and finding replacement for critical but end-of-life equipment in the clean room. A small window of opportunity in early Autumn, between the two pandemic peaks, was used to investigate and select a new surface profiler tool. This critical instrument is used in all IRAM technology steps to measure film heights and film stress. The new surface profiler will arrive early 2021, and will allow these steps to be done in an automated fashion, permitting more reliable quality control and a better device yield.

## SIS junctions on 10 $\mu$ m thick silicon

The major research focus for the Superconducting Devices Group in 2020 as in 2019 has been a continuation of the development of SIS junction technology on 10 micrometer thick silicon substrates. This new process, based on silicon-on-insulator (SOI) technology, has several advantages over the classical approach, most importantly the possibility to design junctions with a wider IF bandwidth. Moreover, it allows to use beam-lead technology for advanced packaging, and in the future advanced integration of functionality on chip. In 2020 two major technology issues have been tackled; they were linked to stress in the beam leads, that rendered packaging and electrical contacting of these fragile devices very difficult. Devices can now reliably be packaged, and first confirmation tests on increased IF bandwidth of these junctions are foreseen for early 2021.

## Dichroic filters

In-house development of dichroic filters for dual-band operation has continued. These filters consist of an assembly of metallic structures on thin quartz substrates. Tiny air gaps between the different substrates severely hamper their performance. Therefore, we have investigated techniques to glue together these wafers without introducing inhomogeneity due to varying glue thickness, nor introducing supplementary dielectric loss in the glue. These developments have significantly improved devices performances, which is now comparable to or better than that of commercially available filters.



**Prototype dichroic filter for NOEMA dual-band operation. The filter consists of 5 layers of 1-3  $\mu$ m thick gold plated patterns (two layers are shown in the inset), deposited on 4 fused silica wafers of 163  $\mu$ m thickness, that are subsequently glued together.**

## Other developments

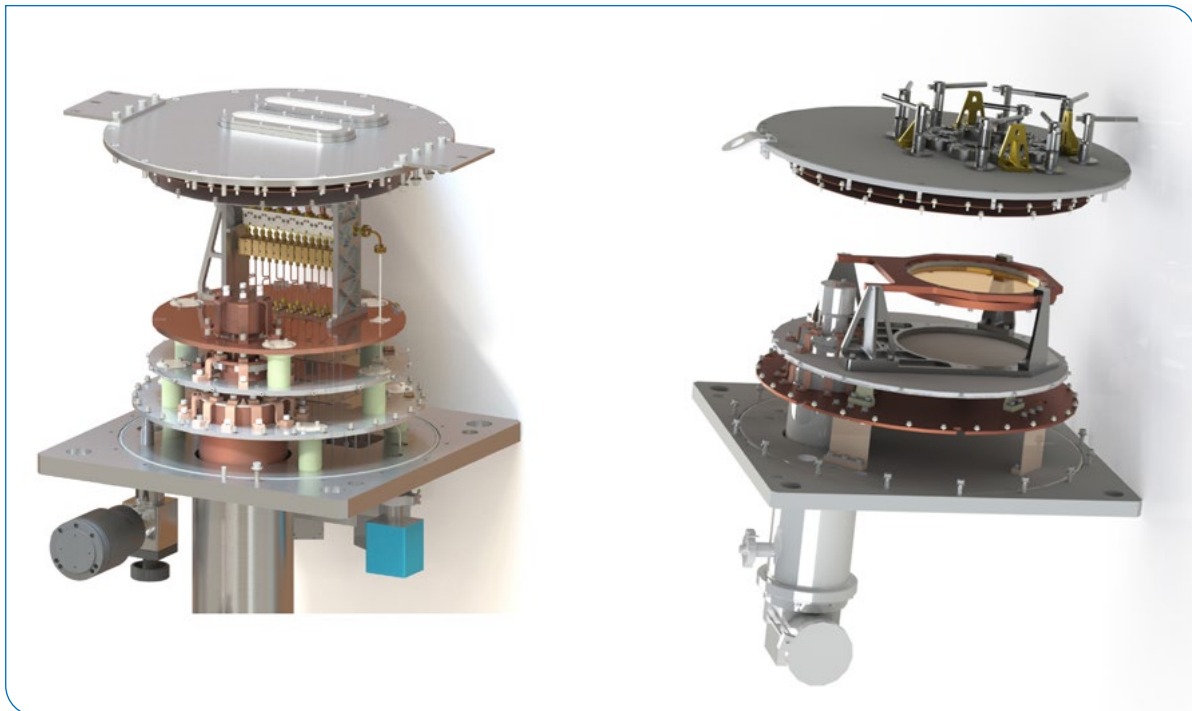
Other development projects from 2020 include production of beam-lead devices for the 100-GHz HEMT prototype receiver array, a thorough investigation of the causes of frequency dispersion in large KID arrays, made possible by the automated measurement routines of our newly acquired e-beam lithography system, and small series productions of devices for various projects.

## MECHANICAL GROUP

The workshop received more than 100 requests for the production of mechanical high-precision elements, in particular many items for frontend projects (mixer blocks, horns, LOs, etc). This served several NOEMA projects, as the new generation Water Vapor Radiometers or the dual-band receivers, as well as the RadioNet AETHRA-supported development of multi-beam prototype arrays.

### Cryostats

Three cryostats were designed almost simultaneously by the Frontend group: two multibeam receiver prototypes and one lab cryostat to study deformations at low temperatures. IRAM adopted a different internal organization for these projects, as compared to the previous generation (NOEMA receivers) cryostats. The mechanical group engineering office has produced the 3D drawings and was also in charge of the procurement of these cryostats, which were produced by external companies.



3D mechanical drawing of the 7-pixels prototype array and CMD test cryostats.



## NOEMA antennas construction

2020 saw the completion of Antenna 11, which was delivered to the commissioning team in August, with a delay of a couple of months only due to the Covid-19 pandemic. The construction of Antenna 12 started during the fall, with the assembling of the large mechanical pieces of the pedestal. IRAM selected a new contractor in charge of the production of the quadruped legs, a critical element of the antenna reflectors.

In parallel, an important development started in 2019 was continued: because the future baseline extension includes a track segment with a slight ( $<2\%$ ) slope, the antennas must be equipped with a security braking system ensuring their velocity can be kept under control in any scenario (e.g. failure of the main drive systems). Each antenna has a weight of approximately 130 tons. Several options were investigated, including passive and active systems, and their pros and cons were carefully assessed. Final choice was to equip antennas with a backstop: in case of emergency, a hydraulic clamp stops the antenna and a disc anti-skid system allows it to be moved only in the upward direction, i.e. back to the flat part of the track. In order to precisely assess the performances of such a system and to optimize its control, a test-bed was conceived and constructed. Tests early 2021 should lead to a final design to be implemented on NOEMA antennas.



**Test-bed of the emergency brake system to be installed on NOEMA antennas.**

## COMPUTER GROUP

Major upgrades of several software tools used at IRAM were implemented, in particular the tools managing the park of computers running under various operating systems. This was even more important in the context of the Covid-19 pandemic, which triggered a huge increase of remote home office work.

### A set of new web tools for home office

To ensure that all IRAM staff working from home can rely on collaboration services, various web-based tools were deployed or upgraded. This included in particular an Intranet wiki (DokuWiki), a video conference (JitsiMeet), an instant messaging (Rocket.Chat), an issue tracker (Zammad) and a file transfer (Lufi) service. All these tools are open-source and operated by the Computer Group on the IRAM computing infrastructure.



Several operating systems are supported.

### Managing Linux...

During the last years, the choice was to run one single application per virtual machine, because it allows updates to be performed with a better granularity. The drawback is that the number of virtual machines has increased to around 100. Specific tools to configure such large farms of virtual servers were needed. Among the different existing software solutions, IRAM has chosen Ansible to manage the configuration of its Linux servers because it is an agent-less and easy-to-learn solution.

### Windows...

Until last year, the park of Windows computers were managed with a set of individual tools like WSUS, MDT, GPO and PowerShell. Nevertheless, with more than 100 managed Windows devices, a more powerful solution

was clearly needed. Microsoft System Center has been chosen as the new systems management software. System Center offers a single console to manage the life cycle of the devices from the commissioning to the decommissioning. Every step can be easily automated to guarantee fast and repeatable procedures. System Center is also compatible with home office: when the computers are in the IRAM office, they are managed directly, when they connect from outside, they are managed through the IRAM VPN. The commissioning of System Center has been completed at the beginning of the year 2020.

### ...and Apple computers

The Computer Group has also studied the possibility to manage Apple laptops like Windows ones. Technically, it is possible to install a plugin to manage MacBooks with Microsoft System Center, but it is a complex and not very convenient solution. Therefore, the Computer Group has preferred to opt for JAMF, a mobile device management (MDM) software for Apple devices.

The most spectacular feature is the zero-touch configuration: the serial number of any new MacBook is automatically added to IRAM's Apple Business Account and linked to IRAM's JAMF instance. Should the MacBook be stolen, the IRAM Computer Group can remotely erase and lock the device. Even if it is reset to its factory configuration, it will connect immediately again to the IRAM JAMF instance and it will be locked again.

## SCIENCE SOFTWARE ACTIVITIES

### Towards new NOEMA observing modes: polarimetry and VLBI

Mid-2020, a first polarimetry measurement was acquired with NOEMA towards a quasar. As the PolyFiX correlator is optimized to cover the widest possible bandwidth, it does not simultaneously measure the cross-polarisation correlations required for full-Stokes polarimetric observations. Instead, the four correlation products are computed in a time sequence. For this purpose, dedicated electronic devices are used to switch the IF signals between the vertical and horizontal polarization at the entrance of the correlator in a predefined time sequence.

In December 2020, the first Very Long Baseline Interferometry (VLBI) fringes were obtained between NOEMA and several other observatories including the IRAM 30-meter telescope. To do this, the signals from each antenna are phased individually so that they can be added coherently. This means that the 12 NOEMA antennas then behave as a single antenna whose collected area is 12 times the area of a single 15-meter antenna. This is an important step to allow NOEMA to bring its high sensitivity to the benefits of VLBI campaigns, such as the EHT at 1mm or the GMVA at 3mm.

In order to achieve these two milestones, many parts of the software had to be updated. In polarimetry mode, new software had to be written to control the cycle of polarization switches and additional bookkeeping had to be integrated into the raw data format through the correlator. For the VLBI mode, an automated phasing loop was introduced in addition to major changes in the correlator software. The test of both observing modes required changes in the NOEMA raw data format.

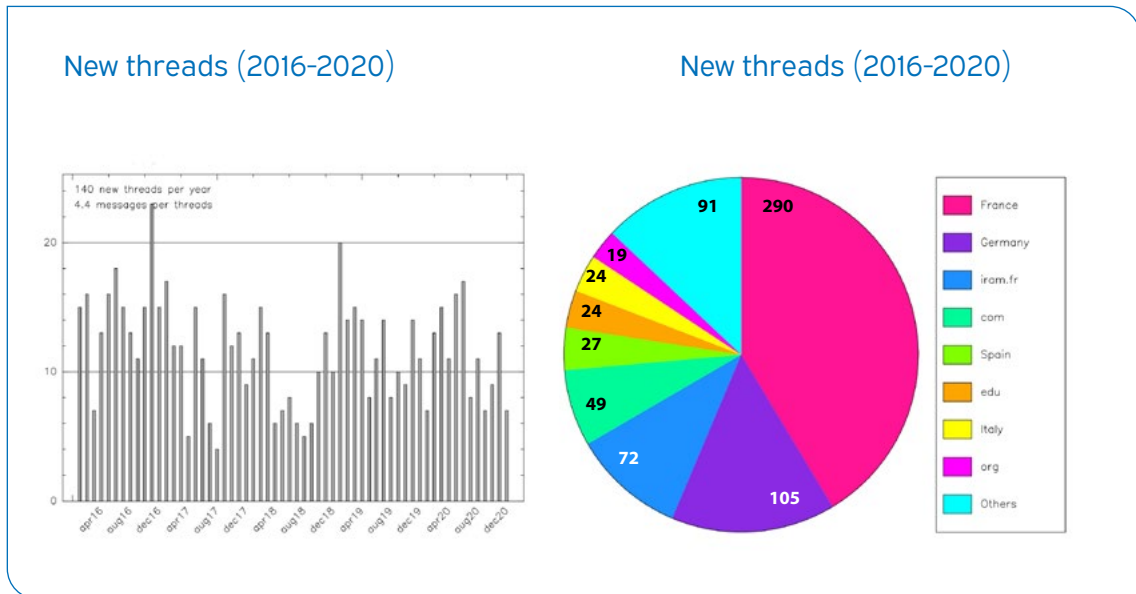
## New tools for NOEMA: Observation Management System

The Observation Management System (OMS) is intended to be a set of independent web-based tools with similar look and feel in order to handle observation projects from proposal submission to distribution of the data to the principal investigators. One of the OMS tools, the Proposal Management System (PMS) has been in operation for many years. In 2020, several major new applications were put in production. First, a web-based sensitivity estimator was introduced to replace the previous tool that required local installation of the GILDAS software. Another major milestone was the release of the Setup Management System (SMS), after several years of development and testing by IRAM astronomers. The SMS allows the principal investigators to easily prepare and validate the details of their NOEMA observing run. In addition to automating many steps such as the selection of calibrators or the setting up of wide-field observations, this tool includes a messaging function and the possibility to check the evolution of the observing setups in order to enable an easy collaboration between the principal investigators and the IRAM staff. Finally, an automated tracking system of the NOEMA status has been implemented. The status of the array (observations, stopped, idle, etc.) is continuously monitored and automatically stored in a database so that unbiased statistics can be calculated.

New functionalities were added to the System Management System (SMS).

## Improvements of the data reduction software

In addition to the major projects described above, several improvements of the data reduction software were implemented. The key IRAM 30-meter software packages PAKO, the astronomer interface to the telescope, and PIIC, the calibration software for the NIKA2 continuum camera, were ported to the gfortran compiler in order to facilitate their installation by end users. A novel bandpass calibration scheme was developed and implemented in the NOEMA data calibration pipeline. The routines that handle the calibrator's spectral index for the absolute flux calibration of NOEMA data were refurbished, tested, and implemented in the calibration pipeline. Although workarounds were already available in 2018, shortly after the PolyFiX correlator was put into operation, the new procedures add robustness to the calibration process. The user manual of CLIC, the calibration software for NOEMA, was fully rewritten. After a period of performance profiling, various software optimizations increased the speed of the NOEMA pipeline by 75%. Last but not least, user support continued in 2020 with statistics similar to those of the last five years.



140 independent threads (one every 2.6 days), with an average flux of 4.4 emails per threads, were treated in 2020 by the science software team.

## IRAM ARC NODE

In the framework of the European ALMA Regional Center (ARC), IRAM is supporting ALMA users, in particular during the data reduction phase. Users can obtain direct help from an IRAM astronomer, in a way similar to the support provided for the NOEMA projects. Travel funding is available for users affiliated to the IRAM funding agencies to visit IRAM and receive face-to-face support. The IRAM ARC node is open to all interested scientists, with an emphasis on the IRAM community (France, Germany, and Spain). One of the goals is to provide to the astronomical community a common support for the IRAM and ALMA facilities, hence maximizing the scientific synergies between the observatories.

In 2020, the Covid-19 pandemic strongly impacted the ALMA operations and led to the cancellation of the Cycle 8 call for proposals. The observatory itself was shut down in March. The "Return to Operations" started on October 1st 2020 with the goal to resume scientific operations in March 2021, after one "blank year". The pandemic also affected the IRAM ARC node, reducing the activity load and preventing any face-to-face support visits. A double remote support solution was implemented, in which both the supported astronomes and the local contact can work from home on the same data reduction session. In 2020, the node supported 80 Cycle 7 projects as contact scientists plus eight Cycle 6 projects carried over. Three face-to-face user support visits were done in Grenoble, and five support sessions were done remotely. An ALMA data reduction training session was organized in the frame of the support of a large program.



Security instructions and evacuation exercise during the Covid pandemic

# Personnel & Finance



## Administration

The Covid-19 pandemic had an obvious important impact on IRAM operations, on all sites. The Grenoble headquarters were totally closed during three weeks in March-April 2020. Since then, a significant part of the work is done remotely from home, whenever possible. A preliminary analysis of the financial impact due to the Covid-19 pandemic showed a balance between additional costs and savings.

The year 2020 highlighted the importance of the dematerialization process in all administrative activities and allowed the Administration group to reach more flexibility and efficiency. As outlook for 2021, the Administration group will work amongst other things to implement a new purchasing software.

## Staff

IRAM employed 121.5 FTEs in 2020 (92.6 in France and 28.9 in Spain). Statistics show a stable proportion of 28% women at IRAM. IRAM continues to have good results in 2020 in terms of the equal pay index between men and women.

IRAM continues to invest in training for the staff, which has a high priority. Unfortunately, due to the Covid-19 pandemic most of the training sessions have been canceled. A side effect was the reduction of the training expenditures in 2020, down -50% in comparison to 2019.

## Financial situation of IRAM

### Operating

Income in k€	Actual 2020
Associates' contribution	12 859
Other income	906
<b>Total income</b>	<b>13 765</b>

Expenses in k€	Actual 2020
Operation (staff costs and operating expenses)	13 801
<b>Total expenditure</b>	<b>13 801</b>

### Investment

Expenses in k€	Actual 2020
Base Investment	1 188
Specific projects	4 075
<b>Total</b>	<b>5 263</b>



## IRAM staff list

### IRAM Headquarters, Grenoble, France

<b>Direction</b>	<b>SCHUSTER Karl-Friedrich</b> <b>GUETH Frédéric</b> DELLA BOSCA Paolo MOREAU Sonja SERLET Murielle ZACHER Karin	Director Deputy Director
<b>Administration</b>	<b>DELAUNAY Isabelle</b> FERREIRA Dina MARCOUX Stéphane MESSMER Romain PALARIC Laurent SIMON Lauriane SIMONE Jeannine	Head of Administration
<b>Astronomy &amp; Science Support Group</b>	<b>NERI Roberto</b> ANTONELLINI Stefano ARUMUGAM Vinodiran BARDEAU Sébastien BERJAUD Catherine BERTA Stefano BREMER Michael BROGUIERE Dominique CASTRO CARRIZO Arancha CHAHINE Loyal CHAPILLON Edwige CONTURSI Alessandra CORTZEN Isabella CUNNINGHAM Nichol DE SOUZA MAGALHAES Victor FEHER Orsolya HERRERA CONTRERAS Cinthya KRAMER Carsten KRIPS Melanie LEFEVRE Charlene LÓPEZ SEPULCRE Ana MELISSE Jean-Paul PETY Jérôme PIETU Vincent REYNIER Emmanuel WINTERS Jan Martin WONG Ka Tat ZYLKA Robert	Head of Astronomy & Science Support Group
<b>Frontend Group</b>	<b>RISACHER Christophe</b> BERTON Marylène BORTOLOTTI Yves FONTANA Anne-Laure GARNIER Olivier LECLERCQ Samuel MAHIEU Sylvain MAIER Doris MOUTOTE Quentin PARIOLEAU Magali PERRIN Guillaume PISSARD Bruno REVERDY Julien SERRES Patrice	Head of Frontend Group
<b>Backend Group</b>	<b>GENTAZ Olivier</b> BALDINO Maryse GARCÍA Roberto GEOFFROY Daniel SASSELLA Rémi	Head of Backend Group
<b>Superconducting Devices Group</b>	<b>DRIESSEN Eduard</b> BARBIER Arnaud BILLON-PIERRON Dominique	Head of Superconducting Devices Group
<b>Computer Group</b>	<b>BLANCHET Sébastien</b> CHALAIN Julien DUMONTROTJY Patrick MICHAUD Jean-Yves REYGAZA Mickaël ROCHE Jean-Christophe	Head of Computer Group

**Mechanical Group**

**LEFRANC Bastien**  
 COUTANSON Laurent  
 DANNEEL Jean-Marc  
 JUBARD Vincent  
 LAZARO Gaëtan  
 PASCAUD Victor

Head of Mechanical Group

**NOEMA, Plateau de Bure, France**

**GAUTIER Bertrand**  
**BOISSIER Jérémie**  
 AZPEITIA Jean-Jacques  
 CASALI Julien  
 CAYOL Alain  
 CHAUDET Patrick  
 COMBE Kevin  
 CONSEIL Yann  
 CONVERS Bruno  
 DAN Michel  
 DI LEONE Cécile  
 LAPEYRE Laurent  
 LE CORRE François-Gildas  
 LEONARDON Sophie  
 MASNADA Lilian  
 MOURIER Yvan  
 OLIVIA Stéphanie  
 RAMBAUD André  
 SALGADO Emmanuel  
 SARRAZIN Jérémy  
 ZANINELLO Pierre

Station Manager  
 Deputy Station Manager

**IRAM 30-meter telescope, Granada, Spain**

**SÁNCHEZ PORTAL Miguel**  
**PEÑALVER Juan**  
 AMAYA Sergio  
 BONGIOVANNI Angel Manuel  
 CÓRDOBA Antonio  
 DAMOUR Frédéric  
 ESPAÑA Gloria  
 GÁLVEZ Gregorio  
 GARCÍA José  
 GARCÍA Verónica  
 GARCÍA RODRIGUEZ Juan Pedro  
 JOHN David  
 KIM Wonju  
 LADJELATE Bilal Smain  
 LARA María  
 LOBATO Enrique  
 MELLADO Pablo  
 MORENO GARCÍA Laura  
 MORENO María  
 MUÑOZ GONZÁLEZ Miguel  
 MYSERLIS Ioannis  
 NAVARRO Santiago  
 PAUBERT Gabriel  
 PEULA Víctor  
 PIERFEDERICI Francesco  
 ROBERTSON II William  
 RODRÍGUEZ MARTÍNEZ Mónica  
 RUIZ Carmen  
 RUIZ Ignacio  
 RUIZ Manuel  
 SÁNCHEZ Antonio  
 SÁNCHEZ Rosa María  
 SÁNCHEZ Salvador  
 SANTARÉN Juan Luis  
 SANTIAGO Joaquín  
 SERRANO David  
 SIEVERS Albrecht  
 TORNE Pablo

Station Manager  
 Deputy Station Manager

# Telescope schedules

## 30-METER TELESCOPE

Project	Title	Authors
122-16	NIKA2 GT-LP set 1: Galactic Star Formation with NIKA2 - GASTON	Nicolas Peretto, Philippe Andre, Alexandre Beelen, Alain Benoit, Aurelien Bideaud, Nicolas Billot, O. Bourrion, M. Calvo, A. Catalano, Gregoire Coiffard, Barbara Comis, Francois-Xavier Desert, S. Doyle, Carsten Kramer, Samuel Leclercq, Juan Macias-Perez, Frederic Mayet, A. Monfardini, Francois Pajot, Enzo Pascale, Laurence Perotto, Giampaolo Pisano, Nicolas Ponthieu, Vincent Reveret, Alessia Ritacco, Louis Rodriguez, Charles Romero, Florian Ruppin, Karl-Friedrich Schuster, Albrecht Sievers, Robert Zylka, Remi Adam, Peter Ade, Frederique Motte, Aurore Bacmann, Andrew Rigby, Isabelle Ristorcelli, Pablo Garcia, Anaëlle Maury, Jean-Francois Lestrade, Yoshito Shimajiri, Andrea Bracco, Bilal Ladjelate, Ana Duarte Cabral, Sarah Ragan, Jane Greaves
124-16	ORION B: The anatomy of a Giant Molecular Cloud	Jerome Pety, Maryvonne Gerin, Emeric Bron, Viviana Guzman Veloso, Jan Orkisz, Sebastien Bardeau, Javier R. Goicoechea, Pierre Gratier, Franck Le Petit, Francois Levrier, Harvey Liszt, Karin Oberg, Nicolas Peretto, Evelyne Roueff, Albrecht Sievers, Pascal Tremblin
160-16	Interpreting the Millimetre Emission of Galaxies with IRAM and NIKA (IMEGIN) - a set 1 NIKA2 GT-LP	Suzanne Madden, Jonathan Davies, Carsten Kramer, Nicolas Peretto, Enzo Pascale, W. Gear, Steve Eales, Matthew Smith, Israel Hermelo, Remi Adam, Francois-Xavier Desert, S. Doyle, Ruth Evans, Christopher Clark, Helene Roussel, Annie Hughes, Peter Ade, Philippe Andre, Alexandre Beelen, Alain Benoit, Aurelien Bideaud, Nicolas Billot, O. Bourrion, M. Calvo, A. Catalano, Gregoire Coiffard, Barbara Comis, Samuel Leclercq, Juan Macias-Perez, Frederic Mayet, A. Monfardini, Francois Pajot, Laurence Perotto, Giampaolo Pisano, Nicolas Ponthieu, Vincent Reveret, Alessia Ritacco, Louis Rodriguez, Charles Romero, Florian Ruppin, Karl-Friedrich Schuster, Albrecht Sievers, Robert Zylka
192-16	The NIKA2 Cosmological Legacy Survey (NIKA2 GT-LP Set1 -N2CLS)	Guilaine Lagache, Alexandre Beelen, Nicolas Ponthieu, Remi Adam, H. Aussel, Matthieu Bethermin, Veronique Buat, Frederic Boone, Emanuele Daddi, David Elbaz, Daizhong Liu, Morgane Cousin, Francois-Xavier Desert, Juan Macias-Perez, Denis Burgarella, Herve Dole, Peter Ade, Philippe Andre, Alain Benoit, Aurelien Bideaud, Nicolas Billot, O. Bourrion, M. Calvo, A. Catalano, Gregoire Coiffard, Barbara Comis, S. Doyle, Carsten Kramer, Samuel Leclercq, Frederic Mayet, A. Monfardini, Francois Pajot, Enzo Pascale, Laurence Perotto, Giampaolo Pisano, Vincent Reveret, Alessia Ritacco, Louis Rodriguez, Charles Romero, Florian Ruppin, Karl-Friedrich Schuster, Albrecht Sievers, Robert Zylka
199-16	NIKA2 GT-LP set 1: High-resolution tSZ observations of a large sample of clusters of galaxies (NIKA2SZ)	Frederic Mayet, Barbara Comis, Remi Adam, Peter Ade, Nabila Aghanim, Philippe Andre, Monique Arnaud, Rafael Barrena Delgado, Iacopo Bartalucci, Alexandre Beelen, Alain Benoit, Aurelien Bideaud, Nicolas Billot, O. Bourrion, M. Calvo, A. Catalano, Nicolas Clerc, Gregoire Coiffard, Marco De Petris, Francois-Xavier Desert, Marian Douspis, S. Doyle, Chiara Ferrari, Carsten Kramer, Samuel Leclercq, Juan Macias-Perez, Jean-Baptiste Melin, A. Monfardini, Francois Pajot, Enzo Pascale, Laurence Perotto, Giampaolo Pisano, Etienne Pointecouteau, Nicolas Ponthieu, Gabriel Pratt, Vincent Reveret, Alessia Ritacco, Louis Rodriguez, Charles Romero, Jose Alberto Rubino Martin, Florian Ruppin, Karl-Friedrich Schuster, Albrecht Sievers, Robert Zylka, H. Aussel
084-17	Imaging the Shadows of Supermassive Black Holes	Ciriaco Goddi, Pablo Torne, Thomas Krichbaum, Eduardo Ros, Michael Kramer, Luciano Rezzolla, Anton Zensus, Karl-Friedrich Schuster, Michael Bremer, Freek Roelofs, Monika Moscibrodzka, H. Rottmann, Remo Tilanus
183-17	LEGO: Studying Milky Way Line Emission to assess Galaxy Observations	Jens Kauffmann, Paul F. Goldsmith, Karl M. Menten, Frank Bigiel, Friedrich Wyrowski, Simon Glover, Susanne Aalto, Andres Guzman, Dario Colombo, Nina Brinkmann, Laszlo Szucs, Carsten Kramer, Neal Evans, Serena Viti, Valentine Wakelam, Wonju Kim
096-18	Dynamic and Radiative Feedback of Massive Stars	Javier R. Goicoechea, Nuria Marcelino, O. Berne, Alexander Tielens, David Teyssier, Cornelia Pabst, Ronan Higgins, Jurgen Stutzki, Mark Wolfire, Slawa Kabanovic, Sumeyye Suri, Christof Buchbender, Alvaro Hacar, Carsten Kramer, Sara Cuadrado
114-19	Composition and the origin of formaldehyde in a bright comet	Nicolas Biver, Dominique Bockelee-Morvan, Jacques Crovisier, Raphael Moreno, Gabriel Paubert, Stefanie Milam, Dariusz C. Lis, Jeremie Boissier, Neil Dello Russo, Katia Hadraoui, Ronald Vervack, Martin Cordiner, Nathan Roth
115-19	Determining the magnetic field morphology and the relative strength of self-gravity in Serpens	Alex Lazarian, Yue Hu, Ka Ho Yuen, Ka Wai Ho, Snezana Stanimirovic, Richard Crutcher
116-19	Disentangling the fibers of L1495/B213	Mario Tafalla, Ana Chacon-Tanarro, Alvaro Hacar
117-19	The one-sided illumination of L183 and L134 as traced by <sup>12</sup> CO	Laurent Pagani, Charlene Lefevre
119-19	Measuring nitrogen isotopic ratio across the Galaxy using PGCCs and IRDCs	Shaoshan Zeng, Izaskun Jimenez-Serra, Giuliana Cosentino, Sarolta Zahorevcz, Jesus Martin-Pintado

Project	Title	Authors
120-19	CH <sub>3</sub> OD: a key to understanding deuterium fractionation	Aurore Bacmann, Alexandre Faure, Quirico Eric, Patrice Theule
122-19	NKA2 insights into the dust evolution in prestellar cores	Isabelle Ristorcelli, Mika Juvela, Karine Demyk, Nathalie Ysard, DeborahParadis, Julien Montillaud, L. Montier, Jean-Philippe Bernard, Alessia Ritacco, Nicolas Ponthieu, V.-M. Pelkonen, Tie Liu, Peregrine McGehee
123-19	FIR/mm dust emissivity in L183 and L134	Charlene Lefevre, Laurent Pagani, Hiroyuki Hirashita, Bilal Ladjelate
125-19	The origin of the shocks in starless clump candidates	Feng-Yao Zhu, Junzhi Wang, Juan Li
126-19	Understanding the coupling between dust properties in interstellar filaments and young stellar objects in low-mass star-forming regions	Bilal Ladjelate, Jean-Francois Lestrade, Charlene Lefevre, James di Francesco, Juan Macias-Perez, Mathilde Gaudel
128-19	Dust and gas evolution in the prototypical starless cores in TMC1	Carsten Kramer, Asuncion Fuente, Paola Caselli, Santiago Garcia-Burillo, Rafael Bachiller, Valentine Wakelam, Nuria Marcelino, Izaskun Jimenez-Serra, Jason Kirk, Jaime Pineda, Belen Tercero, Pierre Gratier, Alvaro Hacar, Sandra Trevino-Morales, Tony Mroczkowski, Charles Romero, Ana Chacon-Tanarro, Mario Tafalla, David Navarro Almada
129-19	Kinematical Transition from Cores to Envelopes around Evolved Protostars	Jinshi SAJ, Nagayoshi Ohashi, Sebastien Maret, Anaëlle Maury, Yusuke Aso, Mathilde Gaudel, Yen Hsi-Wei
131-19	A search for phosphorus carriers towards protosolar analogs	Jennifer Bergner, Karin Oberg, Fred Ciesla
132-19	NKA2 mapping of the dense core Barnard 5	Anika Schmiedeke, Jaime Pineda, Dominique Segura-Cox, Maria Maureira
133-19	Mapping a Giant Complex Organic Molecular Cloud	Victor Rivilla, Sergio Martin Ruiz, Jesus Martin-Pintado, Shaoshan Zeng, Izaskun Jimenez-Serra, Miguel Angel Requena-Torres, Jairo Vladimir Armijos Abendano
134-19	Spectroscopic characterization of a new interstellar molecule	Marcelino Agundez, Nuria Marcelino, Jose Cernicharo, Carlos Cabezas, Celina Bermudez
135-19	The Deuterium Abundance in the Extreme Outer Galaxy	Don Lubowich, Romane Le Gal, Evelyne Roueff, Christian Henkel, Jay Pasachoff, David Weinberg, Yan Gong
136-19	Nitrogen chemistry in proto-brown dwarfs	Basmah Riaz
137-19	The <sup>14</sup> N/ <sup>15</sup> N ratio in low mass protostars: a new step towards understanding nitrogen chemistry	Elena Redaelli, Paola Caselli, Luca Bizzocchi
139-19	Complex Organic vs. Warm Carbon Chain Molecules in High Mass Star Forming Regions	Sandrine Bottinelli, Rene Plume, Emmanuel Caux, Bhaswati Mookerjee, Pamela Freeman
140-19	Confirming the first detection of CH <sub>2</sub> OH towards IRAS4A	Silvia Spezzano, Paola Caselli, Cecilia Ceccarelli, Holger Muller, Charlotte Vastel, Izaskun Jimenez-Serra, Jaime Pineda, Ana Lopez-Sepulcre, Valerio Lattanzi
141-19	Core and filament formation: kinematics of G1592-8.4	Siju Zhang, Hongli Liu, Amelia Stutz, Annie Zavagno, Jinghua Yuan
143-19	Linking density structures and fragmentation in high-mass star formation	Henrik Beuther, Caroline Gieser, Aida Ahmadi, Sumeyye Suri, Hendrik Linz, Dmitry Semenov, Karl M. Menten, Thomas Henning, Rolf Kuiper, Riccardo Cesaroni, Pamela Klaassen, Sarah Ragan, Juan Diego Soler, Siyi Feng, Aina Palau, Luca Moscadelli
144-19	A high spectral resolution view of the Orion Bar PDR at 2 mm	Sara Cuadrado, Javier R. Goicoechea, Jose Cernicharo, Belen Tercero
145-19	Large scale cloud properties of Cygnus X	Friedrich Wyrowski, Henrik Beuther, Karl M. Menten, Gisela Ortiz Leon, Antonio Hernandez-Gomez, Thanh Dat Hoang, Sumeyye Suri, Caroline Gieser, Nicola Schneider, Tímea Csengeri, Sylvain Bontemps, Frederique Motte, Jan Martin Winters, Ka Tat Wong, Nichol Cunningham, Wonju Kim
147-19	HCN 1-0 and H <sup>13</sup> CN 1-0 mapping toward massive star forming regions with accurate distances	Kai Yang, Shu Liu, Junzhi Wang, Yan Duan, Shanghuo Li, Fei Li, Juan Li
148-19	Is Water deuterium exchange at work in NGC7538-IRS1 ?	Juan Ospina-Zamudio, Bertrand Lefloch, Cecile Favre, Isabelle Kleiner, Alexandre Faure
150-19	A project for Master students of Grenoble University: Radiation-driven implosion in M20	Bertrand Lefloch
151-19	California as a laboratory for filament evolution	Rodrigo Hernan Alvarez Gutierrez, Amelia Stutz, Ralf Klessen, Law Chi Yan, Stefan Reissl, Hongli Liu
152-19	Extended SiO Emission in IRDCs: Tracing the Assembly of Massive Clumps?	Wonju Kim, Gary Fuller, Jinjin Xie, Nicolas Peretto, Di Li, Fabien Louvet, Kenichi Tatematsu, Adam Avison
153-19	Mapping the North America Nebula	Alvaro Sanchez-Monge, Shuo Kong, Hector Arce, John Carpenter, Volker Ossenkopf-Okada, Fumitaka Nakamura, Yoshito Shimajiri, Peregrine McGehee, Adam Ginsburg, Sumeyye Suri, Peter Schilke, Darek LIS, John Bally, Paul F. Goldsmith
155-19	Turbulence and protostellar outflows in the Cepheus dense clumps	Pierre Guillard, Anaëlle Maury, Matthias Gonzalez, Bilal Ladjelate
158-19	The physical and radiative interaction of the supernova remnant CTB 109 with a giant molecular cloud	Seamus Clarke, Alvaro Sanchez-Monge, Peter Schilke, Manami Sasaki, Prof. Dr. Stefanie Walch
159-19	Mapping the interaction of supernova remnant with its progenitor's wind bubble.	Vladimir Domcek, Maria Arias, Ping Zhou, Jacco Vink, Sophia Derlopa, Alexandros Chiotellis, Panayotis Boumbs
160-19	Mapping O <sup>18</sup> O emission in SNR IC443 B region with IRAM 30-meter	Shu Liu, Junzhi Wang, Yan Duan, Kai Yang

Project	Title	Authors
161-19	Search for cosmic ray-induced multi-molecular lines near supernova remnant IC 443	Qiancheng Liu, Yang Chen
162-19	Molecular survey of water bearing disks in Taurus	Pablo Riviere-Marichalar, Asuncion Fuente, David Navarro Almada, Benjamin Montesinos, Ignacio Mendigutia, Tomas Alonso-Albi, David Barrado y Navascues, Alvaro Ribas
163-19	Spectral inversion in SED's of debris disks : a signature of the collisional cascade of planetesimals ?	Jean-Francois Lestrade, Jean-Charles Augereau, Mark Booth, Philippe Thebault, Charlene Lefevre, Bilal Ladjelate
165-19	Molecular Content of the C-rich Red Supergiant star AFGL2233	Guillermo Quintana-Lacaci, Jose Pablo Fonfria, Jose Cernicharo, Marcelino Agundez, Luis Velilla Prieto
166-19	Density profiles of extended PNe and their implications for mass-loss histories	Juan Luis Verbena, Javier Alcolea, Valentin Bujarrabal, Klaus-Peter Schroder
167-19	Confirmation of KO in VY Canis Majoris	Lucy Ziurys, Deborah Rose Schmidt, Mark Burton, Phil Sheridan
169-19	The Dawn of Helium Chemistry	Helmut Wiesemeyer, Rolf Gusten, David A. Neufeld, Karl M. Menten
170-19	The formation of Fullerenes in Planetary Nebulae: A radio astronomy view	Jose Jairo Diaz-Luis, Javier Alcolea, Domingo Anibal Garcia Hernandez, Valentin Bujarrabal, Arturo Manchado, J-F. Desmurs
171-19	Circumstellar envelopes of AGB stars: exploring the onset of axisymmetric nebulae	Jose Jairo Diaz-Luis, Javier Alcolea, Valentin Bujarrabal, Miguel Santander-Garcia, Arancha Castro-Carrizo, Miguel Gomez-Garrido, J-F. Desmurs
172-19	HCN masers and high velocity winds in IRC+10216	Jose Cernicharo, Marcelino Agundez, Guillermo Quintana-Lacaci, Michel Guelin, Arancha Castro-Carrizo, Jose Pablo Fonfria, Juan R. Pardo, Luis Velilla Prieto
173-19	A sensitive line survey of IRC+10216 between 200 and 320 GHz	Jose Cernicharo, Juan R. Pardo, Michel Guelin, Luis Velilla Prieto, Carlos Cabezas, Celina Bermudez, Jose Pablo Fonfria, Guillermo Quintana-Lacaci, Marcelino Agundez
175-19	R Aqr: the first radio-spectroscopic binary	Javier Alcolea, Valentin Bujarrabal, Joanna Mikolajewska, Miguel Gomez-Garrido, Krystian Ilkiewicz, Arancha Castro-Carrizo, Miguel Santander-Garcia, J-F. Desmurs
176-19	Constraining the Molecular Emission Size in Envelopes around AGB Stars	Sarah Massalkhi, Jose Cernicharo, Juan R. Pardo, Jose Pablo Fonfria, Marcelino Agundez, Luis Velilla Prieto
177-19	Looking for high-density tracers in maser-emitting PNe	Lucero Uscanga, Jose F. Gomez, Luis F. Miranda, Gerardo Ramos-Larios, Roldan Cala
178-19	Surviving in the Helix: a study of isotopic selective photodissociation	Luis Velilla Prieto, Hans Olofsson, Wouter Vlemmings, Theo Khouri, Elvire De Beck, Maryam Saberi
179-19	The long term evolution of the structure, dynamics and photochemistry of CRL618 - continuation	Juan R. Pardo, Jose Cernicharo, Marcelino Agundez, Guillermo Quintana-Lacaci, Luis Velilla Prieto
180-19	A Search for $^{12}\text{C}^{16}\text{O}$ & $^{12}\text{C}^{18}\text{O}$ in the Dust Envelope of R Coronae Borealis	Edward J Montiel, Jose Pablo Fonfria
182-19	Mapping Jet-ISM Interaction Zones near Black Hole X-ray Binaries with HERA	Alexandra Tetarenko, Erik Rosolowsky, James Miller-Jones, Gregory Sivakoff
183-19	Variability monitoring of magnetars after the reactivation of AXP J1810-197 (continuation)	Pablo Torne, Gabriel Paubert, Gregory Desvignes, Ramesh Karuppusamy, Kuo Liu, Ralph Eatough, Clemens Thum
185-19	IRAM 30m CO(1-0) mapping of the nuclear ring of M31	Zongnan Li, Zhiyuan Li, Yu Gao, Matthew Smith, Ping Zhou, Xuejian Jiang, Jinjin Xie
186-19	Ram pressure stripped molecular gas in NGC 4396 ?	Thomas Lizee, Jonathan Braine, Bernd Vollmer
190-19	Star formation from atomic hydrogen in metal-poor galaxies?	Miriam Garcia, Jesus Martin-Pintado, Francisco Najarro
191-19	Explore the sub-mm water maser emission in NGC 4258	Feng Gao, Jim Braatz, Violette Impellizzeri, Christian Henkel, Liz Humphreys, Dom Pesce, Cheng-Yu Kuo
192-19	IRAM 30m high angular follow-up observations on large scale molecular outflows in NGC 3628	An-Li Tsai, Jose Ricardo Rizzo, Chornng-Yuan Hwang, Edwige Chapillon
193-19	Relic Compact Elliptical Galaxies (following)	Francoise Combes, Philippe Salome, Valeria Olivares
196-19	The IRAM COCO survey: CO in the Coma cluster	Nikki Zabel, Timothy Davis, Paolo Serra, Christine Wilson, G. Bendo, Freeke van de Voort, Toby Brown
198-19	Star formation and molecular gas in double-peak galaxies	Anne-Laure Melchior, Daniel Maschmann, Francoise Combes
199-19	Molecular gas in low-mass star-forming S0 galaxies	Xue Ge, Qiusheng Gu, Zhiyu Zhang, Ruben Garcia-Benito, Mengyuan Xiao, Zongnan Li, Zhengyi Chen
200-19	Constraining the variability of the most active Brightest Cluster Galaxies in the mm	Philippe Salome, Francoise Combes, Thomas Rose, Jae-Woo Kim, Aeree Chung, Junhyun Baek, Alastair Edge
201-19	Searching for Cold, Molecular Gas in Low-Mass, Quenched Galaxies Hosting AGN	Catherine Witherspoon, Eric Wilcots
202-19	Plugging a hole in studies of molecular outflows from galaxies	Dieter Lutz, Eckhard Sturm, Sylvain Veilleux, Thomas Taro Shimizu, Rodrigo Herrera-Camus, Richard Davies, Linda Tacconi, Alessandra Contursi
203-19	Gas-to-Dust Ratios in Herschel-Detected Early-Type Galaxies - Extending the Parameter Space	David Glass, Anne Sansom, Timothy Davis, Sebastien Viaene, Cristina Popescu
204-19	Probing Molecular Gas in Extremely Compact Starbursts as Major Merger Remnants	Mengyuan Xiao, Longji Bing, Qiusheng Gu, Yong Shi, Yifei Jin

Project	Title	Authors
205-19	Measuring the molecular gas in super spirals at $z < 0.3$	Ute Lisenfeld, Patrick Ogle, Phil Appleton, Lauranne Lanz, David Frayer
206-19	Time sequence of post-merger galaxies at $z=0.06$	Anne-Laure Melchior, Barbara Mazzilli-Ciraulo, Francoise Combes, Daniel Maschmann
207-19	Search and Analysis of Giant radio galaxies with Associated Nuclei (SAGAN)-I: Studying host properties with IRAM	Francoise Combes, Pratik Dabhade, Mousumi Mahato
208-19	Measuring the ICM conditions that trigger AGN feedback in MAXBCG J201.08197+04.31863	Ewan O'Sullivan, Douglas Burke, Aneta Siemiginowska, Magdalena Kunert-Bajraszewska, Francoise Combes, Philippe Salome
209-19	Probing the effect of the cluster environment on molecular gas of distant brightest cluster galaxies	Gianluca Castignani, Francoise Combes, Philippe Salome, Pascale Jablonka, Jonathan Freundlich
210-19	MAPI: Monitoring AGN with Polarimetry at the IRAM 30-meter telescope	Ivan Agudo, Carolina Casadio, Efthalia Traianou, Jae-Young Kim, Ioannis Myserlis, Nicholas MacDonald, Thomas Krichbaum, Anton Zensus, Helmut Wiesemeyer, Clemens Thum, Alessia Ritacco, Antonio Fuentes, Jose L. Gomez, Venkatesh Ramakrishnan, Alan Marscher, Svetlana Jorstad
212-19	A systematic search for ultra-bright high- $z$ strongly lensed galaxies in Planck catalogues	Matteo Bonato, Gianfranco De Zotti, Marcella Massardi, Mattia Negrello, Tiziana Trombetti, Carlo Burigana, Diego Herranz, Vincenzo Galluzzi, Stefano Berta
213-19	Molecular gas properties of an over-density of LOFAR and Herschel galaxies	Maria del Carmen Polletta, Matthew Lehnert, Herve Dole, Brenda Frye, Clement Martinache
216-19	First Characterisation of the Gas Content within a New and Promising Strong Lensing Cluster	Florian Ruppin, Alexandre Beelen, Raoul Canameras, Francois-Xavier Desert, Florian Keruzore, Guilaine Lagache, Marceau Limousin, Juan Macias-Perez, Frederic Mayet, Laurence Perotto, Nicolas Ponthieu
217-19	Unveiling the intra-cluster gas physics at intermediate redshift	Iacopo Bartalucci, Monique Arnaud, Stefano Ettori, Florian Keruzore, Juan Macias-Perez, Frederic Mayet, Tony Mroczkowski, Laurence Perotto, Etienne Pointecouteau, Gabriel Pratt, Jack Sayers
218-19	Sunyaev-Zel'dovich follow-up of XXL galaxy clusters at $z \sim 1$ with NIKA2	Marina Ricci, Remi Adam, Bruno Altieri, Mark Birkinshaw, Alberto Cappi, Dominique Eckert, Sotiria Fotopoulou, Fabio Gastaldello, Oliver Hahn, Cathy Horellou, Elias Koulouridis, Adam Mantz, Ben Maughan, Sophie Maurogordato, Florian Pacaud, Marguerite Pierre, Emanuela Pompei, Mauro Sereno
219-19	Studying the Properties of the Intra-cluster Medium of Distant, $z \geq 1$ , Galaxy Clusters	Hans Boehringer, Karl-Friedrich Schuster, Gayoung Chon, Juan Macias-Perez, Piero Rosati, Paolo Tozzi
220-19	High Angular Resolution tSZ Mapping of the Most Massive Galaxy Clusters at $z > 0.9$	Mark Brodwin, Marshall Bautz, Bandon Decker, Peter Eisenhardt, Daniel Marrone, Michael McDonald, Alexandra Pope, Florian Ruppin, Adam Stanford, Dominika Wylezalek
221-19	First Map of the Gas Temperature in a Galaxy Cluster using the Relativistic Sunyaev-Zel'dovich Effect	Florian Ruppin, Francois-Xavier Desert, Florian Keruzore, Juan Macias-Perez, Frederic Mayet, Laurence Perotto, Nicolas Ponthieu
222-19	Intracluster medium properties of the first massive clusters selected independently of their baryon content	Stefano Andreon, Bilal Ladjelate, Ginevra Trinchieri, Alberto Moretti
223-19	A Pilot Cosmological NIKA2 Survey in The North Ecliptic Pole Field ("A PicNik in the NEP Field")	Denis Burgarella, Stephen Serjeant, Samuel Boissier, David Clements, Gianfranco De Zotti, Michal J. Michalowski, Kouichiro Nakanishi, Alain Omont, M. Ouchi, Chris Pearson, Tsutomu Takeuchi, M. Vaccari, I. Valtchanov, Glenn White, Fangting Yuan, Nicolas Ponthieu, Veronique Buat, Ambra Nanni, Jana Bogdanoska
225-19	Knocking on giant's door: A large-scale view of candidate $z > 4$ dusty galaxies	Darko Donevski, Daizhong Liu, Carlos Gomez-Guijarro, Andrea Lapi, William Pearson, Kasia Malek, Anna Feltre, Allison Man
227-19	Towards the first Radio Galaxies in the Universe	Stergios Amarantidis, Luca Bizzocchi, Jose Afonso, Israel Matute, Ciro Pappalardo
228-19	Chemical and dynamical evolution of starless cores	David Navarro Almada, Asuncion Fuente, Carsten Kramer, Benoit Commercon, Paola Caselli, Valentine Wakelam, Stephanie Cazaux, Santiago Garcia-Burillo, Rafael Bachiller, Mario Tafalla, Nuria Marcelino, Izaskun Jimenez-Serra, Rachel Friesen, Tomas Alonso-Albi, Evelyne Roueff, Maryvonne Gerin, Jaime Pineda, Silvia Spezzano, Jean-Christophe Loison, Sandra Trevino-Morales, Ana Chacon-Tanarro, Pablo Riviere-Marichalar, Marcelino Agundez, Valerio Lattanzi, Roberto Neri
229-19	Ionization: explaining the split between big and small Protostellar Disks	Maria Maureira, Jaime Pineda, Dominique Segura-Cox, Paola Caselli, Bo Zhao
230-19	Are disk asymmetries driven by large scale accretion flows?	Jaime Pineda, Anika Schmiedeke, Paola Caselli, Dominique Segura-Cox, Bo Zhao, Nichol Cunningham, Roberto Neri, Maria Maureira
231-19	Characterizing diffusive processes in the B335 protostar	Anaëlle Maury, Josep Miquel Girart, Victoria Cabedo Soto
232-19	2MASS J0233+6156: a newly discovered eruptive star	Orsolya Feher, Agnes Kospal, Peter Abraham, Carlos Contreras Pena, Fernando Cruz-Saenz de Miera
233-19	Caught in the act: Varying infall towards a periodically brightening protostar	Hendrik Linz, Bringfried Stecklum, Henrik Beuther, Alessio Caratti o Garatti, Marian Szymczak
234-19	The protostellar and interstellar content of the IC443 SNR	Antoine Gusdorf, Pierre Dell'Ova, Maryvonne Gerin, Fabien Louvet, Denise Riquelme, Marco Padovani, Martin Houde, Bilal Ladjelate
235-19	Radiation-driven Molecular Chemistry in the Planetary Nebula NGC 7027	Joel Kastner, Javier Alcolea, Pierre Hily-Blant, Thierry Forveille, Jesse Bublitz
236-19	Streams, disk and chemistry in the S-type AGB star RS Cnc	Thibaut Le Bertre, Jan Martin Winters, Ka Tat Wong, Do Thi Hoai, Pham Thi Tuyet Nhung, Pham Tuan-Anh, Pierre Lesaffre, Diep Pham Ngoc, Pierre Darrigat

Project	Title	Authors
237-19	Resolved molecular gas in the SN factory NGC 2770	Christina Thone, Michal J. Michalowski, Antonio de Ugarte Postigo, Sergio Martin Ruiz, David Alexander Kann, Katarzyna Bensch, Natalia Gotkiewicz
238-19	The First Cloud-by-Cloud Dense Gas Map of an External Galaxy	Eva Schinnerer, Frank Bigiel, Jerome Pety, Antonio Usero, Adam Leroy, Annie Hughes, Miguel Querejeta, Cinthya Herrera Contreras, Ashley Thomas Barnes, Ilin Lazar, Cosima Eibensteiner, Jakob den Brok, Daizhong Liu, Johannes Puschignig, Toshiki Saito, Axel Garcia-Rodriguez, Sharon Meidt, Eric Emsellem, Jonathan Henshaw, Melanie Chevance, Diederik Kruijssen, Alex Hygate, Andreas Schrubba, Maria Jesus Jimenez Donaire
D01-19	The activity and composition of Interstellar comet C/2019 Q4 (Borisov)	Nicolas Biver, Dominique Bockelee-Morvan, Jacques Crovisier, Raphael Moreno, Gabriel Paubert, Jeremie Boissier, Barbara Handzlik, Michal Drahus, Piotr Guzik, Nathan Roth, Martin Cordiner, Stefanie Milam
D02-19	Characterizing the millimeter emission in nearby galaxies using NIKA-2	Isabella Lamperti, Amelie Saintonge
D07-19	Follow up of the newly-discovered magnetar Swift J1818-1607 at millimetre wavelengths	Pablo Torne, Ramesh Karuppusamy, Gregory Desvignes, Michael Kramer, Kuo Liu, Ralph Eatough, Salvador Sanchez, Gabriel Paubert, Clemens Thum, Juan Macias-Perez, Bilal Ladjelate, Stefano Berta, Miguel Sanchez Portal, Santiago Navarro, Angel Bongiovanni
EHT-1	EHT: Resolving the gamma-ray emission region and the jet collimation profile in TeV blazar Mrk 501	Michael Nowak, Rocco Lico, Mislav Balokovic, Venkatesh Ramakrishnan, Monica Orienti, Zhiqiang Shen, Guangyao Zhao, Shoko Koyama, Anton Zensus, Kotaro Niinuma, Marcello Giroletti, Silke Britzen, Svetlana Jorstad, Sunil Chandra, Gabriele Giovannini, Jan Carlos Algaba, Feng Yuan, Timothy Davis, Jose F. Gomez, Kazuhiro Hada, Motoki Kino, Kazunori Akiyama, Rusen Lu, Tuomas Savolainen, David James, Keiichi Asada, Wen-Ping Lo, Eduardo Ros, Mark Gurwell, Hiroshi Nagai, Norbert Schartel, David Paneque, Thomas Krichbaum, Masanori Nakamura, Yuzhu Cui, Heino Falcke
EHT-4	EHT: Magnetic field structure in the jet acceleration and collimation zone of quasar 3C273	V. Fish, Feng Yuan, J. Wagner, Anton Zensus, Keiichi Asada, Venkatesh Ramakrishnan, Thomas Krichbaum, Masanori Nakamura, Alan Roy, Maciek Wielgus, Alexander Tchekhovskoy, Jose L. Gomez, H. Rottmann, Tuomas Savolainen, Katherine Bouman, Kazunori Akiyama, Yosuke Mizuno, Eduardo Ros, Geoffrey Crew, Jae-Young Kim, Svetlana Jorstad, Alan Marscher, Kazuhiro Hada, Daniel Marrone, Rusen Lu, Lindy Blackburn, Michael Janssen, C. Goddi, Ewan O'Sullivan, Talvikki Hovatta
GMVA-19B-127	ALMA revealing the fine structure of shocks in the extreme blazar CTA 102	Carolina Casadio, Nicholas MacDonald, Thomas Krichbaum, Alan Marscher, Svetlana Jorstad, Jae-Young Kim, H. Rottmann, Efthalia Traianou, Ivan Agudo, Jose L. Gomez, Shoko Koyama, Keiichi Asada, Ruben Herrero-Illana, David Hughes, Anton Zensus, Victor Manuel Patino Alvarez, Gopal Narayanan, Antonio Fuentes
GMVA-19B-134	Imaging massive binary black hole candidate OJ287 with the GMVA+ALMA	Jose L. Gomez, Thomas Krichbaum, Andrei Lobanov, Antonio Fuentes, Stefanie Komossa, Alan Marscher, Svetlana Jorstad, Gabriele Bruni, Yuri Kovalev, Carolina Casadio, Jae-Young Kim, Laura Vega-Garcia, Ivan Marti-Vidal, Jeffrey Hodgson, Roman Gold, Kazunori Akiyama, Michael Johnson, Sera Markoff, Laurent Loinard, Brissa Gomez-Miller, Uwe Bach, Ivan Agudo, Sol N. Molina, Yosuke Mizuno, Josep Marti, Manel Perucho, Eduardo Ros, Silke Britzen, Rusen Lu, Geoffrey Crew, Anton Zensus, H. Rottmann, Tuomas Savolainen, Efthalia Traianou, Sara Issaoun, Michael Janssen, Keiichi Asada, Lindy Blackburn, Masanori Nakamura, Venkatesh Ramakrishnan, Rocco Lico, Marshall Cohen, Achamveedu Gopakumar, Stanislaw Zola, Shoko Koyama, Elisabetta Liuzzo, Violette Impellizzeri, Ruben Herrero-Illana, Hugo Messias, Ilje Cho
GMVA-19B-147	Resolving the counter-jet of 3C 84 at 3 mm with GMVA+ALMA	Ilje Cho, Jae-Young Kim, Thomas Krichbaum, Jeffrey Hodgson, Junghwan Oh, Guangyao Zhao, Eduardo Ros, Svetlana Jorstad, Alan Marscher, Hiroshi Nagai, Motoki Kino, Silke Britzen, Kiyooki Wajima, Bong Won Sohn, Taehyun Jung, Michael Bremer, Keiichi Asada, Masanori Nakamura, Shoko Koyama, Jun Yi Koay, Satoki Matsushita, Yosuke Mizuno, Jose L. Gomez, David Sanchez-Arguelles, David Hughes, Gopal Narayanan
GMVA-19B-208	Millimeter-VLBI Observations of TeV-Blazars at the dawn of the CTA Era	Matthias Kadler, Eduardo Ros, Julian Sitarek, Karl Mannheim, Thomas Krichbaum, Anton Zensus, David Hughes, David Sanchez-Arguelles, Gopal Narayanan
GMVA-19B-212	Sharpening the Source Model for Sgr A* with GMVA+ALMA	Sara Issaoun, Lindy Blackburn, Michael Johnson, Christiaan Brinkerink, Maciek Wielgus, Ciriaco Goddi, Thomas Krichbaum, Monika Moscibrodzka, Sera Markoff, S. Doleman, Michael Janssen, Freek Roelofs, V. Fish, Eduardo Ros, Heino Falcke, Geoffrey Bower, Daniel Marrone, Jason Dexter, Kazunori Akiyama, Katherine Bouman, Rusen Lu, Guangyao Zhao, Ilje Cho, Motoki Kino, Silke Britzen, David Hughes, Gopal Narayanan, Laurent Loinard, Antonio Hernandez, David Sanchez-Arguelles, Kazuhiro Hada, Remo Tilanus, Anton Zensus, Keiichi Asada, Dimitrios Psaltis, Feryal Ozel, Avery Broderick, Roman Gold, Raquel Fraga-Encinas, Andrew Chael, James Moran, Jose L. Gomez, Luciano Rezzolla, Michael Kramer, Kuo Liu, Gregory Desvignes, Robert Wharton, James Cordes, John Wardle, Shami Chatterjee, Scott Ransom, H. Rottmann, J. Wagner, Yurii Pidopryhora, Gunther Witzel, Jae-Young Kim, Dom Pesce, David James, Tomohisa Kawashima, Yosuke Mizuno, Jordy Davelaar, Kazi Rygl, Elisabetta Liuzzo

Project	Title	Authors
GMVA-19B-233	Imaging Jet and Magnetic Field near the Spinning SMBH in M87	Jae-Young Kim, Kazuhiro Hada, Thomas Krichbaum, Masanori Nakamura, Rusen Lu, Keiichi Asada, Tomohisa Kawashima, Jordy Davelaar, Kenji Toma, Kazunori Akiyama, Walter Alef, Rebecca Azulay, Lindy Blackburn, Katherine Bouman, Geoffrey Bower, Michael Bremer, Silke Britzen, Avery Broderick, Sunil Chandra, Ilje Cho, Geoffrey Crew, S. Doleman, Akihiro Doi, Heino Falcke, V. Fish, Gabriele Giovannini, Marcello Giroletti, Jose L. Gomez, Ruben Herrero-Illana, Paul Ho, Mareki Honma, David Hughes, Violette Impellizzeri, Makoto Inoue, Sara Issaoun, David James, Michael Janssen, Wu Jiang, Michael Johnson, Motoki Kino, Shoko Koyama, Rocco Lico, Michael Lindqvist, Elisabetta Liuzzo, Andrei Lobanov, Nicholas MacDonald, Sera Markoff, Ivan Marti-Vidal, Alan Marscher, Satoki Matsushita, Jonathan McKinney, Hugo Messias, Shin Mineshige, Yosuke Mizuno, Monika Moscibrodzka, Hiroshi Nagai, Gopal Narayanan, Scott Noble, Monica Orienti, Yurii Pidopryhora, Oliver Porth, Hung-Yi Pu, Luciano Rezzolla, Eduardo Ros, H. Rottmann, Kazi Rygl, David Sanchez-Arguelles, Tuomas Savolainen, Karl-Friedrich Schuster, Zhiqiang Shen, Hotaka Shiokawa, Fumie Tazaki, Pablo de Vicente, John Wardle, Maciek Wielgus, Anton Zensus
GMVA-20A-349	Search for candidate twin-jet sources at 86GHz	Anne-Kathrin Baczko, Dhanya Nair, Dongjin Kim, Biagina Boccardi
003-20	The molecular content of the diffuse interstellar medium	David Neufeld, Edith Falgarone, Maryvonne Gerin, Benjamin Godard, Peter Schilke, Karl M. Menten, Friedrich Wyrowski
004-20	Measurements of the gradients of isotope ratios $^{12}\text{C}/^{13}\text{C}$ and $^{14}\text{N}/^{15}\text{N}$ in our Galaxy from CN	Yaoting Yan, Christian Henkel, Jiangshui Zhang, Jinjin Xie, Yan Gong, Kai Yang, Hongzhi Yu, Jialiang Chen, Youxin Wang
005-20	Derive accurate $^{12}\text{C}/^{13}\text{C}$ ratio with HCCCN and its isotopic lines	Junzhi Wang, Bo Zhang, Shu Liu, Juan Li
006-20	Dust and gas evolution in two prestellar GEMS cores of TMC1	Carsten Kramer, Asuncion Fuente, Paola Caselli, Santiago Garcia-Burillo, Rafael Bachiller, Valentine Wakelam, Nuria Marcelino, Izaskun Jimenez-Serra, Jason Kirk, Jaime Pineda, Belen Tercero, Pierre Gratier, Alvaro Hacar, Sandra Trevino-Morales, Tony Mroczkowski, Charles Romero, Ana Chacon-Tanarro, Mario Tafalla, David Navarro Almaya, Marina Rodriguez Baras
007-20	NIKA2 insights into the dust evolution in prestellar cores	Isabelle Ristorcelli, Mika Juvela, Karine Demyk, Nathalie Ysard, Deborah Paradis, Julien Montillaud, Jean-Philippe Bernard, Alessia Ritacco, Nicolas Ponthieu, V.-M. Pelkonen, Tie Liu, Peregrine McGehee, Helene Roussel, R. Paladini, Alexy Louis
008-20	Influence of the environment on the molecular complexity of prestellar cores	Charlotte Vastel, Chenlin Zhou, Julien Montillaud, Cecilia Ceccarelli
009-20	The onset of collapse in a magnetized core	Felipe Alves, Paola Caselli, Elena Redaelli, Silvia Spezzano, Bo Zhao, Maria Maureira, Valerio Lattanzi, Luca Bizzocchi, Olli Sipilä
010-20	Characterizing the velocity fluctuations along molecular filaments	Philippe Andre, Hamza Ajeddig, Doris Arzoumanian, Yoshito Shimajiri, Shuichiro Inutsuka
011-20	Tracing the evolutionary stage of starless-cores through deuteration fraction and isotopically substituted molecules	Gisela Esplugues, Asuncion Fuente, David Navarro Almaya, Marina Rodriguez Baras, Izaskun Jimenez-Serra, Marcelino Agundez, Tomas Alonso-Albi, Rafael Bachiller, Paola Caselli, Benoit Commercon, Santiago Garcia-Burillo, Maryvonne Gerin, Barbara Michela Giuliano, Javier R. Goicoechea, Alvaro Hacar, Jason Kirk, Carsten Kramer, Valerio Lattanzi, Jean-Christophe Loison, Nuria Marcelino, Rafael Martin-Domenech, Guillermo M. Munoz Caro, Jaime Pineda, Evelyne Roueff, Pablo Riviere-Marichalar, Octavio Roncero, Mario Tafalla, Belen Tercero, Sandra Trevino-Morales, Derek Ward-Thompson, Valentine Wakelam, Stephanie Cazaux, Romane Le Gal, Silvia Spezzano, Luca Bizzocchi
012-20	First evidence for the extreme fractionation of ammonia in pre-stellar cores	Pierre Hily-Blant, Guillaume Pineau des Forêts, Alexandre Faure, Victor de Souza Magalhaes, Lydie Bonal, David Flower, Thomas R. Govers, Dahbia Talbi, Olivier Poch
013-20	O-bearing vs. N-bearing complex organic chemistry in starless cores	Izaskun Jimenez-Serra, Paola Caselli, Serena Viti, Silvia Spezzano, Nuria Marcelino, Anton Vasyunin
014-20	A search for molecular complexes in space: the van der Waals complex CO-CO and the charge transfer complex Ar-N <sub>2</sub> <sup>+</sup>	Alexey Potapov, Thomas Henning, Harold Linnartz
016-20	Origin of enhanced DCO <sup>+</sup> in cold molecular clouds	Shu Liu, Junzhi Wang
017-20	Mapping Observation of Molecular Clumps with Characteristic Infall Profile	Yang Yang, Zhibo Jiang, Zhiwei Chen, Yiping Ao, Andrey Sobolev
018-20	Is H <sub>2</sub> S tracing the snowline in cold cores?	David Navarro Almaya, Asuncion Fuente, Evelyne Roueff, Paola Caselli, Carsten Kramer, Mario Tafalla, Santiago Garcia-Burillo, Rafael Bachiller, Maryvonne Gerin, Stephanie Cazaux, Valentine Wakelam, Nuria Marcelino, Marcelino Agundez, Izaskun Jimenez-Serra, Tomas Alonso-Albi, Derek Ward-Thompson, Jason Kirk, Jaime Pineda, Belen Tercero, Pierre Gratier, Alvaro Hacar, Guillermo M. Munoz Caro, Sandra Trevino-Morales, Valerio Lattanzi, Rafael Martin-Domenech, Jean-Christophe Loison, Ana Chacon-Tanarro, Barbara Michela Giuliano, Octavio Roncero, Pablo Riviere-Marichalar, Romane Le Gal, Gisela Esplugues, Silvia Spezzano, Marina Rodriguez Baras
020-20	Extended SiO Emission in IRDCs: Tracing the Assembly of Massive Clumps?	Wonju Kim, Gary Fuller, Fabien Louvet, Nicolas Peretto, Adam Avison, Di Li, Ken'ichi Tatematsu, Jinjin Xie, Bethany Jones, James Urquhart
021-20	Complex Organic vs. Warm Carbon Chain Molecules in High Mass Star Forming Regions	Sandrine Bottinelli, Rene Plume, Emmanuel Caux, Bhaswati Mookerjee, Pamela Freeman



Project	Title	Authors
022-20	Measuring the Galactic sulfur isotope ratios toward massive star forming regions: a radial $^{32}\text{S}/^{34}\text{S}$ gradient?	Hongzhi Yu, Jiangshui Zhang, Yaoting Yan, Jialiang Chen, Youxin Wang
024-20	Mapping the $\text{HCO}^+$ gas irradiated by an X-ray-luminous bomb in the Galaxy	Ping Zhou, Xin Zhou, Maria Arias, Bon-Chul Koo, Yong-Hyun Lee, Jacco Vink
027-20	A second source with the elusive $\text{HOOH}$ molecule: Confirmation toward S 140	Karl M. Menten, Arshia Jacob, Henrik Olofsson, Yan Gong, Per Bergman
028-20	Understanding the initial conditions of massive star formation induced by cloud-cloud collisions.	Giuliana Cosentino, Izaskun Jimenez-Serra, Francesco Fontani, Paola Caselli, Serena Viti, Jonathan Tan, Jonathan Henshaw, Shaoshan Zeng, Chi Yan Law
029-20	Unveiling the cold material in high-mass star formation regions	Bilal Ladjelate, Frederique Motte, Pierre Didelon, Fabien Louvet, Sylvain Bontemps, Nicola Schneider, Caroline Gieser
031-20	Large scale cloud properties of Cygnus X	Friedrich Wyrowski, Henrik Beuther, Karl M. Menten, Gisela Ortiz Leon, Antonio Hernandez-Gomez, Thanh Dat Hoang, Sumeyye Suri, Caroline Gieser, Nicola Schneider, Timea Csengeri, Sylvain Bontemps, Frederique Motte, Jan Martin Winters, Ka Tat Wong, Nichol Cunningham, Wonju Kim
033-20	Mapping the $^{18}\text{O}/^{17}\text{O}$ Isotope Abundance Ratio in the Galactic Center	Pablo Garcia, Martin Steinke, Robert Simon
034-20	SN-driven star formation in CMa?	Bertrand Lefloch, Jane Gregorio-Hetem, Jacques Lepine, Beatriz Fernandes, Thierry Montmerle
035-20	Ionisation triggered by the HB3 supernova remnant: combining FERMI and IRAM	Valentine Wakelam, Pierre Gratier, Marianne Lemoine, Nathalie Brouillet, E. Dartois, Marin Chabot, Marie-Helene Grondin, Jean-Christophe Loison
036-20	Cosmic rays and shocked gas around a hadronic source	Rebeca Aladro, Rolf Gusten, Denise Riquelme, Serena Viti, Helmut Wiesemeyer, Antoine Gusdorf
037-20	Characterizing the region that interacts with gamma-rays in the IC443 SNR	Pierre Dell'Ova, Maryvonne Gerin, Denise Riquelme, Rolf Gusten, Martin Houde, Marco Padovani, Alexandre Marcowith, Antoine Gusdorf, Alessia Ritacco
038-20	Characterizing the Disk Fraction of M Dwarfs	William Schap, Elizabeth Lada, Adam Ginsburg, Carlos Roman-Zuniga, Matthew De Furio
039-20	Spectral inversion in SED's of debris disks: a signature of the collisional cascade of planetesimals?	Jean-Francois Lestrade, Jean-Charles Augereau, Mark Booth, Bilal Ladjelate, Charlene Lefevre
040-20	Circumstellar chemistry of X-ray emitting AGB stars	Carmen Sanchez Contreras, Raghvendra Sahai, Guillermo Quintana-Lacaci, Marcelino Agundez, Jose Cernicharo, Luis Velilla Prieto
041-20	The O-rich to C-rich transition in AGB stars	Marcelino Agundez, Jose Pablo Fonfria, Sarah Massalkhi, Jose Cernicharo
042-20	The molecular content of post-AGB disks	Ivan Gallardo Cava, Miguel Gomez-Garrido, Valentin Bujarrabal, Javier Alcolea, Miguel Santander-Garcia
044-20	Forsaken pre-Planetary Nebulae: CO emission observations	Carmen Sanchez Contreras, Javier Alcolea, Valentin Bujarrabal, Guillermo Quintana-Lacaci, Wouter Vlemmings, Raghvendra Sahai, Elvire De Beck, Joel Kastner, Daniel Tafoya, Andres Perez-Sanchez, Albert Zijlstra, Foteini Lykou, Bruce Balick, Hans Van Winckel, Matt Redman
045-20	New revelations on the nature of the 21- $\mu\text{m}$ emission feature in protoplanetary nebulae	Jose Jairo Diaz-Luis, Javier Alcolea, Domingo Anibal Garcia Hernandez, Valentin Bujarrabal, Arturo Manchado
046-20	Exploring the Chemical Complexity of the Unusual Planetary Nebula NGC 6445	Deborah Rose Schmidt, Lucy Ziurys
049-20	Search for the molecular clouds associated with GeV source Fermi J1913+0515	Jian Li, Diego Torres, Qiancheng Liu, Ruoyu Liu, Yang Su, Emma de Ona Wilhelmi, Matthew Kerr
050-20	3D CO and dust mapping towards Aql X-1	Sebastian Heinz
051-20	Amount of molecular gas in NGC205	Frank Israel
053-20	Mapping molecular gas in the third closest massive spiral galaxy M81	Zongnan Li, Ruben Garcia-Benito, Christine Wilson, Zhiyuan Li
054-20	Resolving $\text{N}_2\text{H}^+$ (1-0) emission for the first time across the disk of a normal, star-forming galaxy: NGC6946.	Maria Jesus Jimenez Donaire, Mario Tafalla, Ana Chacon-Tanarro, Antonio Usero, Axel Garcia-Rodriguez, Frank Bigiel, Jens Kauffmann, Ivana Beslic, Diederik Kruijssen, Thomas Williams, Toshiki Saito, Daizhong Liu, Miguel Querejeta, Ashley Thomas Barnes, Eva Schinnerer, Melanie Chevance, Simon Glover, Jerome Pety, Johannes Puschignig
055-20	Deriving carbon abundance ratios for the first time in a normal disk galaxy: NGC 6946	Maria Jesus Jimenez Donaire, Antonio Usero, Mario Tafalla, Frank Bigiel, Adam Leroy, Glen Petitpas, Amanda Kepley, Johannes Puschignig
056-20	The diffuse dust emission in NGC4214	Katharina Lutz, Caroline Bot, Chris Clark
058-20	On the formation of massive stars in intergalactic clouds	Edvige Corbelli, Filippo Mannucci, G. Cresci, David Thilker
061-20	Characterizing the millimeter emission in nearby galaxies with NIKA-2	Isabella Lamperti, Amelie Saintonge, Ilse De Looze, Elias Brinks, Christine Wilson, Mark T. Sargent, Ho Seong Hwang, Christopher Clark, Matthew Smith, Lihwai Lin
062-20	Do Changing-look AGNs reside in the gas-rich environment?	Xiaoling Yu, Yong Shi, Jianhang Chen, Zhiyu Zhang, Xue Ge
063-20	Molecular gas in an HI-bearing ultra-diffuse galaxy	Chengpeng Zhang, Qiong Li, Ran Wang

Project	Title	Authors
064-20	Time sequence of merging galaxies, and evolution path at $z=0.07$	Barbara Mazzilli-Ciraulo, Anne-Laure Melchior, Daniel Maschmann, Françoise Combes
065-20	A survey of molecular gas in NLSy1 Galaxies with X-ray Ultra Fast Out-flows	Anna Lia Longinotti, Quentin Salome, Manuela Bischetti, Maria Vittoria Zanchettin, Olga Vega, Yair Krongold, Miguel Sanchez Portal, Chiara Feruglio
066-20	Cooling filaments in the high-velocity merging group NGC 6338	Ewan O'Sullivan, Gerrit Schellenberger, Françoise Combes, Laurence P. David, Jan M. Vrtilik, Douglas Burke, Lihwai Lin, Hsi-An Pan
068-20	Comparing molecular gas in fast and slowly rotating super spiral galaxies	Ute Lisenfeld, David Frayer, Phil Appleton, Patrick Ogle, Lauranne Lanz
069-20	Monitoring AGN with Polarimetry at the IRAM 30-meter telescope	Ivan Agudo, Carolina Casadio, Efthalia Traianou, Jae-Young Kim, Nicholas MacDonald, Thomas Krichbaum, Eduardo Ros, Anton Zensus, Helmut Wiesemeyer, Clemens Thum, Ioannis Myserlis, Antonio Fuentes, Jose L. Gomez, Alan Marscher, Svetlana Jorstad, Emmanouil Angelakis, Venkatesh Ramakrishnan
071-20	NIKA2 Sunyaev-Zel'dovich Imaging of the AGN-driven X-ray Cavities in MS 0735.6+7421	Tony Mroczkowski, Paola Andreani, Robert Laing, Brian Mason, Daniel Marrone, Kaustuv Basu, Etienne Pointecouteau, P. Nulsen, Luca Di Mascolo, Eugene Churazov, Frederic Mayet, Remi Adam, Helen Russell, Simon Dicker, Mark Devlin, Charles Romero, Jean-Paul Breuer, Norbert Werner
072-20	First Characterisation of the Gas Content within a New and Promising Strong Lensing Cluster	Florian Ruppin, Alexandre Beelen, Raoul Canameras, Francois-Xavier Desert, Florian Keruzore, Guilaine Lagache, Marceau Limousin, Juan Macias-Perez, Frederic Mayet, Laurence Perotto, Nicolas Ponthieu
073-20	Molecular gas in cluster galaxies at intermediate redshift: the case of Cl0024+1652	Miguel Sanchez Portal, Angel Bongiovanni, Jordi Cepa, Ana M. Perez Garcia, Carmen P. Padilla-Torres, J. Ignacio Gonzalez Serrano, Irene Pintos-Castro, Ricardo Perez Martinez, Irene Cruz-Gonzalez, Alenka Negrete, Zeleke Beyoro-Amado, Mirjana Povic
074-20	First Map of the Gas Temperature in a Galaxy Cluster using the Relativistic Sunyaev-Zel'dovich Effect	Florian Ruppin, Francois-Xavier Desert, Florian Keruzore, Juan Macias-Perez, Frederic Mayet, Laurence Perotto, Nicolas Ponthieu
075-20	Intracluster medium properties of the first massive clusters selected independently of their baryon content	Stefano Andreon, Alberto Moretti, Bilal Ladjelate, Ginevra Trinchieri
076-20	Sunyaev-Zel'dovich follow-up of XXL galaxy clusters at $z \sim 1$ with NIKA2	Marina Ricci, Remi Adam, Bruno Altieri, Mark Birkinshaw, Alberto Cappi, Dominique Eckert, Sotiria Fotopoulou, Fabio Gastaldello, Oliver Hahn, Cathy Horellou, Elias Koulouridis, Adam Mantz, Ben Maughan, Sophie Maurogordato, Florian Pacaud, Emanuela Pompei, Chiara Ferrari, Malcolm Bremer
077-20	High Angular Resolution tSZ Mapping of the Most Massive Galaxy Clusters at $z > 0.9$	Mark Brodwin, Marshall Bautz, Bandon Decker, Daniel Marrone, Michael McDonald, Alexandra Pope, Adam Stanford, Dominika Wylezalek, Florian Ruppin, Frederic Mayet, Laurence Perotto, Juan Macias-Perez, Florian Keruzore
078-20	Redshift scan of gravitationally lensed galaxies	Denis Burgarella, Firas Mazyed, Veronique Buat, Stephen Serjeant, Tomo Goto
079-20	Gas and grain interactions: unraveling the methanol story with JWST and NOEMA	Valentine Wakelam, Pierre Gratier, Daniel Harsono, Jacqueline Keane, Adwin Boogert, Jennifer Noble, E. Dartois, Marin Chabot
080-20	The protostellar and interstellar content of the IC443 SNR	Antoine Gusdorf, Maryvonne Gerin, Marco Padovani, Denise Riquelme, Martin Houde, Fabien Louvet, Bilal Ladjelate, Pierre Dell'Ova, Rolf Gusten
081-20	What is the true evolutionary state of the First Hydrostatic Core candidate CB 17 MMS?	Maria Maureira, Paola Caselli, Hector Arce, Jaime Pineda, Stephanie Spear, Dominique Segura-Cox
082-20	Chemical and dynamical evolution of starless cores	David Navarro Almaida, Asuncion Fuente, Evelyne Roueff, Paola Caselli, Carsten Kramer, Mario Tafalla, Santiago Garcia-Burillo, Rafael Bachiller, Maryvonne Gerin, Stephanie Cazaux, Valentine Wakelam, Nuria Marcelino, Roberto Neri, Marcelino Agundez, Izaskun Jimenez-Serra, Rachel Friesen, Tomas Alonso-Albi, Jaime Pineda, Silvia Spezzano, Sandra Trevino-Morales, Valerio Lattanzi, Jean-Christophe Loison, Ana Chacon-Tanarro, Pablo Riviere-Marichalar, Marina Rodriguez Baras, Romane Le Gal, Gisela Esplugues
083-20	Circumstellar environment of new FUor: Gaia18dvy	Fernando Cruz-Saenz de Miera, Agnes Kospal, Peter Abraham, Zsafia Nagy, Orsolya Feher
084-20	The origin of complex organic molecules in the young protostellar binary system Aqu-mm2	Yan Gong, Yuxin Lin, Arnaud Belloche, Karl M. Menten, Christian Henkel, Friedrich Wyrowski, Fajun Du, Miaomiao Zhang
085-20	Evolution of a massive clump at the intersection of colliding filaments	Julien Montillaud, Cecile Favre, Charlotte Vastel, Mika Juvela, Isabelle Ristorcelli, Tie Liu, David Cornu, Rebeka Bogner
086-20	How to make massive protostellar cluster?	Shanghuo li, Qizhou Zhang, Ian Stephens, Junzhi Wang, Kai Yang, Thushara Pillai, Fei Li
087-20	Disruption or Assembly? The Origin of the Widespread SiO Emission in a Massive IRDC	Wonju Kim, Gary Fuller, Nichol Cunningham, Nicolas Peretto, Fabien Louvet, Di Li, Jinjin Xie, Bethany Jones, Ken'ichi Tatematsu, Adam Avison, James Urquhart, Ka Tat Wong
088-20	Resolving Ongoing Star Formation in Orion A	Sumeyye Suri, Shuo Kong, Alvaro Sanchez-Monge, Hector Arce, Volker Ossenkopf-Okada, John Bally, Henrik Beuther
089-20	First cloud-scale measurement of $N_2H^+$ in a normal star-forming galaxy	Axel Garcia-Rodriguez, Antonio Usero, Maria Jesus Jimenez Donaire, Frank Bigiel, Ivana Beslic, Johannes Puschign, Melanie Chevance, Diederik Kruijssen, Ashley Thomas Barnes, Eva Schinnerer, Toshiki Saito, Christopher Faesi, Daizhong Liu, Andreas Schrubba, Miguel Querejeta, Adam Leroy, Cinthya Herrera Contreras, Jerome Pety, Simon Glover
D01-20	Investigation of the Great Comet of 2020: C/2020 F3 (NEOWISE)	Nicolas Biver, Dominique Bockelee-Morvan, Jacques Crovisier, Raphael Moreno, Gabriel Paubert, Jeremie Boissier, Katia Hadraoui, Herve Cottin

Project	Title	Authors
D03-20	B0218+35 in flare: An exceptional laboratory for AGN jet physics at the highest energies	Ivan Agudo, Ioannis Myserlis, Carolina Casadio, Julian Sitarek
D04-20	NIKA2 follow-up of the Swift GRB20102412 afterglow	Angel Bongiovanni, Bilal Ladjelate, Miguel Sanchez Portal
D05-20	Is phosphine present in Venus' atmosphere?	Raphael Moreno, Carsten Kramer, Emmanuel Lellouch, Roberto Neri, Gabriel Paubert, Miguel Sanchez Portal
GMVA-20B-178-MH5	Ultra-high-resolution Imaging of the Nearest Gamma-ray Emitting NLSy1 1H0323+342	Kazuhiro Hada, Filippo D'Ammando, Akihiro Doi, Monica Orienti, Kiyooki Wajima, Gabriele Giovannini, Marcello Giroletti, Bong Won Sohn, Mahito Sasada, Lang Cui, Keiichi Asada, Masanori Nakamura, Valentina Vacca
GMVA-20B-179-MI9	Ultra-deep Imaging the Acceleration and Collimation Zone in the jet of 4C+73.18	Kunwoo Lee, Jongho Park, Masanori Nakamura, Sascha Trippe
GMVA-20B-243-MK16	Extreme blazars under the GMVA microscope	Matthias Kadler, Eduardo Ros, Marcello Giroletti, Daniela Dorner, Shoko Koyama, Thomas Krichbaum, Rocco Lico, Karl Mannheim, Roopesh Ojha, Julian Sitarek, Luis Wachter
GMVA-20B-339-MK18	The nature of molecular gas in the jet- launching region of young radio galaxy.	Dongjin Kim, Thomas Krichbaum, Biagina Boccardi, Alan L. Roy, Eduardo Ros, Anton Zensus, Anne-Kathrin Baczko, Jae-Young Kim, Violette Impellizzeri, Uwe Bach, Matthias Kadler

## NOEMA INTERFEROMETER

Project	Title	Authors
D20AA	A novel method to identify the most massive, dusty starburst galaxies and AGN/starburst composites at $z > 4$ with IRAM and LOFAR?	Nicole Nesvadba, Rachel Cochrane, Philip Best, Rohit Kondapally, Kenneth Duncan
D20AB	Completing z-GAL: the Comprehensive Redshift Survey of Bright Herschel Galaxies	Pierre Cox, Tom Bakx, Helmut Dannerbauer, Roberto Neri
D20AC	The nucleus and inner coma of the great comet C/2020 F3 (NEOWISE)	Jeremie Boissier, Dominique Bockelee-Morvan, Nicolas Biver, Raphael Moreno, Katia Hadraoui, Jacques Crovisier, Martin Cordiner, Stefanie Milam
D20AD	Monitoring the Abnormal Behaviour of Betelgeuse	Thavisha Dharmawardena, Karl M. Menten, Ka Tat Wong, Peter Scicluna, Steve Mairs, Albert Zijlstra, Iain McDonald
D20AE	The Evolving Pulsar Wind Nebula in SN 2012au	Joseph Bright, Raffaella Margutti, Deanne Coppejans, Giacomo Terreran, Lindsay DeMarchi
D20AF	Search for Millimeter Emission From AT2020xnd, an AT2018cow Analog	Anna Ho, Daniel Perley, Yuhan Yao
D20AG	Request for Continued Observations of AT2020xnd: Establishing A New Class of Millimeter-Bright Transients	Anna Ho, Yuhan Yao, Daniel Perley, David Kaplan, Dougal Dobie, Andrew O'Brien
E19AA	Confirming the detection of the [CII] line in the $z = 7.12$ galaxy GN-108036	Rodrigo Herrera-Camus, Linda Tacconi, Natascha Förster Schreiber, Reinhard Genzel, Dieter Lutz, Alessandra Contursi
E19AB	Water deuteration in the Class 0 protostar CepE-mm	Bertrand Lefloch, Juan Ospina-Zamudio, Cecile Favre, Jaime Pineda, Dominique Segura-Cox, Ana Lopez-Sepulcre, Claudio Codella, Paola Caselli, Cecilia Ceccarelli
E19AD	Gas and Dust Properties in a Red Quasar Firstly Discovered at $z > 7$	Seiji Fujimoto, Gabriel Brammer, Johan Fynbo, Georgios Magdis, Sune Toft, Charles Steinhardt, Francesco Valentino, Isabella Cortzen
L19MA	Galactic star formation MIOP: From clouds to cores	Karl M. Menten, Friedrich Wyrowski, Henrik Beuther, Gisela Ortiz Leon, Thanh Dat Hoang, Antonio Hernandez-Gomez, Sumeyye Suri, Caroline Gieser, Nicola Schneider, Timea Csengeri, Sylvain Bontemps, Frederique Motte, Nichol Cunningham, Jan Martin Winters, Ka Tat Wong, Wonju Kim
L19MB	Redshift determination of high-redshift Herschel lensed galaxies	Alain Omont, Roberto Neri, Alexandre Beelen, Steve Eales, Tom Bakx, R. Gavazzi, Simon Dye, Rob Ivison, Ismael Perez-Fournon, Ivan Oteo, Helmut Dannerbauer, Frank Bertoldi, Matthew Lehnert, Chentao Yang, Zhiyu Zhang, Gianfranco De Zotti, Dominik A. Riechers, David Clements, Lucia Marchetti, Joshua Greenslade, Melanie Krips, Catherine Vlahakis, Michal J. Michalowski, Andrew Baker, Paul van der Werf, Pierre Cox
L19ME	From Protostars to Planet-Forming Disks	Paola Caselli, Thomas Henning, Jaime Pineda, Dominique Segura-Cox, Dmitry Semenov, Bo Zhao, Mario Tafalla, Grigori Smirnov-Pinchukov, Cecilia Ceccarelli, Edwige Chapillon, Nichol Cunningham, Anne Dutrey, Stephane Guilloteau, Izaskun Jimenez-Serra, Ana Lopez-Sepulcre, Sebastian Marino, Maria Maureira, Roberto Neri, Vincent Pietu, Asuncion Fuente
L19MC	Search for molecular absorption in AGNs.	Dongjin Kim, Rainer Mauersberger, Thomas Krichbaum, Biagina Boccasardi, Anton Zensus, Michael Bremer, Christian Henkel, Françoise Combes
L19MD	NOEMA3D: a Comprehensive Census of the Molecular Gas Distribution and Kinematics of Massive Main-Sequence Star Forming Galaxies at the Peak and Winding Down of Galaxy Formation Activity	Reinhard Genzel, Roberto Neri, Linda Tacconi, Natascha Förster Schreiber, Dieter Lutz, Karl-Friedrich Schuster, Alessandra Contursi, Melanie Krips, Stefano Berta, Fabian Walter, Axel Weiss, T. Naab, Richard Davies, Minju Lee, Sedona Price, Thomas Taro Shimizu, Eckhard Sturm, Hannah Uebler, Françoise Combes, David Elbaz, Pierre Cox, Santiago Garcia-Burillo, Antonio Usero, Alberto D. Bolatto, Monica Rubio, Tadayuki Kodama, Rodrigo Herrera-Camus, Ken-Ichi Tadaki, Alvio Renzini, Amiel Sternberg, Andreas Burkert, Avishai Dekel, S. Wuyts, Cinthya Herrera Contreras
M18AB	A Comprehensive NOEMA Redshift Survey of the Brightest Herschel Galaxies	Pierre Cox, Tom Bakx, Helmut Dannerbauer, Roberto Neri, Alain Omont, Steve Eales, Rob Ivison, Matthew Lehnert, R. Gavazzi, Stephen Serjeant, Lucia Marchetti, Mattia Negrello, Simon Dye, Dominik A. Riechers, Melanie Krips, Asantha Cooray, Guilaine Lagache, Ismael Perez-Fournon, Ivan Oteo, David Hughes, Hugo Messias, Veronique Buat, Andrew Baker, Catherine Vlahakis, Paul van der Werf, Loretta Dunne, Chentao Yang, Stefano Berta, Alexandre Beelen, Axel Weiss, Cinthya Herrera Contreras
M19AA	The First Cloud-by-Cloud Dense Gas Map of an External Galaxy	Eva Schinnerer, Frank Bigiel, Jérôme Pety, Antonio Usero, Adam Leroy, Annie Hughes, Miguel Querejeta, Cinthya Herrera Contreras, Ashley Thomas Barnes, Ilin Lazar, Cosima Eibensteiner, Jakob den Brok, Daizhong Liu, Johannes Puschignig, Toshiaki Saito, Axel Garcia-Rodriguez, Sharon Meidt, Eric Emsellem, Jonathan Henshaw, Melanie Chevance, Diederik Kruijssen, Alex Hygate, Andreas Schrubba, Maria Jesus Jimenez Donaire
S19AW	Ionization Structure of Protoplanetary Disks: Is there a connection with turbulence?	Grigori Smirnov-Pinchukov, Richard Teague, Dmitry Semenov, Stephane Guilloteau, Thomas Henning, Anne Dutrey, Mario Flock
S19BB	Testing time-dependent chemistry in the expanding CSE IRC+10216	Michel Guélin, Jose Cernicharo, Marcelino Agundez, Jan Martin Winters, Carl Gottlieb, Guillermo Quintana-Lacaci
S19BM	CO(1-0) in a Candidate Accretion-Induced Starburst in a Local Dwarf Galaxy	Monica Rubio, Bruce Elmegreen, Cinthya Herrera Contreras, Debra Elmegreen, Jorge Sanchez Almeida, Casiana Munoz-Tunon, Elias Brinks, Deidre Hunter, Leslie Hunt, Juan Cortes

Project	Title	Authors
S19BP	Mapping molecular gas in one of the most extended Halpha nebulae in X-ray cool cores	Ming Sun, Alastair Edge, Francoise Combes, William R. Forman, Hao Chen
S19BV	Probing the molecular gas content of galaxies in an over-dense group at $z \sim 0.7$ : a test case for environmental quenching	Thierry Contini, Jonathan Freundlich, Benoit Epinat, Philippe Salomé, Avishai Dekel, G. Soucaill, Léo Michel-Dansac, Sandro Tacchella, Leindert Boogaard
S19BY	CO survey of the most strongly lensed galaxies	Johan Richard, Miroslava Dessauges-Zavadsky, Francoise Combes, Frederic Boone, Daniel Schaerer, Vera Patricio, Wiphu Rujopakarn, John Chisholm
S19CC	At the end of the Cosmic Noon: Molecular gas census in intermediate-redshift lensed quasars	Matus Rybak, Jacqueline Hodge, Paul van der Werf, Gabriela Calistro Rivera, Hannah Stacey, John Mckean
S19DM	Unraveling the powering mechanism of the cold ISM in $z > 6$ quasars	Roberto Decarli, Bram Venemans, Fabian Walter, Mladen Novak, Eduardo Banados, Dominik A. Riechers, Axel Weiss, Feige Wang, Jinyi Yang, Xiaohui Fan, Jianan Li, Ran Wang, Antonio Pensabene
S20AA	Gas and grain interactions: unraveling the methanol story with JWST and NOEMA	Valentine Wakelam, Pierre Gratier, Daniel Harsono, Jacqueline Keane, Adwin Boogert, Jennifer Noble, E. Dartois, Marin Chabot
S20AB	NOEMA-SPONGE: the role of neutral hydrogen in diffuse interstellar chemistry	Daniel Rybarczyk, Snezana Stanimirovic, Claire Murray, Ellen Zweibel, Shuichiro Inutsuka, John Dickey, Antoine Gusdorf, Anne Klitsch, Celine Peroux, John Wu, Martin Zwaan
S20AD	What is the true evolutionary state of the First Hydrostatic Core candidate CB 17 MMS?	Maria Maureira, Paola Caselli, Hector Arce, Jaime Pineda, Stephanie Spear, Dominique Segura-Cox
S20AE	Chemical and dynamical evolution of starless cores	David Navarro Almada, Asuncion Fuente, Evelyne Roueff, Paola Caselli, Carsten Kramer, Mario Tafalla, Santiago Garcia-Burillo, Rafael Bachiller, Maryvonne Gerin, Stephanie Cazaux, Valentine Wakelam, Nuria Marcelino, Roberto Neri, Marcelino Agundez, Izaskun Jimenez-Serra, Tomas Alonso-Albi, Jaime Pineda, Silvia Spezzano, Sandra Trevino-Morales, Valerio Lattanzi, Jean-Christophe Loison, Ana Chacón-Tanarro, Pablo Riviere-Marichalar, Marina Rodriguez Baras, Romane Le Gal, Gisela Esplugues
S20AH	Distinguishing between envelope and embedded disk chemistry of Class I YSOs	Romane Le Gal, Karin Öberg, Ana Lopez-Sepulcre, Charlotte Vastel, Jane Huang, Francois Menard, Charles Law, Bertrand Lefloch, Cecilia Ceccarelli, Cecile Favre, Eleonora Bianchi, Clement Baruteau, Asuncion Fuente, Pablo Riviere-Marichalar, Anaëlle Maury, David Navarro Almada, Edwin A. Bergin, Emmanuel Caux
S20AI	Evolution of a massive clump at the intersection of colliding filaments	Julien Montillaud, Cecile Favre, Charlotte Vastel, Mika Juvela, Isabelle Ristorcelli, Tie Liu, David Cornu, Rebeka Bögner
S20AJ	Hunting for the coldest cores in Cygnus-X	Keping Qiu, Yue Cao, Bo Hu, Junhao Liu
S20AL	Disruption or Assembly? The Origin of the Widespread SiO Emission in a Massive IRDC	Wonju Kim, Gary Fuller, Nichol Cunningham, Nicolas Peretto, Fabien Louvet, Di Li, Jinjin Xie, Bethany Jones, Ken'ichi Tatematsu, Adam Avison, James Urquhart, Ka Tat Wong
S20AM	Marking the End of Evolution: The association of class II methanol masers with high-mass star formation	Nichol Cunningham, Gary Fuller, Adam Avison, Alessio Traficante, Bethany Jones, Shari Breen, Wonju Kim
S20AR	CO as a Tracer of Pebble Growth and Drift in Protoplanetary disks	Ke Zhang, Edwin A. Bergin, Arthur Bosman
S20AT	A tale of two masses: HD and CO	Ewine F. Van Dishoeck, Alice Booth, Margot Leemker, Melissa McClure, Leon Trapman
S20AX	Dust properties, temperatures, and the HCN X-factor of individual Giant Molecular Clouds in the Andromeda Galaxy, using unique NOEMA/SMA synergies	Jan Forbrich, Charles Lada, Christopher Faesi, Glen Petitpas, Sebastien Viaene, Jérôme Pety, Jonathan Toomey
S20AZ	First cloud-scale measurement of $N_2H^+$ in a normal star-forming galaxy	Axel García-Rodríguez, Antonio Usero, Maria Jesus Jimenez Donaïre, Frank Bigiel, Ivana Beslic, Johannes Puschignig, Melanie Chevance, Diederik Kruijssen, Ashley Thomas Barnes, Eva Schinnerer, Toshiki Saito, Christopher Faesi, Daizhong Liu, Andreas Schrubba, Miguel Querejeta, Adam Leroy, Cinthya Herrera Contreras, Jérôme Pety, Simon Glover
S20BB	Searching for molecular gas in HI-rich red spirals	Jianhang Chen, Yong Shi, Zhiyu Zhang
S20BD	Mapping two Relic Compact Elliptical Galaxies	Francoise Combes, Philippe Salomé, Valeria Olivares
S20BH	Feedback from low luminosity radio AGN: Strong jet-ISM interaction in B2 0258+35	Suma Murthy, Pierre Guillard, Raffaella Morganti, Tom Oosterloo, Dipanjan Mukherjee
S20BJ	Probing Merger-driven Gas Inflows in Dual-AGNs	Meicun Hou, Zhiyuan Li, Zongnan Li, Xin Liu
S20BQ	A systematic search for ultra-bright strongly lensed galaxies in the Planck all-sky survey	Mattia Negrello, Gianfranco De Zotti, Matteo Bonato, Andrea Enia, Pierre Cox, Stefano Berta, Tiziana Trombetti, Carlo Burigana, Lucia Marchetti, Roberto Neri, Amvrosiadis Aristeidis, Alain Omont, Matthew Smith
S20BT	Tracing starburst HyLIRGs in host galaxies of high-z QSOs	Y. Sophia Dai, Alain Omont, Pierre Cox, Xue-Bing Wu, Rob Ivison, Chentao Yang, Roberto Neri, Belinda Wilkes, Jacqueline Bergeron, Melanie Krips
S20BV	How thermalized is the molecular ISM at $z \sim 2$ ?	Melanie Kaasinen, Daizhong Liu, Fabian Walter, Leindert Boogaard, Manuel Aravena, Ian Smail, Chelsea Sharon, Dominik A. Riechers, Gergo Popping
S20BY	Gas Properties in the Early Universe: collisional excitation or IR pumping in the Cloverleaf Quasar?	Michel Guélin, Carsten Kramer
S20BZ	Looking down the barrel through a multi-phase quasar outflow at high redshift with VLT and NOEMA	Pasquier Noterdaeme, Raghunathan Srianand, Francoise Combes, Sergei Balashev, Jens-Kristian Krogager, Peter Laursen, Neeraj Gupta

Project	Title	Authors
S20CA	Redshift Scans of Submillimeter Galaxies in the Hubble Frontier Fields: A Pilot Program	Logan Jones, Amy Barger, Lennox Cowie
S20CD	Unveiling the host galaxies of the most luminous quasars at $z \sim 3.5$	Jan-Torge Schindler, Bram Venemans, Fabian Walter, Eduardo Banados, Marcel Neeleman
S20CE	Coming out from the curtain: Molecular gas condition in an optical/near-IR dark sub-mm bright AGN host	Zhiyu Zhang, Chentao Yang, Chao-Wei Tsai, Natsuki H. Hayatsu, Ping Zhou, Rob Ivison
S20CK	Exploiting a snapshot survey of the 3,083 reddest Herschel sources to reveal distant protoclusters	Vinodiran Arumugam, Melanie Krips (NOEMA coordinator), Rob Ivison, Helmut Dannerbauer, Loretta Dunne, Malcolm Bremer, Tom Bakx, Seiji Fujimoto, Geraint Lewis, Jianhang Chen
S20CL	A Band 2 Follow-up to Candidate Protoclusters in NIKA2 Science Verification Field	Longji Bing, Alexandre Beelen, Guilaine Lagache, Matthieu Bethermin, Rémi Adam, Nicolas Ponthieu, Juan Macias-Perez, Alain Omont, Roberto Neri, Stefano Berta
S20CP	How fast could the Universe form a massive galaxy?	Pablo Pérez-González, Jesus Martin-Pintado, Helmut Dannerbauer, Giovanni Fazio, Guillermo Barro, Miguel Pereira Santaella, Belén Alcalde Pampliega, Ángela García Argumánez
S20CS	NOEMA line scans toward $z > 5$ candidate AzTEC-ALMA SMGs	Soh Ikarashi, Rob Ivison, Karina Caputi, Kotaro Kohno
S20CV	First insights into the ISM of the most distant radio galaxy at $z = 5.72$	Bram Venemans, Fabian Walter, Marcel Neeleman, Aayush Saxena, Eduardo Banados, Chris L. Carilli
S20CW	Probing the CO spectral line energy distributions (SLEDs) in two luminous quasars at $z \sim 6$	Jianan Li, Karl M. Menten, Frank Bertoldi, Fabian Walter, Roberto Neri, Alain Omont, Pierre Cox, Xiaohui Fan, Michael A. Strauss, Dominik A. Riechers, Ran Wang, Jeff Wagg, Desika Narayanan, Roberto Decarli, Eduardo Banados, Yali Shao, Yuanqi Liu, Qiong Li, Bram Venemans, Yu Gao, Chris L. Carilli
S20CY	The host galaxies of the most distant radio-loud quasars at $z > 6$	Eduardo Banados, Yana Khusanova, Sofia Rojas, Chiara Mazzucchelli, Bram Venemans, Roberto Decarli, Fabian Walter
S20DA	Dense Gas Content of Star-Forming Cores in the Best-Studied AGN Host and Starburst at $z \sim 6.5$	Dominik A. Riechers, Fabian Walter, Roberto Decarli, Axel Weiss, Pierre Cox, Roberto Neri
S20DB	Probing "Cosmic Dawn": The physical properties of a $z = 8.78$ galaxy	Nicolas Laporte, Frederic Boone, Richard Ellis, Guido Roberts-Borsani, Romain Meyer, Roberto Maiolino, Gareth Jones
W18BY	50pc imaging of the molecular outflow in M82	Nico Krieger, Fabian Walter, Axel Weiss, Adam Leroy, Alberto D. Bolatto, Laura Zschaechner, Sylvain Veilleux
W18CS	Probing the molecular gas content in galaxies with gas flows: a test case for self-regulated star formation models	Nicolas Bouche, Thierry Contini, Jonathan Freundlich, Léo Michel-Dansac, Ilane Schroetter, Johan Richard, Johannes Zabl
W19AA	Protostellar Chemistry and the Carbon Content of Terrestrial Worlds	Edwin A. Bergin, Jes Jorgensen, Ke Zhang, Thomas Rice, Merel van 't Hoff
W19AG	Envelope to Disk: The Composition of Accretion	Dominique Segura-Cox, Jaime Pineda, Paola Caselli, Anika Schmiedeke, Nichol Cunningham, Maria Maureira
W19AH	Ionization: explaining the split between big and small Protostellar Disks	Maria Maureira, Jaime Pineda, Dominique Segura-Cox, Paola Caselli, Bo Zhao
W19AI	Are disk asymmetries driven by large scale accretion flows?	Jaime Pineda, Anika Schmiedeke, Paola Caselli, Dominique Segura-Cox, Bo Zhao, Nichol Cunningham, Roberto Neri, Maria Maureira
W19AL	2MASS J0233+6156: a newly discovered eruptive star	Orsolya Feher, Agnes Kospal, Carlos Contreras Pena, Fernando Cruz-Saenz de Miera
W19AM	Caught in the act: Varying infall towards a periodically brightening protostar	Hendrik Linz, Bringfried Stecklum, Henrik Beuther, Alessio Caratti O Garatti, Marian Szymczak
W19AN	Catching the missing: NOEMA survey of massive cold cores in Cygnus-X	Keping Qiu, Yue Cao, Yuwei Wang
W19AP	Investigation for mass growth of massive young stellar objects by the feedback of companion gas clump	Chen Xi
W19AQ	AU-scale structure in the diffuse ISM: shocks and multi-phase nature	Daniel Rybarczyk, Snezana Stanimirovic, Ellen Zweibel, John Dickey, Shuichiro Inutsuka, Antoine Gusdorf
W19AR	The protostellar and interstellar content of the IC443 SNR	Antoine Gusdorf, Pierre Dell'Ova, Maryvonne Gerin, Fabien Louvet, Denise Riquelme, Marco Padovani, Martin Houde, Bilal Ladjelate
W19AU	The Molecular Content of Small Protoplanetary Disks	Vincent Pietu, Jean-Paul Melisse, Anne Dutrey, Stephane Guilloteau, Edwige Chapillon
W19AV	GG Tau A: a 3mm Large spectral Survey in the densest binary T Tauri disk	Anne Dutrey, Edwige Chapillon, Stephane Guilloteau, Vincent Pietu, Ya-Wen Tang, Jeffrey Bary, Audrey Coutens, Diep Pham Ngoc, Liton Majumdar, Emmanuel Di Folco, Otoniel Denis-Alpizar, Jean-Paul Melisse, Tracy Beck, Thi Phuong Nguyen
W19AW	Searching for Cold Circumbinary Disks Around High Mass X-Ray Binaries	Kevin Fogarty, Dimitri Mawet, Julie Hlavacek-Larrondo, Jack Steiner, Andy C. Fabian, Dom Walton, Lauren Weiss, David Lafreniere, Myriam Prasow-vâmond
W19AX	Streams, disk and chemistry in the S-type AGB star RS Cnc	Thibaut Le Bertre, Jan Martin Winters, Ka Tat Wong, Do Thi Hoai, Pham Thi Tuyet Nhung, Pham Tuan-Anh, Pierre Lesaffre, Diep Pham Ngoc, Pierre Darriulat
W19BJ	CO observation of a star-forming SO galaxy PGC 34107	Xue Ge, Qiusheng Gu, Zhiyu Zhang, Rubén García-Benito, Mengyuan Xiao, Zhengyi Chen
W19BK	Mapping Molecular Gas in Shell Galaxies	Brisa Mancillas, Françoise Combes, Pierre-Alain Duc

Project	Title	Authors
W19BL	SFE distributions in interacting galaxies -- Difference between S+E and S+S pairs	Cong Kevin Xu, Ute Lisenfeld, Yu Gao, Min Yun
W19BN	Search for a cool accretion disk around M31 black hole	Anne-Laure Melchior, Françoise Combes, Igor Chilingarian, Ivan Katkov, Daniel Maschmann
W19BR	A CO survey and molecular gas scaling relations of the SUBWAYS AGN sample	Chiara Feruglio, Marcella Brusa, Stefano Bianchi, Francesco Tombesi, Smita Mathur, Fabio La Franca, Cristian Vignali, Yair Krongold, Raffaella Morganti, Enrico Piconcelli, Anna Lia Longinotti, Fabrizio Fiore, Michele Perna, Gerard Kriss, Ehud Behar, Massimo Gaspari, Alessandro Marconi
W19BS	Molecular gas content in post starburst E+A galaxies with massive AGN-driven winds	Richard Davies, Dieter Lutz, H. Netzer, Dalya Baron
W19BV	Unveiling the MS to SB transition with a sample of intermediate redshift ULIRGs	Santiago Garcia-Burillo, Dimitra Rigopoulou, Georgios Magdis, Miguel Pereira Santaella, Françoise Combes, Ismael García-Bernete, Almudena Alonso-Herrero, Axel Weiss
W19BZ	Short depletion scales in cluster LIRGs: the LoCuSS sample	Pascale Jablonka, Françoise Combes, Gianluca Castignani, Chris Haines, Melanie Krips, Monique Arnaud
W19CF	Investigating the molecular component of fast multiphase outflows into the CGM	Christy Tremonti, James Geach, Amanda Kepley, Gregory Rudnick, John Moustakas, Alison Coil, Ryan Hickox, Aleks Diamond-Stanic, David Rupke, Paul Sell
W19CJ	Characterizing Molecular Gas in Quenching Galaxies at $z > 1$	Sirio Belli, Alessandra Contursi, Natascha Förster Schreiber, Dieter Lutz, Linda Tacconi, Rodrigo Herrera-Camus, Hannah Uebler, Thomas Taro Shimizu, Sedona Price, Rebecca Davies, Erica Nelson, Minju Lee, Jinyi Shangquan
W19CL	A titanic wind destroying the interstellar medium of a massive starburst galaxy at $z=1.4$ ?	Annagrazia Puglisi, Emanuele Daddi, Marcella Brusa, Chiara Mancini, Giulia Rodighiero, Ivan Delvecchio, Andrea Enia
W19CR	Completion: A survey of molecular gas in the Hubble Deep Field North (HDF-N)	Fabian Walter, Roberto Decarli, Mladen Novak, Dominik A. Riechers, Manuel Aravena, Axel Weiss, Gergo Popping, Emanuele Daddi, Daizhong Liu, Mark T. Sargent, Frank Bertoldi, Benjamin Magnelli, Roberto Neri, Jérôme Pety, Pierre Cox, Elisabete Da Cunha, Pascal Oesch, Rychard Bouwens, Richard Ellis, Dan Stark
W19CS	Resolving the [CI] and Mid-J CO Line Emission from Giant Molecular Clouds in Strongly Lensed Starbursts at $z = 2-3$	Kevin Harrington, Axel Weiss, Benjamin Magnelli, Eric Faustino Jiménez-Andrade, Min Yun, Frank Bertoldi, David Frayer, Patrick Kamienieski, Q. Daniel Wang, Amit Vishwas, T.K. Daisy Leung, Nichol Cunningham
W19CW	Probing the dense gas star formation law in intense dusty starbursts at $z \sim 2-4$	Raoul Canameras, Nicole Nesvadba, Chentao Yang, Sabine König, Alexandre Beelen, Ryley Hill, Ruediger Kneissl, Emeric Le Floch, Sangeeta Malhotra, Alain Omont, Douglas Scott
W19DA	Gas Properties in the Early Universe from the study of molecular lines: 15 mm observations of high excitation lines in the Cloverleaf Quasar	Michel Guélin, Chentao Yang, Carsten Kramer, Robert Zylka, Alain Omont
W19DB	Probing the excess gas origin in QSO2343+12	Scott Chapman, Axel Weiss, Axel Weiss
W19DD	Rise of the Titans: Molecular Gas Excitation in Hyper-Luminous Starbursts at $z=3-6$	Dominik A. Riechers, Ismael Perez-Fournon, Rob Ivison, Roberto Neri, Alain Omont, Pierre Cox, David Clements
W19DE	Exploring the Nature of the Broad Line Bright Herschel Galaxy HerBS-89a at $z=2.95$	Stefano Berta, Pierre Cox, Roberto Neri, Alain Omont, Alexandre Beelen, Tom Bakx, Matthew Lehnert, Andrew Baker, Veronique Buat, Helmut Dannerbauer, Loretta Dunne, Simon Dye, Steve Eales, R. Gavazzi, Andrew Harris, Cinthya Herrera Contreras, Rob Ivison, Shuowen Jin, Melanie Krips, Guilaine Lagache, Lucia Marchetti, Hugo Messias, Mattia Negrello, Ismael Perez-Fournon, Stephen Serjeant, Sheona Urquhart, Catherine Vlahakis, Axel Weiss, Paul van der Werf, Chentao Yang, Anthony Young, Dominik A. Riechers
W19DF	$\text{CH}^+(1-0)$ in high-redshift starburst galaxies : probes of massive turbulent reservoirs	Alba Vidal Garcia, Edith Falgarone, Benjamin Godard, Roberto Neri, Paola Andreani, Rob Ivison, Chentao Yang, Martin Zwaan, Alain Omont, Fabian Walter, Edwin A. Bergin, Nick Indriolo
W19DG	Redshift Scans of Bright Submm Galaxies in a Candidate Proto-cluster in the GOODS-N Field	Logan Jones, Amy Barger, Lennox Cowie
W19DI	A critical test of the nature of cold dust in submillimeter bright galaxies at $z \sim 4$	Emanuele Daddi, Shuowen Jin, Georgios Magdis, Daizhong Liu, Eva Schinnerer, Francesco Valentino, Yu Gao, Antonello Calabro', Padelis Papadopoulos, Isabella Cortzen
W19DN	Measuring for the first time the massive-end of the dust mass function of galaxies at $z \sim 4$	Benjamin Magnelli, Eva Schinnerer, Mark T. Sargent, Eric Faustino Jiménez-Andrade, Caitlin Casey, Jorge Zavala, Manuel Aravena, Dominik A. Riechers, Daizhong Liu, Frank Bertoldi, Alexander Karim, Tsan-Ming Wang
W19DO	Capitalising on an ALMA snapshot survey of the 3,083 reddest Herschel sources	Vinodiran Arumugam, Rob Ivison, Melanie Krips, Loretta Dunne, Helmut Dannerbauer
W19DQ	Final Piece to The Most Puzzling $z > 4$ SMG in GOODS-North, New Chapter for A Blind Line Emitter Field?	Daizhong Liu, Emanuele Daddi, Eva Schinnerer
W19DS	Exploration of a Small Angular Separation Quasar/SMG Pair	Marcel Neeleman, Nissim Kanekar, Fabian Walter
W19DU	The Formation and Growth of Supermassive Black Holes in the Early Universe	Anna-Christina Eilers, Bram Venemans, Fabian Walter, Joseph Hennawi, Roberto Decarli, Eduardo Banados, Feige Wang, Chiara Mazzucchelli, Frederick Davies

Project	Title	Authors
W19EB	Witnessing the formation of the first large-scale structures in the universe	Roberto Decarli, R. Gilli, M. Mignoli, Cristian Vignali, Eros Vanzella, Marcella Brusa, Andrea Comastri, Antonio Pensabene, Riccardo Nanni, Alessandro Peca, Nico Cappellutti, Barbara Balmaverde
W20AA	The intriguing mm-spectrum of Iapetus	Emmanuel Lellouch, Alice Le Gall, Lea E Bonnefoy, Cedric Leyrat, Raphael Moreno, Jeremie Boissier
W20AF	Connecting scales in protostellar disk formation	Edwin A. Bergin, Merel van 't Hoff, Felipe Alarcon, Arthur Bosman, Jane Huang, Kamber Schwarz, Jenny Calahan, John Tobin
W20AQ	The OMC-2 FIR6c outflow: A new astrochemical laboratory	Mathilde Bouvier, Ana Lopez-Sepulcre, Cecilia Ceccarelli, Nadia Balucani, Claudio Codella, Marta De Simone, Joan Enrique-Romero, Bertrand Lefloch, Pedro Ruben Rivera-Ortiz, Nami Sakai, Andre Schutzer, Fanny Vazart, Satoshi Yamamoto
W20BB	Investigating the deuterium fraction in the diffuse and translucent clouds through sensitive absorption observations	Luo Gan, Zhiyu Zhang, Siyi Feng, Thomas Bisbas
W20BC	The Molecular Content of Small Protoplanetary Disks	Vincent Pietu, Jean-Paul Melisse, Anne Dutrey, Stephane Guilloteau, Edwige Chapillon, Emmanuel Di Folco
W20BK	Determining the cause of the extremely unusual behaviour of Betelgeuse with NOEMA	Thavisha Dharmawardena, Karl M. Menten, Ka Tat Wong, Iain McDonald, Albert Zijlstra, Steve Mairs, Peter Scicluna, Miguel Montargès, Anita M. S. Richards, Fabrice Herpin
W20CM	At the end of the Cosmic Noon: Completing the molecular gas census in lensed quasars at $z=1.0-1.5$	Matus Rybak, Paul van der Werf, Jacqueline Hodge, Hannah Stacey, Gabriela Calistro Rivera, Marta Frias Castillo
W20CW	The molecular gas properties of high- $z$ galaxies as traced by [C I] and CO	Isabella Cortzen, Roberto Neri, Pierre Cox, Stefano Berta, Anthony Young, Alain Omont, Flora Stanley, Tom Bakx, Helmut Dannerbauer, Alexandre Beelen, Dominik A. Riechers, Axel Weiss, Andrew Baker, Steve Eales, Rob Ivison, Shuowen Jin, R. Gavazzi, Stephen Serjeant, Lucia Marchetti, Mattia Negrello, Matthew Lehnert, Melanie Krips, Ismael Perez-Fournon, Asantha Cooray, Chentao Yang, Sheona Urquhart, Hugo Messias, Veronique Buat, Catherine Vlahakis, Paul van der Werf, Loretta Dunne, Andrew Harris
W20DB	Molecular gas across the circum-galactic medium of Enormous Ly $\alpha$ Nebulae	Qiong Li, Jiangtao Li, Ran Wang, Jianan Li
W20DC	A multi-phase, multi-scale, multi-wavelength investigation of quasar feedback at high redshift. NOEMA: The dense molecular component.	Pasquier Noterdaeme, Sergei Balashev, Jens-Kristian Krogager, Françoise Combes, Neeraj Gupta, Raghunathan Srianand
W20DD	A Survey of CO(3-2) in the 20Mpc environment of HSI549+19, the most overdense protocluster known at $z>2$	Scott Chapman, Frank Bertoldi, Ian Smail, Chuck Steidel, Yuichi Matsuda, Manuel Aravena, Nikolaus Sulzenauer
W20DX	NOEMA line scans toward $z>5$ candidate ALMA-AzTEC SMGs (Continue)	Soh Ikarashi, Rob Ivison, Karina Caputi, Kotaro Kohno
W20EO	A Vigorously Star-forming Red Quasar Firstly Discovered at $z>7$	Seiji Fujimoto, Gabriel Brammer, Sune Toft, Georgios Magdis, Francesco Valentino, Charles Steinhardt, Isabella Cortzen, Luis Colina, Rui Marques-Chaves, Thomas R. Greve, M. Vestergaard, Peter Jakobsen, Vasily Kokorev



# Publications

## IRAM USERS' COMMUNITY

n°	Titre	Auteurs	Référence
2578	Cold Molecular Gas and PAH Emission in the Nuclear and Circumnuclear Regions of Seyfert Galaxies	Alonso-Herrero, A.; Pereira-Santaella, M.; Rigopoulou, D.; García-Bernete, I.; García-Burillo, S.; Domínguez-Fernández, A. J.; Combes, F.; Davies, R. I.; Díaz-Santos, T.; Esparza-Arredondo, D.; González-Martín, O.; Hernán-Caballero, A.; Hicks, E. K. S.; Hönl, S. F.; Levenson, N. A.; Ramos Almeida, C.; Roche, P. F.; Rosario, D.	2020, A&A, 639, A43
2579	Propargylimine in the Laboratory and in Space: Millimetre-Wave Spectroscopy and Its First Detection in the ISM	Bizzocchi, L.; Prudenzano, D.; Rivilla, V. M.; Pietropoli-Charmet, A.; Giuliano, B. M.; Caselli, P.; Martín-Pintado, J.; Jiménez-Serra, I.; Martín, S.; Requena-Torres, M. A.; Rico-Villas, F.; Zeng, S.; Guillemin, J.-C.	2020, A&A, 640, A98
2580	Toward a Large Bandwidth Photonic Correlator for Infrared Heterodyne Interferometry. A First Laboratory Proof of Concept	Bourdarot, G.; Guillet de Chatellus, H.; Berger, J.-P.	2020, A&A, 639, A53
2581	Rotational Spectroscopy and Astronomical Search for Glutaronitrile	Cabezas, C.; Bermúdez, C.; Endo, Y.; Tercero, B.; Cernicharo, J.	2020, A&A, 636, A33
2582	The Millimeter-Wave Spectrum and Astronomical Search for Ethyl Methyl Sulfide	Cabezas, C.; Bermúdez, C.; Tercero, B.; Cernicharo, J.	2020, A&A, 639, A129
2583	Environmental Processing in Cluster Core Galaxies at $z \approx 1.7$	Castignani, G.; Combes, F.; Salomé, P.	2020, A&A, 635, L10
2584	Molecular Gas in Distant Brightest Cluster Galaxies	Castignani, G.; Combes, F.; Salomé, P.; Freundlich, J.	2020, A&A, 635, A32
2585	Molecular Gas in CLASH Brightest Cluster Galaxies at $z \sim 0.2 - 0.9$	Castignani, G.; Pandey-Pommier, M.; Hamer, S. L.; Combes, F.; Salomé, P.; Freundlich, J.; Jablonka, P.	2020, A&A, 640, A65
2586	Discovery of $\text{HC}_3\text{O}^+$ in Space: The Chemistry of O-Bearing Species in TMC-1	Cernicharo, J.; Marcelino, N.; Agúndez, M.; Endo, Y.; Cabezas, C.; Bermúdez, C.; Tercero, B.; de Vicente, P.	2020, A&A, 642, L17
2587	Discovery of $\text{HC}_3\text{O}^+$ in Space: The Chemistry of O-Bearing Species in TMC-1 (Corrigendum)	Cernicharo, J.; Marcelino, N.; Agúndez, M.; Endo, Y.; Cabezas, C.; Bermúdez, C.; Tercero, B.; de Vicente, P.	2020, A&A, 644, C2.
2588	Interstellar Nitrile Anions: Detection of $\text{C}_3\text{N}^-$ and $\text{C}_5\text{N}^-$ in TMC-1	Cernicharo, J.; Marcelino, N.; Pardo, J. R.; Agúndez, M.; Tercero, B.; de Vicente, P.; Cabezas, C.; Bermúdez, C.	2020, A&A, 641, L9
2589	The First Steps of Interstellar Phosphorus Chemistry	Chantzos, J.; Rivilla, V. M.; Vasyunin, A.; Redaelli, E.; Bizzocchi, L.; Fontani, F.; Caselli, P.	2020, A&A, 633, A54
2590	Anisotropy of Random Motions of Gas in Messier 33	Chemin, L.; Braine, J.; Combes, F.; Kam, Z. S.; Carignan, C.	2020, A&A, 639, A145
2591	Enhanced UV Radiation and Dense Clumps in the Molecular Outflow of Mrk 231	Cicone, C.; Maiolino, R.; Aalto, S.; Müller, S.; Feruglio, C.	2020, A&A, 633, A163
2592	A Hyper Luminous Starburst at $z = 4.72$ Magnified by a Lensing Galaxy Pair at $z = 1.48$	Ciesla, L.; Béthermin, M.; Daddi, E.; Richard, J.; Díaz-Santos, T.; Sargent, M. T.; Elbaz, D.; Boquien, M.; Wang, T.; Schreiber, C.; Yang, C.; Zabl, J.; Fraser, M.; Aravena, M.; Assef, R. J.; Baker, A. J.; Beelen, A.; Boselli, A.; Bournaud, F.; Burgarella, D.; Charmandaris, V.; Côté, P.; Epinat, B.; Ferrarese, L.; Gobat, R.; Ilbert, O.	2020, A&A, 635, A27
2593	Evolutionary Study of Complex Organic Molecules in High-Mass Star-Forming Regions	Coletta, A.; Fontani, F.; Rivilla, V. M.; Mininni, C.; Colzi, L.; Sánchez-Monge, Á.; Beltrán, M. T.	2020, A&A, 641, A54
2594	A Wide Field-of-View Low-Resolution Spectrometer at APEX: Instrument Design and Scientific Forecast	Concerto Collaboration; Ade, P.; Aravena, M.; Barria, E.; Beelen, A.; Benoit, A.; Béthermin, M.; Bounmy, J.; Bourrion, O.; Bres, G.; De Breuck, C.; Calvo, M.; Cao, Y.; Catalano, A.; Desert, F.-X.; Durán, C. A.; Fasano, A.; Fenouillet, T.; Garcia, J.; Garde, G.; Goupy, J.; Groppi, C.; Hoarau, C.; Lagache, G.; Lambert, J.-C.; Leggeri, J.-P.; Levy-Bertrand, F.; Macías-Pérez, J.; Mani, H.; Marpaud, J.; Maukopf, P.; Monfardini, A.; Pisano, G.; Ponthieu, N.; Prieur, L.; Roni, S.; Roudier, S.; Tourres, D.; Tucker, C.	2020, A&A, 642, A60
2595	Deceptively Cold Dust in the Massive Starburst Galaxy GN20 at $z \sim 4$	Cortzen, I.; Magdis, G. E.; Valentino, F.; Daddi, E.; Liu, D.; Rigopoulou, D.; Sargent, M.; Riechers, D.; Cormier, D.; Hodge, J. A.; Walter, F.; Elbaz, D.; Béthermin, M.; Greve, T. R.; Kokorev, V.; Toft, S.	2020, A&A, 634, L14
2596	Search and Analysis of Giant Radio Galaxies with Associated Nuclei (SAGAN). II. Molecular Gas Content of Giant Radio Galaxies	Dabhade, P.; Combes, F.; Salomé, P.; Bagchi, J.; Mahato, M.	2020, A&A, 643, A111
2597	Interstellar Anatomy of the TeV Gamma-Ray Peak in the IC443 Supernova Remnant	Dell'Ova, P.; Gusdorf, A.; Gerin, M.; Riquelme, D.; Güsten, R.; Noriega-Crespo, A.; Tram, L. N.; Houde, M.; Guillard, P.; Lehmann, A.; Lesaffre, P.; Louvet, F.; Marcowith, A.; Padovani, M.	2020, A&A, 644, A64
2598	Searching for Molecular Gas Inflows and Outflows in the Nuclear Regions of Five Seyfert Galaxies	Domínguez-Fernández, A. J.; Alonso-Herrero, A.; García-Burillo, S.; Davies, R. I.; Usero, A.; Labiano, A.; Levenson, N. A.; Pereira-Santaella, M.; Imanishi, M.; Ramos Almeida, C.; Rigopoulou, D.	2020, A&A, 643, A127
2599	Measuring Elemental Abundance Ratios in Protoplanetary Disks at Millimeter Wavelengths	Fedele, D.; Favre, C.	2020, A&A, 638, A110

n°	Titre	Auteurs	Référence
2600	Deep Search for Hydrogen Peroxide toward Pre- and Protostellar Objects. Testing the Pathway of Grain Surface Water Formation	Fuchs, G. W.; Witsch, D.; Herberth, D.; Kempkes, M.; Stancik, B.; Chantzou, J.; Linnartz, H.; Menten, K.; Giesen, T. F.	2020, A&A, 636, A114
2601	Simulating the Circumstellar H <sub>2</sub> CO and CH <sub>3</sub> OH Chemistry of Young Stellar Objects Using a Spherical Physical-Chemical Model	Fuchs, G. W.; Witsch, D.; Herberth, D.; Kempkes, M.; Stancik, B.; Chantzou, J.; Linnartz, H.; Menten, K. M.; Giesen, T. F.	2020, A&A, 639, A143
2602	An Observational Correlation between Magnetic Field, Angular Momentum and Fragmentation in the Envelopes of Class 0 Protostars?	Galametz, M.; Maury, A.; Girart, J. M.; Rao, R.; Zhang, Q.; Gaudel, M.; Valdivia, V.; Hennebelle, P.; Cabedo-Soto, V.; Keto, E.; Lai, S.-P.	2020, A&A, 644, A47
2603	More Insights into Bar Quenching. Multi-Wavelength Analysis of Four Barred Galaxies	George, K.; Joseph, P.; Mondal, C.; Subramanian, S.; Subramanian, A.; Paul, K. T.	2020, A&A, 644, A79
2604	Scaling Relations and Baryonic Cycling in Local Star-Forming Galaxies. I. The Sample	Ginolfi, M.; Hunt, L. K.; Tortora, C.; Schneider, R.; Cresci, G.	2020, A&A, 638, A4
2605	Very Fast Variations of SiO Maser Emission in Evolved Stars	Gómez-Garrido, M.; Bujarrabal, V.; Alcolea, J.; Soria-Ruiz, R.; de Vicente, P.; Desmurs, J.-F.	2020, A&A, 642, A213
2606	HCN-to-HNC Intensity Ratio: A New Chemical Thermometer for the Molecular ISM	Hacar, A.; Bosman, A. D.; van Dishoeck, E. F.	2020, A&A, 635, A4
2607	APEX-SEPIA660 Early Science: Gas at Densities above 10 <sup>7</sup> cm <sup>-3</sup> towards OMC-1	Hacar, A.; Hogerheijde, M. R.; Harsono, D.; Portegies Zwart, S.; De Breuck, C.; Torstenson, K.; Boland, W.; Baryshev, A. M.; Hesper, R.; Barkhof, J.; Adema, J.; Bekema, M. E.; Koops, A.; Khudchenko, A.; Stark, R.	2020, A&A, 644, A133
2608	Missing Water in Class I Protostellar Disks	Harsono, D.; Persson, M. V.; Ramos, A.; Murillo, N. M.; Maud, L. T.; Hogerheijde, M. R.; Bosman, A. D.; Kristensen, L. E.; Jørgensen, J. K.; Bergin, E. A.; Visser, R.; Mottram, J. C.; van Dishoeck, E. F.	2020, A&A, 636, A26
2609	AGN Feedback in a Galaxy Merger: Multi-Phase, Galaxy-Scale Outflows with a Fast Molecular Gas Blob ~6 Kpc Away from IRAS F08572+3915	Herrera-Camus, R.; Janssen, A.; Sturm, E.; Lutz, D.; Veilleux, S.; Davies, R.; Shimizu, T.; González-Alfonso, E.; Rupke, D. S. N.; Tacconi, L.; Genzel, R.; Ciccone, C.; Maiolino, R.; Contursi, A.; Graciá-Carpio, J.	2020, A&A, 635, A47
2610	Sulphur and Carbon Isotopes towards Galactic Centre Clouds	Humire, P. K.; Thiel, V.; Henkel, C.; Belloche, A.; Loison, J.-C.; Pillai, T.; Riquelme, D.; Wakelam, V.; Langer, N.; Hernández-Gómez, A.; Mauersberger, R.; Menten, K. M.	2020, A&A, 642, A222
2611	Central Molecular Zones in Galaxies: <sup>12</sup> CO-to- <sup>13</sup> CO Ratios, Carbon Budget, and X Factors	Israel, F. P.	2020, A&A, 635, A131
2612	Rotational Spectroscopic Study of S-Methyl Thioformate. A Global Laboratory Analysis of Ground and Excited Torsional States up to 660 GHz	Jabri, A.; Tercero, B.; Margulès, L.; Motiyenko, R. A.; Alekseev, E. A.; Kleiner, I.; Cernicharo, J.; Guillemin, J.-C.	2020, A&A, 644, A102
2613	Impact of Polarised Extragalactic Sources on the Measurement of CMB B-Mode Anisotropies	Lagache, G.; Béthermin, M.; Montier, L.; Serra, P.; Tucci, M.	2020, A&A, 642, A232
2614	Molecular Complexity in Pre-Stellar Cores: A 3 mm-Band Study of L183 and L1544	Lattanzi, V.; Bizzocchi, L.; Vasyunin, A. I.; Harju, J.; Giuliano, B. M.; Vastel, C.; Caselli, P.	2020, A&A, 633, A118
2615	Submillimeter-Wave Spectroscopy and the Radio-Astronomical Investigation of Propynethial (HC-CCHS)	Margulès, L.; McGuire, B. A.; Evans, C. J.; Motiyenko, R. A.; Remijan, A.; Guillemin, J. C.; Wong, A.; McNaughton, D.	2020, A&A, 642, A206
2616	Millimeter Wave Spectroscopy of Cyanoketene (NC-CH=C=O) and an Observational Search in the ISM	Margulès, L.; McGuire, B. A.; Motiyenko, R. A.; Brogan, C.; Hunter, T.; Remijan, A.; Guillemin, J. C.	2020, A&A, 638, A3
2617	Massive Molecular Gas Reservoir around the Central AGN in the CARLA J1103 + 3449 Cluster at z = 1.44	Markov, V.; Mei, S.; Salomé, P.; Combes, F.; Stern, D.; Galametz, A.; De Breuck, C.; Wylezalek, D.; Amodeo, S.; Cooke, E. A.; Gonzalez, A. H.; Hatch, N. A.; Noiro, G.; Rettura, A.; Seymour, N.; Stanford, S. A.; Vernet, J.	2020, A&A, 641, A22
2618	The Abundance of S- and Si-Bearing Molecules in O-Rich Circumstellar Envelopes of AGB Stars	Massalkhi, S.; Agúndez, M.; Cernicharo, J.; Velilla-Prieto, L.	2020, A&A, 641, A57
2619	The Galaxy Population within the Virial Radius of the Perseus Cluster	Meusinger, H.; Rudolf, C.; Stecklum, B.; Hoeft, M.; Mauersberger, R.; Apai, D.	2020, A&A, 640, A30
2620	Orientation of the Crescent Image of M 87*	Nalewajko, K.; Sikora, M.; Rózańska, A.	2020, A&A, 634, A38
2621	Gas, Dust, and Star Formation in the Positive AGN Feedback Candidate 4C 4117 at z = 3.8	Nesvadba, N. P. H.; Bicknell, G. V.; Mukherjee, D.; Wagner, A. Y.	2020, A&A, 639, L13
2622	Expanding Bubbles in Orion A: [C II] Observations of M 42, M 43, and NGC 1977	Pabst, C. H. M.; Goicoechea, J. R.; Teyssier, D.; Berné, O.; Higgins, R. D.; Chambers, E. T.; Kabanovic, S.; Güsten, R.; Stutzki, J.; Tielens, A. G. G. M.	2020, A&A, 639, A2
2623	Theoretical Modelling of Two-Component Molecular Discs in Spiral Galaxies	Patra, N. N.	2020, A&A, 638, A66
2624	The Lyman Alpha Reference Sample. XI. Efficient Turbulence-Driven Ly $\alpha$ Escape and an Analysis of IR, CO, and [C II] $\lambda$ 158 $\mu$ m	Puschnig, J.; Hayes, M.; Östlin, G.; Cannon, J.; Smirnova-Pinchukova, I.; Husemann, B.; Kunth, D.; Bridge, J.; Herenz, E. C.; Messa, M.; Oteo, I.	2020, A&A, 644, A10

n°	Titre	Auteurs	Référence
2625	$\lambda = 2$ Mm Spectroscopy Observations toward the Circumnuclear Disk of NGC 1068	Qiu, J.; Zhang, J.; Zhang, Y.; Jia, L.; Tang, X.	2020, A&A, 634, A125
2626	First Sample of N <sup>15</sup> H+ Nitrogen Isotopic Ratio Measurements in Low-Mass Protostars	Redaelli, E.; Bizzocchi, L.; Caselli, P.	2020, A&A, 644, A29
2627	Survey of Ortho-H <sup>2</sup> D <sup>+</sup> in High-Mass Star-Forming Regions	Sabatini, G.; Bovino, S.; Giannetti, A.; Wyrowski, F.; Órdenes, M. A.; Pascale, R.; Pillai, T.; Wielen, M.; Csengeri, T.; Menten, K. M.	2020, A&A, 644, A34
2628	Dust Evolution across the Horsehead Nebula	Schirmer, T.; Abergel, A.; Verstraete, L.; Ysard, N.; Juvela, M.; Jones, A. P.; Habart, E.	2020, A&A, 639, A144
2629	Sub-Milliarcsecond Imaging of a Bright Flare and Ejection Event in the Extragalactic Jet 3C 111	Schulz, R.; Kadler, M.; Ros, E.; Perucho, M.; Krichbaum, T. P.; Agudo, I.; Beuchert, T.; Lindqvist, M.; Mannheim, K.; Wilms, J.; Zensus, J. A.	2020, A&A, 644, A85
2630	Distribution of Methanol and Cyclopropenylidene around Starless Cores	Spezzano, S.; Caselli, P.; Pineda, J. E.; Bizzocchi, L.; Prudeniano, D.; Nagy, Z.	2020, A&A, 643, A60
2631	Localizing the $\gamma$ -Ray Emitting Region in the Blazar TXS 2013+370	Traianou, E.; Krichbaum, T. P.; Boccardi, B.; Angioni, R.; Rani, B.; Liu, J.; Ros, E.; Bach, U.; Sokolovsky, K. V.; Lisakov, M. M.; Kiehlmann, S.; Gurwell, M.; Zensus, J. A.	2020, A&A, 634, A112
2632	Dense Gas in a Giant Molecular Filament	Wang, Y.; Beuther, H.; Schneider, N.; Meidt, S. E.; Linz, H.; Ragan, S.; Zucker, C.; Battersby, C.; Soler, J. D.; Schinnerer, E.; Bigiel, F.; Colombo, D.; Henning, Th.	2020, A&A, 641, A53
2633	Probing the Initial Conditions of High-Mass Star Formation. IV. Gas Dynamics and NH <sub>2</sub> D Chemistry in High-Mass Precluster and Protocluster Clumps	Zhang, C.-P.; Li, G.-X.; Pillai, T.; Csengeri, T.; Wyrowski, F.; Menten, K. M.; Pestalozzi, M. R.	2020, A&A, 638, A105
2634	On the Effects of UV Photons/X-Rays on the Chemistry of the Sgr B2 Cloud	Armijos-Abendaño, J.; Martín-Pintado, J.; López, E.; Llerena, M.; Harada, N.; Requena-Torres, M. A.; Martín, S.; Rivilla, V. M.; Riquelme, D.; Aldas, F.	2020, ApJ, 895, 57
2635	Exploring the Possibility of Identifying Hydride and Hydroxyl Cations of Noble Gas Species in the Crab Nebula Filament	Das, A.; Sil, M.; Bhat, B.; Gorai, P.; Chakrabarti, S. K.; Caselli, P.	2020, ApJ, 902, 131
2636	Detecting and Characterizing Young Quasars. I. Systemic Redshifts and Proximity Zone Measurements	Eilers, A.-C.; Hennawi, J. F.; Decarli, R.; Davies, F. B.; Venemans, B.; Walter, F.; Bañados, E.; Fan, X.; Farina, E. P.; Mazzucchelli, C.; Novak, M.; Schindler, J.-T.; Simcoe, R. A.; Wang, F.; Yang, J.	2020, ApJ, 900, 37
2637	The Chemical Structure of Young High-Mass Star-Forming Clumps. II. Parsec-Scale CO Depletion and Deuterium Fraction of HCO <sup>+</sup>	Feng, S.; Li, D.; Caselli, P.; Du, F.; Lin, Y.; Sipilä, O.; Beuther, H.; Sanhueza, P.; Tatematsu, K.; Liu, S. Y.; Zhang, Q.; Wang, Y.; Hogge, T.; Jimenez-Serra, I.; Lu, X.; Liu, T.; Wang, K.; Zhang, Z. Y.; Zahorecz, S.; Li, G.; Liu, H. B.; Yuan, J.	2020, ApJ, 901, 145
2638	A Low-Velocity Bipolar Outflow from a Deeply Embedded Object in Taurus Revealed by the Atacama Compact Array	Fujishiro, K.; Tokuda, K.; Tachihara, K.; Takashima, T.; Fukui, Y.; Zahorecz, S.; Saigo, K.; Matsumoto, T.; Tomida, K.; Machida, M. N.; Inutsuka, S.; André, P.; Kawamura, A.; Onishi, T.	2020, ApJ, 899, L10
2639	The Physical Properties of S0 Galaxy PGC 26218: The Origin of Starburst and Star Formation	Ge, X.; Gu, Q.-S.; García-Benito, R.; Xiao, M.-Y.; Li, Z.-N.	2020, ApJ, 889, 132
2640	Mapping Circumstellar Magnetic Fields of Late-Type Evolved Stars with the Goldreich-Kylafis Effect: CARMA Observations at $\lambda 1.3$ Mm of R CrA and R Leo	Huang, K.-Y.; Kemball, A. J.; Vlemmings, W. H. T.; Lai, S.-P.; Yang, L.; Agudo, I.	2020, ApJ, 899, 152
2641	The Redshift and Star Formation Mode of AzTEC2: A Pair of Massive Galaxies at $z = 4.63$	Jiménez-Andrade, E. F.; Zavala, J. A.; Magnelli, B.; Casey, C. M.; Liu, D.; Romano-Díaz, E.; Schinnerer, E.; Harrington, K.; Aretxaga, I.; Karim, A.; Staguhn, J.; Burnham, A. D.; Montaña, A.; Smolčić, V.; Yun, M.; Bertoldi, F.; Hughes, D.	2020, ApJ, 890, 171
2642	Biases and Cosmic Variance in Molecular Gas Abundance Measurements at High Redshift	Keenan, R. P.; Marrone, D. P.; Keating, G. K.	2020, ApJ, 904, 127
2643	Probing the Full CO Spectral Line Energy Distribution (SLED) in the Nuclear Region of a Quasar-Starburst System at $z = 6.003$	Li, J.; Wang, R.; Riechers, D.; Walter, F.; Decarli, R.; Venemans, B. P.; Neri, R.; Shao, Y.; Fan, X.; Gao, Y.; Carilli, C. L.; Omont, A.; Cox, P.; Menten, K. M.; Wagg, J.; Bertoldi, F.; Narayanan, D.	2020, ApJ, 889, 162
2644	CO Emission and CO Hot Spots in Diffuse Molecular Gas	Liszt, H. S.	2020, ApJ, 897, 104
2645	A Small-Scale Investigation of Molecular Emission toward the Tip of the Western Lobe of W50/SS 433	Liu, Q.-C.; Chen, Y.; Zhou, P.; Zhang, X.; Jiang, B.	2020, ApJ, 892, 143
2646	Confirmation of Enhanced Long-Wavelength Dust Emission in OMC 2/3	Mason, B.; Dicker, S.; Sadavoy, S.; Stanchfield, S.; Mroczkowski, T.; Romero, C.; Friesen, R.; Sarazin, C.; Sievers, J.; Stanke, T.; Devlin, M.	2020, ApJ, 893, 13
2647	SDSS-IV MaNGA: The Nature of an Off-Galaxy H $\alpha$ Blob—A Multiwavelength View of Offset Cooling in a Merging Galaxy Group	Pan, H.-A.; Lin, L.; Hsieh, B.-C.; Michałowski, M. J.; Bothwell, M. S.; Huang, S.; Moiseev, A. V.; Oparin, D.; O'Sullivan, E.; Worrall, D. M.; Sánchez, S. F.; Gwyn, S.; Law, D. R.; Stark, D. V.; Bizyaev, D.; Li, C.; Lee, C.-H.; Fu, H.; Belfiore, F.; Bundy, K.; Fernández-Trincado, J. G.; Gelfand, J.; Peirani, S.	2020, ApJ, 903, 16

n°	Titre	Auteurs	Référence
2648	A Measurement of the Degree-Scale CMB B-Mode Angular Power Spectrum with POLARBEAR	Polarbear Collaboration; Adachi, S.; Aguilar Faúndez, M. A. O.; Arnold, K.; Baccigalupi, C.; Barron, D.; Beck, D.; Beckman, S.; Bianchini, F.; Boettger, D.; Borrill, J.; Carron, J.; Chapman, S.; Cheung, K.; Chinone, Y.; Crowley, K.; Cukierman, A.; Dobbs, M.; El Bouhargani, H.; Elleflot, T.; Errard, J.; Fabbian, G.; Feng, C.; Fujino, T.; Galitzki, N.; Goeckner-Wald, N.; Groh, J.; Hall, G.; Halverson, N.; Hamada, T.; Hasegawa, M.; Hazumi, M.; Hill, C. A.; Howe, L.; Inoue, Y.; Jaehnig, G.; Jeong, O.; Kaneko, D.; Katayama, N.; Keating, B.; Keskitalo, R.; Kikuchi, S.; Kisner, T.; Krachmalnicoff, N.; Kusaka, A.; Lee, A. T.; Leon, D.; Linder, E.; Lowry, L. N.; Mangu, A.; Matsuda, F.; Minami, Y.; Navaroli, M.; Nishino, H.; Pham, A. T. P.; Poletti, D.; Puglisi, G.; Reichardt, C. L.; Segawa, Y.; Silva-Feaver, M.; Siritanasak, P.; Stebor, N.; Stompor, R.; Suzuki, A.; Tajima, O.; Takakura, S.; Takatori, S.; Tanabe, D.; Teply, G. P.; Tsai, C.; Verges, C.; Westbrook, B.; Zhou, Y.	2020, ApJ, 897, 55
2649	A Hard X-Ray Test of HCN Enhancements As a Tracer of Embedded Black Hole Growth	Privon, G. C.; Ricci, C.; Aalto, S.; Viti, S.; Armus, L.; Díaz-Santos, T.; González-Alfonso, E.; Iwasawa, K.; Jeff, D. L.; Treister, E.; Bauer, F.; Evans, A. S.; Garg, P.; Herrero-Illana, R.; Mazzarella, J. M.; Larson, K.; Blecha, L.; Barcos-Muñoz, L.; Charmandaris, V.; Stierwalt, S.; Pérez-Torres, M. A.	2020, ApJ, 893, 149
2650	Prebiotic Precursors of the Primordial RNA World in Space: Detection of NH <sub>2</sub> OH	Rivilla, V. M.; Martín-Pintado, J.; Jiménez-Serra, I.; Martín, S.; Rodríguez-Almeida, L. F.; Requena-Torres, M. A.; Rico-Villas, F.; Zeng, S.; Briones, C.	2020, ApJ, 899, L28
2651	Atacama Compact Array Measurements of the Molecular Mass in the NGC 5044 Cooling-Flow Group	Schellenberger, G.; David, L. P.; Vrtilek, J.; O'Sullivan, E.; Lim, J.; Forman, W.; Sun, M.; Combes, F.; Salome, P.; Jones, C.; Giacintucci, S.; Edge, A.; Gastaldello, F.; Temi, P.; Brighenti, F.; Bardelli, S.	2020, ApJ, 894, 72
2652	Isomers in Interstellar Environments. I. The Case of Z- and E-Cyanomethanimine	Shingledecker, C. N.; Molpeceres, G.; Rivilla, V. M.; Majumdar, L.; Kästner, J.	2020, ApJ, 897, 158
2653	Physical Conditions and Kinematics of the Filamentary Structure in Orion Molecular Cloud 1	Teng, Y.-H.; Hirano, N.	2020, ApJ, 893, 63
2654	Fragmentation and Evolution of Dense Cores Judged by ALMA (FREJA). I. Overview: Inner ~1000 au Structures of Prestellar/Protostellar Cores in Taurus	Tokuda, K.; Fujishiro, K.; Tachihara, K.; Takashima, T.; Fukui, Y.; Zahorecz, S.; Saigo, K.; Matsumoto, T.; Tomida, K.; Machida, M. N.; Inutsuka, S.; André, P.; Kawamura, A.; Onishi, T.	2020, ApJ, 899, 10
2655	The Properties of the Interstellar Medium of Galaxies across Time as Traced by the Neutral Atomic Carbon [C I]	Valentino, F.; Magdis, G. E.; Daddi, E.; Liu, D.; Aravena, M.; Bournaud, F.; Cortzen, I.; Gao, Y.; Jin, S.; Juneau, S.; Kartaltepe, J. S.; Kokorev, V.; Lee, M.-Y.; Madden, S. C.; Narayanan, D.; Popping, G.; Puglisi, A.	2020, ApJ, 890, 24
2656	A Significantly Neutral Intergalactic Medium Around the Luminous z = 7 Quasar J0252-0503	Wang, F.; Davies, F. B.; Yang, J.; Hennawi, J. F.; Fan, X.; Barth, A. J.; Jiang, L.; Wu, X.-B.; Mudd, D. M.; Bañados, E.; Bian, F.; Decarli, R.; Eilers, A.-C.; Farina, E. P.; Venemans, B.; Walter, F.; Yue, M.	2020, ApJ, 896, 23
2657	Formation of the Hub-Filament System G33.92+0.11: Local Interplay between Gravity, Velocity, and Magnetic Field	Wang, J.-W.; Koch, P. M.; Galván-Madrid, R.; Lai, S.-P.; Liu, H. B.; Lin, S.-J.; Pattle, K.	2020, ApJ, 905, 158
2658	Molecular Oxygen in the Nearest QSO Mrk 231	Wang, J.; Li, D.; Goldsmith, P. F.; Zhang, Z.-Y.; Gao, Y.; Shi, Y.; Li, S.; Fang, M.; Li, J.; Zhang, J.	2020, ApJ, 889, 129
2659	Galactic Interstellar Sulfur Isotopes: A Radial <sup>32</sup> S/ <sup>34</sup> S Gradient?	Yu, H. Z.; Zhang, J. S.; Henkel, C.; Yan, Y. T.; Liu, W.; Tang, X. D.; Langer, N.; Luan, T. C.; Chen, J. L.; Wang, Y. X.; Deng, G. G.; Zou, Y. P.	2020, ApJ, 899, 145
2660	Excess C/H in Protoplanetary Disk Gas from Icy Pebble Drift Across the CO Snowline	Zhang, K.; Bosman, A. D.; Bergin, E. A.	2020, ApJ, 891, L16
2661	Rapid Evolution of Volatile CO from the Protostellar Disk Stage to the Protoplanetary Disk Stage	Zhang, K.; Schwarz, K. R.; Bergin, E. A.	2020, ApJ, 891, L17
2662	Unraveling the Complex Behavior of Mrk 421 with Simultaneous X-Ray and VHE Observations during an Extreme Flaring Activity in 2013 April	Acciari, V. A.; Ansoldi, S.; Antonelli, L. A.; Arbet Engels, A.; Baack, D.; Babić, A.; Banerjee, B.; Barres de Almeida, U.; Barrio, J. A.; Becerra González, J.; Bednarek, W.; Bellizzi, L. K.; Bernardini, E.; Berti, A.; Besenrieder, J.; Bhattacharyya, W.; Bigongiari, C.; Biland, A.; Blanch, O.; Bonnoli, G.; Bošnjak, Ž.; Busetto, G.; Carosi, R.; Ceribella, G.; Cerruti, M.; Chai, Y.; Chilingarian, A.; Cikota, S.; Colak, S. M.; Colin, U.; Colombo, E.; Contreras, J. L.; Cortina, J.; Covino, S.; D'Elia, V.; da Vela, P.; Dazzi, F.; de Angelis, A.; de Lotto, B.; Del Puppo, F.; Delfino, M.; Delgado, J.; Depaoli, D.; di Pierro, F.; di Venere, L.; Do Souto Espiñeira, E.; Prester, D. D.; Donini, A.; Dorner, D.; Doro, M.; Elsaesser, D.; Ramazani, V. F.; Fattorini, A.; Ferrara, G.; Foffano, L.; Fonseca, M. V.; Font, L.; Fruck, C.; Fukami, S.; García López, R. J.; Garczarczyk, M.; Gasparyan, S.; Gaug, M.; Giglietto, N.; Giordano, F.; Gliwny, P.; Godinović, N.; Green, D.; Hadasch, D.; Hahn, A.; Hassan, T.; Herrera, J.; Hoang, J.; Hrupec, D.; Hütten, M.; Inada, T.; Inoue, S.; Ishio, K.; Iwamura, Y.; Jouvin, L.; Kajiwara, Y.; Kerszberg, D.; Kobayashi, Y.; Kubo, H.; Kushida, J.; Lamastra, A.; Lelas, D.; Leone, F.; Lindfors, E.; Lombardi, S.; Longo, F.; López, M.; López-Coto, R.; López-Oramas, A.; Loporchio, S.; Machado de Oliveira Fraga, B.; Maggio, C.; Majumdar, P.; Makariev, M.; Mallamaci, M.; Maneva, G.; Manganaro, M.; Mannheim, K.; Maraschi, L.; Mariotti, M.; Martínez, M.; Mazin, D.; Mender, S.; Mićanović, S.; Miceli, D.; Miener, T.; Mineev, M.; Miranda, J. M.; Mirzoyan, R.; Molina, E.; Moralejo, A.; Morcuende, D.; Moreno, V.; Moretti, E.; Munar-Adrover, P.; Neustroev, V.; Nigro, C.; Nilsson, K.; Ninci, D.; Nishijima, K.; Noda, K.; Nogués, L.; Nozaki, S.; Ohtani, Y.; Oka, T.; Otero-Santos, J.; Palatiello, M.; Paneque, D.; Paoletti, R.; Paredes, J. M.; Pavletić, L.	2020, ApJ Supp. Series, 248, 29

.../...

n°	Titre	Auteurs	Référence
2662 (cont)	Unraveling the Complex Behavior of Mrk 421 with Simultaneous X-Ray and VHE Observations during an Extreme Flaring Activity in 2013 April	Peñil, P.; Peresano, M.; Persic, M.; Moroni, P. G. P.; Prandini, E.; Puljak, I.; Rhode, W.; Ribó, M.; Rico, J.; Righi, C.; Rugliancich, A.; Saha, L.; Sahakyan, N.; Saito, T.; Sakurai, S.; Satalecka, K.; Schleicher, B.; Schmidt, K.; Schweizer, T.; Sitarek, J.; Šnidarić, I.; Sobczynska, D.; Spolon, A.; Stamerra, A.; Strom, D.; Strzys, M.; Suda, Y.; Surić, T.; Takahashi, M.; Tavecchio, F.; Temnikov, P.; Terzić, T.; Teshima, M.; Torres-Albà, N.; Tosti, L.; van Scherpenberg, J.; Vanzo, G.; Vazquez Acosta, M.; Ventura, S.; Verguillo, V.; Vigorito, C. F.; Vitale, V.; Vovk, I.; Will, M.; Zarić, D.; MAGIC Collaboration; Finke, J.; D'Ammando, F.; Baloković, M.; Madejski, G.; Mori, K.; Puccetti, S.; Leto, C.; Perri, M.; Verrecchia, F.; Villata, M.; Raiteri, C. M.; Agudo, I.; Bachev, R.; Berdyugin, A.; Blinov, D. A.; Chanishvili, R.; Chen, W. P.; Chigladze, R.; Damjanovic, G.; Eswaraiah, C.; Grishina, T. S.; Ibryamov, S.; Jordan, B.; Jorstad, S. G.; Joshi, M.; Kopatskaya, E. N.; Kurtanidze, O. M.; Kurtanidze, S. O.; Larionova, E. G.; Larionova, L. V.; Larionov, V. M.; Latev, G.; Lin, H. C.; Marscher, A. P.; Mokrushina, A. A.; Morozova, D. A.; Nikolashvili, M. G.; Semkov, E.; Smith, P. S.; Strigachev, A.; Troitskaya, Yu. V.; Troitsky, I. S.; Vince, O.; Barnes, J.; Güver, T.; Moody, J. W.; Sadun, A. C.; Hovatta, T.; Richards, J. L.; Max-Moerbeck, W.; Readhead, A. C. S.; Lähteenmäki, A.; Tornikoski, M.; Tammi, J.; Ramakrishnan, V.; Reinthal, R.	2020, ApJ Supp. Series, 248, 29
2663	A Systematic Observational Study on Galactic Interstellar Ratio $^{18}\text{O}/^{17}\text{O}$ . I. $\text{C}^{18}\text{O}$ and $\text{C}^{17}\text{O}$ J = 1-0 Data Analysis	Zhang, J. S.; Liu, W.; Yan, Y. T.; Yu, H. Z.; Liu, J. T.; Zheng, Y. H.; Romano, D.; Zhang, Z.-Y.; Wang, J. Z.; Chen, J. L.; Wang, Y. X.; Zhang, W. J.; Lu, H. H.; Chen, L. S.; Zou, Y. P.; Yang, H. Q.; Wen, T.; Lu, F. S.	2020, ApJ Supp. Series, 249, 6
2664	Structure and Kinematics of Shocked Gas in Sgr B2: Further Evidence of a Cloud-Cloud Collision from SiO Emission Maps	Armijos-Abendaño, J.; Banda-Barragán, W. E.; Martín-Pintado, J.; Dénes, H.; Federrath, C.; Requena-Torres, M. A.	2020, MNRAS, 499, 4918-4939
2665	Deuterium Fractionation of Nitrogen Hydrides: Detections of NHD and $\text{ND}_2$	Bacmann, A.; Faure, A.; Hily-Blant, P.; Kobayashi, K.; Ozeki, H.; Yamamoto, S.; Pagani, L.; Lique, F.	2020, MNRAS, 499, 1795-1804
2666	IRAM 30-m-EMIR Redshift Search of $z = 3$ -4 Lensed Dusty Starbursts Selected from the HerBS Sample	Bakx, T. J. L. C.; Dannerbauer, H.; Frayer, D.; Eales, S. A.; Pérez-Fournon, I.; Cai, Z.-Y.; Clements, D. L.; De Zotti, G.; González-Nuevo, J.; Ivison, R. J.; Lapi, A.; Michałowski, M. J.; Negrello, M.; Serjeant, S.; Smith, M. W. L.; Temi, P.; Urquhart, S.; van der Werf, P.	2020, MNRAS, 496, 2372-2390
2667	Simultaneous Millimetre-Wave and X-Ray Monitoring of the Seyfert Galaxy NGC 7469	Behar, E.; Kaspi, S.; Paubert, G.; Billot, N.; Peretz, U.; Baldi, R. D.; Laor, A.; Kaastra, J.; Mehdipour, M.	2020, MNRAS, 491, 3523-3534
2668	What Drives Galaxy Quenching? Resolving Molecular Gas and Star Formation in the Green Valley	Brownson, S.; Belfiore, F.; Maiolino, R.; Lin, L.; Carniani, S.	2020, MNRAS, 498, L66-L71
2669	SiO Emission as a Probe of Cloud-Cloud Collisions in Infrared Dark Clouds	Cosentino, G.; Jiménez-Serra, I.; Henshaw, J. D.; Caselli, P.; Viti, S.; Barnes, A. T.; Tan, J. C.; Fontani, F.; Wu, B.	2020, MNRAS, 499, 1666-1681
2670	Galaxy Cold Gas Contents in Modern Cosmological Hydrodynamic Simulations	Davé, R.; Crain, R. A.; Stevens, A. R. H.; Narayanan, D.; Saintonge, A.; Catinella, B.; Cortese, L.	2020, MNRAS, 497, 146-166
2671	Gas Kinematics of Key Prebiotic Molecules in GV Tau N Revealed with an ALMA, PdBI, and Herschel Synergy	Fuente, A.; Treviño-Morales, S. P.; Le Gal, R.; Rivière-Marichalar, P.; Pilleri, P.; Rodríguez-Baras, M.; Navarro-Almada, D.	2020, MNRAS, 496, 5330-5340
2672	Predicting Fully Self-Consistent Satellite Richness, Galaxy Growth, and Star Formation Rates from the Statistical SEMI-Empirical Model STEEL	Grylls, P. J.; Shankar, F.; Leja, J.; Menci, N.; Moster, B.; Behroozi, P.; Zanisi, L.	2020, MNRAS, 491, 634-654
2673	Differentiating Disc and Black Hole-Driven Jets with EHT Images of Variability in M87	Jeter, B.; Broderick, A. E.; Gold, R.	2020, MNRAS, 493, 5606-5616
2674	Constraints on the Electron-to-Proton Mass Ratio Variation at the Epoch of Reionization	Levshakov, S. A.; Kozlov, M. G.; Agafonova, I. I.	2020, MNRAS, 498, 3624-3632
2675	Isotopologues of Dense Gas Tracers in Nearby Infrared Bright Galaxies	Li, F.; Wang, J.; Fang, M.; Li, S.; Zhang, Z.-Y.; Gao, Y.; Kong, M.	2020, MNRAS, 494, 1095-1113
2676	The HASHTAG Project I. A Survey of CO(3-2) Emission from the Star Forming Disc of M31	Li, Z.; Li, Z.; Smith, M. W. L.; Wilson, C. D.; Gao, Y.; Eales, S. A.; Ao, Y.; Bureau, M.; Chung, A.; Davis, T. A.; de Grijs, R.; Eden, D. J.; He, J.; Hughes, T. M.; Jiang, X.; Kemper, F.; Lamperti, I.; Lee, B.; Lee, C.-H.; Michałowski, M. J.; Parsons, H.; Ragan, S.; Scicluna, P.; Shi, Y.; Tang, X.; Tomičić, N.; Viaene, S.; Williams, T. G.; Zhu, M.	2020, MNRAS, 492, 195-209
2677	What Has Quenched the Massive Spiral Galaxies?	Luo, Y.; Li, Z.; Kang, X.; Li, Z.; Wang, P.	2020, MNRAS, 496, L116-L121
2678	Observability of Dusty Debris Discs around M-Stars	Luppe, P.; Krivov, A. V.; Booth, M.; Lestrade, J.-F.	2020, MNRAS, 499, 3932-3942
2679	A Panchromatic Spatially Resolved Analysis of Nearby Galaxies - II. The Main Sequence - Gas Relation at Sub-Kpc Scale in Grand-Design Spirals	Morselli, L.; Rodighiero, G.; Enia, A.; Corbelli, E.; Casasola, V.; Rodríguez-Muñoz, L.; Renzini, A.; Tacchella, S.; Baronchelli, I.; Bianchi, S.; Cassata, P.; Franceschini, A.; Mancini, C.; Negrello, M.; Popesso, P.; Romano, M.	2020, MNRAS, 496, 4606-4623
2680	Multiwavelength Modelling of the Circumstellar Environment of the Massive Protostar AFGL 2591 VLA 3	Olguin, F. A.; Hoare, M. G.; Johnston, K. G.; Motte, F.; Chen, H.-R. V.; Beuther, H.; Mottram, J. C.; Ahmadi, A.; Gieser, C.; Semenov, D.; Peters, T.; Palau, A.; Klaassen, P. D.; Kuiper, R.; Sánchez-Monge, Á.; Henning, T.	2020, MNRAS, 498, 4721-4744
2681	Cosmic Evolution of Molecular Gas Mass Density from an Empirical Relationship between L1.4 GHz and LCO	Orellana-González, G.; Ibar, E.; Leiton, R.; Thomson, A. P.; Cheng, C.; Ivison, R. J.; Herrera-Camus, R.; Messias, H.; Calderón-Castillo, P.; Hughes, T. M.; Leeuw, L.	2020, MNRAS, 495, 1760-1770
2682	H I Scale Height in Spiral Galaxies	Patra, N. N.	2020, MNRAS, 499, 2063-2075
2683	DC <sub>3</sub> N Observations towards High-Mass Star-Forming Regions	Rivilla, V. M.; Colzi, L.; Fontani, F.; Melosso, M.; Caselli, P.; Bizzocchi, L.; Tamassia, F.; Dore, L.	2020, MNRAS, 496, 1990-1999

n°	Titre	Auteurs	Référence
2684	Molecular Hydrogen in IllustrisTNG Galaxies: Carefully Comparing Signatures of Environment with Local CO & SFR Data	Stevens, A. R. H.; Lagos, C. del P.; Cortese, L.; Catinella, B.; Diemer, B.; Nelson, D.; Pillepich, A.; Hernquist, L.; Marinacci, F.; Vogelsberger, M.	2020, MNRAS, staa3662
2685	Constructing a Multivariate Distribution Function with a Vine Copula: Towards Multivariate Luminosity and Mass Functions	Takeuchi, T. T.; Kono, K. T.	2020, MNRAS, 498, 4365–4378
2686	Molecular Line Ratio Diagnostics along the Radial Cut and Dusty Ultraviolet-Bright Clumps in a Spiral Galaxy NGC 0628	Topal, S.	2020, MNRAS, 495, 2682–2712
2687	CO Observations towards H=I-Rich Ultradiffuse Galaxies	Wang, J.; Yang, K.; Zhang, Z.-Y.; Fang, M.; Shi, Y.; Liu, S.; Li, J.; Li, F.	2020, MNRAS, 499, L26–L30
2688	Cloud-Cloud Collision as Drivers of the Chemical Complexity in Galactic Centre Molecular Clouds	Zeng, S.; Zhang, Q.; Jiménez-Serra, I.; Terceiro, B.; Lu, X.; Martín-Pintado, J.; de Vicente, P.; Rivilla, V. M.; Li, S.	2020, MNRAS, 497, 4896–4909
2689	Chemical Models of Interstellar Cyanomethanimine Isomers	Zhang, X.; Quan, D.; Chang, Q.; Herbst, E.; Esimbek, J.; Webb, M.	2020, MNRAS, 497, 609–625
2690	HCN 3-2 Survey towards a Sample of Local Galaxies	Li, F.; Wang, J.; Fang, M.; Tan, Q.-H.; Zhang, Z.-Y.; Gao, Y.; Li, S.	2020, PASJ, 72, 41
2691	86-GHz SiO Masers in Galactic Centre OH/IR Stars	Messineo, M.; Sjouwerman, L. O.; Habing, H. J.; Omont, A.	2020, PASJ, 72, 63
2692	Probing UV-Sensitive Pathways for CN and HCN Formation in Protoplanetary Disks with the Hubble Space Telescope	Arulanantham, N.; France, K.; Cazzoletti, P.; Miotello, A.; Manara, C. F.; Schneider, P. C.; Hoadley, K.; van Dishoeck, E. F.; Günther, H. M.	2020, Astron. J., 159, 168
2693	Time-Variable Radio Recombination Line Emission in W49A	De Pree, C. G.; Wilner, D. J.; Kristensen, L. E.; Galván-Madrid, R.; Goss, W. M.; Klessen, R. S.; Mac Low, M.-M.; Peters, T.; Robinson, A.; Sloman, S.; Rao, M.	2020, Astron. J., 160, 234
2694	The Physical Parameters of Clumps Associated with Class I Methanol Masers	Ladeyschikov, D. A.; Urquhart, J. S.; Sobolev, A. M.; Breen, S. L.; Bayandina, O. S.	2020, Astron. J., 160 (5), 213
2695	Star-Forming Galaxies at Cosmic Noon	Förster Schreiber, N. M.; Wuyts, S.	2020, Annu. Rev. Astron. Astrophys., 58, 661–725
2696	The Evolution of the Star-Forming Interstellar Medium Across Cosmic Time	Tacconi, L. J.; Genzel, R.; Sternberg, A.	2020, Annu. Rev. Astron. Astrophys., 58, 157–203
2697	Tracing High-Energy Irradiation in Molecular Gas: Radio Studies of Nearby Planetary Nebulae	Bublitz, J.	2020, BAAS, 235, 152.04
2698	Observational Constraints and Modeling Dust at $5 < z < 10$	Burgarella, D.; Nanni, A.; Hirashita, H.; Theulé, P.; Inoue, A.; Takeuchi, T. T.	2020, BAAS, 235, 459.02
2699	Tending the Fire: A Molecular Gas Study of Hard X-Ray Selected AGN from the BASS Survey	Koss, M.; BASS Survey Team; Treister, E.; Cicone, C.; Shimizu, T.; Saintonge, A.; Privon, G.; Sanders, D.; Schawinski, K.; Lamperti, I.; Mushotzky, R.	2020, BAAS, 235, 325.03
2700	The Unexpected Molecular Complexity of Planetary Nebulae as Revealed by Millimeter-Wave Observations	Schmidt, D. R.	2020, BAAS, 236, 320.02
2701	2 mm GISMO Observations of the Galactic Center: Dust Emission, Nonthermal Filament in the Radio Arc, and Compact Sources	Staguhn, J.; Arendt, R.; Dwek, E.; Morris, M.; Yusef-Zadeh, F.; Benford, D.; Kovacs, A.; Gonzalez-Quiles, J.	2020, BAAS, 235, 158.02
2702	The Complete Local-Volume Groups Sample (CLOGS): Recent Results from X-Ray, Radio Continuum, and CO Line Observations	Vrtilek, J. M.; O'Sullivan, E.; Kolokythas, K.; David, L.; Schellenberger, G.; Gitti, M.; Giacintucci, S.; Babul, A.; Raychaudhury, S.; Combes, F.; Salome, P.	2020, BAAS, 235, 127.06
2703	Dense Gas Tracers in the Most Massive Infrared Dark Cloud	Walters, L. C.; Tan, J.; Viti, S.; Caselli, P.; Jones, D.; Walsh, C.	2020, BAAS, 235, 216.06
2704	Imaging Black Holes and Jets with a VLBI Array Including Multiple Space-Based Telescopes	Fish, V. L.; Shea, M.; Akiyama, K.	2020, Adv. Space Res., 65, 821–830
2705	Toward the RNA-World in the Interstellar Medium—Detection of Urea and Search of 2-Amino-Oxazole and Simple Sugars	Jiménez-Serra, I.; Martín-Pintado, J.; Rivilla, V. M.; Rodríguez-Almeida, L.; Alonso Alonso, E. R.; Zeng, S.; Cocinero, E. J.; Martín, S.; Requena-Torres, M.; Martín-Domenech, R.; Testi, L.	2020, Astrobiology, 20, 1048–1066
2706	Deuterium Fractionation in the Oph-H-MMI Dense Core of the L1688 Low Mass Star-Forming Region	Petrashkevich, I. V.; Punanova, A. F.; Caselli, P.; Pineda, J.; Pon, A.; Friesen, R.	2020, Astron. Rep., 64, 637–640
2707	Accretion Disks around Young Stars: The Cradles of Planet Formation	Semenov, D. A.; Teague, R. D.	2020, Europhys. News, 51, 29–32
2708	Irradiation Investigation: Exploring the Molecular Gas in NGC 7293	Bublitz, J.; Kastner, J.; Hily-Blant, P.; Forveille, T.; Santander-García, M.; Bujarrabal, V.; Alcolea, J.; Montez, R., Jr.	2020, Galaxies, 8, 32
2709	Submillimeter-Wave Spectroscopy of and Interstellar Search for Thioacetaldehyde	Margulès, L.; Ilyushin, V. V.; McGuire, B. A.; Belloche, A.; Motiyenko, R. A.; Remijan, A.; Alekseev, E. A.; Dorovskaya, O.; Guillemin, J.-C.	2020, J. Mol. Spectrosc., 371, 111304

n°	Titre	Auteurs	Référence
2710	From Diffuse Gas to Dense Molecular Cloud Cores	Ballesteros-Paredes, J.; André, P.; Hennebelle, P.; Klessen, R. S.; Kruijssen, J. M. D.; Chevance, M.; Nakamura, F.; Adamo, A.; Vázquez-Semadeni, E.	2020, Space Sci. Rev., 216, 76
2711	Nitrogen Atmospheres of the Icy Bodies in the Solar System	Scherf, M.; Lammer, H.; Erkaev, N. V.; Mandt, K. E.; Thaller, S. E.; Marty, B.	2020, Space Sci. Rev., 216, 123
2712	Recurrent Cometary Activity in Near-Earth Object (3552) Don Quixote	Mommert, M.; Hora, J. L.; Trilling, D. E.; Biver, N.; Wierzchos, K.; Harrington Pinto, O.; Agarwal, J.; Kim, Y.; McNeill, A.; Womack, M.; Knight, M. M.; Polishook, D.; Moskovitz, N.; Kelley, M. S. P.; Smith, H. A.	2020, The Planetary Science Journal, 1, 12
2713	DYNAMO: An Upclose View of Turbulent, Clumpy Galaxies	Fisher, D.	2020, IAU, 352, 317-317
2714	Galaxy Build-up at Cosmic Dawn: Insights from Deep Observations with Hubble, Spitzer, and ALMA	Oesch, P.	2020, IAU, 352, 12-12
2715	Characterizing the Youngest Protostellar Disks with the IRAM-PdBI and ALMA Interferometers	Maury, A.	2020, IAU, 345, 91-95
2716	Statistical Trends of the GEMS Molecular Database	Rodríguez-Baras, M.; Fuente, A.; Rivière-Marichalar, P.; Navarro, D. G.; Tercero, B.; Esplugues, G. B.; Alonso-Albi, T.; GEMS Collaboration	2020, XIV <sup>o</sup> Scientific Meeting (virtual) of the Spanish Astronomical Society, 183
2717	Astrophysics Research at DAP	Diep, P. N.; Hoai, D. T.; Nhung, P. T.; Phuong, N. T.; Thai, T. T.; Tuan-Anh, P.; Darriulat, P.	2020, EPJ Web of Conferences, 240, 03001
2718	Complex Organics in Protostellar Disks: The First Stage of a Long Chemical Journey to Planetary Systems	Codella, C.; Ceccarelli, C.; Lee, C.-F.; De Simone, M.; Bianchi, E.; Podio, L.; Mercimek, S.	2020, EPSC, 14, 288
2719	Observing Atmospheric HCN on Titan from Space and Ground-Based Observatories: An Inter-Comparison Study from Herschel, APEX and IRAM 30-meter Telescopes	Rengel, M.; Shulyak, D.; Hartogh, P.; Sagawa, H.; Moreno, R.; Jarchow, C.	2020, EPSC, 14, 570
2720	The Power of PolyFiX at NOEMA: New Insights into Sulfur Chemistry in DM Tau	Semenov, D.; Favre, C.; Fedele, D.; Teague, R.; Dutrey, A.; Guilloteau, S.; Henning, T.; Smirnov-Pinchukov, G.	2020, EPSC, 14, 304
2721	The Interstellar Medium Properties of High Redshift Galaxies	Leung, T. K. D.	2020, PhD Thesis

## IRAM (CO) AUTHORS

N°	Titre	Auteurs	Référence
2499	Exploring the Formation Pathways of Formamide. Near Young O-Type Stars.	Allen, V.; van der Tak, F. F. S.; López-Sepulcre, A.; Sánchez-Monge, Á.; Rivilla, V. M.; Cesaroni, R.	2020, A&A, 636, A67
2500	Probing Episodic Accretion with Chemistry: CALYPSO Observations of the Very-Low-Luminosity Class 0 Protostar IRAM 04191+1522. Results from the CALYPSO IRAM-PdBI Survey	Anderl, S.; Maret, S.; Cabrit, S.; Maury, A. J.; Belloche, A.; André, Ph.; Bacmann, A.; Codella, C.; Podio, L.; Gueth, F.	2020, A&A, 643, A123
2501	Absolute Calibration of the Polarisation Angle for Future CMB B-Mode Experiments from Current and Future Measurements of the Crab Nebula	Aumont, J.; Macías-Pérez, J. F.; Ritacco, A.; Ponthieu, N.; Mangilli, A.	2020, A&A, 634, A100
2502	The Multi-Phase ISM in the Nearby Composite AGN-SB Galaxy NGC 4945: Large-Scale (Parsecs) Mechanical Heating	Bellochchi, E.; Martín-Pintado, J.; Güsten, R.; Requena-Torres, M. A.; Harris, A.; van der Werf, P. P.; Israel, F. P.; Weiss, A.; Kramer, C.; García-Burillo, S.; Stutzki, J.	2020, A&A, 642, A166
2503	Questioning the Spatial Origin of Complex Organic Molecules in Young Protostars with the CALYPSO Survey	Belloche, A.; Maury, A. J.; Maret, S.; Anderl, S.; Bacmann, A.; André, Ph.; Bontemps, S.; Cabrit, S.; Codella, C.; Gaudel, M.; Gueth, F.; Lefèvre, C.; Lefloch, B.; Podio, L.; Testi, L.	2020, A&A, 635, A198
2504	Possible Evidence of Ongoing Planet Formation in AB Aurigae. A Showcase of the SPHERE/ALMA Synergy	Boccaletti, A.; Di Folco, E.; Pantin, E.; Dutrey, A.; Guilloteau, S.; Tang, Y. W.; Piétu, V.; Habart, E.; Milli, J.; Beck, T. L.; Maire, A.-L.	2020, A&A, 637, L5
2505	The OTELO Survey. A Case Study of [O III] $\lambda 4959,5007$ Emitters at $z = 0.83$	Bongiovanni, Á.; Ramón-Pérez, M.; Pérez García, A. M.; Cerviño, M.; Cepa, J.; Nadolny, J.; Pérez Martínez, R.; Alfaro, E. J.; Castañeda, H. O.; Cedrés, B.; de Diego, J. A.; Ederoclite, A.; Fernández-Lorenzo, M.; Gallego, J.; de Jesús González, J.; González-Serrano, J. I.; Lara-López, M. A.; Oteo Gómez, I.; Padilla Torres, C. P.; Pintos-Castro, I.; Pović, M.; Sánchez-Portal, M.; Heath Jones, D.; Bland-Hawthorn, J.; Cabrera-Lavers, A.	2020, A&A, 635, A35
2506	The OTELO Survey. A Case Study of [O III] $\lambda 4959,5007$ Emitters at $z = 0.83$ (Corrigendum)	Bongiovanni, Á.; Ramón-Pérez, M.; Pérez García, A. M.; Cerviño, M.; Cepa, J.; Nadolny, J.; Pérez Martínez, R.; Alfaro, E. J.; Castañeda, H. O.; Cedrés, B.; de Diego, J. A.; Ederoclite, A.; Fernández-Lorenzo, M.; Gallego, J.; de Jesús González, J.; González-Serrano, J. I.; Lara-López, M. A.; Oteo Gómez, I.; Padilla Torres, C. P.; Pintos-Castro, I.; Pović, M.; Sánchez-Portal, M.; Heath Jones, D.; Bland-Hawthorn, J.; Cabrera-Lavers, A.	2020, A&A, 637, C2
2507	Hunting for Hot Corinos and WCCC Sources in the OMC-2/3 Filament.	Bouvier, M.; López-Sepulcre, A.; Ceccarelli, C.; Kahane, C.; Imai, M.; Sakai, N.; Yamamoto, S.; Dagdigan, P. J.	2020, A&A, 636, A19
2508	High-Resolution Observations of the Symbiotic System R Aqr. Direct Imaging of the Gravitational Effects of the Secondary on the Stellar Wind (Corrigendum).	Bujarrabal, V.; Alcolea, J.; Mikofajewska, J.; Castro-Carrizo, A.; Ramstedt, S.	2020, A&A, 633, C1
2509	Molecular Gas and Star Formation Activity in Luminous Infrared Galaxies in Clusters at Intermediate Redshifts	Castignani, G.; Jablonka, P.; Combes, F.; Haines, C. P.; Rawle, T.; Jauzac, M.; Egami, E.; Krips, M.; Spérone-Longin, D.; Arnaud, M.; García-Burillo, S.; Schinnerer, E.; Bigiel, F.	2020, A&A, 640, A64
2510	Seeds of Life in Space (SOLIS). V. Methanol and Acetaldehyde in the Protostellar Jet-Driven Shocks L1157-B0 and B1.	Codella, C.; Ceccarelli, C.; Bianchi, E.; Balucani, N.; Podio, L.; Caselli, P.; Feng, S.; Lefloch, B.; López-Sepulcre, A.; Neri, R.; Spezzano, S.; De Simone, M.	2020, A&A, 635, A17
2511	FRIPON: A Worldwide Network to Track Incoming Meteoroids	Colas, F.; Zanda, B.; Bouley, S.; Jeanne, S.; Malgouyre, A.; Birlan, M.; Blanpain, C.; Gattacceca, J.; Jorda, L.; Lecubin, J.; Marmo, C.; Rault, J. L.; Vaubaillon, J.; Vernazza, P.; Yohia, C.; Gardiol, D.; Nedelcu, A.; Poppe, B.; Rowe, J.; Forcier, M.; Koschny, D.; Trigo-Rodríguez, J. M.; Lamy, H.; Behrend, R.; Ferrière, L.; Barghini, D.; Buzzoni, A.; Carbognani, A.; Di Carlo, M.; Di Martino, M.; Knapic, C.; Londero, E.; Pratesi, G.; Rasetti, S.; Riva, W.; Stirpe, G. M.; Valsecchi, G. B.; Volpicelli, C. A.; Zorba, S.; Coward, D.; Drolshagen, E.; Drolshagen, G.; Hernandez, O.; Jehin, E.; Jobin, M.; King, A.; Nitschelm, C.; Ott, T.; Sanchez-Lavega, A.; Toni, A.; Abraham, P.; Affaticati, F.; Albani, M.; Andreis, A.; Andrieu, T.; Anghel, S.; Antaluca, E.; Antier, K.; Appéré, T.; Armand, A.; Ascione, G.; Audureau, Y.; Auxepaules, G.; Avoscan, T.; Baba Aissa, D.; Bacci, P.; Bădescu, O.; Baldini, R.; Baldo, R.; Balestrero, A.; Baratoux, D.; Barbotin, E.; Bardy, M.; Basso, S.; Bautista, O.; Bayle, L. D.; Beck, P.; Bellitto, R.; Belluso, R.; Benna, C.; Benammi, M.; Beneteau, E.; Benkhaldoun, Z.; Bergamini, P.; Bernardi, F.; Bertaina, M. E.; Bessin, P.; Betti, L.; Bettonvil, F.; Bihel, D.; Birnbaum, C.; Blagoi, O.; Blouri, E.; Boacă, I.; Boată, R.; Bobiet, B.; Bonino, R.; Boros, K.; Bouchet, E.; Borgeot, V.; Bouchez, E.; Boust, D.; Boudon, V.; Bouman, T.; Bourget, P.; Brandenburg, S.; Bramond, Ph.; Braun, E.; Bussi, A.; Cacault, P.; Caillier, B.; Calegario, A.; Camargo, J.; Caminade, S.; Campana, A. P. C.; Campbell-Burns, P.; Canal-Domingo, R.; Carell, O.; Carreau, S.; Cascone, E.; Cattaneo, C.; Cauhape, P.; Cavier, P.; Celestin, S.; Cellino, A.; Champenois, M.; Chennaoui Aoudjehane, H.; Chevrier, S.; Cholvy, P.; Chomier, L.	2020, A&A, 644, A53



N°	Titre	Auteurs	Référence
2511	FRIPON: A Worldwide Network to Track Incoming Meteoroids (cont.)	Christou, A.; Cricchio, D.; Coadou, P.; Cocaign, J. Y.; Cochard, F.; Cointin, S.; Colombi, E.; Colque Saavedra, J. P.; Corp, L.; Costa, M.; Costard, F.; Cottier, M.; Courmoyer, P.; Coustal, E.; Cremonese, G.; Cristea, O.; Cuzon, J. C.; D'Agostino, G.; Daifallah, K.; Dănescu, C.; Dardon, A.; Dasse, T.; Davadan, C.; Debs, V.; Defaix, J. P.; Deleflie, F.; D'Elia, M.; De Luca, P.; De Maria, P.; Deverchère, P.; Devillepoix, H.; Dias, A.; Di Dato, A.; Di Luca, R.; Dominici, F. M.; Drouard, A.; Dumont, J. L.; Dupouy, P.; Duvignac, L.; Egal, A.; Erasmus, N.; Esseiva, N.; Ebel, A.; Eisengarten, B.; Federici, F.; Feral, S.; Ferrant, G.; Ferreol, E.; Finitzer, P.; Foucault, A.; Francois, P.; Frínco, M.; Froger, J. L.; Gaborit, F.; Gagliarducci, V.; Galard, J.; Gardavot, A.; Garmier, M.; Garnung, M.; Gautier, B.; Gendre, B.; Gerard, D.; Gerardi, A.; Godet, J. P.; Grandchamps, A.; Grouiez, B.; Groult, S.; Guidetti, D.; Giuli, G.; Hello, Y.; Henry, X.; Herbreteau, G.; Herpin, M.; Hewins, P.; Hillairet, J. J.; Horak, J.; Hueso, R.; Huet, E.; Huet, S.; Hyaumé, F.; Interrante, G.; Isselin, Y.; Jeangeorges, Y.; Janeux, P.; Jeanneret, P.; Jobse, K.; Jouin, S.; Jouvard, J. M.; Joy, K.; Julien, J. F.; Kacerek, R.; Kaire, M.; Kempf, M.; Koschny, D.; Krier, C.; Kwon, M. K.; Lacassagne, L.; Lachat, D.; Lagain, A.; Laisné, E.; Lanchares, V.; Laskar, J.; Lazzarin, M.; Leblanc, M.; Lebreton, J. P.; Lecomte, J.; Le Dô, P.; Lelong, F.; Lera, S.; Leoni, J. F.; Le Pichon, A.; Le Poupon, P.; Leroy, A.; Leto, G.; Levansuu, A.; Lewin, E.; Lienard, A.; Licchelli, D.; Locatelli, H.; Loehle, S.; Loizeau, D.; Luciani, L.; Maignan, M.; Manca, F.; Mancuso, S.; Mandon, E.; Mangold, N.; Mannucci, F.; Maquet, L.; Marant, D.; Marchal, Y.; Marin, J. L.; Martin-Brisset, J. C.; Martin, D.; Mathieu, D.; Maury, A.; Mespoulet, N.; Meyer, F.; Meyer, J. Y.; Meza, E.; Moggi Cecchi, V.; Moiroud, J. J.; Millan, M.; Montesarchio, M.; Misiano, A.; Molinari, E.; Molau, S.; Monari, J.; Monflier, B.; Monkos, A.; Montemaggi, M.; Monti, G.; Moreau, R.; Morin, J.; Mourgues, R.; Mousis, O.; Nablanc, C.; Nastasi, A.; Niaçsu, L.; Notez, P.; Ory, M.; Pace, E.; Paganelli, M. A.; Pagola, A.; Pajuelo, M.; Palacián, J. F.; Pallier, G.; Paraschiv, P.; Pardini, R.; Pavone, M.; Pavy, G.; Payen, G.; Pegoraro, A.; Peña-Asensio, E.; Perez, L.; Pérez-Hoyos, S.; Perlerin, V.; Peyrot, A.; Peth, F.; Pic, V.; Pietronave, S.; Pilger, C.; Piquel, M.; Pisanu, T.; Poppe, M.; Portois, L.; Prezeau, J. F.; Pugno, N.; Quantin, C.; Quitté, G.; Rambaux, N.; Ravier, E.; Repetti, U.; Ribas, S.; Richard, C.; Richard, D.; Rigoni, M.; Rivet, J. P.; Rizzi, N.; Rochain, S.; Rojas, J. F.; Romeo, M.; Rotaru, M.; Rotger, M.; Rougier, P.; Rousset, P.; Rousset, J.; Rousseau, D.; Rubiera, O.; Rudawska, R.; Rudelle, J.; Ruguet, J. P.; Russo, P.; Sales, S.; Sauzereau, O.; Salvati, F.; Schieffer, M.; Schreiner, D.; Scribano, Y.; Selvestrel, D.; Serra, R.; Shengold, L.; Shuttleworth, A.; Smareglia, R.; Sohy, S.; Soldi, M.; Stanga, R.; Steinhäusser, A.; Strafella, F.; Sylla Mbaye, S.; Smedley, A. R. D.; Tagger, M.; Tanga, P.; Taricco, C.; Teng, J. P.; Tercu, J. O.; Thizy, O.; Thomas, J. P.; Tombelli, M.; Trangosi, R.; Tregon, B.; Trivero, P.; Tukkers, A.; Turcu, V.; Umbriaco, G.; Unda-Sanzana, E.; Vairetti, R.; Valenzuela, M.; Valente, G.; Varennes, G.; Vauclair, S.; Vergne, J.; Verlinden, M.; Vidal-Alaiz, M.; Vieira-Martins, R.; Viel, A.; Vintdevarã, D. C.; Vinogradoff, V.; Volpini, P.; Wendling, M.; Wilhelm, P.; Wohlgemuth, K.; Yanguas, P.; Zagarella, R.; Zollo, A.	2020, A&A, 644, A53
2512	Galaxy Classification: Deep Learning on the OTELO and COSMOS Databases	de Diego, J. A.; Nadolny, J.; Bongiovanni, Á.; Cepa, J.; Pović, M.; Pérez García, A. M.; Padilla Torres, C. P.; Lara-López, M. A.; Cerviño, M.; Pérez Martínez, R.; Alfaro, E. J.; Castañeda, H. O.; Fernández-Lorenzo, M.; Gallego, J.; González, J. J.; González-Serrano, J. I.; Pintos-Castro, I.; Sánchez-Portal, M.; Cedrés, B.; González-Otero, M.; Heath Jones, D.; Bland-Hawthorn, J.	2020, A&A, 638, A134
2513	Seeds of Life in Space (SOLIS). X. Interstellar Complex Organic Molecules in the NGC 1333 IRAS 4A Outflows	De Simone, M.; Codella, C.; Ceccarelli, C.; López-Sepulcre, A.; Witzel, A.; Neri, R.; Balucani, N.; Caselli, P.; Favre, C.; Fontani, F.; Lefloch, B.; Ospina-Zamudio, J.; Pineda, J. E.; Taquet, V.	2020, A&A, 640, A75
2514	An ALMA/NOEMA Study of Gas Dissipation and Dust Evolution in the 5 Myr-Old HD 141569A Hybrid Disc	Di Folco, E.; Péricaud, J.; Dutrey, A.; Augereau, J.-C.; Chapillon, E.; Guilloteau, S.; Piétu, V.; Boccaletti, A.	2020, A&A, 635, A94
2515	The Structure and Characteristic Scales of Molecular Clouds	Dib, S.; Bontemps, S.; Schneider, N.; Elia, D.; Ossenkopf-Okada, V.; Shadmehri, M.; Arzoumanian, D.; Motte, F.; Heyer, M.; Nordlund, Å.; Ladjelate, B.	2020, A&A, 642, A177
2516	Seeds of Life in Space (SOLIS). VII. Discovery of a Cold Dense Methanol Blob toward the L1521F VeLLO System	Favre, C.; Vastel, C.; Jimenez-Serra, I.; Quénard, D.; Caselli, P.; Ceccarelli, C.; Chacón-Tanarro, A.; Fontani, F.; Holdship, J.; Oya, Y.; Punanova, A.; Sakai, N.; Spezzano, S.; Yamamoto, S.; Neri, R.; López-Sepulcre, A.; Alves, F.; Bachiller, R.; Balucani, N.; Bianchi, E.; Bizzocchi, L.; Codella, C.; Caux, E.; De Simone, M.; Enrique Romero, J.; Dulieu, F.; Feng, S.; Jaber Al-Edhari, A.; Lefloch, B.; Ospina-Zamudio, J.; Pineda, J.; Podio, L.; Rimola, A.; Segura-Cox, D.; Sims, I. R.; Taquet, V.; Testi, L.; Theulé, P.; Ugliengo, P.; Vasyunin, A. I.; Vazart, F.; Viti, S.; Witzel, A.	2020, A&A, 635, A189
2517	Angular Momentum Profiles of Class 0 Protostellar Envelopes	Gaudel, M.; Maury, A. J.; Belloche, A.; Maret, S.; André, Ph.; Hennebelle, P.; Galametz, M.; Testi, L.; Cabrit, S.; Palmeirim, P.; Ladjelate, B.; Codella, C.; Podio, L.	2020, A&A, 637, A92
2518	Molecular Globules in the Veil Bubble of Orion. IRAM 30-m <sup>12</sup> CO, <sup>13</sup> CO, and C <sup>18</sup> O (2-1) Expanded Maps of Orion A	Goicoechea, J. R.; Pabst, C. H. M.; Kabanovic, S.; Santa-Maria, M. G.; Marcelino, N.; Tielens, A. G. G. M.; Hacar, A.; Berné, O.; Buchbender, C.; Cuadrado, S.; Higgins, R.; Kramer, C.; Stutzki, J.; Suri, S.; Teyssier, D.; Wolfire, M.	2020, A&A, 639, A1
2519	The Headlight Cloud in NGC 628: An Extreme Giant Molecular Cloud in a Typical Galaxy Disk	Herrera, C. N.; Pety, J.; Hughes, A.; Meidt, S. E.; Kreckel, K.; Querejeta, M.; Saito, T.; Lang, P.; Jiménez-Donaire, M. J.; Pessa, I.; Cormier, D.; Usero, A.; Sliwa, K.; Faesi, C.; Blanc, G. A.; Bigiel, F.; Chevance, M.; Dale, D. A.; Grasha, K.; Glover, S. C. O.; Hygate, A. P. S.; Kruijssen, J. M. D.; Leroy, A. K.; Rosolowsky, E.; Schinnerer, E.; Schrubba, A.; Sun, J.; Utomo, D.	2020, A&A, 634, A121
2520	ATOMIUM: A High-Resolution View on the Highly Asymmetric Wind of the AGB Star ΠIGruis. I. First Detection of a New Companion and Its Effect on the Inner Wind	Homan, W.; Montargès, M.; Pimpanuwat, B.; Richards, A. M. S.; Wallström, S. H. J.; Kervella, P.; Decin, L.; Zijlstra, A.; Danilovich, T.; de Koter, A.; Menten, K.; Sahai, R.; Plane, J.; Lee, K.; Waters, R.; Baudry, A.; Tat Wong, K.; Millar, T. J.; Van de Sande, M.; Lagadec, E.; Gobrecht, D.; Yates, J.; Price, D.; Cannon, E.; Bolte, J.; De Ceuster, F.; Herpin, F.; Nuth, J.; Philip Sindel, J.; Kee, D.; Grey, M. D.; Etoka, S.; Jeste, M.; Gottlieb, C. A.; Gottlieb, E.; McDonald, I.; El Mellah, I.; Müller, H. S. P.	2020, A&A, 644, A61

N°	Titre	Auteurs	Référence
2521	Molecular Remnant of Nova 1670 (CK Vulpeculae). I. Properties and Enigmatic Origin of the Gas	Kamiński, T.; Menten, K. M.; Tylenda, R.; Wong, K. T.; Belloche, A.; Mehner, A.; Schmidt, M. R.; Patel, N. A.	2020, A&A, 644, A59
2522	Exploiting NIKA2/XMM-Newton Imaging Synergy for Intermediate-Mass High-z Galaxy Clusters within the NIKA2 SZ Large Program. Observations of ACT-CLJ0215.4+0030 at $z \sim 0.9$	Kéruszoré, F.; Mayet, F.; Pratt, G. W.; Adam, R.; Ade, P.; André, P.; Andrianasolo, A.; Arnaud, M.; Aussel, H.; Bartalucci, I.; Beelen, A.; Benoît, A.; Berta, S.; Bourrion, O.; Calvo, M.; Catalano, A.; De Petris, M.; Désert, F.-X.; Doyle, S.; Driessen, E. F. C.; Gomez, A.; Goupy, J.; Kramer, C.; Ladjelate, B.; Lagache, G.; Leclercq, S.; Lestrade, J.-F.; Macías-Pérez, J. F.; Mauskopf, P.; Monfardini, A.; Perotto, L.; Pisano, G.; Pointecouteau, E.; Ponthieu, N.; Revéret, V.; Ritacco, A.; Romero, C.; Roussel, H.; Ruppin, F.; Schuster, K.; Shu, S.; Sievers, A.; Tucker, C.	2020, A&A, 644, A93
2523	Event Horizon Telescope Imaging of the Archetypal Blazar 3C 279 at an Extreme 20 Microarcsecond Resolution	Kim, J.-Y.; Krichbaum, T. P.; Broderick, A. E.; Wielgus, M.; Blackburn, L.; Gómez, J. L.; Johnson, M. D.; Bouman, K. L.; Chael, A.; Akiyama, K.; Jorstad, S.; Marscher, A. P.; Issaoun, S.; Janssen, M.; Chan, C.; Savolainen, T.; Pesce, D. W.; Özel, F.; Alberdi, A.; Alef, W.; Asada, K.; Azulay, R.; Baczko, A.-K.; Ball, D.; Baloković, M.; Barrett, J.; Bintley, D.; Boland, W.; Bower, G. C.; Bremer, M.; Brinkerink, C. D.; Brissenden, R.; Britzen, S.; Brogiere, D.; Bronzwaer, T.; Byun, D. Y.; Carlstrom, J. E.; Chatterjee, S.; Chatterjee, K.; Chen, M.-T.; Chen, Y.; Cho, I.; Christian, P.; Conway, J. E.; Cordes, J. M.; Crew, G. B.; Cui, Y.; Davelaar, J.; De Laurentis, M.; Deane, R.; Dempsey, J.; Desvignes, G.; Dexter, J.; Doeleman, S. S.; Eatough, R. P.; Falcke, H.; Fish, V. L.; Fomalont, E.; Fraga-Encinas, R.; Friberg, P.; Fromm, C. M.; Galisp, P.; Gammie, C. F.; García, R.; Gentaz, O.; Georgiev, B.; Goddi, C.; Gold, R.; Gómez-Ruiz, A. I.; Gu, M.; Gurwell, M.; Hada, K.; Hecht, M. H.; Hesper, R.; Ho, L. C.; Ho, P.; Honma, M.; Huang, C.-W. L.; Huang, L.; Hughes, D. H.; Ikeda, S.; Inoue, M.; James, D. J.; Jannuzi, B. T.; Jeter, B.; Jiang, W.; Jimenez-Rosales, A.; Jung, T.; Karami, M.; Karuppusamy, R.; Kawashima, T.; Keating, G. K.; Kettenis, M.; Kim, J.; Kim, J.; Kino, M.; Koay, J. Y.; Koch, P. M.; Koyama, S.; Kramer, M.; Kramer, C.; Kuo, C. Y.; Lauer, T. R.; Lee, S.-S.; Li, Y.-R.; Li, Z.; Lindqvist, M.; Lico, R.; Liu, K.; Liuzzo, E.; Lo, W.-P.; Lobanov, A. P.; Loinard, L.; Lonsdale, C.; Lu, R.-S.; MacDonald, N. R.; Mao, J.; Markoff, S.; Marrone, D. P.; Martí-Vidal, I.; Matsushita, S.; Matthews, L. D.; Medeiros, L.; Menten, K. M.; Mizuno, Y.; Mizuno, I.; Moran, J. M.; Moriyama, K.; Moscibrodzka, M.; Musoke, G.; Müller, C.; Nagai, H.; Nagar, N. M.; Nakamura, M.; Narayan, R.; Narayanan, G.; Natarajan, I.; Neri, R.; Ni, C.; Noutsos, A.; Okino, H.; Olivares, H.; Ortiz-León, G. N.; Oyama, T.; Palumbo, D. C. M.; Park, J.; Patel, N.; Pen, U.-L.; Piétu, V.; Plambeck, R.; PopStefanija, A.; Porth, O.; Prather, B.; Preciado-López, J. A.; Psaltis, D.; Pu, H.-Y.; Ramakrishnan, V.; Rao, R.; Rawlings, M. G.; Raymond, A. W.; Rezzolla, L.; Ripperda, B.; Roelofs, F.; Rogers, A.; Ros, E.; Rose, M.; Roshanineshat, A.; Rottmann, H.; Roy, A. L.; Ruszczyk, C.; Ryan, B. R.; Rygl, K. L. J.; Sánchez, S.; Sánchez-Arguelles, D.; Sasada, M.; Schloerb, F. P.; Schuster, K.-F.; Shao, L.; Shen, Z.; Small, D.; Sohn, B. W.; Soohoo, J.; Tazaki, F.; Tiede, P.; Tilanus, R. P. J.; Titus, M.; Toma, K.; Torne, P.; Trent, T.; Traianou, E.; Trippe, S.; Tsuda, S.; van Bemmelen, I.; van Langevelde, H. J.; van Rossum, D. R.; Wagner, J.; Wardle, J.; Ward-Thompson, D.; Weintroub, J.; Wex, N.; Wharton, R.; Wong, G. N.; Wu, Q.; Yoon, D.; Young, A.; Young, K.; Younsi, Z.; Yuan, F.; Yuan, Y.-F.; Zensus, J. A.; Zhao, G.; Zhao, S.-S.; Zhu, Z.; Algaba, J.-C.; Allardi, A.; Amestica, R.; Anczarski, J.; Bach, U.; Baganoff, F. K.; Beaudoin, C.; Benson, B. A.; Berthold, R.; Blanchard, J. M.; Blundell, R.; Bustamente, S.; Cappallo, R.; Castillo-Domínguez, E.; Chang, C.-C.; Chang, S.-H.; Chang, S. C.; Chen, C.-C.; Chilson, R.; Chuter, T. C.; Rosado, R. C.; Coulson, I. M.; Crowley, J.; Derome, M.; Dexter, M.; Dornbusch, S.; Dudevoir, K. A.; Dzib, S. A.; Eckart, A.; Eckert, C.; Erickson, N. R.; Everett, W. B.; Faber, A.; Farah, J. R.; Fath, V.; Folkers, T. W.; Forbes, D. C.; Freund, R.; Gale, D. M.; Gao, F.; Geertsema, G.; Graham, D. A.; Greer, C. H.; Grosslein, R.; Gueth, F.; Haggard, D.; Halverson, N. W.; Han, C.-C.; Han, K.-C.; Hao, J.; Hasegawa, Y.; Henning, J. W.; Hernández-Gómez, A.; Herrero-Illana, R.; Heyminck, S.; Hirota, A.; Hoge, J.; Huang, Y.-D.; Violette Impellizzeri, C. M.; Jiang, H.; John, D.; Kamble, A.; Keisler, R.; Kimura, K.; Kono, Y.; Kubo, D.; Kuroda, J.; Lacasse, R.; Laing, R. A.; Leitch, E. M.; Li, C.-T.; Lin, L. C.-C.; Liu, C.-T.; Liu, K.-Y.; Lu, L.-M.; Marson, R. G.; Martin-Cocher, P. L.; Massingill, K. D.; Matulonis, C.; McColl, M. P.; McWhirter, S. R.; Messias, H.; Meyer-Zhao, Z.; Michalik, D.; Montaña, A.; Montgomerie, W.; Mora-Klein, M.; Muders, D.; Nadolski, A.; Navarro, S.; Neilsen, J.; Nguyen, C. H.; Nishioka, H.; Norton, T.; Nowak, M. A.; Nystrom, G.; Ogawa, H.; Oshiro, P.; Oyama, T.; Parsons, H.; Peñalver, J.; Phillips, N. M.; Poirier, M.; Pradel, N.; Primiani, R. A.; Raffin, P. A.; Rählin, A. S.; Reiland, G.; Risacher, C.; Ruiz, I.; Sáez-Madaín, A. F.; Sassella, R.; Schellart, P.; Shaw, P.; Silva, K. M.; Shiokawa, H.; Smith, D. R.; Snow, W.; Souccar, K.; Sousa, D.; Sridharan, T. K.; Srinivasan, R.; Stahm, W.; Stark, A. A.; Story, K.; Timmer, S. T.; Vertatschitsch, L.; Walther, C.; Wei, T.-S.; Whitehorn, N.; Whitney, A. R.; Woody, D. P.; Wouterloot, J. G. A.; Wright, M.; Yamaguchi, P.; Yu, C. Y.; Zeballos, M.; Zhang, S.; Ziurys, L.; Event Horizon Telescope Collaboration	2020, A&A, 640, A69
2524	ATLASGAL-Selected Massive Clumps in the Inner Galaxy. VIII. Chemistry of Photodissociation Regions	Kim, W.-J.; Wyrowski, F.; Urquhart, J. S.; Pérez-Beaupuits, J. P.; Pillai, T.; Tiwari, M.; Menten, K. M.	2020, A&A, 644, A160
2525	Properties of the Dense Core Population in Orion B as Seen by the Herschel Gould Belt Survey	Könyves, V.; André, Ph.; Arzoumanian, D.; Schneider, N.; Men'shchikov, A.; Bontemps, S.; Ladjelate, B.; Didelon, P.; Pezzuto, S.; Benedettini, M.; Bracco, A.; Di Francesco, J.; Goodwin, S.; Rygl, K. L. J.; Shimajiri, Y.; Spinoglio, L.; Ward-Thompson, D.; White, G. J.	2020, A&A, 635, A34
2526	Gas and Dust Cooling along the Major Axis of M 33 (HerM33es). Herschel/PACS [C II] and [O I] Observations	Kramer, C.; Nikola, T.; Anderl, S.; Bertoldi, F.; Boquien, M.; Braine, J.; Buchbender, C.; Combes, F.; Henkel, C.; Hermelo, I.; Israel, F.; Relaño, M.; Röllig, M.; Schuster, K.; Tabatabaei, F.; van der Tak, F.; Verley, S.; van der Werf, P.; Wiedner, M.; Xilouris, E. M.	2020, A&A, 639, A61
2527	The Herschel View of the Dense Core Population in the Ophiuchus Molecular Cloud	Ladjelate, B.; André, Ph.; Könyves, V.; Ward-Thompson, D.; Men'shchikov, A.; Bracco, A.; Palmeirim, P.; Roy, A.; Shimajiri, Y.; Kirk, J. M.; Arzoumanian, D.; Benedettini, M.; Di Francesco, J.; Fiorellino, E.; Schneider, N.; Pezzuto, S.; Motte, F.; Herschel Gould Belt Survey Team	2020, A&A, 638, A74

N°	Titre	Auteurs	Référence
2528	Physical and Chemical Modeling of the Starless Core L 1512	Lin, S.-J.; Pagani, L.; Lai, S.-P.; Lefèvre, C.; Lique, F.	2020, A&A, 635, A188
2529	Molecular Outflows in Local Galaxies: Method Comparison and a Role of Intermittent AGN Driving	Lutz, D.; Sturm, E.; Janssen, A.; Veilleux, S.; Aalto, S.; Cicone, C.; Contursi, A.; Davies, R. I.; Feruglio, C.; Fischer, J.; Fluetsch, A.; García-Burillo, S.; Genzel, R.; González-Alfonso, E.; Graciá-Carpio, J.; Herrera-Camus, R.; Maiolino, R.; Schrubba, A.; Shimizu, T.; Sternberg, A.; Tacconi, L. J.; Weiß, A.	2020, A&A, 633, A134
2530	Searching for Kinematic Evidence of Keplerian Disks around Class 0 Protostars with CALYPSO	Maret, S.; Maury, A. J.; Belloche, A.; Gaudel, M.; André, Ph.; Cabrit, S.; Codella, C.; Lefèvre, C.; Podio, L.; Anderl, S.; Gueth, F.; Hennebelle, P.	2020, A&A, 635, A15
2531	From Clump to Disc Scales in W3 IRS4. A Case Study of the IRAM NOEMA Large Programme CORE	Mottram, J. C.; Beuther, H.; Ahmadi, A.; Klaassen, P. D.; Beltrán, M. T.; Csengeri, T.; Feng, S.; Gieser, C.; Henning, Th.; Johnston, K. G.; Kuiper, R.; Leurini, S.; Linz, H.; Longmore, S. N.; Lumsden, S.; Maud, L. T.; Moscadelli, L.; Palau, A.; Peters, T.; Pudritz, R. E.; Ragan, S. E.; Sánchez-Monge, Á.; Semenov, D.; Urquhart, J. S.; Winters, J. M.; Zinnecker, H.	2020, A&A, 636, A118
2532	Detection of Deuterated Molecules, but Not of Lithium Hydride, in the $z = 0.89$ Absorber toward PKS 1830-211	Muller, S.; Roueff, E.; Black, J. H.; Gérin, M.; Guélin, M.; Menten, K. M.; Henkel, C.; Aalto, S.; Combes, F.; Martín, S.; Martí-Vidal, I.	2020, A&A, 637, A7
2533	The OTELO Survey. Nature and Mass-Metallicity Relation for H $\alpha$ Emitters at $z \sim 0.4$	Nadolny, J.; Lara-López, M. A.; Cerviño, M.; Bongiovanni, Á.; Cepa, J.; de Diego, J. A.; Pérez García, A. M.; Pérez Martínez, R.; Sánchez-Portal, M.; Alfaro, E.; Castañeda, H. O.; Gallego, J.; González, J. J.; González-Serrano, J. I.; Padilla Torres, C. P.; Pintos-Castro, I.; Povič, M.	2020, A&A, 636, A84
2534	Gas Phase Elemental Abundances in Molecular Clouds (GEMS). II. On the Quest for the Sulphur Reservoir in Molecular Clouds: The H2S Case	Navarro-Almaida, D.; Le Gal, R.; Fuente, A.; Rivière-Marichalar, P.; Wakelam, V.; Cazaux, S.; Caselli, P.; Laas, J. C.; Alonso-Albi, T.; Loison, J. C.; Gerin, M.; Kramer, C.; Roueff, E.; Bachiller, R.; Commerçon, B.; Friesen, R.; García-Burillo, S.; Goicoechea, J. R.; Giuliano, B. M.; Jiménez-Serra, I.; Kirk, J. M.; Lattanzi, V.; Malinen, J.; Marcelino, N.; Martín-Domènech, R.; Muñoz Caro, G. M.; Pineda, J.; Tercero, B.; Treviño-Morales, S. P.; Roncero, O.; Hacar, A.; Tafalla, M.; Ward-Thompson, D.	2020, A&A, 637, A39
2535	NOEMA Redshift Measurements of Bright Herschel Galaxies	Neri, R.; Cox, P.; Omont, A.; Beelen, A.; Berta, S.; Bakx, T.; Lehnert, M.; Baker, A. J.; Buat, V.; Cooray, A.; Dannerbauer, H.; Dunne, L.; Dye, S.; Eales, S.; Gavazzi, R.; Harris, A. I.; Herrera, C. N.; Hughes, D.; Ivison, R.; Jin, S.; Krips, M.; Lagache, G.; Marchetti, L.; Messias, H.; Negrello, M.; Perez-Fournon, I.; Riechers, D. A.; Serjeant, S.; Urquhart, S.; Vlahakis, C.; Weiß, A.; van der Werf, P.; Yang, C.; Young, A. J.	2020, A&A, 635, A7
2536	Radio Telescope Total Power Mode: Improving Observation Efficiency	Pagani, L.; Frayer, D.; Pagani, B.; Lefèvre, C.	2020, A&A, 643, A126
2537	Detection of Vibrationally Excited HC <sub>3</sub> N and HC <sub>5</sub> N in IRC +10216	Pardo, J. R.; Bermúdez, C.; Cabezas, C.; Agúndez, M.; Gallego, J. D.; Fonfría, J. P.; Velilla-Prieto, L.; Quintana-Lacaci, G.; Tercero, B.; Guélin, M.; Cernicharo, J.	2020, A&A, 640, L13
2538	Calibration and Performance of the NIKA2 Camera at the IRAM 30-meter telescope	Perotto, L.; Ponthieu, N.; Macías-Pérez, J. F.; Adam, R.; Ade, P.; André, P.; Andrianasolo, A.; Aussel, H.; Beelen, A.; Benoît, A.; Berta, S.; Bideaud, A.; Bourrion, O.; Calvo, M.; Catalano, A.; Comis, B.; De Petris, M.; Désert, F.-X.; Doyle, S.; Driessen, E. F. C.; García, P.; Gomez, A.; Goupy, J.; John, D.; Kéruszoré, F.; Kramer, C.; Ladjelate, B.; Lagache, G.; Leclercq, S.; Lestrade, J.-F.; Maury, A.; Mouskópif, P.; Mayet, F.; Monfardini, A.; Navarro, S.; Peñalver, J.; Pierfederici, F.; Pisano, G.; Revéret, V.; Ritacco, A.; Romero, C.; Roussel, H.; Ruppín, F.; Schuster, K.; Shu, S.; Sievers, A.; Tucker, C.; Zylka, R.	2020, A&A, 637, A71
2539	Planet-Induced Spirals in the Circumbinary Disk of GG Tauri A	Phuong, N. T.; Dutrey, A.; Di Folco, E.; Guilloteau, S.; Pierens, A.; Bary, J.; Beck, T. L.; Chapillon, E.; Denis-Alpizar, O.; Diep, P. N.; Majumdar, L.; Piétu, V.; Tang, Y.-W.	2020, A&A, 635, L9
2540	GG Tauri A: Gas Properties and Dynamics from the Cavity to the Outer Disk	Phuong, N. T.; Dutrey, A.; Diep, P. N.; Guilloteau, S.; Chapillon, E.; Di Folco, E.; Tang, Y.-W.; Piétu, V.; Bary, J.; Beck, T.; Hersant, F.; Hoai, D. T.; Huré, J. M.; Nhung, P. T.; Pierens, A.; Tuan-Anh, P.	2020, A&A, 635, A12
2541	The XXL Survey. XLIV. Sunyaev-Zel'dovich Mapping of a Low-Mass Cluster at $z \sim 1$ : A Multi-Wavelength Approach	Ricci, M.; Adam, R.; Eckert, D.; Ade, P.; André, P.; Andrianasolo, A.; Altieri, B.; Aussel, H.; Beelen, A.; Benoist, C.; Benoît, A.; Berta, S.; Bideaud, A.; Birkinshaw, M.; Bourrion, O.; Boutigny, D.; Bremer, M.; Calvo, M.; Cappi, A.; Chiappetti, L.; Catalano, A.; De Petris, M.; Désert, F.-X.; Doyle, S.; Driessen, E. F. C.; Faccioli, L.; Ferrari, C.; Fotopoulou, S.; Gastaldello, F.; Giles, P.; Gomez, A.; Goupy, J.; Hahn, O.; Horellou, C.; Kéruszoré, F.; Koulouridis, E.; Kramer, C.; Ladjelate, B.; Lagache, G.; Leclercq, S.; Lestrade, J.-F.; Macías-Pérez, J. F.; Maughan, B.; Maurogordato, S.; Mouskópif, P.; Monfardini, A.; Pacaud, F.; Perotto, L.; Pierre, M.; Pisano, G.; Pompei, E.; Ponthieu, N.; Revéret, V.; Ritacco, A.; Romero, C.; Roussel, H.; Ruppín, F.; Sánchez Portal, M.; Schuster, K.; Sereno, M.; Shu, S.; Sievers, A.; Tucker, C.; Umetsu, K.	2020, A&A, 642, A126
2542	AB Aur, a Rosetta Stone for Studies of Planet Formation. I. Chemical Study of a Planet-Forming Disk	Rivière-Marichalar, P.; Fuente, A.; Le Gal, R.; Baruteau, C.; Neri, R.; Navarro-Almaida, D.; Treviño-Morales, S. P.; Macías, E.; Bachiller, R.; Osorio, M.	2020, A&A, 642, A32
2543	SYMBA: An End-to-End VLBI Synthetic Data Generation Pipeline. Simulating Event Horizon Telescope Observations of M 87	Roelofs, F.; Janssen, M.; Natarajan, I.; Deane, R.; Davelaar, J.; Olivares, H.; Porth, O.; Paine, S. N.; Bouman, K. L.; Tilanus, R. P. J.; van Bemmell, I. M.; Falcke, H.; Akiyama, K.; Alberdi, A.; Alef, W.; Asada, K.; Azulay, R.; Baczkó, A.; Ball, D.; Baloković, M.; Barrett, J.; Bintley, D.; Blackburn, L.; Boland, W.; Bower, G. C.; Bremer, M.; Brinkerink, C. D.; Brissenden, R.; Britzen, S.; Broderick, A. E.; Brogiere, D.; Bronzwaer, T.; Byun, D.; Carlstrom, J. E.; Chael, A.; Chan, C.; Chatterjee, S.; Chatterjee, K.; Chen, M.; Chen, Y.; Cho, I.; Christian, P.; Conway, J. E.; Cordes, J. M.; Crew, G. B.; Cui, Y.; De Laurentis, M.; Dempsey, J.; Desvignes, G.; Dexter, J.; Doeleman, S. S.; Eatough, R. P.; Fish, V. L.; Fomalont, E.; Fraga-Encinas, R.; Friberg, P.; Fromm, C. M.; Gómez, J. L.; Galison, P.; Gammie, C. F.; García, R.; Gentaz, O.; Georgiev, B.; Goddi, C.; Gold, R.; Gu, M.; Gurwell, M.; Hada, K.; Hecht, M. H.; Hesper, R.; Ho, L. C.; Ho, P.; Honma, M.; Huang, C. L.	2020, A&A, 636, A5

.../...

N°	Titre	Auteurs	Référence
2543 (cont)	SYMBA: An End-to-End VLBI Synthetic Data Generation Pipeline. Simulating Event Horizon Telescope Observations of M 87 (cont)	Huang, L.; Hughes, D. H.; Ikeda, S.; Inoue, M.; Issaoun, S.; James, D. J.; Jannuzi, B.T.; Jeter, B.; Jiang, W.; Johnson, M. D.; Jorstad, S.; Jung, T.; Karami, M.; Karuppusamy, R.; Kawashima, T.; Keating, G. K.; Kettens, M.; Kim, J.; Kim, J.; Kim, J.; Kino, M.; Koay, J. Y.; Koch, P. M.; Koyama, S.; Kramer, M.; Kramer, C.; Krichbaum, T. P.; Kuo, C.; Lauer, T. R.; Lee, S.; Li, Y.; Li, Z.; Lindqvist, M.; Lico, R.; Liu, K.; Liuzzo, E.; Lo, W.; Lobanov, A. P.; Loinard, L.; Lonsdale, C.; Lu, R.; MacDonald, N. R.; Mao, J.; Markoff, S.; Marrone, D. P.; Marscher, A. P.; Martí-Vidal, I.; Matsushita, S.; Matthews, L. D.; Medeiros, L.; Menten, K. M.; Mizuno, Y.; Mizuno, I.; Moran, J. M.; Moriyama, K.; Moscibrodzka, M.; Müller, C.; Nagai, H.; Nagar, N. M.; Nakamura, M.; Narayan, R.; Narayanan, G.; Neri, R.; Ni, C.; Noutsos, A.; Okino, H.; Olivares, H.; Ortiz-León, G. N.; Oyama, T.; Özel, F.; Palumbo, D. C. M.; Patel, N.; Pen, U.; Pesce, D. W.; Piétu, V.; Plambeck, R.; PopStefanija, A.; Prather, B.; Preciado-López, J. A.; Psaltis, D.; Pu, H.; Ramakrishnan, V.; Rao, R.; Rawlings, M. G.; Raymond, A. W.; Rezzolla, L.; Ripperda, B.; Rogers, A.; Ros, E.; Rose, M.; Roshanineshat, A.; Rottmann, H.; Roy, A. L.; Ruszczyk, C.; Ryan, B. R.; Rygl, K. L. J.; Sánchez, S.; Sánchez-Arguelles, D.; Sasada, M.; Savolainen, T.; Schloerb, F. P.; Schuster, K.; Shao, L.; Shen, Z.; Small, D.; Won Sohn, B.; SooHoo, J.; Tazaki, F.; Tiede, P.; Titus, M.; Toma, K.; Torne, P.; Traianou, E.; Trent, T.; Trippe, S.; Tsuda, S.; van Langevelde, H. J.; van Rossum, D. R.; Wagner, J.; Wardle, J.; Weintroub, J.; Wex, N.; Wharton, R.; Wielgus, M.; Wong, G. N.; Wu, Q.; Young, A.; Young, K.; Younsi, Z.; Yuan, F.; Yuan, Y.; Zensus, J. A.; Zhao, G.; Zhao, S.; Zhu, Z.	2020, A&A, 636, A5
2544	Seeds of Life in Space (SOLIS). VIII. SiO Isotopic Fractionation, and a New Insight into the Shocks of L1157-B1	Spezzano, S.; Codella, C.; Podio, L.; Ceccarelli, C.; Caselli, P.; Neri, R.; López-Sepulcre, A.	2020, A&A, 640, A74
2545	Constraining MHD Disk Winds with ALMA. Apparent Rotation Signatures and Application to HH212	Tabone, B.; Cabrit, S.; Pineau des Forêts, G.; Ferreira, J.; Gusdorf, A.; Podio, L.; Bianchi, E.; Chapillon, E.; Codella, C.; Gueth, F.	2020, A&A, 640, A82
2546	Seeds of Life in Space (SOLIS). VI. Chemical Evolution of Sulfuretted Species along the Outflows Driven by the Low-Mass Protostellar Binary NGC 1333-IRAS4A	Taquet, V.; Codella, C.; De Simone, M.; López-Sepulcre, A.; Pineda, J. E.; Segura-Cox, D.; Ceccarelli, C.; Caselli, P.; Gusdorf, A.; Persson, M. V.; Alves, F.; Caux, E.; Favre, C.; Fontani, F.; Neri, R.; Oya, Y.; Sakai, N.; Vastel, C.; Yamamoto, S.; Bachiller, R.; Balucani, N.; Bianchi, E.; Bizzocchi, L.; Chacón-Tanarro, A.; Dulieu, F.; Enrique-Romero, J.; Feng, S.; Holdship, J.; Lefloch, B.; Jaber Al-Edhari, A.; Jiménez-Serra, I.; Kahane, C.; Lattanzi, V.; Ospina-Zamudio, J.; Podio, L.; Punanova, A.; Rimola, A.; Sims, I. R.; Spezzano, S.; Testi, L.; Theulé, P.; Ugliengo, P.; Vasyunin, A. I.; Vazart, F.; Viti, S.; Witzel, A.	2020, A&A, 637, A63
2547	New Molecular Species at Redshift $z = 0.89$	Tercero, B.; Cernicharo, J.; Cuadrado, S.; de Vicente, P.; Guélin, M.	2020, A&A, 636, L7
2548	Cause and Effects of the Massive Star Formation in Messier 8 East	Tiwari, M.; Menten, K. M.; Wyrowski, F.; Giannetti, A.; Lee, M.-Y.; Kim, W.-J.; Pérez-Beaupuits, J. P.	2020, A&A, 644, A25
2549	Detection of the Magnetar XTE J1810-197 at 150 and 260 GHz with the NIKA2 Kinetic Inductance Detector Camera	Torne, P.; Macías-Pérez, J.; Ladjelate, B.; Ritacco, A.; Sánchez-Portal, M.; Berta, S.; Paubert, G.; Calvo, M.; Desvignes, G.; Karuppusamy, R.; Navarro, S.; John, D.; Sánchez, S.; Peñalver, J.; Kramer, M.; Schuster, K.	2020, A&A, 640, L2
2550	An ALMA Survey of the SCUBA-2 Cosmology Legacy Survey UKIDSS/UDS Field: The Far-Infrared/Radio Correlation for High-Redshift Dusty Star-Forming Galaxies	Algera, H. S. B.; Smail, I.; Dudzevičiūtė, U.; Swinbank, A. M.; Stach, S.; Hodge, J. A.; Thomson, A. P.; Almaini, O.; Arumugam, V.; Blain, A. W.; Calistro-Rivera, G.; Chapman, S. C.; Chen, C.-C.; da Cunha, E.; Farrah, D.; Leslie, S.; Scott, D.; van der Vlugt, D.; Wardlow, J. L.; van der Werf, P.	2020, ApJ, 903, 138
2551	Local Starburst Conditions and Formation of GRB 980425/SN 1998bw within a Collisional Ring	Arabsalmani, M.; Renaud, F.; Roychowdhury, S.; Arumugam, V.; Floch, E. L.; Bournaud, F.; Cormier, D.; Zwaan, M. A.; Christensen, L.; Pian, E.; Madden, S.; Levan, A.	2020, ApJ, 899, 165
2552	On the Nature of the T Tauri Triple System	Beck, T. L.; Schaefer, G. H.; Guilloteau, S.; Simon, M.; Dutrey, A.; Di Folco, E.; Chapillon, E.	2020, ApJ, 902, 132
2553	THEMIS: A Parameter Estimation Framework for the Event Horizon Telescope	Broderick, A. E.; Gold, R.; Karami, M.; Preciado-López, J. A.; Tiede, P.; Pu, H.-Y.; Akiyama, K.; Alberdi, A.; Alef, W.; Asada, K.; Azulay, R.; Baczkó, A.-K.; Baloković, M.; Barrett, J.; Bintley, D.; Blackburn, L.; Boland, W.; Bouman, K. L.; Bower, G. C.; Bremer, M.; Brinkerink, C. D.; Brissenden, R.; Britzen, S.; Brogiere, D.; Bronzwaer, T.; Byun, D.-Y.; Carlstrom, J. E.; Chael, A.; Chatterjee, S.; Chatterjee, K.; Chen, M.-T.; Chen, Y.; Cho, I.; Conway, J. E.; Cordes, J. M.; Crew, G. B.; Cui, Y.; Davelaar, J.; De Laurentis, M.; Deane, R.; Dempsey, J.; Desvignes, G.; Doleman, S. S.; Eatough, R. P.; Falcke, H.; Fish, V. L.; Fomalont, E.; Fraga-Encinas, R.; Friberg, P.; Fromm, C. M.; Galison, P.; Gammie, C. F.; García, R.; Gentaz, O.; Georgiev, B.; Goddi, C.; Gómez, J. L.; Gu, M.; Gurwell, M.; Hada, K.; Hecht, M. H.; Hesper, R.; Ho, L. C.; Ho, P.; Honma, M.; Huang, C.-W. L.; Huang, L.; Hughes, D. H.; Inoue, M.; Issaoun, S.; James, D. J.; Janssen, M.; Jeter, B.; Jiang, W.; Jiménez-Rosales, A.; Johnson, M. D.; Jorstad, S.; Jung, T.; Karuppusamy, R.; Kawashima, T.; Keating, G. K.; Kettens, M.; Kim, J.-Y.; Kim, J.; Kino, M.; Koay, J. Y.; Koch, P. M.; Koyama, S.; Kramer, M.; Kramer, C.; Krichbaum, T. P.; Kuo, C.-Y.; Lee, S.-S.; Li, Y.-R.; Li, Z.; Lindqvist, M.; Lico, R.; Liu, K.; Liuzzo, E.; Lo, W.-P.; Lobanov, A. P.; Loinard, L.; Lonsdale, C.; Lu, R. S.; MacDonald, N. R.; Mao, J.; Marscher, A. P.; Martí-Vidal, I.; Matsushita, S.; Matthews, L. D.; Menten, K. M.; Mizuno, Y.; Mizuno, I.; Moran, J. M.; Moriyama, K.; Moscibrodzka, M.; Müller, C.; Nagai, H.; Nagar, N. M.; Nakamura, M.; Narayan, R.; Narayanan, G.; Natarajan, I.; Neri, R.; Ni, C.; Noutsos, A.; Okino, H.; Olivares, H.; Ortiz-León, G. N.; Oyama, T.; Palumbo, D. C. M.; Park, J.; Pen, U.-L.; Pesce, D. W.; Piétu, V.; Plambeck, R.; PopStefanija, A.; Porth, O.; Prather, B.; Ramakrishnan, V.; Rao, R.; Rawlings, M. G.; Raymond, A. W.; Rezzolla, L.; Ripperda, B.; Roelofs, F.; Rogers, A.; Ros, E.; Rose, M.; Rottmann, H.; Ruszczyk, C.; Ryan, B. R.; Rygl, K. L. J.; Sánchez, S.; Sánchez-Arguelles, D.; Sasada, M.; Savolainen, T.; Schloerb, F. P.	2020, ApJ, 897, 139

.../...

N°	Titre	Auteurs	Référence
2553 (cont.)	THEMIS: A Parameter Estimation Framework for the Event Horizon Telescope	Schuster, K. F.; Shao, L.; Shen, Z.; Small, D.; Sohn, B. W.; SooHoo, J.; Tazaki, F.; Tilanus, R. P. J.; Titus, M.; Toma, K.; Torne, P.; Traianou, E.; Trippe, S.; Tsuda, S.; van Bommel, I.; van Langevelde, H. J.; van Rossum, D. R.; Wagner, J.; Wardle, J.; Weintraub, J.; Wex, N.; Wharton, R.; Wielgus, M.; Wong, G. N.; Wu, Q.; Yoon, D.; Young, A.; Young, K.; Younsi, Z.; Yuan, F.; Yuan, Y.-F.; Zensus, J. A.; Zhao, G.; Zhao, S.-S.; Zhu, Z.; Event Horizon Telescope Collaboration	2020, ApJ, 897, 139
2554	From Nuclear to Circumgalactic: Zooming in on AGN-Driven Outflows at $z \sim 2.2$ with SINFONI	Davies, R. L.; Förster Schreiber, N. M.; Lutz, D.; Genzel, R.; Belli, S.; Shimizu, T. T.; Contursi, A.; Davies, R. I.; Herrera-Camus, R.; Lee, M. M.; Naab, T.; Price, S. H.; Renzini, A.; Schrubba, A.; Sternberg, A.; Tacconi, L. J.; Übler, H.; Wisnioski, E.; Wuyts, S.	2020, ApJ, 894, 28
2555	Hot Corinos Chemical Diversity: Myth or Reality?	De Simone, M.; Ceccarelli, C.; Codella, C.; Svoboda, B. E.; Chandler, C.; Bouvier, M.; Yamamoto, S.; Sakai, N.; Caselli, P.; Favre, C.; Loinard, L.; Lefloch, B.; Liu, H. B.; López-Sepulcre, A.; Pineda, J. E.; Taquet, V.; Testi, L.	2020, ApJ, 896, L3
2556	Herschel Gould Belt Survey Observations of Dense Cores in the Cepheus Flare Clouds	Di Francesco, J.; Keown, J.; Fallscheer, C.; André, P.; Ladjelate, B.; Könyves, V.; Men'shchikov, A.; Stephens-Whale, S.; Nguyen-Luong, Q.; Martin, P.; Sadavoy, S.; Pezzuto, S.; Fiorellino, E.; Benedettini, M.; Schneider, N.; Bontemps, S.; Arzoumanian, D.; Palmeirim, P.; Kirk, J. M.; Ward-Thompson, D.	2020, ApJ, 904, 172
2557	Seeds of Life in Space (SOLIS). IX. Chemical Segregation of SO <sub>2</sub> and SO toward the Low-Mass Protostellar Shocked Region of L1157	Feng, S.; Codella, C.; Ceccarelli, C.; Caselli, P.; Lopez-Sepulcre, A.; Neri, R.; Fontani, F.; Podio, L.; Lefloch, B.; Liu, H. B.; Bachiller, R.; Viti, S.	2020, ApJ, 896, 37
2558	Rotation Curves in $z \sim 1-2$ Star-Forming Disks: Evidence for Cored Dark Matter Distributions	Genzel, R.; Price, S. H.; Übler, H.; Förster Schreiber, N. M.; Shimizu, T. T.; Tacconi, L. J.; Bender, R.; Burkert, A.; Contursi, A.; Coogan, R.; Davies, R. L.; Davies, R. I.; Dekel, A.; Herrera-Camus, R.; Lee, M.-J.; Lutz, D.; Naab, T.; Neri, R.; Nestor, A.; Renzini, A.; Saglia, R.; Schuster, K.; Sternberg, A.; Wisnioski, E.; Wuyts, S.	2020, ApJ, 902, 98
2559	Verification of Radiative Transfer Schemes for the EHT	Gold, R.; Broderick, A. E.; Younsi, Z.; Fromm, C. M.; Gammie, C. F.; Mościbrodzka, M.; Pu, H.-Y.; Bronzwaer, T.; Davelaar, J.; Dexter, J.; Ball, D.; Chan, C.; Kawashima, T.; Mizuno, Y.; Ripperda, B.; Akiyama, K.; Alberdi, A.; Alef, W.; Asada, K.; Azulay, R.; Baczkó, A.-K.; Baloković, M.; Barrett, J.; Bintley, D.; Blackburn, L.; Boland, W.; Bouman, K. L.; Bower, G. C.; Bremer, M.; Brinkerink, C. D.; Brissenden, R.; Britzen, S.; Brogiere, D.; Byun, D.-Y.; Carlstrom, J. E.; Chael, A.; Chatterjee, K.; Chatterjee, S.; Chen, M.-T.; Chen, Y.; Cho, I.; Christian, P.; Conway, J. E.; Cordes, J. M.; Crew, G. B.; Cui, Y.; De Laurentis, M.; Deane, R.; Dempsey, J.; Desvignes, G.; Doeleman, S. S.; Eatough, R. P.; Falcke, H.; Fish, V. L.; Fomalont, E.; Fraga-Encinas, R.; Freeman, B.; Friberg, P.; Gómez, J. L.; Galison, P.; García, R.; Gentaz, O.; Georgiev, B.; Goddi, C.; Gu, M.; Gurwell, M.; Hada, K.; Hecht, M. H.; Hesper, R.; Ho, L. C.; Ho, P.; Honma, M.; Huang, C. W. L.; Huang, L.; Hughes, D. H.; Inoue, M.; Issaoun, S.; James, D. J.; Jannuzi, B. T.; Janssen, M.; Jeter, B.; Jiang, W.; Jimenez-Rosales, A.; Johnson, M. D.; Jorstad, S.; Jung, T.; Karami, M.; Karuppusamy, R.; Keating, G. K.; Kettenis, M.; Kim, J.-Y.; Kim, J.; Kim, J.; Kino, M.; Koay, J. Y.; Koch, P. M.; Koyama, S.; Kramer, M.; Kramer, C.; Krichbaum, T. P.; Kuo, C.-Y.; Lauer, T. R.; Lee, S.-S.; Li, Y.-R.; Li, Z.; Lico, R.; Lindqvist, M.; Liu, K.; Liuzzo, E.; Lo, W.-P.; Lobanov, A. P.; Loinard, L.; Lonsdale, C.; Lu, R.-S.; MacDonald, N. R.; Markoff, S.; Mao, J.; Marrone, D. P.; Marscher, A. P.; Martí-Vidal, I.; Matsushita, S.; Matthews, L. D.; Medeiros, L.; Menten, K. M.; Mizuno, I.; Moran, J. M.; Moriyama, K.; Müller, C.; Nagai, H.; Nakamura, M.; Nagar, N. M.; Narayan, R.; Narayanan, G.; Natarajan, I.; Neri, R.; Ni, C.; Noutsos, A.; Okino, H.; Ortiz-León, G. N.; Oyama, T.; Özel, F.; Palumbo, D. C. M.; Park, J.; Patel, N.; Pen, U.-L.; Pesce, D. W.; Plambeck, R.; Piétu, V.; PopStefanija, A.; Porth, O.; Preciado-López, J. A.; Psaltis, D.; Ramakrishnan, V.; Rao, R.; Rawlings, M. G.; Raymond, A. W.; Rezzolla, L.; Roelofs, F.; Rogers, A.; Ros, E.; Rose, M.; Roshanineshat, A.; Rottmann, H.; Roy, A. L.; Ruszczyk, C.; Rygl, K. L. J.; Sánchez, S.; Sánchez-Argüelles, D.; Sasada, M.; Savolainen, T.; Schuster, K.-F.; Schloerb, F. P.; Shao, L.; Shen, Z.; Small, D.; Sohn, B. W.; SooHoo, J.; Tiede, P.; Tazaki, F.; Tilanus, R. P. J.; Titus, M.; Toma, K.; Torne, P.; Trent, T.; Traianou, T.; Trippe, S.; Tsuda, S.; van Langevelde, H. J.; van Bommel, I.; van Rossum, D. R.; Wagner, J.; Wardle, J.; Wex, N.; Weintraub, J.; Wharton, R.; Wielgus, M.; Wong, G. N.; Wu, Q.; Yoon, D.; Young, K.; Young, A.; Yuan, F.; Yuan, Y.-F.; Zensus, J. A.; Zhao, G.; Zhao, S.-S.; Zhu, Z.; Event Horizon Telescope Collaboration	2020, ApJ, 897, 148
2560	The CO(3-2)/CO(1-0) Luminosity Line Ratio in Nearby Star-Forming Galaxies and Active Galactic Nuclei from XCOLD GASS, BASS, and SLUGS	Lamperti, I.; Saintonge, A.; Koss, M.; Viti, S.; Wilson, C. D.; He, H.; Shimizu, T. T.; Greve, T. R.; Mushotzky, R.; Treister, E.; Kramer, C.; Sanders, D.; Schawinski, K.; Tacconi, L. J.	2020, ApJ, 889, 103
2561	PHANGS CO Kinematics: Disk Orientations and Rotation Curves at 150 Pc Resolution	Lang, P.; Meidt, S. E.; Rosolowsky, E.; Nofech, J.; Schinnerer, E.; Leroy, A. K.; Emsellem, E.; Pessa, I.; Glover, S. C. O.; Groves, B.; Hughes, A.; Kruijssen, J. M. D.; Querejeta, M.; Schrubba, A.; Bigiel, F.; Blanc, G. A.; Chevance, M.; Colombo, D.; Faesi, C.; Henshaw, J. D.; Herrera, C. N.; Liu, D.; Pety, J.; Puschnig, J.; Saito, T.; Sun, J.; Usero, A.	2020, ApJ, 897, 122
2562	A 3 Mm Chemical Exploration of Small Organics in Class I YSOs	Le Gal, R.; Öberg, K. I.; Huang, J.; Law, C. J.; Ménard, F.; Lefloch, B.; Vastel, C.; Lopez-Sepulcre, A.; Favre, C.; Bianchi, E.; Ceccarelli, C.	2020, ApJ, 898, 131
2563	Ionized and Atomic Interstellar Medium in the $z = 6.003$ Quasar SDSS J2310+1855	Li, J.; Wang, R.; Cox, P.; Gao, Y.; Walter, F.; Wagg, J.; Menten, K. M.; Bertoldi, F.; Shao, Y.; Venemans, B. P.; Decarli, R.; Riechers, D.; Neri, R.; Fan, X.; Omont, A.; Narayanan, D.	2020, ApJ, 900, 131
2564	A Model for the Onset of Self-Gravitation and Star Formation in Molecular Gas Governed by Galactic Forces. II. The Bottleneck to Collapse Set by Cloud-Environment Decoupling	Meidt, S. E.; Glover, S. C. O.; Kruijssen, J. M. D.; Leroy, A. K.; Rosolowsky, E.; Hughes, A.; Schinnerer, E.; Schrubba, A.; Usero, A.; Bigiel, F.; Blanc, G.; Chevance, M.; Pety, J.; Querejeta, M.; Utomo, D.	2020, ApJ, 892, 73

N°	Titre	Auteurs	Référence
2565	A SOFIA Survey of [C II] in the Galaxy M51. II. [C II] and CO Kinematics across the Spiral Arms	Pineda, J. L.; Stutzki, J.; Buchbender, C.; Koda, J.; Fischer, C.; Goldsmith, P. F.; Glover, S. C. O.; Klessen, R. S.; Kramer, C.; Mookerjee, B.; Smith, R.; Treß, R.; Ziebart, M.	2020, ApJ, 900, 132
2566	COLDz: A High Space Density of Massive Dusty Starburst Galaxies ~1 Billion Years after the Big Bang	Riechers, D. A.; Hodge, J. A.; Pavesi, R.; Daddi, E.; Decarli, R.; Ivison, R. J.; Sharon, C. E.; Smail, I.; Walter, F.; Aravena, M.; Capak, P. L.; Carilli, C. L.; Cox, P.; Cunha, E. da; Dannerbauer, H.; Dickinson, M.; Neri, R.; Wagg, J.	2020, ApJ, 895, 81
2567	Unveiling the Merger Dynamics of the Most Massive MaDCoWS Cluster at $z = 1.2$ from a Multiwavelength Mapping of Its Intracluster Medium Properties	Ruppin, F.; McDonald, M.; Brodwin, M.; Adam, R.; Ade, P.; André, P.; Andrianasolo, A.; Arnaud, M.; Aussel, H.; Bartalucci, I.; Bautz, M. W.; Beelen, A.; Benoît, A.; Bideaud, A.; Bourrion, O.; Calvo, M.; Catalano, A.; Comis, B.; Decker, B.; De Petris, M.; Désert, F.-X.; Doyle, S.; Driessen, E. F. C.; Eisenhardt, P. R. M.; Gomez, A.; Gonzalez, A. H.; Goupy, J.; Kéruzoré, F.; Kramer, C.; Ladjelate, B.; Lagache, G.; Leclercq, S.; Lestrade, J.-F.; Macías-Pérez, J. F.; Mauskopf, P.; Mayet, F.; Monfardini, A.; Moravec, E.; Perotto, L.; Pisano, G.; Pointecouteau, E.; Ponthieu, N.; Pratt, G. W.; Revéret, V.; Ritacco, A.; Romero, C.; Roussel, H.; Schuster, K.; Shu, S.; Sievers, A.; Stanford, S. A.; Stern, D.; Tucker, C.; Zylka, R.	2020, ApJ, 893, 74
2568	Dynamical Equilibrium in the Molecular ISM in 28 Nearby Star-Forming Galaxies	Sun, J.; Leroy, A. K.; Ostriker, E. C.; Hughes, A.; Rosolowsky, E.; Schrub, A.; Schinnerer, E.; Blanc, G. A.; Faesi, C.; Kruijssen, J. M. D.; Meidt, S.; Utomo, D.; Bigiel, F.; Bolatto, A. D.; Chevance, M.; Chiang, I.-D.; Dale, D.; Emsellem, E.; Glover, S. C. O.; Grasha, K.; Henshaw, J.; Herrera, C. N.; Jimenez-Donaire, M. J.; Lee, J. C.; Pety, J.; Querejeta, M.; Saito, T.; Sandstrom, K.; Usero, A.	2020, ApJ, 892, 148
2569	Molecular Gas Properties on Cloud Scales across the Local Star-Forming Galaxy Population	Sun, J.; Leroy, A. K.; Schinnerer, E.; Hughes, A.; Rosolowsky, E.; Querejeta, M.; Schrub, A.; Liu, D.; Saito, T.; Herrera, C. N.; Faesi, C.; Usero, A.; Pety, J.; Kruijssen, J. M. D.; Ostriker, E. C.; Bigiel, F.; Blanc, G. A.; Bolatto, A. D.; Boquien, M.; Chevance, M.; Dale, D. A.; Deger, S.; Emsellem, E.; Glover, S. C. O.; Grasha, K.; Groves, B.; Henshaw, J.; Jimenez-Donaire, M. J.; Kim, J. J.; Klessen, R. S.; Kreckel, K.; Lee, J. C.; Meidt, S.; Sandstrom, K.; Sardone, A. E.; Utomo, D.; Williams, T. G.	2020, ApJ, 901, L8
2570	A Study of Millimeter Variability in FUor Objects	Wendeborn, J.; Espallat, C. C.; Macías, E.; Fehér, O.; Kóspál, Á.; Hartmann, L.; Zhu, Z.; Dunham, M. M.; Kounkel, M.	2020, ApJ, 897, 54
2571	Monitoring the Morphology of M87* in 2009-2017 with the Event Horizon Telescope	Wielgus, M.; Akiyama, K.; Blackburn, L.; Chan, C.; Dexter, J.; Doeleman, S. S.; Fish, V. L.; Issaoun, S.; Johnson, M. D.; Krichbaum, T. P.; Lu, R.-S.; Pesce, D. W.; Wong, G. N.; Bower, G. C.; Broderick, A. E.; Chael, A.; Chatterjee, K.; Gammie, C. F.; Georgiev, B.; Hada, K.; Loinard, L.; Markoff, S.; Marrone, D. P.; Plambeck, R.; Weintraub, J.; Dexter, M.; MacMahon, D. H. E.; Wright, M.; Alberdi, A.; Alef, W.; Asada, K.; Azulay, R.; Bacsko, A.-K.; Ball, D.; Baloković, M.; Barausse, E.; Barrett, J.; Bintley, D.; Boland, W.; Bouman, K. L.; Bremer, M.; Brinkerink, C. D.; Brissenden, R.; Britzen, S.; Brogiere, D.; Bronzwaer, T.; Byun, D.-Y.; Carlstrom, J. E.; Chatterjee, S.; Chen, M.-T.; Chen, Y.; Cho, I.; Christian, P.; Conway, J. E.; Cordes, J. M.; Crew, G. B.; Cui, Y.; Davelaar, J.; Laurentis, M. D.; Deane, R.; Dempsey, J.; Desvignes, G.; Dzib, S. A.; Eatough, R. P.; Falcke, H.; Fomalont, E.; Fraga-Encinas, R.; Friberg, P.; Fromm, C. M.; Galison, P.; García, R.; Gentaz, O.; Goddi, C.; Gold, R.; Gómez, J. L.; Gómez-Ruiz, A. I.; Gu, M.; Gurwell, M.; Hecht, M. H.; Hesper, R.; Ho, L. C.; Ho, P.; Honma, M.; Huang, C.-W. L.; Huang, L.; Hughes, D. H.; Inoue, M.; James, D. J.; Jannuzi, B. T.; Janssen, M.; Jeter, B.; Jiang, W.; Jimenez-Rosales, A.; Jorstad, S.; Jung, T.; Karami, M.; Karuppusamy, R.; Kawashima, T.; Keating, G. K.; Kettenis, M.; Kim, J.-Y.; Kim, J.; Kim, J.; Kino, M.; Koay, J. Y.; Koch, P. M.; Koyama, S.; Kramer, M.; Kramer, C.; Kuo, C.-Y.; Lauer, T. R.; Lee, S.-S.; Li, Y.-R.; Li, Z.; Lindqvist, M.; Lico, R.; Liu, K.; Liuzzo, E.; Lo, W.-P.; Lobanov, A. P.; Lonsdale, C.; MacDonald, N. R.; Mao, J.; Marchili, N.; Marscher, A. P.; Martí-Vidal, I.; Matsushita, S.; Matthews, L. D.; Medeiros, L.; Menten, K. M.; Mizuno, Y.; Mizuno, I.; Moran, J. M.; Moriyama, K.; Moscibrodzka, M.; Müller, C.; Musoke, G.; Nagai, H.; Nagar, N. M.; Nakamura, M.; Narayan, R.; Narayanan, G.; Natarajan, I.; Nathanail, A.; Neri, R.; Ni, C.; Noutsos, A.; Okino, H.; Olivares, H.; Ortiz-León, G. N.; Oyama, T.; Özel, F.; Palumbo, D. C. M.; Park, J.; Patel, N.; Pen, U.-L.; Piétu, V.; PopStefanija, A.; Porth, O.; Prather, B.; Preciado-López, J. A.; Psaltis, D.; Pu, H.-Y.; Ramakrishnan, V.; Rao, R.; Rawlings, M. G.; Raymond, A. W.; Rezzolla, L.; Ripperda, B.; Roelofs, F.; Rogers, A.; Ros, E.; Rose, M.; Roshaninshat, A.; Rottmann, H.; Roy, A. L.; Ruszczyk, C.; Ryan, B. R.; Rygl, K. L. J.; Sánchez, S.; Sánchez-Argüelles, D.; Sasada, M.; Savolainen, T.; Schloerb, F. P.; Schuster, K.-F.; Shao, L.; Shen, Z.; Small, D.; Sohn, B. W.; SooHoo, J.; Tazaki, F.; Tiede, P.; Tilanus, R. P. J.; Titus, M.; Toma, K.; Torne, P.; Trent, T.; Traianou, E.; Trippe, S.; Tsuda, S.; Bemmell, I. van; van Langevelde, H. J.; van Rossum, D. R.; Wagner, J.; Wardle, J.; Ward-Thompson, D.; Wex, N.; Wharton, R.; Wu, Q.; Yoon, D.; Young, A.; Young, K.; Younsi, Z.; Yuan, F.; Yuan, Y.-F.; Zensus, J. A.; Zhao, G.; Zhao, S.-S.; Zhu, Z.	2020, ApJ, 901, 67
2572	Molecular Cloud Cores with a High Deuterium Fraction: Nobeyama Single-Pointing Survey	Kim, G.; Tatematsu, K.; Liu, T.; Yi, H.-W.; He, J.; Hirano, N.; Liu, S.-Y.; Choi, M.; Sanhueza, P.; Tóth, L. V.; Evans, N. J., II; Feng, S.; Juvela, M.; Kim, K.-T.; Vastel, C.; Lee, J.-E.; Nguyễn Lu'ong, Q.; Kang, M.; Ristorcelli, I.; Fehér, O.; Wu, Y.; Ohashi, S.; Wang, K.; Kandori, R.; Hirota, T.; Sakai, T.; Lu, X.; Thompson, M. A.; Fuller, G. A.; Li, D.; Shinnaga, H.; Kim, J.	2020, ApJ, 249, 33
2573	LEGO - II. A 3 mm Molecular Line Study Covering 100 Pc of One of the Most Actively Star-Forming Portions within the Milky Way Disc	Barnes, A. T.; Kauffmann, J.; Bigiel, F.; Brinkmann, N.; Colombo, D.; Guzmán, A. E.; Kim, W. J.; Szűcs, L.; Wakelam, V.; Aalto, S.; Albertsson, T.; Evans, N. J.; Glover, S. C. O.; Goldsmith, P. F.; Kramer, C.; Menten, K.; Nishimura, Y.; Viti, S.; Watanabe, Y.; Weiss, A.; Wienen, M.; Wiesemeyer, H.; Wyrowski, F.	2020, MNRAS, 497, 1972-2001
2574	ATLASGAL - Relationship between Dense Star-Forming Clumps and Interstellar Masers	Billington, S. J.; Urquhart, J. S.; König, C.; Beuther, H.; Breen, S. L.; Menten, K. M.; Campbell-White, J.; Ellingsen, S. P.; Thompson, M. A.; Moore, T. J. T.; Eden, D. J.; Kim, W.-J.; Leurini, S.	2020, MNRAS, 499, 2744-2759

N°	Titre	Auteurs	Référence
2575	High-Cadence Observations and Variable Spin Behaviour of Magnetar Swift J1818.0-1607 after Its Outburst	Champion, D.; Cognard, I.; Cruces, M.; Desvignes, G.; Jankowski, F.; Karuppusamy, R.; Keith, M. J.; Kouveliotou, C.; Kramer, M.; Liu, K.; Lyne, A. G.; Micaliger, M. B.; O'Connor, B.; Parthasarathy, A.; Porayko, N.; Rajwade, K.; Stappers, B. W.; Torne, P.; van der Horst, A. J.; Weltevrede, P.	2020, MNRAS, 498, 6044-6056
2576	The Lifecycle of Molecular Clouds in Nearby Star-Forming Disc Galaxies	Chevance, M.; Kruijssen, J. M. D.; Hygate, A. P. S.; Schrupa, A.; Longmore, S. N.; Groves, B.; Henshaw, J. D.; Herrera, C. N.; Hughes, A.; Jeffreson, S. M. R.; Lang, P.; Leroy, A. K.; Meidt, S. E.; Pety, J.; Razza, A.; Rosolowsky, E.; Schinnerer, E.; Bigiel, F.; Blanc, G. A.; Emsellem, E.; Faesi, C. M.; Glover, S. C. O.; Haydon, D. T.; Ho, I.-T.; Kreckel, K.; Lee, J. C.; Liu, D.; Querejeta, M.; Saito, T.; Sun, J.; Usero, A.; Utomo, D.	2020, MNRAS, 493, 2872-2909
2577	An ALMA Survey of the SCUBA-2 CLS UDS Field: Physical Properties of 707 Sub-Millimetre Galaxies	Dudzevičiūtė, U.; Smail, I.; Swinbank, A. M.; Stach, S. M.; Almaini, O.; da Cunha, E.; An, F. X.; Arumugam, V.; Birkin, J.; Blain, A. W.; Chapman, S. C.; Chen, C.-C.; Conzelmann, C. J.; Coppin, K. E. K.; Dunlop, J. S.; Farrah, D.; Geach, J. E.; Gullberg, B.; Hartley, W. G.; Hodge, J. A.; Ivison, R. J.; Maltby, D. T.; Scott, D.; Simpson, C. J.; Simpson, J. M.; Thomson, A. P.; Walter, F.; Wardlow, J. L.; Weiss, A.; van der Werf, P.	2020, MNRAS, 494, 3828-3860
2578	No Nitrogen Fractionation on 600 au Scale in the Sun Progenitor Analogue OMC-2 FIR4	Fontani, F.; Quaiá, G.; Ceccarelli, C.; Colzi, L.; López-Sepulcre, A.; Favre, C.; Kahane, C.; Caselli, P.; Codella, C.; Podio, L.; Viti, S.	2020, MNRAS, 493, 3412-3421
2579	ALMA Unveils Wider Environment of Distant Red Protocluster Core	Ivison, R. J.; Biggs, A. D.; Bremer, M.; Arumugam, V.; Dunne, L.	2020, MNRAS, 496, 4358-4365
2580	Giant Star-Forming Clumps?	Ivison, R. J.; Richard, J.; Biggs, A. D.; Zwaan, M. A.; Falgarone, E.; Arumugam, V.; van der Werf, P. P.; Rujopakarn, W.	2020, MNRAS, 495, L1-L6
2581	Multiwavelength Behaviour of the Blazar 3C 279: Decade-Long Study from $\gamma$ -Ray to Radio	Larionov, V. M.; Jorstad, S. G.; Marscher, A. P.; Villata, M.; Raiteri, C. M.; Smith, P. S.; Agudo, I.; Savchenko, S. S.; Morozova, D. A.; Acosta-Pulido, J. A.; Aller, M. F.; Aller, H. D.; Andreeva, T. S.; Arkharov, A. A.; Bachev, R.; Bonnoli, G.; Borman, G. A.; Bozhilov, V.; Calciolase, P.; Carnerero, M. I.; Carosati, D.; Casadio, C.; Chen, W.-P.; Damjanovic, G.; Dementyev, A. V.; Di Paola, A.; Frasca, A.; Fuentes, A.; Gómez, J. L.; González-Morales, P.; Giunta, A.; Grishina, T. S.; Gurwell, M. A.; Hagen-Thorn, V. A.; Hovatta, T.; Ibryamov, S.; Joshi, M.; Kiehlmann, S.; Kim, J.-Y.; Kimeridze, G. N.; Kopatskaya, E. N.; Kovalev, Y. A.; Kovalev, Y. Y.; Kurtanidze, O. M.; Kurtanidze, S. O.; Lähteenmäki, A.; Lázaro, C.; Larionova, L. V.; Larionova, E. G.; Leto, G.; Marchini, A.; Matsumoto, K.; Mihov, B.; Mineev, M.; Mingaliev, M. G.; Mirzaqulov, D.; Muñoz Dimitrova, R. V.; Myserlis, I.; Nikiforova, A. A.; Nikolashvili, M. G.; Nizhelsky, N. A.; Ovcharov, E.; Pressburger, L. D.; Rakhimov, I. A.; Righini, S.; Rizzi, N.; Sadakane, K.; Sadun, A. C.; Samal, M. R.; Sanchez, R. Z.; Semkov, E.; Sergeev, S. G.; Sigua, L. A.; Slavcheva-Mihova, L.; Sola, P.; Sotnikova, Y. V.; Strigachev, A.; Thum, C.; Traianou, E.; Troitskaya, Y. V.; Troitsky, I. S.; Tsybulev, P. G.; Vasilyev, A. A.; Vince, O.; Weaver, Z. R.; Williamson, K. E.; Zhekanis, G. V.	2020, MNRAS, 492, 3829-3848
2582	ALMA Observations of CS in NGC 1068: Chemistry and Excitation	Scourfield, M.; Viti, S.; García-Burillo, S.; Saintonge, A.; Combes, F.; Fuente, A.; Henkel, C.; Alonso-Herrero, A.; Harada, N.; Takano, S.; Nakajima, T.; Martín, S.; Krips, M.; van der Werf, P. P.; Aalto, S.; Usero, A.; Kohno, K.	2020, MNRAS, 496, 5308-5329
2583	Gravitational Test beyond the First Post-Newtonian Order with the Shadow of the M87 Black Hole	Psaltis, D.; Medeiros, L.; Christian, P.; Özel, F.; Akiyama, K.; Alberdi, A.; Alef, W.; Asada, K.; Azulay, R.; Ball, D.; Baloković, M.; Barrett, J.; Bintley, D.; Blackburn, L.; Boland, W.; Bower, G. C.; Bremer, M.; Brinkerink, C. D.; Brissenden, R.; Britzen, S.; Brogiuere, D.; Bronzwaer, T.; Byun, D.-Y.; Carlstrom, J. E.; Chael, A.; Chan, C.; Chatterjee, S.; Chatterjee, K.; Chen, M.-T.; Chen, Y.; Cho, I.; Conway, J. E.; Cordes, J. M.; Crew, G. B.; Cui, Y.; Davelaar, J.; De Laurentis, M.; Deane, R.; Dempsey, J.; Desvignes, G.; Dexter, J.; Eatough, R. P.; Falcke, H.; Fish, V. L.; Fomalont, E.; Fraga-Encinas, R.; Friberg, P.; Fromm, C. M.; Gammie, C. F.; García, R.; Gentaz, O.; Goddi, C.; Gómez, J. L.; Gu, M.; Gurwell, M.; Hada, K.; Hesper, R.; Ho, L. C.; Ho, P.; Honma, M.; Huang, C.-W. L.; Huang, L.; Hughes, D. H.; Inoue, M.; Issaoun, S.; James, D. J.; Jannuzi, B. T.; Janssen, M.; Jiang, W.; Jimenez-Rosales, A.; Johnson, M. D.; Jorstad, S.; Jung, T.; Karami, M.; Karuppusamy, R.; Kawashima, T.; Keating, G. K.; Kettenis, M.; Kim, J.-Y.; Kim, J.; Kino, M.; Koay, J. Y.; Koch, P. M.; Koyama, S.; Kramer, M.; Kramer, C.; Krichbaum, T. P.; Kuo, C.-Y.; Lauer, T. R.; Lee, S.-S.; Li, Y.-R.; Li, Z.; Lindqvist, M.; Lico, R.; Liu, J.; Liu, K.; Liuzzo, E.; Lo, W.-P.; Lobanov, A. P.; Lonsdale, C.; Lu, R.-S.; Mao, J.; Markoff, S.; Marrone, D. P.; Marscher, A. P.; Martí-Vidal, I.; Matsushita, S.; Mizuno, Y.; Mizuno, I.; Moran, J. M.; Moriyama, K.; Moscibrodzka, M.; Müller, C.; Musoke, G.; Mus Mejías, A.; Nagai, H.; Nagar, N. M.; Narayan, R.; Narayanan, G.; Natarajan, I.; Neri, R.; Noutsos, A.; Okino, H.; Olivares, H.; Oyama, T.; Palumbo, D. C. M.; Park, J.; Patel, N.; Pen, U.-L.; Piétu, V.; Plambeck, R.; PopStefanija, A.; Prather, B.; Preciado-López, J. A.; Ramakrishnan, V.; Rao, R.; Rawlings, M. G.; Raymond, A. W.; Ripperda, B.; Roelofs, F.; Rogers, A.; Ros, E.; Rose, M.; Roshanineshat, A.; Rottmann, H.; Roy, A. L.; Ruszczyk, C.; Ryan, B. R.; Rygl, K. L. J.; Sánchez, S.; Sánchez-Argüelles, D.; Sasada, M.; Savolainen, T.; Schloerb, F. P.; Schuster, K.-F.; Shao, L.; Shen, Z.; Small, D.; Sohn, B. W.; SooHoo, J.; Takaki, F.; Tilanus, R. P. J.; Titus, M.; Torne, P.; Trent, T.; Traianou, E.; Trippe, S.; van Bemmelen, I.; van Lamsweerde, H. J.; van Rossum, D. R.; Wagner, J.; Wardle, J.; Ward-Thompson, D.; Weintraub, J.; Wex, N.; Wharton, R.; Wielgus, M.; Wong, G. N.; Wu, Q.; Yoon, D.; Young, A.; Young, K.; Younsi, Z.; Yuan, F.; Yuan, Y.-F.; Zhao, S.-S.; EHT Collaboration	2020, Phys. Rev. Lett., 125, 141104
2584	(Sub)Stellar Companions Shape the Winds of Evolved Stars	Decin, L.; Montargès, M.; Richards, A. M. S.; Gottlieb, C. A.; Homan, W.; McDonald, I.; El Mellah, I.; Danilovich, T.; Wallström, S. H. J.; Zijlstra, A.; Baudry, A.; Bolte, J.; Cannon, E.; De Beck, E.; De Ceuster, F.; de Koter, A.; De Ridder, J.; Etoka, S.; Gobrecht, D.; Gray, M.; Herpin, F.; Jests, M.; Lagadec, E.; Kervella, P.; Khouri, T.; Menten, K.; Millar, T. J.; Müller, H. S. P.; Plane, J. M. C.; Sahai, R.; Sana, H.; Van de Sande, M.; Waters, L. B. F. M.; Wong, K. T.; Yates, J.	2020, Science, 369, 1497-1500

N°	Titre	Auteurs	Référence
2585	Plateau de Bure High-z Blue Sequence Survey 2 (PHIBSS2): Search for Secondary Sources, CO Luminosity Functions in the Field, and the Evolution of Molecular Gas Density through Cosmic Time	Lenkić, L.; Bolatto, A. D.; Förster Schreiber, N. M.; Tacconi, L. J.; Neri, R.; Combes, F.; Walter, F.; García-Burillo, S.; Genzel, R.; Lutz, D.; Cooper, M. C.	2020, Astron. J., 159, 190
2586	Unusually High CO Abundance of the First Active Interstellar Comet	Cordiner, M. A.; Milam, S. N.; Biver, N.; Bockelée-Morvan, D.; Roth, N. X.; Bergin, E. A.; Jehin, E.; Remijan, A. J.; Charnley, S. B.; Mumma, M. J.; Boissier, J.; Crovisier, J.; Paganini, L.; Kuan, Y.-J.; Lis, D. C.	2020, Nat. Astron., 4, 861–866
2587	Ubiquitous Velocity Fluctuations throughout the Molecular Interstellar Medium	Henshaw, J. D.; Kruijssen, J. M. D.; Longmore, S. N.; Riener, M.; Leroy, A. K.; Rosolowsky, E.; Ginsburg, A.; Battersby, C.; Chevance, M.; Meidt, S. E.; Glover, S. C. O.; Hughes, A.; Kainulainen, J.; Klessen, R. S.; Schinnerer, E.; Schrubba, A.; Beuther, H.; Bigiel, F.; Blanc, G. A.; Emsellem, E.; Henning, T.; Herrera, C. N.; Koch, E. W.; Pety, J.; Ragan, S. E.; Sun, J.	2020, Nat. Astron., 4, 1064–1071
2588	A Protostellar System Fed by a Streamer of 10,500 au Length	Pineda, J. E.; Segura-Cox, D.; Caselli, P.; Cunningham, N.; Zhao, B.; Schmiedeke, A.; Maureira, M. J.; Neri, R.	2020, Nat. Astron., 4, 1158–1163
2589	An Era Comes to an End: The Legacy of LABOCA at APEX	Lundgren, A.; De Breuck, C.; Siringo, G.; Weiß, A.; Agurto, C.; Azagra, F.; Belloche, A.; Dumke, M.; Durán, C.; Eckart, A.; González, E.; Güsten, R.; Hacar, A.; Kovács, A.; Kreysa, E.; Mac-Auliffe, F.; Martínez, M.; Menten, K. M.; Montenegro, F.; Nyman, L.-Å.; Parra, R.; Pérez-Beaupuits, J. P.; Reveret, V.; Risacher, C.; Schuller, F.; Stanke, T.; Torstensson, K.; Venegas, P.; Wiesemeyer, H.; Wyrowski, F.	2020, The Messenger, 181, 7–15
2590	Probing the Chemical Composition of Interstellar Comet 2I/Borisov Using ALMA	Cordiner, M.; Milam, S.; Biver, N.; Bockelée-Morvan, D.; Roth, N.; Bergin, E.; Jehin, E.; Remijan, A.; Charnley, S.; Mumma, M.; Boissier, J.; Crovisier, J.; Paganini, L.; Kuan, Y.; Lis, D.	2020, BAAS, 52, 313.04
2591	PHANGS-ALMA: Star Formation at Molecular Cloud Scales	Schinnerer, E.; Leroy, A. K.; Rosolowski, E.; Hughes, A.; Blanc, G.; Schrubba, A.; Pety, J.; Emsellem, E.	2020, BAAS, 235, 255.04
2592	An Attempt to Detect Transient Changes in Io's SO <sub>2</sub> and NaCl Atmosphere	Roth, L.; Boissier, J.; Moullet, A.; Sánchez-Monge, Á.; de Kleer, K.; Yoneda, M.; Hikida, R.; Kita, H.; Tsuchiya, F.; Blöcker, A.; Gladstone, G. R.; Grodent, D.; Ivchenko, N.; Lellouch, E.; Retherford, K. D.; Saur, J.; Schilke, P.; Strobel, D.; Thorwirth, S.	2020, Icarus, 350, 113925
2593	IRAM 30-meter telescope Detection of the Magnetar Swift J1818.0-1607 between 86 and 154 GHz	Torne, P.; Liu, K.; Cognard, I.; Desvignes, G.; Karuppusamy, R.; Kramer, M.; Paubert, G.; Lyne, A.; Rajwade, K.; Stappers, B.; Eatough, R.; Sanchez, S.; Macias-Perez, J.; Ladjelate, B.; Berta, S.; Sanchez-Portal, M.; Navarro, S.; Bongiovanni, A.; Kramer, C.; Schuster, K.	2020, ATel, 14001, 1
2594	Episodic Accretion in Focus: Revealing the Environment of FU Orionis-Type Stars	Fehér, O.; Kóspál, Á.; Ábrahám, P.; Hogerheijde, M. R.; Brinch, Ch.; Semenov, D.	2020, IAU, 345, 87–90
2595	HCL1 and HCL2 - Low Mass Star Formation in Violent and Quiet Environments	Tóth, L. V.; Fehér, O.; Juvela, M.; Montillaud, J.; Pintér, S.	2020, IAU, 345, 333–334
2596	Large Reservoirs of Turbulent Diffuse Gas around High-z Starburst Galaxies	Falgarone, E.; Vidal-García, A.; Godard, B.; Zwaan, M. A.; Herrera, C.; Ivison, R. J.; Bergin, E.; Andreani, P. M.; Omont, A.; Walter, F.	2020, IAU, 352, 200–204
2597	A MUSE Inquiry into the Physical Processes Taking Place within the Abell 2667 Brightest Cluster Galaxy	Iani, E.; Rodighiero, G.; Fritz, J.; Cresci, G.; Mancini, C.; Tozzi, P.; Rodríguez-Muñoz, L.; Rosati, P.; Caminha, G. B.; Berta, S.; Cassata, P.; Concas, A.; Enia, A.; Fadda, D.; Franceschini, A.; Liu, A.; Mercurio, A.; Morselli, L.; Pérez-González, P. G.; Popesso, P.; Sabatini, G.; Zanella, A.	2020, IAU, 341, 83–87
2598	First Application of a Kinetic Inductance Detector (KID) Camera to Pulsar Science in the Millimetre Regime	Torne, P.; Macías-Perez, J.; Ladjelate, B.; Ritacco, A.; Sánchez-Portal, M.; Berta, S.; Paubert, G.; Calvo, M.; Desvignes, G.; Karuppusamy, R.; Navarro, S.; John, D.; Sánchez, S.; Peñalver, J.; Kramer, M.; Schuster, K.	2020, XIV <sup>0</sup> Scientific Meeting (virtual) of the Spanish Astronomical Society, 243.
2599	Chemical Inventory of Class I Protostars with IRAM-30m: A Bridge between Protostars and Planet-Forming Disks	Mercimek, S.; Codella, C.; Podio, L.; Bianchi, E.; Chahine, L.; López-Sepulcre, A.; Neri, R.; Ceccarelli, C.	2020, EPSC2020, 14, 326
2600	Evidence of Enhanced Ionization During Early Planet Formation	Schwarz, K.; Maret, S.; Lefevre, C.; Andre, P.; Belloche, A.; Bergin, E.; Codella, C.	2020, EPSC2020, 14, 361
2601	TREASUREHUNT: Hubble's UV-Visible Treasury Imaging of the JWST NEP Time-Domain Field	Jansen, R. A.; Alpaslan, M.; Ashby, M. L. N.; Ashcraft, T. A.; Bonoli, S.; Briskin, W.; Cappelluti, N.; Civano, F.; Cohen, S. H.; Conselice, C. J.; Cotton, W.; Dhillon, V.; Driver, S. P.; Duncan, K. J.; Dupke, R. A.; Elvis, M.; Fazio, G. G.; Finkelstein, S. L.; Frye, B. L.; Griffiths, A.; Grogin, N.; Hammel, H. B.; Hathi, N. P.; Hyun, M.; Im, M.; Jones, V. R.; Kim, D.; Koekemoer, A. M.; Ladjelate, B.; Larson, R. L.; Maksym, W. P.; Malhotra, S.; Marshall, M.; Messias, H.; Milam, S. N.; Perley, R. A.; Rhoads, J.; Roberts-Pierel, J.; Rodney, S.; Rottgering, H.; Rutkowski, M. J.; Ryan, R. E.; Smail, I.; Smith, B. M.; Ward, M. J.; White, C. W.; Willmer, C. N. A.; Windhorst, R. A.; van Weeren, R. J.	2020, HST proposal, 16252
2602	Preliminary Results on the Instrumental Polarization of NIKA2-Pol at the IRAM 30-meter telescope	Ajeddig, H.; Adam, R.; Ade, P.; André, Ph.; Andrianasolo, A.; Aussel, H.; Beelen, A.; Benoît, A.; Bideaud, A.; Bourrion, O.; Calvo, M.; Catalano, A.; Comis, B.; De Petris, M.; Désert, F.-X.; Doyle, S.; Driessen, E. F. C.; Gomez, A.; Goupy, J.; Kéruzoré, F.; Kramer, C.; Ladjelate, B.; Lagache, G.; Leclercq, S.; Lestrade, J.-F.; Macías-Pérez, J. F.; Maury, A.; Mauskopf, P.; Mayet, F.; Monfardini, A.; Perotto, L.; Pisano, G.; Ponthieu, N.; Revéret, V.; Ritacco, A.; Romero, C.; Roussel, H.; Ruppini, F.; Schuster, K.; Shimajiri, Y.; Shu, S.; Sievers, A.; Tucker, C.; Zylka, R.	2020, EPJ Web of Conferences, 228, 00002
2603	Absolute Calibration of the Polarisation Angle for Future CMB B-Mode Experiments from Current and Future Measurements of the Crab Nebula	Aumont, J.; Ritacco, A.; Macías-Pérez, J. F.; Ponthieu, N.; Mangilli, A.	2020, EPJ Web of Conferences, 228, 00003



N°	Titre	Auteurs	Référence
2604	Probing the Subsurface of the Two Faces of Iapetus	Bonnefoy, L. E.; Lestrade, J.-F.; Lellouch, E.; Le Gall, A.; Leyrat, C.; Ponthieu, N.; Ladjelate, B.	2020, EPJ Web of Conferences, 228, 00006
2605	A Low-Mass Galaxy Cluster as a Test-Case Study for the NIKA2 SZ Large Program	Kéruzoré, F.; Adam, R.; Ade, P.; André, P.; Andrianasolo, A.; Arnaud, M.; Aussel, H.; Bartalucci, I.; Beelen, A.; Benoît, A.; Bideaud, A.; Bourrion, O.; Calvo, M.; Catalano, A.; Comis, B.; De Petris, M.; Désert, F.-X.; Doyle, S.; Driessen, E. F. C.; Gomez, A.; Goupy, J.; Kramer, C.; Ladjelate, B.; Lagache, G.; Leclercq, S.; Lestrade, J.-F.; Macías-Pérez, J. F.; Mausekopf, P.; Mayet, F.; Monfardini, A.; Perotto, L.; Pisano, G.; Pointecouteau, E.; Ponthieu, N.; Pratt, G. W.; Revéret, V.; Ritacco, A.; Romero, C.; Roussel, H.; Ruppín, F.; Schuster, K.; Shu, S.; Sievers, A.; Tucker, C.; Zylka, R.	2020, EPJ Web of Conferences, 228, 00012
2606	NOEMA Complementarity with NIKA2	Lefèvre, C.; Kramer, C.; Neri, R.; Berta, S.; Schuster, K.	2020, EPJ Web of Conferences, 228, 00014
2607	Dust Evolution in Pre-Stellar Cores	Lefèvre, C.; Pagani, L.; Ladjelate, B.; Min, M.; Hirashita, H.; Zylka, R.	2020, EPJ Web of Conferences, 228, 00013
2608	Debris Disks around Stars in the NIKA2 Era	Lestrade, J.-F.; Augereau, J.-C.; Booth, M.; Adam, R.; Ade, P.; André, P.; Andrianasolo, A.; Aussel, H.; Beelen, A.; Benoît, A.; Bideaud, A.; Bourrion, O.; Calvo, M.; Catalano, A.; Comis, B.; De Petris, M.; Désert, F.-X.; Doyle, S.; Driessen, E. F. C.; Gomez, A.; Goupy, J.; Holland, W.; Kéruzoré, F.; Kramer, C.; Ladjelate, B.; Lagache, G.; Leclercq, S.; Lefèvre, C.; Macías-Pérez, J. F.; Mausekopf, P.; Mayet, F.; Monfardini, A.; Perotto, L.; Pisano, G.; Ponthieu, N.; Revéret, V.; Ritacco, A.; Romero, C.; Roussel, H.; Ruppín, F.; Schuster, K.; Shu, S.; Sievers, A.; Thébaud, P.; Tucker, C.; Zylka, R.	2020, EPJ Web of Conferences, 228, 00015
2609	NIKA: A mm Camera for Sunyaev-Zel'dovich Science in Clusters of Galaxies	Macías-Pérez, J. F.; Adam, R.; Ade, P.; André, P.; Andrianasolo, A.; Aussel, H.; Arnaud, M.; Bartalucci, I.; Beelen, A.; Benoît, A.; Bideaud, A.; Bourrion, O.; Calvo, M.; Catalano, A.; Comis, B.; De Petris, M.; Désert, F.-X.; Doyle, S.; Driessen, E. F. C.; Gomez, A.; Goupy, J.; Kéruzoré, F.; Kramer, C.; Ladjelate, B.; Lagache, G.; Leclercq, S.; Lestrade, J.-F.; Mausekopf, P.; Mayet, F.; Monfardini, A.; Perotto, L.; Pisano, G.; Pointecouteau, E.; Ponthieu, N.; Pratt, G. W.; Revéret, V.; Ritacco, A.; Romero, C.; Roussel, H.; Ruppín, F.; Schuster, K.; Shu, S.; Sievers, A.; Tucker, C.; Zylka, R.	2020, EPJ Web of Conferences, 228, 00016
2610	Cluster Cosmology with the NIKA2 SZ Large Program	Mayet, F.; Adam, R.; Ade, P.; André, P.; Andrianasolo, A.; Arnaud, M.; Aussel, H.; Bartalucci, I.; Beelen, A.; Benoît, A.; Bideaud, A.; Bourrion, O.; Calvo, M.; Catalano, A.; Comis, B.; De Petris, M.; Désert, F.-X.; Doyle, S.; Driessen, E. F. C.; Gomez, A.; Goupy, J.; Kéruzoré, F.; Kramer, C.; Ladjelate, B.; Lagache, G.; Leclercq, S.; Lestrade, J.-F.; Macías-Pérez, J. F.; Mausekopf, P.; Monfardini, A.; Perotto, L.; Pisano, G.; Pointecouteau, E.; Ponthieu, N.; Pratt, G. W.; Revéret, V.; Ritacco, A.; Romero, C.; Roussel, H.; Ruppín, F.; Schuster, K.; Shu, S.; Sievers, A.; Tucker, C.; Zylka, R.	2020, EPJ Web of Conferences, 228, 00017
2611	GASTON: Galactic Star Formation with NIKA2 A New Population of Cold Massive Sources Discovered	Peretto, N.; Rigby, A.; Adam, R.; Ade, P.; André, P.; Andrianasolo, A.; Aussel, H.; Bacmann, A.; Beelen, A.; Benoît, A.; Bideaud, A.; Bourrion, O.; Calvo, M.; Catalano, A.; Comis, B.; De Petris, M.; Désert, F.-X.; Doyle, S.; Driessen, E. F. C.; Gomez, A.; Goupy, J.; Kéruzoré, F.; Kramer, C.; Ladjelate, B.; Lagache, G.; Leclercq, S.; Lestrade, J.-F.; Macías-Pérez, J. F.; Mausekopf, P.; Mayet, F.; Monfardini, A.; Motte, F.; Perotto, L.; Pisano, G.; Ponthieu, N.; Revéret, V.; Ristorcelli, I.; Ritacco, A.; Romero, C.; Roussel, H.; Ruppín, F.; Schuster, K.; Shu, S.; Sievers, A.; Tucker, C.; Zylka, R.	2020, EPJ Web of Conferences, 228, 00018
2612	NIKA2 Observations around LBV Stars Emission from Stars and Circumstellar Material	Ricardo Rizzo, J.; Ritacco, A.; Bordiu, C.	2020, EPJ Web of Conferences, 228, 00023
2613	Observing with NIKA2Pol from the IRAM 30-meter telescope : Early Results on the Commissioning Phase	Ritacco, A.; Adam, R.; Ade, P.; Ajeddig, H.; André, P.; Andrianasolo, A.; Aussel, H.; Beelen, A.; Benoît, A.; Bideaud, A.; Bourrion, O.; Calvo, M.; Catalano, A.; Comis, B.; De Petris, M.; Désert, F.-X.; Doyle, S.; Driessen, E. F. C.; Gomez, A.; Goupy, J.; Kéruzoré, F.; Kramer, C.; Ladjelate, B.; Lagache, G.; Leclercq, S.; Lestrade, J.-F.; Macías-Pérez, J. F.; Mausekopf, P.; Maury, A.; Mayet, F.; Monfardini, A.; Perotto, L.; Pisano, G.; Ponthieu, N.; Revéret, V.; Romero, C.; Roussel, H.; Ruppín, F.; Schuster, K.; Shimajiri, Y.; Shu, S.; Sievers, A.; Tucker, C.; Zylka, R.	2020, EPJ Web of Conferences, 228, 00022
2614	The NIKA Polarimeter on Science Targets: Crab Nebula Observations at 150 GHz and Dual-Band Polarization Images of Orion Molecular Cloud OMC-1	Ritacco, A.; Adam, R.; Ade, P.; André, P.; Andrianasolo, A.; Aussel, H.; Beelen, A.; Benoît, A.; Bideaud, A.; Bourrion, O.; Calvo, M.; Catalano, A.; Comis, B.; De Petris, M.; Désert, F.-X.; Doyle, S.; Driessen, E. F. C.; Gomez, A.; Goupy, J.; Kéruzoré, F.; Kramer, C.; Ladjelate, B.; Lagache, G.; Leclercq, S.; Lestrade, J.-F.; Macías-Pérez, J. F.; Mausekopf, P.; Maury, A.; Mayet, F.; Monfardini, A.; Perotto, L.; Pisano, G.; Ponthieu, N.; Revéret, V.; Romero, C.; Roussel, H.; Ruppín, F.; Schuster, K.; Shu, S.; Sievers, A.; Tucker, C.; Zylka, R.	2020, EPJ Web of Conferences, 228, 00021
2615	NIKA2 Mapping and Cross-Instrument SED Extraction of Extended Sources with Scanamorphos	Roussel, H.; Ponthieu, N.; Adam, R.; Ade, P.; André, P.; Andrianasolo, A.; Aussel, H.; Beelen, A.; Benoît, A.; Bideaud, A.; Bourrion, O.; Calvo, M.; Catalano, A.; Comis, B.; De Petris, M.; Désert, F.-X.; Doyle, S.; Driessen, E. F. C.; Gomez, A.; Goupy, J.; Kéruzoré, F.; Kramer, C.; Ladjelate, B.; Lagache, G.; Leclercq, S.; Lestrade, J.-F.; Macías-Pérez, J. F.; Mausekopf, P.; Mayet, F.; Monfardini, A.; Perotto, L.; Pisano, G.; Revéret, V.; Ritacco, A.; Romero, C.; Ruppín, F.; Schuster, K.; Shu, S.; Sievers, A.; Tucker, C.; Zylka, R.	2020, EPJ Web of Conferences, 228, 00024

N°	Titre	Auteurs	Référence
2616	Mapping the Gas Thermodynamic Properties of the Massive Cluster Merger MOO J1142+1527 at $z = 1.2$	Ruppin, F.; Adam, R.; Ade, P.; André, P.; Andrianasolo, A.; Arnaud, M.; Aussel, H.; Bartalucci, I.; Bautz, M. W.; Beelen, A.; Benoît, A.; Bideaud, A.; Bourrion, O.; Brodwin, M.; Calvo, M.; Catalano, A.; Comis, B.; Decker, B.; De Petris, M.; Désert, F.-X.; Doyle, S.; Driessen, E. F. C.; Eisenhardt, P. R. M.; Gomez, A.; Gonzalez, A. H.; Goupy, J.; Kéruzoré, F.; Kramer, C.; Ladjelate, B.; Lagache, G.; Leclercq, S.; Lestrade, J.-F.; Macías-Pérez, J. F.; Mauskopf, P.; Mayet, F.; McDonald, M.; Monfardini, A.; Moravec, E.; Perotto, L.; Pisano, G.; Pointecouteau, E.; Ponthieu, N.; Pratt, G. W.; Revéret, V.; Ritacco, A.; Romero, C.; Roussel, H.; Schuster, K.; Shu, S.; Sievers, A.; Stanford, S. A.; Stern, D.; Tucker, C.; Zylka, R.	2020, EPJ Web of Conferences, 228, 00026
2617	The NOEMA Correlator Software	Broguière, D.; Blanchet, S.; Chavatte, P.; Garcia, R. G.; Gentaz, O.	2020, ASP Conference Series, 522, 485

# Committees

## STEERING COMMITTEE

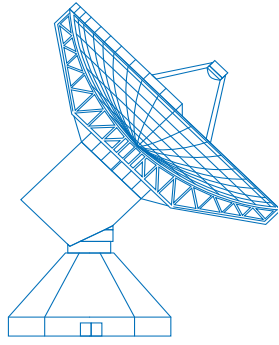
Rafael Bachiller, OAN, Madrid, Spain  
Reinhard Genzel, MPE, Garching, Germany  
Mónica Groba López, IGN, Madrid, Spain  
Eric Humler, CNRS, Paris, France  
José Antonio López Fernández, IGN, Madrid, Spain  
Karl Menten, MPIfR, Bonn, Germany  
Guy Perrin, INSU, Paris, France  
Jean-Loup Puget, IAS, Orsay, France  
Markus Schleier, MPG, Munich, Germany

## SCIENTIFIC ADVISORY COMMITTEE

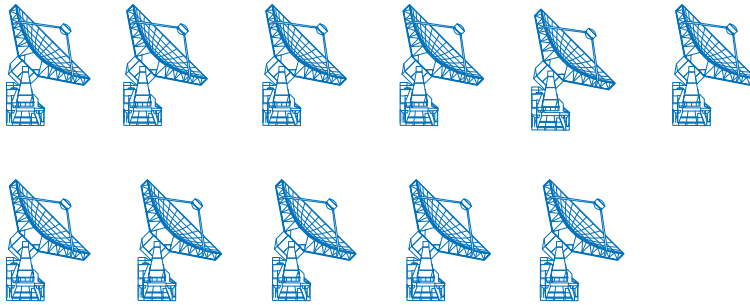
Santiago García Burillo, OAN, Madrid, Spain  
Maryvonne Gerin, LERMA/ENS, Paris, France  
Guilaine Lagache, LAM, Marseille, France  
Raphaël Moreno, LESIA, Observatoire de Paris, France  
Gordon J. Stacey, Cornell University, Ithaca, USA  
Linda Tacconi, MPE, Garching, Germany  
Mario Tafalla, OAN, Madrid, Spain  
Fabian Walter, MPIA, Heidelberg, Germany  
Friedrich Wyrowski, MPIfR, Bonn, Germany

## PROGRAM COMMITTEE

Peter Abraham, Konkoly Observatory, Budapest, Hungary  
Marcelino Agúndez, IFF-CSIC, Madrid, Spain  
Javier Alcolea, OAN, Madrid, Spain  
Elias Brinks, University Hertfordshire, Hatfield, United Kingdom  
Natascha Förster Schreiber, MPE, Garching, Germany  
John S. Gallagher, University Wisconsin-Madison, USA  
Yu Gao, CAS Purple Mountain Observatory, Nanjing, China  
Pierre Guillard, IAP, Paris, France  
Lee Hartmann, Univ. of Michigan, Ann Arbor, USA  
Vianney Lebouteiller, DAp CEA, Saclay, France  
François Levrier, LERMA/ENS, Paris, France  
Miguel Querejeta, ESO Garching, Germany  
Amélie Saintonge, University College London, United Kingdom  
Dimitri Semenov, MPIA, Heidelberg, Germany  
Axel Weiss, MPIfR, Bonn, Germany



**30-meter telescope, Pico Veleta**



**11 x 15-meter Interferometer, NOEMA**

The Institut de Radioastronomie Millimétrique (IRAM) is a multi-national scientific institute covering all aspects of radio astronomy at millimeter wavelengths. IRAM operates two observatories – the 30-meter Telescope on Pico Veleta in the Sierra Nevada and NOEMA, an interferometer of eleven 15-meter antennas on the Plateau de Bure in the French Alps.

IRAM was founded in 1979 by two national research organizations: the CNRS and the Max-Planck-Gesellschaft – the Spanish Instituto Geográfico Nacional, initially an associate member, became a full member in 1990.

The technical and scientific staff of IRAM develops instrumentation and software for the specific needs of millimeter radioastronomy and for the benefit of the international astronomical community.

IRAM scientists conduct forefront research in several domains of astrophysics, from nearby star-forming regions to objects at cosmological distances.

IRAM Partner Organizations:

Centre National de la Recherche Scientifique (CNRS) – Paris, France

Max-Planck-Gesellschaft (MPG) – München, Deutschland

Instituto Geográfico Nacional (IGN) – Madrid, España

